VEGETATION SENSITIVITY TO DROUGHTS (1982 – 2011) THROUGH REMOTE SENSING IN THE YUCATAN PENINSULA, MEXICO

Betsabé de la Barreda Bautista, BSc., MSc.

Thesis submitted to the University of Nottingham
for the degree of Doctor of Philosophy

September 2016

ABSTRACT

Ecosystems undergo permanent alteration and degradation as a result of the pressure exerted upon them by anthropogenic activities and natural causes. Amongst the natural causes, drought can have considerable impacts on vegetation productivity; these impacts include biomass reduction and changes in vegetation cycles, growth, and vitality. Such impacts have important implications for society, and understanding the impacts of drought in natural systems will help minimise vulnerability to it. The Yucatan Peninsula is a vulnerable area in climate change scenarios, where increased intensity and frequency of droughts is already occurring.

This thesis aims to analyse how droughts impact upon vegetation on the Yucatan Peninsula, Mexico using both remotely sensed data (in particular the Advanced Very High Resolution Radiometer – AVHRR - data) and meteorological data (*in situ* precipitation data). Three major elements are addressed: (1) spatial and temporal precipitation variability, and the occurrence of droughts during the period 1980-2011; (2) vegetation productivity trends, focusing on the persistence and resilience of the different vegetation types present across the Yucatan Peninsula using remotely sensed data sets, specifically, the Normalised Difference Vegetation Index (NDVI) from the National Oceanic and Atmosphere Administration Advanced Very High Resolution Radiometer (NOAA-AVHRR) as a proxy for productivity in the period 1982 to 2011; and (3) the relationship between vegetation productivity and rainfall and the lack of it (i.e. droughts) at a more detailed temporal scale (monthly) with two vegetation indices (NDVI from AVHRR and MTCI from the MEdium Resolution Imaging Spectrometer (MERIS)).

The main findings indicate that precipitation in the area follows a gradient from north to south which is linked to vegetation types in the area, from deciduous forest to evergreen forest. NDVI trends in the Yucatan Peninsula are generally stable during the period 1980-2011; however, negative trends are persistent in areas where human impacts and intensive agriculture are present. Analysis of resilience also shows that deciduous forest and grasslands are much less resilient

to disturbance and have a longer recovery period compared to other vegetation types. Per-pixel regression analysis between precipitation and vegetation productivity shows high explained variances between NDVI and rainfall with a time-lag of 1 and 2 months and tropical dry forest is the biome most affected by droughts. These results are valuable for decreasing the vulnerability of the Yucatan Peninsula and they could be used for increasing the understanding of the area and therefore go further in the creation of warning and management programmes.

ACKNOWLEDGEMENTS

First, I would like to express my sincere gratitude to my two supervisors Sarah Metcalfe and Doreen Boyd for their support, patience, motivation and immense knowledge during these years. Many thanks indeed for encouraging me and especially in the difficult moments, for reading meticulously every chapter and analysis in this thesis. Without her guidance and constant feedback this PhD would not have been achievable.

I would like to thank Georgina Endfield, my internal assessor, for her brilliant and useful comments and suggestions every year. Thanks to Kevin White, my external assessor, and Georgina for letting me know that the *viva voce* can be enjoyable and again for the great discussion we had on it.

I gratefully acknowledge the funding received towards my PhD from my sponsorship (CONACYT).

My PhD was indeed something that changed my life for good and without the support of my family, friends and colleagues this stage of my life would have never been possible. Thus, I want to thank principally my family, mamá, papá, Bere, Güicho, Güichito and Fabiola. Thanks a lot for all your support, for all the skype calls we had in the happiest and the most difficult moments, for encouraging me to stay here when I just wanted to give up, for making my time here always better with your words and life lessons and for all the sacrifices you have made on my behalf. Mil gracias!

I would like to thank my Nottingham friends who became my family here. Thank you Hugo for always listening to me, teaching me new things and making uni a nice place to work in. To my chicas de oro: Michele for the innumerable moments, fun, advises and pastas and for making me smile even in the worst moments, Nayra for all the love and motivation without forgetting all the meals and laughs together, Giada for being a great friend and being always there cheering me up and giving me love and laughs. To Darren and Anja for making me part of your family and being the first perfect example of the amazing people you can find in the UK. To Matteo, for being my first friend in Notts and for all the great moments we've shared together. To Heather for all the love, fun and advises. To Rowan (Rogüen) for making the day a day at uni different and fun. To Andres, for making me laugh, bringing more happiness to my life and making me feel the joy of the butterflies. To Alice for her infinite support. To Yiannis for all his unconditional and valuable help and his patience teaching me time series and his great company. To Ivan, for an amazing friendship as we have known from ages ago. To Tania and Tona, always there full of love. For all their friendship and encouragement to Emil, Linda, David, Pietro, Raffaella, Robert,

Paco, Diego, Javier, Jose, Camille, Francesca, Laura, Matteo, Alex. Igone, Wil, Teresa, Cordy, Raico, Cris, Vic, Normann, and Mark.

And to my friends in Mexico who from there were always there for me and these years made me realise what exactly having friends for the whole life means. To Nico, Amaya, Dago, Goyo, Guille, Arge, Clau, Andrea, Fabian, Mara, Mariel and Mariana.

Finally, I want to dedicate this work to my mum and dad for all the love and support and because I am who I am because of them. To my grandma, doña Pavita, who always was proud of me and I know if she were here she would be happy for this achievement. And to Silvana Levy because she trusted me and made this dream happened and she was the person to whom I owe being in Nottingham; I wish you could see that it was worth and that I finished.

Abstract **0**
Acknowledgements ..... **iii**
LIST of figures ..... **ix**
LIST of tables ..... **xvii**
CHAPTER 1. Context and Aims **1**
1.1 Importance of droughts 1
1.2 Drought definition 3
1.2.1 Types of droughts 4
1.3 Drought causes 5
1.4 Droughts impacts 6
1.4.1 Impacts on vegetation 6
1.5 Measuring and detecting droughts 7
1.5.1 Drought indices 7
1.6 The use of remote sensing for droughts 9
1.6.1 Drought impact assessment from an ecosystem perspective 10
1.6.2 Vegetation indices 13
1.6.2.1 Spectral characteristics of vegetation 14
1.6.2.2 Vegetation indices overview 15
1.6.2.3 Vegetation indices vs climatological variables 19
1.7 The Normalized Difference Vegetation Index (NDVI) 24
1.7.1 NDVI time series analysis 26
1.7.1.1 TIMESAT 28
1.8 Motivation and contribution to knowledge 28
1.9 Aims and objectives 30
1.10 Thesis outline 32
CHAPTER 2. Site description: Physical setting, vegetation, and human activities at the Yucatan Peninsula, Mexico **35**
2.1 Overview 35
2.2 Geology and hydrology 37
2.3 Climatology 39
2.3.1 Spatial and temporal precipitation variability 40
2.3.2 Temperature across the Peninsula 45
2.3.3 Extreme meteorological events 45
2.4 Vegetation 47

2.5 Principal human activities in the Peninsula 51

CHAPTER 3. Precipitation patterns and droughts across the Yucatan Peninsula 54

3.1 Introduction 54

3.2 Dataset and methods 55

3.2.1 Precipitation dataset 55

3.2.1.1 Precipitation data cleaning 58

3.2.2 Methods 60

3.2.2.1 Cluster analysis 61

3.2.2.2 Interpolation analysis (Kriging) 62

3.2.2.2.1 Kriging validation 64

3.2.2.3 Monthly precipitation in clusters 65

3.2.2.4 Precipitation Anomalies 66

3.3 Results 68

3.3.1 Cluster precipitation trends 68

3.3.2 Kriging 76

3.3.3 Monthly analysis 85

3.4 Precipitation anomalies 91

3.4.1 Drought detection in clusters 91

3.4.2 Precipitation anomalies maps 97

3.4.3 Kriging SPI 99

3.5 Chapter summary 102

CHAPTER 4. Vegetation productivity dynamics at the Yucatan Peninsula 105

4.1 Introduction 105

4.2 Datasets and pre-processing 106

4.2.1 Normalised Difference Vegetation Index (NDVI) dataset 106

4.2.2 Vegetation types 107

4.2.3 Precipitation dataset 108

4.3 Methodology 108

4.3.1 NDVI Smoothing and extraction of metrics: TIMESAT 108

4.3.2 Persistent and resilient vegetation behaviour analysis 110

4.3.2.1 Persistence probabilities: recovery times 111

4.3.3 NDVI anomalies 113

4.3.4 Understanding the relationship with precipitation 114
4.4 Results 115
4.4.1 Small integral analysis 115
4.4.2 Vegetation persistence 117
4.4.2.1 Persistence probabilities (resilience): recovery times in each type of vegetation 119
4.4.3 Evaluation of the NDVI anomalies 123
4.4.4 Correlation between NDVI and precipitation 125
4.5 Chapter summary 127

CHAPTER 5. Relationship between vegetation productivity and precipitation 130

5.1 Introduction 130
5.2 Correlation analysis between vegetation productivity and precipitation 131
5.3 Regression analysis between vegetation productivity and rainfall 132
5.4 Datasets and Methodology 134
5.4.1 Rainfall dataset 134
5.4.2 Normalised Difference Vegetation Index dataset (NDVI) and MERIS Terrestrial Chlorophyll Index (MTCI) 135
5.4.3 Standardised Precipitation Index (SPI) 135
5.4.4 Regression analyses 136
5.4.4.1 Precipitation lags 137
5.4.4.2 Vegetation productivity decay 138
5.4.4.3 Seasonality 138
5.4.4.4 Drought detection 139
5.5 Results and discussion 140
5.5.1 Precipitation lags 140
5.5.2 Vegetation productivity decay 145
5.5.3 Seasonality 149
5.5.4 Drought detection 153
5.6 Chapter summary 158

CHAPTER 6. Discussion, conclusions and suggestions for future work 160

6.1 Discussion of key findings 161

6.2 Knowledge gaps addressed and thesis novelty 165
6.3 Reflections on datasets and methods 166
6.4 Monitoring droughts and conservation implications 169
6.5 Future work 170
6.6 Conclusions 171

References 173
Appendix 1 194
Appendix 2 200
Appendix 3 203
Appendix 4 204

LIST OF FIGURES

Figure 1-1. Drought events and impacts through time for different drought types. Modified from National Drought Mitigation Center, University of Nebraska-Lincoln, U.S.A. 5

Figure 1-2. Spectral signatures of dry bare soil, vegetation and water in different wavelengths of the electromagnetic spectrum. Modified from: http://landsat.usgs.gov/remote_sensing_applications.php 14

Figure 1-3. Thesis structure 33

Figure 2-1 Location of the Yucatan Peninsula (21 - 17° N; 91 -87° W) with the political division which includes the states of Yucatan, Campeche and Quintana Roo and the two adjacent countries (Guatemala and Belize). Red borders in inset map show the Natural Protected Areas. 36

Figure 2-2. Topography of the Yucatan Peninsula. Image taken from: http://en-ca.topographic-map.com/places/Yucatan-Peninsula-8159035/ 38

Figure 2-3. Climates types present in the Yucatan Peninsula according to the Köppen system modified by García (1998a). 40

Figure 2-4. Position and movement of the ITCZ (dashed lines) for boreal hemisphere during summer (black) and during winter (blue). Arrows represent the direction of the prevailing moisture-bearing winds in summer (black) and in winter (blue). Modified from: http://soundwaves.usgs.gov/2008/04/ 41

Figure 2-5. Annual precipitation map across the Yucatan Peninsula. Data from (García, 1998b). Note: The dates used by García (1998b) for the creation of this map are not reported and was constructed taking into account orography and wind direction. The source can be found in: http://www.conabio.gob.mx/informacion/metadata/gis/isoyt1mgw.xml?_httpcache=yes&_xsl=/db/metadata/xsl/fgdc_html.xsl&_indent=no 42

Figure 2-6. Map of the Yucatan Peninsula with contours of mean annual precipitation in millimetres. Taken from Hodell et al. (2007) 43

Figure 2-7. Average annual precipitation (1941-2010) and temperature (1971-2010) at the Yucatan Peninsula (CONAGUA, 2010b). 44

Figure 2-8. Vegetation types across the Yucatan Peninsula. The colours of each class are grouped according to the same type of vegetation including

secondary vegetation and some perturbed areas. Data from the National Forest Inventory (INEGI, 2010). 49
Figure 2-9. Natural protected areas in the Yucatan Peninsula including Belize and Guatemala. Data from (CONANP, 2010) and http://www.protectedplanet.net/ 51
Figure 3-1. Spatial distribution of the 229 existing meteorological stations in the Yucatan Peninsula. Red points represent the stations selected with more than 60% of reliable data. The points on the sea are stations located in small land areas called *cayos*. 56
Figure 3-2. Number of meteorological stations in the Yucatan Peninsula through time. Bars show the number of stations set up in each decade. Darker bars show the stations with more than 60% reliable data and lighter bars show the total number of station in the current year. 57
Figure 3-3. Champoton station (in the east of Campeche). This is the station with the longest period of data. The black solid line represents the daily precipitation for this station; the blue dashed line represents the trend line. 57
Figure 3-4. Semivariogram with the fitted model for the estimation of kriging as an example for the year 2005. Parameters: Nugget = 0.74; sill = 1.59; range: 6.4. Parameters estimated in RStudio and semivariogram created in ArcGIS. 64
Figure 3-5. Meteorological station dendrogram resulting from cluster hierarchical analysis. Each rectangle represents each cluster. Yellow: Cluster B; Black: Cluster E; Purple: Cluster C; Red: Cluster A; Green: Cluster D 68
Figure 3-6. Dissimilarity plot shows the distance between clusters. In the x-axis the ideal number of clusters is represented according to the dissimilarity between them (y-axis) 69
Figure 3-7. Silhouette plot analysis. It shows the separation significance between clusters. Each colour represents each cluster. Yellow: Cluster B; Black: Cluster E; Purple: Cluster C; Red: Cluster A; Green: Cluster D. In the right margin it also shows (right hand column) the strength of the affinity of each cluster within cluster. The overall significance in the bottom left corner (average silhouette width). 70

Figure 3-8. Spatial distribution of the clusters (A-E) resulting from the hierarchical cluster analysis on a map that represents the annual precipitation totals across the Yucatan Peninsula. 71
Figure 3-9. Daily precipitation average data grouped in clusters. The bars represent the standard deviation for each cluster. Each colour represents each cluster. Yellow: Cluster B; Black: Cluster E; Purple: Cluster C; Red: Cluster A; Green: Cluster D 72
Figure 3-10. Cluster daily precipitation average (in mm) from 1980 to 2010. Each line represent the time series of each cluster. Red bars indicate the dry years and blue bars the wet years for all clusters. 73
Figure 3-11.a) Vegetation types map overlapped with the five clusters (A-E) across the Yucatan Peninsula; b) Temperature ranges map overlapped with the five clusters (A-E) across the Yucatan Peninsula; c) Altitude in m.a.s.l overlapped with the five clusters (A-E) across the Yucatan Peninsula. 75
Figure 3-12. Long-term average (1980-2011) maps resulted from Kriging analysis. a) Long-term precipitation average from daily data. b) Long-term accumulated precipitation. 77
Figure 3-13. Maps (1980-2011) resulting from Kriging analysis. Each map represents the average daily precipitation for a given year in millimetres across the Yucatan Peninsula. Highlighted maps were validated with TRMM data. The number of stations used for creating each map are shown in Table 3-1. 78
Figure 3-14. TRMM 3B42 v7 precipitation data (1998 – 2011). All maps were created with the TRMM Online Visualization and Analysis System (TOVAS) and they are a product from daily TRMM and Other Rainfall Estimate (3B42 V7) derived. 79
Figure 3-15. Relationships between resulting kriging maps and precipitation from TRMM 3B42 product. Every plot represent each year from 1998-2011. R^2 shows the square root of Pearson correlations 82
Figure 3-16. Boxplots of daily average precipitation by month. X-axis represents the months and y-axis represent the daily precipitation average. The lines in the middle of the boxes represent the mean and the whiskers

represent the standard deviation, while the points represent outliers. a) Cluster A; b) Cluster B; c) Cluster D; d) Cluster E 86
Figure 3-17. Matrix plots of daily average precipitation by month. X-axis represent the years (1980-2011) and y-axis are the months. a) Cluster A; b) Cluster B; c) Cluster D; d) Cluster E. Different colours represent the amount of precipitation in mm. 88
Figure 3-18. Routes of hurricanes and tropical storms from 1980 – 2011. Different colours represent the hurricane category (Taken from: NOAA (2016)). Strongest hurricanes are labelled. 90
Figure 3-19. Standardized Precipitation Index (SPI) computed for each cluster at different time scales (1 to 12 months). Year from 1980 – 2011 on x-axis and y-axis represents the SPI time scale (months) from SPI-1 to SPI-12 for each cluster. 92
Figure 3-20. 3, 6, and 12-month SPI values for cluster A. c) shows the 12-month SPI in the primary axis and the Oceanic Niño Index in the secondary axis 93
Figure 3-21. 3, 6, and 12-month SPI values for cluster B. c) shows the 12-month SPI in the primary axis and the Oceanic Niño Index in the secondary axis 94
Figure 3-22. 3, 6, and 12-month SPI values for cluster D. c) shows the 12-month SPI in the primary axis and the Oceanic Niño Index in the secondary axis 95
Figure 3-23. 3, 6, and 12-month SPI values for cluster E. c) shows the 12-month SPI in the primary axis and the Oceanic Niño Index in the secondary axis 96
Figure 3-24. Maps showing the difference between the long-term average precipitation and annual average precipitation in mm. Each map represent each year from 1980-2011. 98
Figure 3-25. Maps showing the krigged annual SPI. Each map represent each year from 1980-2011. The scale is based on the North American Drought Monitor (NADM): i) closer to -2: low precipitation over 12 months; ii) approximately 0: normal precipitation over 12 months; iii) closer to 2: heavy precipitation over 12 months. 101

Figure 4-1. Forest classification according to its deciduousness in the Yucatan Peninsula. Data obtained by INEGI (2010). 108
Figure 4-2. Possible seasonality parameters derived in TIMESAT. (a) start of season, (b) end of season, (e) maximum value, (g) length of season, (h) small integrated value, (i) large integrated value. Figure modified from Jönsson and Eklundh (2004). 110
Figure 4-3. Normalized difference vegetation index (NDVI) based on growing season NDVI integral. Data resulting from TIMESAT. 116
Figure 4-4. Cumulative persistence map $PtiT_{x,y}$ for the period 1992-2011. Base period is from 1982-1991. Persistence values are expressed in number of years from 1992-2011 (20 years). Sign indicates the trend tendency (positive or negative). Yucatan Peninsula is demarcated with the black line. 118
Figure 4-5. Positive (○) and negative (Δ) persistent probability plots for different vegetation type fitting an exponential decay. Each plot represents different vegetation type; a) Semi-deciduous forest, b) Grasslands, c) Spiny forest, d) Hydrophytic vegetation, e) Evergreen forest, f) Deciduous forest , g) Agriculture and livestock. The estimation of τ represents the mean time life and the R^2 the goodness of fit of the exponential model to the data. Red and green lines represent the best persistence probability fit (exponential model) for negative and positive trends respectively. 120
Figure 4-6. NDVI annual anomalies in the Yucatan Peninsula for the period 1982-2011. Coloured pixels represent those anomalies that are significant and have 5% probability of occurrence. Negative values (red colours) represent negative anomalies and positive values denote positive anomalies (blue colours). 124
Figure 4-7. R-squared annual NDVI and annual rainfall krigged maps from the period 1982-2011 for the Yucatan Peninsula. 126
Figure 5-1. Estimations of the regressions. Every map has 122 points showing the significance of the coefficient of a specific variable when the regression is run in that pixel. Having confidence level $\alpha = 0.05$, the critical values are -1.64 and 1.64, the scale is constructed to show them. Each map contains the values of the t-statistics of $\beta 1$ in the following

regression: $yt = a + \beta 1xt + \beta 2xt - 1 + \beta 3xt - 2 + \beta 4xt - 3 + \beta 5xt - 4 + \beta 5xt - 5 + \varepsilon t$ 142
Figure 5-2. R-squares resultant from the first regression model. Each point represent the R-squares for every regression $yt = a + \beta 1xt + \beta 2xt - 1 + \beta 3xt - 2 + \beta 4xt - 3 + \beta 5xt - 4 + \beta 5xt - 5 + \varepsilon t$ 143
Figure 5-3. Estimations of the regressions (MTCI). Every map has 93 points showing the coefficient of a specific variable when the regression is run in that pixel. Having confidence level $\alpha = 0.05$, the critical values are -1.64 and 1.64, the scale is constructed to show them. Each map contains the values of the t-statistics of $\beta 1$ in the following regression model: $yt = a + \beta 1xt + \beta 2xt - 1 + \beta 3xt - 2 + \beta 4xt - 3 + \beta 5xt - 4 + \beta 5xt - 5 + \varepsilon t$ 144
Figure 5-4 R-squares resultant from the first regression model (MTCI). Each point represent the R-squares for every regression. $yt = a + \beta 1xt + \beta 2xt - 1 + \beta 3xt - 2 + \beta 4xt - 3 + \beta 5xt - 4 + \beta 5xt - 5 + \varepsilon t$ 145
Figure 5-5. Estimations of the regressions. Every map has 122 points showing the coefficient of a specific variable when the regression is run in that pixel. Having confidence level $\alpha = 0.05$, the critical values are -1.64 and 1.64, the scale is constructed to show them. Each map contains the values of the t-statistics of $\beta 1$ in the following regression model: $yt = a + \beta 1xt + \beta 2xt - 1 + \beta 3xt - 2 + \beta 4xt - 3 + \beta 5xt - 4 + \beta 5xt - 5 + \beta 6yt - 1 + \varepsilon t$ 146
Figure 5-6 R-squares resultant from the second regression model. Each point represent the R-squares for every regression. $yt = a + \beta 1xt + \beta 2xt - 1 + \beta 3xt - 2 + \beta 4xt - 3 + \beta 5xt - 4 + \beta 5xt - 5 + \beta 6yt - 1 + \varepsilon t$ 147
Figure 5-7. Estimations of the regressions (MTCI). Every map has 122 points showing the coefficient of a specific variable when the regression is run in that pixel. Having confidence level $\alpha = 0.05$, the critical values are -1.64 and 1.64, the scale is constructed to show them. Each map contains the values of the t-statistics of $\beta 1$ in the following regression: $yt = a + \beta 1xt + \beta 2xt - 1 + \beta 3xt - 2 + \beta 4xt - 3 + \beta 5xt - 4 + \beta 5xt - 5 + \beta 6yt - 1 + \varepsilon t$ 148

Figure 5-8 R-squares resultant from the second regression model (MTCI). Each point represents the R-squares for every regression. $yt = a + \beta 1xt + \beta 2xt - 1 + \beta 3xt - 2 + \beta 4xt - 3 + \beta 5xt - 4 + \beta 5xt - 5 + \beta 6yt - 1 + \varepsilon t$ 149

Figure 5-9 Estimations of the regressions. Every map has 122 points showing the coefficient of a specific variable when the regression is run in that pixel. Having confidence level $\alpha = 0.05$, the critical values are -1.64 and 1.64, the scale is constructed to show them. Each map contains the values of the t-statistics of $\beta 1$ in the following regression: $yt = a + \beta 1xt + \beta 2xt - 1 + \beta 3xt - 2 + \beta 4xt - 3 + \beta 5xt - 4 + \beta 5xt - 5 + \beta 6yt - 1 + \beta 7St + \varepsilon t$ 150

Figure 5-10 R-squares resulting from the third regression model. Each point represents the R-squares for every regression. $yt = a + \beta 1xt + \beta 2xt - 1 + \beta 3xt - 2 + \beta 4xt - 3 + \beta 5xt - 4 + \beta 5xt - 5 + \beta 6yt - 1 + \beta 7St + \varepsilon t$ 151

Figure 5-11. Estimations of the regressions (MTCI). Every map has 93 points showing the coefficient of a specific variable when the regression is run in that pixel. Having confidence level $\alpha = 0.05$, the critical values are -1.64 and 1.64, the scale is constructed to show them. Each map contains the values of the t-statistics of $\beta 1$ in the following regression: $yt = a + \beta 1xt + \beta 2xt - 1 + \beta 3xt - 2 + \beta 4xt - 3 + \beta 5xt - 4 + \beta 5xt - 5 + \beta 6yt - 1 + \beta 7St + \varepsilon t$ 152

Figure 5-12 R-squares resulting from the third regression model (MTCI). Each point represents the R-squares for every regression. $yt = a + \beta 1xt + \beta 2xt - 1 + \beta 3xt - 2 + \beta 4xt - 3 + \beta 5xt - 4 + \beta 5xt - 5 + \beta 6yt - 1 + \beta 7St + \varepsilon t$ 153

Figure 5-13 Estimations of the regressions (NDVI). Every map has 122 points showing the coefficient of a specific variable when the regression is run in that pixel. Having confidence level $\alpha = 0.05$, the critical values are -1.64 and 1.64, the scale is constructed to show them. Each map contains the values of the t-statistics of $\beta 1$ in the following regression: $yt = a + \beta 1xt + \beta 2xt - 1 + \beta 3xt - 2 + \beta 4xt - 3 + \beta 5xt - 4 + \beta 5xt - 5 + \beta 6yt - 1 + \beta 7St + \beta 8SPIt + \beta 9SPIt - 1 + \varepsilon t$ 155

Figure 5-14 R-squares resulting from the fourth regression model. Each point represents the R-squares for every regression. $yt = a + \beta 1xt + \beta 2xt - 1 + \beta 3xt - 2 + \beta 4xt - 3 + \beta 5xt - 4 + \beta 5xt - 5 + \beta 6yt - 1 + \beta 7St + \beta 8SPIt + \beta 9SPIt - 1 + \varepsilon t$ 156
Figure 5-15 Estimations of the regressions (MTCI). Every map has 122 points showing the coefficient of a specific variable when the regression is run in that pixel. Having confidence level $\alpha = 0.05$, the critical values are -1.64 and 1.64, the scale is constructed to show them. Each map contains the values of the t-statistics of $\beta 1$ in the following regression: $yt = a + \beta 1xt + \beta 2xt - 1 + \beta 3xt - 2 + \beta 4xt - 3 + \beta 5xt - 4 + \beta 5xt - 5 + \beta 6yt - 1 + \beta 7St + \beta 8SPIt + \beta 9SPIt - 1 + \varepsilon t$ 157
Figure 5-16 R-squares resulting from the fourth regression model (MTCI). Each point represents the R-squares for every regression. $yt = a + \beta 1xt + \beta 2xt - 1 + \beta 3xt - 2 + \beta 4xt - 3 + \beta 5xt - 4 + \beta 5xt - 5 + \beta 6yt - 1 + \beta 7St + \beta 8SPIt + \beta 9SPIt - 1 + \varepsilon t$ 158
Figure 6-1. SPI computation from different software and sources of information. 167

LIST OF TABLES

Table 1-1. Principal vegetation indices, mathematical definitions, and authors. 15

Table 3-1. Number of stations used for each annual kriging map. Results of these maps are shown in section 3.3.2. 59

Table 3-2. Table to show the distribution of cluster with different features in the Yucatan Peninsula 74

Table 3-3. Correlation values between the TRMM data and the resulting Kriging data per each year (1998-2011). First column presents the Pearson correlation coefficients, second column the p-values for the test of statistical significance and in the last two columns the 95% confidence intervals 81

Table 3-4. Tropical depressions (TD), tropical storms (TS), and hurricanes (categories I to V) at the Yucatan Peninsula from 1980-2011. 89

Table 4-1. Number of pixels for each vegetation type (sample size). 112

Table 4-2. Summary of the results obtained from the persistence probabilities for each vegetation type. Mean life times (in years) of positive and negative trends (t); R-squared for the negative and positive fitted exponential model. 121

CHAPTER 1. **CONTEXT AND AIMS**

The Yucatan Peninsula, Mexico harbours a rich biodiverse tropical forests and has an interesting history particularly in relation to the Mayan culture (dating back more than 4000 years). This area has been of great interest for the scientific community in terms of conservation and biodiversity. The Peninsula is particularly sensitive to climate perturbations, such as drought; this climatic influence may have implications for biodiversity, food security, water demand, changes in phenological cycles, species competition, carbon stock, forest fires, etc. Even though vegetation on the Peninsula has shown signs of being resilient for these events (Islebe et al., 2015), climate change scenarios, land cover change, and human impacts could threaten this characteristic of the area.

The study of droughts has been approached through different perspectives. One of these perspectives is through climatological variables (i.e. temperature, precipitation, evapotranspiration). The second perspective is analysing droughts indirectly by measuring vegetation condition and health from remote sensing data. The main focus of this thesis is to understand and measure how droughts impact on the vegetation of the Yucatan Peninsula using remote sensing for Earth Observation through changes in vegetation productivity. In this chapter, an overview of the principal research concepts is presented; droughts are defined and explained and an explanation of how remote sensing can assess droughts and their impacts on vegetation is provided.

1.1 **Importance of droughts**

Droughts are considered as one of the most important natural hazards as they are a significant risk in terms of water and food scarcity, thus, they are an economical and financial threat (Wilhite, 2000; AghaKouchak et al., 2015). Every country is exposed to them and various climate change effects; however, these could have more impact in developing countries and those with particular physical and geographical features (e.g. low altitude and arid regions) are the most threatened (Liverman, 1999; Wilhite, 2000). Mexico is a developing

country and it is particularly vulnerable to extreme climatological events because of its location and because it is exposed to important climate variability including tropical storms and droughts (Hernández Cerda et al., 2000; Márdero et al., 2012).

Climate projections indicate that Mexico and in particular the southern part will have an increase in temperature and more frequent and intense extreme climatic events (IPCC, 1997; IPCC, 2013). In addition, the lack of policies and knowledge about droughts make this country more vulnerable than most. These are important reasons to study Mexico, in particular the Yucatan Peninsula since it represents a region where all these conditions are present and it is a very distinct area in Mexico.

The Yucatan Peninsula has a distinctive climatic and vegetation gradient and has an unusual geology and hydrology which have made this area develop an interesting biodiversity, thus it has been classified as a biogeographical unit. The Yucatan Peninsula biogeographical unit includes the Mexican States of Yucatan, Quintana Roo and Campeche, part of Belize and Guatemala (Torrescano-Valle and Folan, 2015). It has a great biodiversity in terms of richness and endemism. For instance, it has more than 2500 species of plants, approximately 3000 species of insects, over 125 species of mammals, around 550 of birds, 118 of reptiles and 24 amphibians species (Islebe et al., 2015) and according to Rada et al. (2015) the Yucatan Peninsula has the largest natural reservoir of carbon in Mexico and it is the second largest forested area in Latin America after the Amazon in South America. Furthermore, this region is affected every year by natural hazards, in particular hurricanes and droughts. For this thesis, the Yucatan Peninsula is limited to the Mexican part. Thus, the Belize and Guatemala regions are excluded from the analysis. In chapter 2 a complete description of the area is provided.

Extreme meteorological events, particularly droughts have important implications for society and the regional economy and some theories suggest that in future, the hydrological cycle will alter to produce more frequent and intense drought periods (IPCC, 2013). Unlike other extreme meteorological

events with a specific location and fast impact (e.g. hurricanes), droughts cover large geographic areas and their consequences can last for months or years reducing the quality of life and the development of the population (Wilhite and Vanyarkho, 2000). Mexico has been affected by intense and prolonged periods of drought through its history. Although there is a lack of exact dates and places where droughts occurred in the past across the Yucatan Peninsula; palaeoenvironmental studies, historical archives, and more contemporaneous climatic records show that the Yucatan Peninsula has experienced important drought events and the phenomenon is now well known and being well documented (Mendoza et al., 2006; 2007; Méndez and Magaña, 2010). Drought is considered as the meteorological phenomenon with the most severe impact on economic activity and may well result in human casualties (Wilhite, 2000; Wilhite and Vanyarkho, 2000). Mexico's economy relies strongly on agriculture and livestock and these are intensely affected by droughts. In addition, in some regions of the country, lack of rain means that many people are left without access to water (Ortega-Gaucin and Velasco, 2014).

1.2 **Drought definition**

Droughts do not have a unique definition and there is a lack of consensus about the definition of them. In general, the definition of a drought is related to water balance and the water availability for society (Mendez Perez, 2003). According to Florescano and Swan (1995) defining a drought is not only about water scarcity, but total lack of water which lasts a considerable period of time and affects plant and animal development. In general, drought could be described as a slow-onset natural hazard with effects that accumulate over a considerable period of time. It is a normal and recurrent climate condition, with uneven temporal and spatial features; it occurs or can occur in every climatological area; however, drought characteristics vary significantly between geographical areas (Bayarjargal et al., 2006; Hayes et al., 2012).

Droughts have been classified in terms of their intensity and depending on the aims of the work, in Mexico the intensity of a drought is based on the North American Drought Monitor, which classifies them as: abnormally dry (D0),

moderate drought (D1), severe drought (D2), extreme drought (D3) and exceptional drought (D4). Abnormally Dry (D0) is defined as a dryness condition, not a drought category. It occurs at the beginning or ending of a drought period. At the beginning of a drought period, due to short term dryness, it may cause delay in annual sowing, limit growing of pastures and crops, and there is risk of fires. At the end of the drought period, there may be lack of water, pastures and crops may not be completely recovered. A moderate drought (D1) is when there is some damage to crops and pastures; there is high risk of fire presence, low levels in rivers, creeks, reservoirs, troughs, and swells; voluntary water restriction is advised. Severe Drought (D2) presents probable pasture and crop loss, high risk of fire presence; lack of water is a common scenario; water use restrictions must be imposed. In an extreme drought (D3) there are big pasture and crop losses; extreme forest fire risk, generalized water use restrictions due to scarcity. Finally, an exceptional drought (D4) is when exceptional and generalized pasture and crop losses occur; there is exceptional fire risk, total water scarcity in reservoirs, creeks, and swells and an emergency situation is likely to happen due to absence of water (USDM, 2016).

1.2.1 Types of droughts

It is difficult to set a unique definition of a drought, instead drought experts have opted for classifying droughts according to the impacts they cause (Figure 1-1). Therefore, there are various types of drought: meteorological, hydrological, agricultural and socio-economic (Mendez Perez, 2003).

A meteorological drought is defined as a precipitation reduction below normal average, while hydrological drought occurs when the level of water resources in both surface and underground stores are below the normal. On the other hand, the agricultural definition of drought is based on the soil humidity content available to satisfy the growth of a crop. Finally the socio-economic one is defined when the lack of rain and scarcity of water starts to affect society and socio-economic activities (Mendez Perez, 2003; Hayes et al., 2012). Since the meteorological definition is based on precipitation deficit and the most complete and available dataset is precipitation, then, in this study a drought is taken to be

using the meteorological definition. In addition, a close relationship between rainfall and vegetation productivity has been noted.

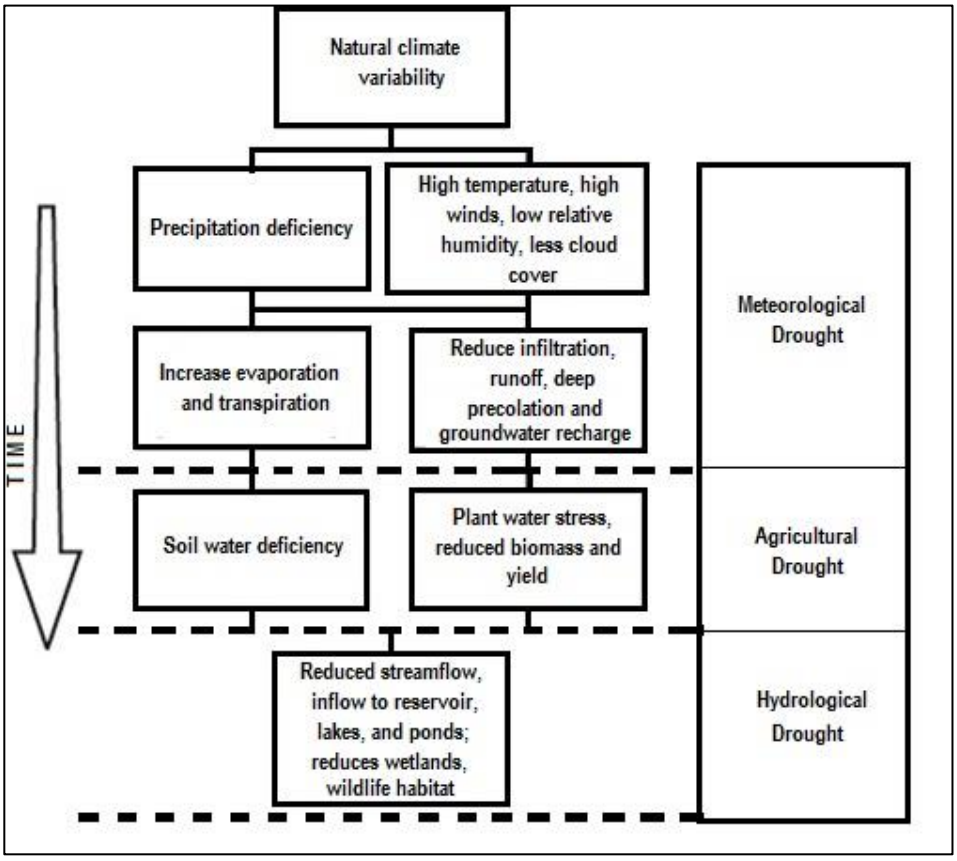


Figure 1-1. Drought events and impacts through time for different drought types. Modified from National Drought Mitigation Center, University of Nebraska-Lincoln, U.S.A.

1.3 **Drought causes**

The causes of meteorological drought are mainly due to the natural variability of climate; it has been noted that they occur when there is a change in the pattern of wind flows (Florescano and Swan, 1995), and they are mostly related to different atmospheric mechanisms and alterations in the atmospheric general circulation, both generated by modifications in the surface albedo, temperature changes on ocean and sea surfaces, among others. In addition, anthropogenic activity (i.e. burning fossil fuels, deforestation, land use change, etc.) is considered as another potential important cause of droughts and their impact. Some studies have suggested that El Niño/La Niña conditions are one of the most

important drivers of droughts in Mexico (as well as in other parts of the world) (Florescano and Swan, 1995; Caviedes and Waylen, 1998; Mendez Perez, 2003; Mendoza et al., 2007; Méndez and Magaña, 2010).

1.4 Droughts impacts

Climate variability has important implications and consequences which have been the focus of study due to their importance to human beings, because these affect society directly and indirectly, as well as natural systems (Easterling et al., 2000). These climate fluctuations may notably impact the structure and function of natural and artificial environments and may modify regional climates. Natural hazards are the consequences of different complex processes between meteorological conditions, land surface characteristics and human activities, and they cause different effects on society and ecosystems. These effects can extend over large geographical regions (Niemeyer and Vogt, 2003).

1.4.1 Impacts on vegetation

Extreme climate events have an impact on biophysical systems and may affect the ecosystems in different ways; these effects are related to particular ecosystem features such as species diversity, functional diversity, time of succession, and stress thresholds of ecosystem resilience. In a functional view, droughts affect physiology, development, competition, phenology, carbon balance and cause important damage to forest ecosystem through the formation of vegetation gaps, droughts can even result in vegetation mortality. They are important drivers for wildfires and play an important role in the establishment of invasive plants species (Rosén, 1995; Breshears et al., 2005; Bréda and Badeau, 2008; Wardlow et al., 2012b). The Figure 1-1 also represents some of the impacts of droughts at different times in natural systems.

Drought impacts on vegetation are related to water and how vegetation is stressed by the lack of this resource (Wardlow et al., 2012b), and the general result is a decrease in biomass; these water deficits have various effects on vegetation growth and vigour (Rossi and Niemeyer, 2012). There are some

studies about how vegetation is affected by droughts (Rosén, 1995; Llorens et al., 2004; Breshears et al., 2005) and different effects such as photosynthetic activity, mortality and biomass in different types of ecosystem and different physiological aspects of vegetation are analysed. Precipitation is a principal determining factor for vegetation, thus, lack of precipitation and subsequent soil moisture deficits have a direct impact on the state of vegetation, causing plant water stress and wilting as demonstrated by Rossi and Niemeyer (2012). According to Bayarjargal et al. (2006) droughts affect vegetation cycles and especially during the green-up onset period and they may accelerate desertification processes. Therefore, detecting and measuring droughts can be done directly with precipitation data or indirectly by studying other vegetation characteristics such as vegetation productivity.

1.5 Measuring and detecting droughts

Normally, the approach used to measure droughts is through indices derived from meteorological data (ground point based records) such as precipitation, humidity, evapotranspiration or temperature observations and they are used to detect and measure droughts, but different indices measure drought in different ways, and no single index works under all circumstances (Heim Jr, 2002). These indices provide information about intensity, duration and point-based spatial location of a drought (Mendez Perez, 2003; Méndez and Magaña, 2010). It has been shown that the use of different drought indices gives different results according to their characteristics as they have been developed for specific climatic conditions (Jain et al., 2015).

1.5.1 Drought indices

The most important indices to monitor droughts are the Palmer Drought Severity Index (PDSI), the Crop Moisture Index (CMI), the Percentage of Average Precipitation (PAP), and the Standardized Precipitation Index (SPI) (Mendez Perez, 2003; Méndez and Magaña, 2010). The Palmer Drought Severity Index (Palmer, 1965) was the first index developed to assess moisture status comprehensively. It uses temperature and precipitation data to calculate water

supply and demand, it incorporates soil moisture (Dai and NCAR, 2016) and it assesses the intensity and the beginning and ending times of a drought. It has been used to identify droughts, monitor droughts, to determine the wet and dry seasons and to compare the dryness between years, as well as for studying the frequency and intensity of droughts all over the world (Alley, 1984). However, according to Akinremi et al. (1996) PDSI does not perform well for every location, so they improved PDSI incorporating the Versatile Soil Moisture Budget (VMB) model. The PDSI has been identified to measure hydrological drought as all its inputs (precipitation, evapotranspiration and soil moisture conditions) are related with the general hydrological cycle (Alley, 1984).

Another index developed from the PDSI was the CMI, which is calculated from evapotranspiration deficits for monitoring short-term agricultural drought conditions that affect crop growth; then, this index is used principally to detect potential agricultural droughts. However, this index has been criticised since it is used for monitoring crop droughts and every crop responds differently to lack of moisture (Alley, 1984; Narasimhan and Srinivasan, 2005).

McKee et al. (1993) proposed another way to measure drought, introducing the SPI, which is an indicator to define a drought, which requires only one input variable (precipitation) for its analysis. This variable could be applied in a similar way to precipitation, snowpack, streamflow, reservoir storage, soil moisture, and ground water; one of the most important features of it, is that it recognises a variety of time scales, and provides information on precipitation deficit, percent of average and probability. The U.S. Monitor Program has been using this index in order to produce monthly maps of deficits in precipitation. This index can be used at different spatial scales over time, which is a good advantage for monitoring droughts in time (see chapter 3). Another indicator to detect anomalies broadly used in precipitation (Werick et al., 1994; Márdero et al., 2012) is the PAP indicator which is used to analyse the precipitation as percentages of precipitation averages in long-term and is used to monitor droughts over different time scales (NADM, 2016).

All the indices mentioned above are some of the most useful to monitor droughts and they fulfil the characteristics that a drought index should have. Those features are, according to Narasimhan and Srinivasan (2005), that the index must be able to reflect developing short-term dry conditions; it should not have any seasonality; and the drought index should be spatially comparable, irrespective of climatic zones (humid or arid). The information obtained by these indices relates to drought intensity in specific areas, and the indices are derived from local meteorological parameters, however these indices do not provide information about drought extent and or give accurate start and end dates, nor do they provide information about the effects that they have in ecosystems. Moreover, the input data for calculating these indices is traditionally extracted by meteorological stations, which need to be located in strategic locations to monitor the local climate. However, in some countries there is a lack of them or there are gaps of information in some regions. In Mexico for example, the sources of information are improving; nevertheless, the historical records are incomplete and many areas of the country do not have meteorological stations.

In order to improve the understanding of a drought, other alternatives to monitor and understand droughts have been developed and give us a broader comprehension about both droughts and the effects of them on ecosystems. Remote sensing is one of these alternatives and it is ideal for understanding droughts through vegetation changes and the impacts of droughts on vegetation dynamics with a spatio-temporal perspective (Wardlow et al., 2012a; AghaKouchak et al., 2015).

1.6 The use of remote sensing for droughts

Remote sensing has been considered an important tool to measure biodiversity and for mapping vegetation cover; it provides information about ecosystem dynamics at different spatial and temporal scales which allows for the analyses of abrupt and gradual changes of vegetation in response to climate variability (AghaKouchak et al., 2015). Remotely sensed archives are an exceptional way to follow up different phenomena through time in inaccessible geographic areas or areas with lack of ground data (Gillespie et al., 2008; Boyd et al., 2011;

Wardlow et al., 2012a; AghaKouchak et al., 2015). It is also a method that can integrate different types of data to study what is and what was happening on the Earth's surface and provides the opportunity to extract information for a specific geographical space. The information acquired from remotely sensed data can be related to other types of variables, and in the context of this thesis includes climatological variables (e.g. precipitation).

According to Chuvieco (1985) the advantages of using remote sensing as a tool to monitor environmental dynamics are based on the following statements: i) it is a synoptic vision of the land surface and in homogenous conditions; ii) the information obtained in different wavelengths beyond the visible spectrum (e.g. infrared and near infrared) is really useful to characterise different land covers (vegetation, urban areas, etc.); iii) it is possible to analyse the terrain at diverse spatial and temporal resolutions due to the orbital features of each sensor; iv) it helps to save time, capital and human resources, and there is specialised software for managing digital information; finally, v) as results are images, it is possible to manipulate them with some basic algebraic operations such as filters, band combination and surfaces measurements, among others.

To understand vegetation dynamics and go further into the description of it, it is necessary to analyse it through different perspectives and ways: field data, geographical data (i.e. maps, georeferenced data, remote sensing products), statistics and models (Gitay et al., 2002) and through a spatial and temporal point of view in order to have a broader understanding of the data and the phenomena studied. Remote sensing, its time series products, and its methodologies is a worthy approach to measure droughts and their impacts on vegetation through the analysis of vegetation productivity; and it allows analysis of the spatial and temporal evolution of droughts.

1.6.1 Drought impact assessment from an ecosystem perspective

Vegetation is in constant change due to natural causes, these changes are basically, vegetation growth/decay and phenology. Phenology is the physiological process of vegetation related to seasonal and interannual variations

in climate; it defines the timing and duration of a photosynthetically active cover and therefore influences the magnitudes of carbon and water fluxes throughout the growing season (Jolly and Running, 2004). The study of vegetation phenology at regional and global levels is a key to comprehend how climate acts over ecosystems at various temporal scales (Myneni et al., 1995).

Many efforts have been undertaken to understand droughts and their impact on vegetation. In the past, the majority of them have been focused on climatological data (Magaña et al., 1999; Mendoza et al., 2007). However, the development of remote sensing has allowed improved understanding in this arena since remote sensing has a strong potential for the monitoring of vegetation dynamics (Anderson et al., 2010; Anyamba and Tucker, 2012; Wardlow et al., 2012a; AghaKouchak et al., 2015).

The remote sensing community has developed many methods and principles to analyse and assess vegetation dynamics in terms of phenology, structure, productivity, and biomass; this has been possible due to the diversity of spaceborne sensors that exist. These developments have opened up a range of opportunities to relate remotely sensed data with droughts. Hayes et al. (2012) stated that remote sensing plays an important role in drought monitoring systems due its synoptic, rapid repeat, and spatially continuous information about regional or local areas affected by droughts. Different missions and sensors have been developed specifically to analyse and understand different aspect of the Earth surface (Tucker and Sellers, 1986). Since the launch of missions such as AVHRR, Landsat and later TRMM, the analysis of droughts through remote sensing has become an important research area to explore (Bayarjargal et al., 2006). Other products developed to measure biomass and vegetation condition started to come on stream in recent decades (Wardlow et al., 2012a). Vegetation condition is related to the spectral signature of vegetation in different parts of the electromagnetic spectrum. Measures of the reflectance of incident light at various wavelengths have been related to plant growth, health and vegetative cover (Tucker and Sellers, 1986; Anyamba and Tucker, 2012; AghaKouchak et al., 2015).

Earlier in this chapter (see section 1.2) a drought was defined as a slow-onset natural hazard related with the lack of precipitation from a climatological perspective. Bayarjargal et al. (2006) defined a drought in the context of remote sensing as a period of abnormally dry weather, which results in a change in vegetation cover or vegetation physiology. Hence, remote sensing and climatological point-based data are two ways that complement each other in the pursuit of a deeper understanding of the impact of droughts on the vegetation ecosystem and what this might mean for a region's natural and socio-economic environment.

There has been much research undertaken to assess and monitor droughts in a geographical perspective and using remote sensing-based data. For instance, the first programme to monitor droughts using satellite imagery was the United States Drought Monitor (USDM) which uses remote sensing data such as Vegetation Index, Vegetation Health Index, Vegetation Drought Response and the Multisensory Hybrid Rainfall, the latter uses radar with rain data acquired from the National Oceanic and Atmospheric Administration (NOAA) and the National Weather Service (NWS). After this programme some other programmes to monitor droughts were been developed such as the North America Drought Monitor (NADM), and the European Drought Observatory, all of them include remote spaceborne-based data in their strategies (Hayes et al., 2012).

Monitoring droughts using remotely sensed data is becoming more popular and the reason for this is that satellite images can capture the physiological effects that droughts produce in vegetation (i.e. vegetation stress and water deficiency) (Rossi and Niemeyer, 2012) (Bayarjargal et al., 2006). As mentioned before (see section 1.2), drought is a complex phenomenon associated with the variability in the global water cycle, and it is tightly associated with climatic circulation patterns which have important implications for the ecosystems (AghaKouchak et al., 2015). Drought analysis origins using remote sensing were based on the analysis of meteorological satellite imagery and information derived by vegetation indices which reflect the state of vegetation in terms of health and photosynthetic activity. In other words and stated by AghaKouchak et al. (2015)

lack of moisture affects the photosynthetic capacity of plants, hence this produces changes in the plants solar radiation absorption, thus creating alterations in the photosynthetically activity of plants. The principal wavelengths used to monitor these changes have been the satellite visible, specifically the red (R) area and the infrared (IR). Therefore, analysing vegetation through satellite imagery is based on the spectral signature of vegetation and some indicators have been created to understand this spectral behaviour.

1.6.2 Vegetation indices

With the premise that climate is one of the most important drivers of vegetation conditions, vegetation indices (VI) obtained from remote sensed data, have been used as an indirect measure of different climatic and environmental changes at different spatial scales and they are, as stated by Steven et al. (2016), one of the best successes of terrestrial remote sensing. VI are related to physiological and structural features of vegetation and have been used as a proxy to estimate vegetation biomass and vegetation vitality (Harris et al., 2014), also as an indirect variable to measure green biomass, leaf area index and vegetation productivity (Steven et al., 2016). Thus, VI also has been related to climatic variables such as temperature, evapotranspiration and rainfall (Nicholson et al., 1990; Tucker et al., 1991; Herrmann et al., 2005; Hickler et al., 2005; Los et al., 2006; Heumann et al., 2007; Fensholt et al., 2013).

Since it has been broadly studied how vegetation behaves in different parts of the electromagnetic spectrum, then the use of information in those parts of the spectrum is useful for extracting vegetation metrics. In general, vegetation indices are spectral transformations of two or more wavelengths/bands and its principal aim is to enhance information about vegetation activity, production, structure and phenology. These transformation allow us to enhance information from the relevant bands, thus avoiding illumination problems (i.e. pixel brightness variations) and topographic effects. Since different bands are highly correlated and the information they provide is similar, VI provide a great opportunity for data reduction and data redundancy. Finally, band transformation helps for better and easier data management, visualisation, and

interpretation. In this research the importance of vegetation changes caused by droughts is the main concern, therefore, a review of the research that has used VI for studying droughts is presented in the following paragraphs.

1.6.2.1 Spectral characteristics of vegetation

To analyse changes in vegetation through remote sensing it is necessary to understand the interaction between vegetation and light, this is, the reflectance properties of vegetation. The vegetation interacts in a specific way from other land covers, such as soils and water bodies (Figure 1-2). This, goes from a minimum value in the red (R) region of the spectrum that relates to the chlorophyll absorption to a maximum value of reflectance in the near infrared (NIR) caused by the cellular structure of the plants; then, most of the information related to vegetation is concentrated in the R and NIR areas in the spectrum (Baret and Guyot, 1991; Hayes et al., 2012).

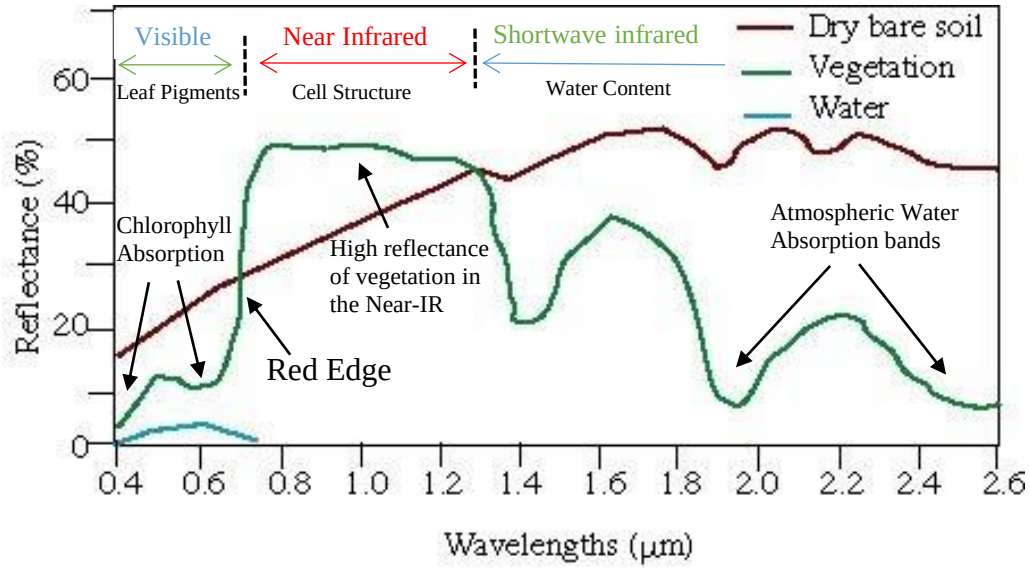


Figure 1-2. Spectral signatures of dry bare soil, vegetation and water in different wavelengths of the electromagnetic spectrum. Modified from: http://landsat.usgs.gov/remote_sensing_applications.php

These properties have been used to combine reflectance and then extract information about vegetation health; as a result of this, vegetation indices (VI) have been developed. Most vegetation indices use the reflectance situated in the (R) and (NIR) region of the spectrum (Hayes et al., 2012); however, a few

indices use the shortwave infrared 1 (SWIR-1), the shortwave infrared 2 (SWIR-2) and the green channels to reflect water content in plants.

1.6.2.2 Vegetation indices overview

Jackson et al. (1983) pointed out that "an ideal vegetation index would be highly sensitive to vegetation, insensitive to soil background changes, and only slightly influenced by atmospheric path radiance." Although there is no ideal VI, they give us an accurate measurement of vegetation productivity and, as they are products from remotely sensed data, it is possible to obtain them and follow vegetation dynamics through time, for example, to follow up seasonal, inter-annual, and long-term variations of vegetation structure (leaf area), phenology, and biophysical parameters (biomass, content of water, and productivity). VIs can be studied in global, regional, and local scales as well.

Many VIs have been developed since the 1970s, every one of them tries to enhance some specific vegetation properties and they have advantages and disadvantages between them. In Table 1-1 some of the first indices developed are shown and explained superficially to have a broad understanding how a VI works; and those that are related with droughts are explained with more detailed.

Table 1-1. Principal vegetation indices, mathematical definitions, and authors.

Vegetation Index	Definition	Author and date
Ratio Vegetation Index	$RVI = \frac{NIR}{R}$	Pearson and Miller (1972)
Normalised Difference Vegetation Index	$NDVI = \frac{(NIR - R)}{(NIR + R)}$	Rouse Jr et al. (1974)
Perpendicular Vegetation Index	$PVI = \sqrt{(\rho Rso_{il} - \rho Rveg)^2 + (\rho IR_{soil} - \rho IR_{veg})^2}$	Richardson and Weigand (1977)
Infrared Index	$II = \frac{(TM4 - TM5)}{(TM4 + TM5)}$	Hardisky et al. (1983)
Moisture Stress Index	$MSI = \frac{TM5}{TM4}$	Rock et al. (1985)
Soil Adjusted Vegetation Index	$SAVI = \frac{NIR - R}{NIR + R + L}(1 + L)$	Huete (1988)
Normalised Difference Vegetation Index	$GEMI = \eta(1 - 0.25\eta)\frac{(\rho_R - 0.125)}{(1 - \rho_R)}$	Pinty and Verstraete (1992)

Standardised Vegetation Index	$SVI = [Z < zijk)$	Kogan and Sullivan (1993)
Vegetation Condition Index	$VCI_{ijk} = \frac{(NDVI_{ijk} - NDVI_{i\ min})}{(NDVI_{i\ max} - NDVI_{i\ min})}$	Kogan (1995)
Optimised SAVI	$OSAVI = \frac{(NIR - R)}{(NIR + R + 0.16)}$	Rondeaux et al. (1996)
Normalised Difference Water Index	$NDWI = \frac{(\rho(0.86\mu m) - \rho(1.24\mu m))}{(\rho(0.86\mu m) + \rho(1.24\mu m))}$	Gao (1996)
Normalised Difference Moisture Index	$NDMI = \frac{(Green - NIR)}{(Green + NIR)}$	McFeeters (1996)
Vegetation Health Index	$VH_{ijk} = 0.5 * VCI_{ijk} + 0.5TCI_{ijk}$	Kogan (1997)
Temperature Condition Index	$TCI_{ijk} = \frac{(BT_{i\ max} - BT_{ijk})}{(BT_{i\ max} - BT_{i\ min})}$	Kogan (2000)
Anomaly of Normalised Difference Vegetation Index	$NDVIA_{ijk} = \overline{NDVI}_{ij} - NDVI_{ijk}$	Anyamba et al. (2001)
Ratio between Land Surface Temperature	$(LST/NDVI)$	McVicar and Bierwirth (2001)
Enhanced Vegetation Index	$EVI = G\frac{\rho_{NIR} _ \rho_R}{\rho_{NIR} - C_1 * \rho_R - C_2 * \rho_{BLUE} + L}$	Huete et al. (2002)
Standardised Vegetation Index	$SVI_{ijk} = \frac{(NDVIij_k - \overline{NDVI}_{ij})}{\sigma NDVIij}$	Peters et al. (2002)
MERIS Terrestrial Chlorophyll Index	$MTCI = \frac{(RBand10 - Rband9)}{(RBand9 - RBand8)}$	Dash and Curran (2004)

Pearson and Miller (1972) developed the first index named the Ratio Vegetation Index (RVI) which is a simple ratio and it is easy to apply; the values of this index go from 0 to 30 where values of 1 are normally bare soils and values close to 30 where more active vegetation is present; however, normally, the values for green vegetation go from 2 to 8. Some studies were carried out analysing phenology in crops using this index. Nevertheless, it is reported in the literature that this index can be saturated in dense vegetation when large amounts of vegetation are presented and it is more influenced by environmental factors (Wu et al., 2008). Afterwards, Rouse Jr et al. (1974) developed the Normalized Difference Vegetation Index (NDVI), this is the index most frequently found in the literature and it is a product of some remotely sensed instruments (e.g. NOAA AHVRR), which have bands in the wave lengths of light ranging from

0.55–0.70 and 0.73–1.0 micrometers (μm). NDVI uses the reflectance in the R and NIR areas.

According to Anyamba and Tucker (2012), NDVI has some advantages comparing it to the simple ratio, since the normalization of this index allows minimization of atmospheric problems, aerosol and water effects, reduces sun angle, shadow and topographic effects and it has a strong correlation with several biophysical parameters of vegetation. Furthermore, they point out that NDVI could follow-up stressed vegetation, and contrast between healthy and unhealthy vegetation could be estimated by it. Nevertheless, according to the same authors, it has an asymptotic pattern in dense vegetated areas; thus in wet ecosystems NDVI is not accurate, since it does not reflect the real changes in these types of ecosystems. Additionally, as other studies reported (Huete, 1988), they found that NDVI is still affected by soil background effect.

Richardson and Weigand (1977) proposed the Perpendicular Vegetation Index (PVI) distinguishing vegetation from soil background information to improve NDVI and RVI soil background effects. With this index the calculation of the coordinates of the intersection of the vegetation and soil background is possible and with this you have information of the background of each pixel. Later on, Huete (1988) developed the Soil-adjusted Vegetation Index (SAVI) in order to minimise soil brightness influences, since he found there were a direct correlation between NDVI and RVI values with darker soil substrates; and direct correlation with PVI values and brighter soils. After the development of this index, other indices were developed to improve the effects of soil background, for example, Transformed SAVI (TSAVI) (Baret et al., 1989), and Optimized SAVI (OSAVI) (Rondeaux et al., 1996).

The Enhanced Vegetation Index (EVI) was developed to improve the NDVI in terms of saturation in areas with great amounts of vegetation and to correct atmospheric influence and those made by soil background (Huete et al., 2002). Subsequently, Peters et al. (2002) developed the Standardized Vegetation Index (SVI) which was derived from NDVI and describes the probability of variation from normal NDVI over multiple years of data, according to Peters et al. (2002),

using this index, it is possible to compare periods over time; it was created to monitor droughts. According to Anyamba and Tucker (2012) this index is useful to monitor vegetation condition since it is able to capture rapidly changing patterns of droughts over large areas.

As stated above, each index has its advantages and disadvantages. However, all indices have some drawbacks in common. According to Baret and Guyot (1991) these problems are related to atmospheric effects, but principally from soil background effects, soil reflectance, leaf optical properties, leaf inclination, leaf area index. Literature has also shown that VIs reach a saturation level when vegetation cover increases (Baret and Guyot, 1991; Dash and Curran, 2004), this is a problem if vegetation change studies are performed in a densely vegetated area (e.g. tropical rain forest). However, the rapid development of new instruments allows the collection of global daily measurements about land cover and different natural phenomena such as those related to hydrological cycles (Anyamba and Tucker, 2012; Hayes et al., 2012), which is relevant for drought research. With these technological developments and in order to improve vegetation indices and their accuracy, new indices have been developed continuously. The development of new indices and new instruments will improve in terms of resolution in the three domains (i.e. spatial, spectral and temporal) and they will help to analyse different aspects of the hydrological cycle which influences in drought conditions (Wardlow et al., 2012a).

More recently and with technological advances, and rapid evolution and launching of new instruments, new indices have been developed using high spectral resolution data (narrow bands) and looking specifically at chlorophyll and plant vigour; this is the case of the MERIS Terrestrial Chlorophyll Index MTCI (Dash and Curran, 2004), which is a product of the Medium Resolution Imaging Spectrometer (MERIS). It is a ratio of the difference in reflectance between band 10 and band 9 and the difference in reflectance between band 9 and band 8 of the MERIS band setting. According to Dash and Curran (2004), the MTCI has some important advantages: it is possible to calculate the MTCI automatically, the red edge position in the spectrum could be calculated from the MTCI, and MTCI is more sensitive at higher contents of chlorophyll. The last is

important for analysing ecosystems in highly vegetated areas. Dash and Curran (2004) compared the performance of MTCI with Red Edge Position (REP). Afterwards they analysed NDVI range from low to high values and compare them with MTCI and REP values, and they found that MTCI is more sensitive at higher concentrations of chlorophyll than REP, since the latter presents an asymptotic form at greater contents of chlorophyll. They also found that MTCI in comparison to NDVI shows low correlation in areas with a low content of chlorophyll and, in vegetated areas with less correlation, MTCI captured more variation. However, they obtained a linear relationship between REP and MTCI, which indicates that REP could be estimated from MTCI as other authors (Gallo et al., 1985; Peng et al., 2012) have found NDVI does.

1.6.2.3 Vegetation indices vs climatological variables

Monitoring vegetation through vegetation indices has been demonstrated as a great tool, since it is possible to extract and highlight information about vegetation conditions. In addition, the historical available remotely sensed data (from 1970s) allow us to analyse time series. Time series are defined as a sequence of data of the same variable (i.e. images) collected in the past with a specific collection frequency (i.e. weekly, monthly, yearly, etc.). Remote sensing time series allow us to characterise what has happened in the terrain. It is a great approach to analyse historical and actual trends, specific events such as disturbances at different times, for identifying natural and land cover changes, and understanding phenology and ecosystem cycles. Also, analysing historical data is powerful for modelling. The information extracted from time series can be related with relevant external variables, such as climatological data. Thus, satellite imagery time series gives the opportunity to increase our understanding of vegetation dynamics, climatological trends and climatological impacts and interaction with vegetation (Boyd et al., 2006; Kuenzer et al., 2015).

Some studies in this regard show us the pertinence to relate some vegetation indices to other climatic variables (i.e. precipitation, temperature). One of the pioneering works that used NDVI in an interannual perspective was conducted by Tucker et al. (1991). They took the NDVI value of one season in a specific

year as the baseline and related it to rainfall data; the differences between this baseline and the following period showed a relation between precipitation anomalies and the NDVI values. Within the works using climatological variables and other variables related to vegetation changes to monitor droughts, there is Kogan (1997) who included rainfall and temperature data, drought indicators-specifically the Palmer Drought Index-,moisture crop data, vegetation density, biomass, and yield into drought analysis, finding a strong correlation between vegetation indices and crops. This study showed one of the most important advantages to analysing vegetation dynamics, since the use of these indices allows us to follow up vegetation at different temporal and spatial scales.

The most predominant area where these studies have been taken place is the African continent, in the Sahelian region (Tucker et al., 1983; Tucker et al., 1985; Hielkema et al., 1986; Justice and Hiernaux, 1986; Townshend and Justice, 1986; Nicholson et al., 1990; Anyamba and Eastman, 1996; Proud and Rasmussen, 2011), others in South Africa (Gaughan et al., 2012), some in United States (Di et al., 1994; Yang et al., 1997) in India (Srivastava et al., 1997) and at a global scale (Schultz and Halpert, 1993). There is a lack of these studies in Mexico, where precipitation and vegetation cycles are different all over the country.

More examples using climatological data and two different indices are the works of Piao et al. (2004) and Boyd et al. (2006). In the first one, they developed a study to understand the relationship between the NDVI and climatological data to follow vegetation activity across different types of vegetation in China using the NDVI, and they found NDVI is a good indicator for the growing season since it increases during this period. Also, they found the same behaviour with temperature, suggesting a relationship between temperature and NDVI values; however, for rain data the relationship was stronger. An important difference between the regional and local scale suggests that NDVI could be related to temperature or rainfall depending on vegetation type and location; some ecosystems are more influenced by temperature fluctuations (i.e. medium to high latitudes) and others by precipitation (i.e. lower latitudes) and some ecosystem are more vulnerable and resilient than others in response to climatological

variables (Harris et al., 2014). Boyd et al. (2006), in turn, studied the Sabah, Borneo rainforest response of droughts provoked by ENSO through NOAA AVHRR indicators and rainfall statistics to create an index capable to monitor drought.

Coupling these types of data is not trivial. Vegetation productivity is related to many factors and vegetation stress could be caused by other factors than just droughts or extreme events. This relationship is far more complex and it is affected and varies according to vegetation type, regional climatology, and soil composition. The most popular approach for coupling VIs and climatological data is by correlation analysis (Schultz and Halpert, 1993; Wang et al., 2001; Ji and Peters, 2003; Lotsch et al., 2003; Evans and Geerken, 2004; Neeti et al., 2012). A less popular method is regression analysis (Los et al., 2006) (Schmidt et al., 2014; Otto et al., 2016). All these studies have shown that there is a statistical association between vegetation productivity and climatological variables. Lotsch et al. (2003) and Schultz and Halpert (1993) coupled precipitation data and drought indices with vegetation indices (NDVI in both cases) at a global scale and they found that seasonal cycles of vegetation are driven by temperature in mid and high latitudes; whereas precipitation is primarily important in low latitudes. Moreover, Schultz and Halpert (1993) found that wetter regions do not show any correlation and they pointed out that could be because precipitation surpasses a minimum threshold, beyond which vegetation is unresponsive. On the other hand, (Lotsch et al., 2003) found that SPI and NDVI have great association and it is important to notice that in their results, the northern part of the Yucatan Peninsula shows there are significant associations between SPI and NDVI.

One piece of research using MTCI and comparing it with other indices and with climatological variables is the study done by Boyd et al. (2011), in which they compare EVI, NDVI and MGVI with MTCI in order to demonstrate MTCI's capability to monitor vegetation phenology. Moreover, they included temperature data to relate it to the growing season. They found that MTCI has success analysing vegetation phenology and they found a relationship between MTCI values and temperature. Regarding the comparison with the other indices,

they found MTCI more accurately represents senescence than the others, and it also could reflect delays in vegetation phenology. This illustrated the importance of considering alternative remotely sensed datasets other than that of the NDVI. That said, the available NDVI datasets cover a much longer temporal range by virtue of the fact that the early satellite sensors tended to have a red and near infrared waveband.

Other indices were developed specifically to monitor vegetation changes produced by droughts, then, these indices use both the R and NIR and the thermal data derived from satellite imagery. Within the most cited indices in the literature are the Anomaly of Normalized Difference Vegetation Index (NDVIA), the Temperature Condition Index (TCI), the Vegetation Health Index (VHI), the Ratio between Land Surface Temperature (LST) and the NDVI (LST/NDVI), the Normalized Difference Moisture Index (NDMI), the Normalized Difference Water Index (NDWI) (Bayarjargal et al., 2006), and Vegetation Anomaly Index (VAI) (Amri et al., 2011).

Bayarjargal et al. (2006) made an assessment for most of the indices used for droughts. They compared four remotely sensed indices and two drought indicators using a change detection technique (Change Vector Analysis) to analyse which of these indices gave better results in terms of drought monitoring, then they used meteorological *in situ* data to compare with the indices and they used it to establish thresholds in order to detect anomalies in precipitation patterns. Their results showed that in dry seasons, all the indices detected the dry condition and they have a significant correlation among them, however there was no agreement between them in the spatial domain. As an interesting result, they found low agreement between the vegetation remotely sensed VIs and the drought indicators and they found better index performance (using the R and NIR) than the index which used the thermal bands. It is important to stress that these results show the necessity to continue with the assessment of drought indices or try another alternative indices. Other work conducted by Lin et al. (2008) compared the performance of drought vegetation indices. They used VCI, TCI and VHI derived using NDVI from MODIS, and they used MCI and NDMI to characterise the relationship between vegetative drought and hydrological

drought indices. They found that the indices utilised generated different spatial patterns, and they found that MCI was a good indicator to monitor hydrological drought, however, in contrast with Bayarjargal et al. (2006) they proposed that indices should use the thermal bands to monitor the water content of vegetation.

Monitoring droughts through remote sensing data now is developing into drought monitoring with a future perspective, doing models and projections to know where and when droughts can occur (Rossi and Niemeyer, 2012). Analysing effects of droughts on vegetation is a difficult task because vegetation condition is dependent not only on climatic patterns but also on complex relationships involving soil characteristics, land use and land cover, topography, and other ecological characteristics (Tadesse et al., 2010). Two similar drought monitoring models have been developed trying to get together all the variables related to droughts; these are the works from Tadesse et al. (2010) and Wardlow et al. (2012b). Both developed two different models (VegOUT and VegDRY respectively) to map droughts and to try to predict where and how intense droughts would be. The principal idea of these models is to incorporate climatological, physical and remotely sensed data to a system and then get it into a training phase, therefore setting up rules to differentiate a real drought from other normal changes (e.g. phenology). The results showed that VegDRY has a high predictive accuracy in the growing seasons and seems to be more accurate than other monitoring programs such as U.S. Drought Monitor (USDM). On the other hand, VegOUT shows success in short-term results; however, the predictions in long term basis are not accurate.

Vegetation is always affected by different natural processes, and all these aforementioned studies demonstrate that the use of remote sensing, in particular the use of vegetation indices is an attractive approach to monitoring changes in vegetation as a result of droughts as they are a good indicator of vegetation condition. VI could monitor changes in vegetation productivity provoked by droughts; that is why the principal application of VI has been analysing vegetation dynamics through time in different spatial and temporal resolutions.

The selected index to accomplish the aim of the thesis is NDVI since there is available data which goes back to the 1980's, thus it is consistent and long enough to analyse climatological events and changes that could have occurred at the Yucatan Peninsula since that time. Therefore, in the following section, a deeper review of the NDVI is given; some important studies are described focused just on NDVI and its relationship with climatological events

1.7 The Normalized Difference Vegetation Index (NDVI)

The Normalized Difference Vegetation Index (NDVI) from AVHRR is a vegetation index widely used to analyse and measure vegetation productivity, greenness, seasonality and biomass (Tucker et al., 1991; Herrmann et al., 2005; Heumann et al., 2007; Neeti et al., 2012; Eastman et al., 2013; Fensholt et al., 2013; Forkel et al., 2013), to monitor extreme events such as droughts (Anyamba et al., 2001; Peters et al., 2002; Bayarjargal et al., 2006; Anyamba and Tucker, 2012; Verbesselt et al., 2012), and to analyse vegetation persistence (Harris et al., 2014). The use of NDVI is extensive because it is a satellite product (pre-processed data) and the data have been freely available since 1982 to the present which allows the analysis of changes in vegetation from a historic perspective. Moreover, NDVI minimises atmospheric problems, aerosol and water effects, reduces sun angle, shadow and topographic effects and has a strong correlation with several biophysical parameters of vegetation (Anyamba and Tucker, 2012).

These studies confirm that NDVI is a good estimator of greenness of vegetation and can be used to study the vegetation condition, including those events that make vegetation be in a stressed condition (e.g. droughts). One of the most recent studies using NDVI monitoring of droughts was performed by Anyamba and Tucker (2012) and they confirm that NDVI responds well when it is related to other climatological data; it is a suitable index to monitor vegetation since it is one of the oldest indices and it can be constructed with images with available data since more than forty years ago.

As mentioned in the previous section, the use of this index relies on distinctive vegetation behaviour across the spectrum, particularly in the contrast between

the red (R) band, which is largely absorbed by the leaves, and the near infrared (NIR) band, which is mostly reflected. Then, it is defined as NDVI = (NIR-R) / (NIR+R) (Rouse Jr et al., 1974).

NDVI has been used as an indicator of climate variables and many applications are important for climate change studies (Holben, 1986; Eastman et al., 2013). Moreover, NDVI has been related to different variables and phenomena such as precipitation, temperature, and El Niño events. According to Jeganathan et al. (2014) in tropical regions the main driver of vegetation cycles is rainfall. Hence, the productivity of vegetation could be an indirect indicator of climatological events related to rainfall.

Herrmann et al. (2005) analysed the relationship and spatial trends between rainfall and greenness in vegetation in the Sahara desert. They used the NDVI to analyse changes in vegetation, and a combination of Tropical Rainfall Measuring Mission (TRMM) and data from the Global Precipitation Climatology Project (GPCP) in order to analyse trends in precipitation regimes. They performed a correlation and regression to understand the correlation between NDVI and precipitation data and to analyse the general trends in NDVI and precipitation changes. They found a strong correlation between NDVI and the three month-cumulative rainfall. According to them and some other research (Nicholson et al., 1990) this strong correlation reflects that vegetation greenness depends more on soil moisture than on immediate precipitation. However, this lag between rainfall and its response reflected in vegetation could be related to vegetation resistance (Manobava, 2003) and could be used to analyse vegetation response and resistance in different types of vegetation caused by droughts. In this regard, Harris et al. (2014) analysed vegetation resilience and persistence using NDVI data, monthly gridded precipitation data and biome data. They assessed vegetation vulnerability in different biomes and analysed vegetation trends (NDVI trends) and its correlation with climatological drivers such as El Niño–Southern Oscillation (ENSO).

Neeti et al. (2012) studied NDVI trends in the Yucatan Peninsula using seasonal trend analysis and a modified Mann-Kendall test; they analysed the relationship

between NDVI and precipitation changes. They found an overall significant greenness decrease in three of the six location they focused on (Cancun, western Campeche, north-eastern Quintana Roo, see Figure 2-1), while in the other three locations (Calakmul Biosphere Reserve, central Yucatan state) there was an increase in overall greenness; however a weak or negative correlation was found between NDVI and precipitation data concluding that NDVI changes in Yucatan Peninsula are driven by land use change, not precipitation. However, research (Herrmann et al., 2005; Fensholt et al., 2013) focused on other countries has found a strong correlation between these two variables. For instance, Fensholt et al. (2013) analysed NDVI greenness trends and its drivers (i.e. precipitation, temperature and incoming shortwave radiation) in semi-arid regions at a global scale and they found that in areas where precipitation is the main constraint for vegetation growth, there was a high correlation between precipitation patterns and NDVI trends. Contrary to what Neeti et al. (2012) have reported and due to the characteristics of the Yucatan Peninsula and the existing climatological studies in the area, as well as the fact that precipitation is the main driver for vegetation in the area, it could be hypothesised that vegetation productivity and precipitation are correlated with time lags to some degree in areas where the precipitation/vegetation is strongly seasonal.

The length and amount of remotely sensed data, in this case the NDVI, allows us to study the changes and trends over time with methods used by econometric and meteorological science (Hostert et al., 2015). Processing long time series data is challenging and the understanding and development of methodologies in this regard is a complete research area (see Kuenzer et al. (2015)).

1.7.1 NDVI time series analysis

There are a variety of methodologies used to understand and analyse the NDVI data time series; these methods range from filtering, smoothing to global, inter-annual, intra-annual trend analysis, etc. According to the literature (Eastman et al., 2013; Fensholt et al., 2013; Tüshaus, 2013) the most cited method to remove noise from NDVI time series is the Maximum Value Composite (MVC), this process helps to remove remaining noise from atmospheric and cloud

contamination (Anyamba and Eastman, 1996; Forkel et al., 2013). However, MVC is still data that could present some noise that could lead to incorrect results. Thus, time-series should be smoothed to remove noise, outliers and to obtain a function that fits the original data to analyse general patterns in the dataset (Atkinson et al., 2012). Different methods have been developed and used for data smoothing such as Fourier decomposition, median smoothing, wavelet decomposition, logistic function, moving average, asymmetric Gaussian function, double logistic, Whitaker filter, and Savitzky-Golay filter among others. According to Atkinson et al. (2012) all these methods have advantages and disadvantages and deciding which method to use depends on the research objectives, the nature of the dataset and the information that needs to be analysed. To test this, they performed a comparison between four fitting models (Fourier, asymmetric Gaussian, double logistic and Whitaker smoother) using randomly noisy data added to an observed vegetation profile and found that all methods performed well, with few differences between them. Different authors report different results in the performance of different smoothing methods (Hird and McDermid, 2009; Dash et al., 2010; Wei et al., 2012; Duncan et al., 2013; Eastman et al., 2013; Forkel et al., 2013), and as Atkinson et al. (2012) pointed out, it is always necessary to analyse the fitted data methods, together with the original data, in order to know which fitted method is the most suitable for the data, also, it is necessary to examine carefully the parameters chosen in the fitted function.

NDVI time–series analysis allow us to summarise and extract information from large datasets and make possible the analysis of phenological changes (annual cycles) and trends in vegetation productivity. However, NDVI values are affected by clouds or atmospheric conditions. Therefore many efforts have been made in order to overcome this problem. Thus, software and different methods have been developed to smooth out the noise present in NDVI time-series, in this way we can make sure that the data analysed is not mistaking trends in vegetation productivity (Bachmann et al., 2015).

1.7.1.1 TIMESAT

Different methodologies and software (e.g. TIMESAT, HANTS, PhenoSat, SPIRITS) have been developed to smooth and pre-process the time series of remotely sensed data (Atkinson et al., 2012). One of the most commonly used is TIMESAT, which was created for this purpose and also for the extraction of phenological information such as start and end of the growing season, the length of the season, amplitude, etc. (Eklundh and Jönsson, 2015). The seasonality metric that this software calculates is one of the most important advantages this software possesses. In addition it has three different smoothing methods (Gaussian, double logistic and Savitzky-Golay) and several parameters to adjust; thus, giving the opportunity to process data from different types of environment. Another advantage of this software compared with others is that it adjusts the data to the upper NDVI envelope, which helps in maintaining the NDVI pattern of change (Chen et al., 2004; Eklundh and Jönsson, 2015). TIMESAT has been created for analysing time-series at middle latitudes, however, its versatility allow us to use in different environments.

1.8 Motivation and contribution to knowledge

There is an increased interest to understand ecosystem dynamics for different perspectives in the world in general as a possible solution to promote a sustainable society, to augment the understanding of ecosystems, thus creating conservation policies. Despite all the effort that has been made to increase knowledge of vegetation dynamics and the relationship with climatological events such as droughts, there are some areas of the Earth which have been less explored (i.e. tropical environments). This is the case of the Yucatan Peninsula. The Yucatan Peninsula is an important area which harbours great biodiversity and different types of vegetation, thus it is an area that provides important ecosystem services that are important for the population living in it. However, these tropical forests have been target of many human activities (i.e. expansion of agriculture, urbanization, tourism, land use and cover change) and it is strongly affected by climatological events (i.e. droughts and hurricanes), therefore this region is characterised and determined by this human-environment

interaction (Turner et al., 2001; Turner, 2010). In addition, this area is vulnerable to the impacts of possible global climate changes and the threats to biodiversity which it presents.

The Yucatan Peninsula has been the focus for many biological and ecological studies. However, there are some difficulties studying a region where there is a lack of available and systematic *in situ* data. Despite the efforts for many years in gathering data in Mexico, there are still many gaps in it and inconsistencies for study of the Peninsula as a whole rather than of small areas. For instance, climatological studies in the Yucatan Peninsula had taken place in regions where more meteorological stations are located or many studies have been done to compare different locations across the Yucatan Peninsula. It is in this situation that remote sensing becomes a great tool for analysing areas where there is limited available data.

This thesis presents the most up to date analysis of the precipitation data available for the Yucatan Peninsula in the last decade. Most of the studies conducted before had focused on certain locations (Márdero et al., 2012; Neeti et al., 2012). In this sense, the work carried out in this thesis adds new knowledge about the recent climatology at the Yucatan Peninsula developing a precipitation analysis and creating the most reliable maps of rainfall for the area that could be useful as a baseline for other studies. No less important, there was an important effort to gather and clean the precipitation data from 1980 until 2011 which could be used for other research.

In order to overcome the lack of data, remote sensing has been used to analyse different aspects of ecosystems in the Yucatan Peninsula. However, all these studies have been focused on human impacts across different type of vegetation and less attention has been paid to understanding the impact of natural disturbances in the area through remote sensing. Therefore, there is a need to understand better the response of vegetation to climatic anomalies. Even though, the Yucatan Peninsula has been catalogued as resistant to natural disturbances (Sánchez-Sánchez et al., 2015), no studies for quantifying this have been done.

Hence, in this thesis an analysis of this is conducted and it is the first research in Mexico of this type.

Understanding the relationship between vegetation productivity and precipitation has been studied more extensively in different areas on the Earth as in the Sahel in Africa, some in the Amazon, a few in United States and others in China. However, in Mexico, and in particular in the Yucatan Peninsula there is no comprehensive study for the whole area explaining the relationship between vegetation productivity and rainfall. One of the major challenges in this thesis is to put together both type of datasets (precipitation and satellite imagery) and analyse the patterns of precipitation, the dynamics of vegetation and how droughts impacts on them.

Droughts are important climatic events that affect Mexico in different scales and there is a lack in understanding the impacts they have in ecosystems and their recovery after a drought occurs. This type of research is crucial in order to increase our understanding of the area and in terms of conservation could help to improve warnings of drought and conservation programs.

1.9 **Aims and objectives**

Analysing vegetation conditions over large geographical areas is essential to understand the dynamics of vegetated ecosystems and their interactions with different type of natural hazards. However, analysing vegetation conditions and the responses and impacts of droughts is challenging since vegetation dynamics are related to different variables such as climate patterns, land use and land cover, topography, ecology and species interaction, among others. Consequently, one of the tasks of this research is trying to understand and analyse droughts through both climatological and remotely sensed data. Due to the temporal record offered by the NOAA AVHRR series of sensors, this thesis will primarily focus on using the vegetation index of the AVHRR NDVI, however in chapter 5 other index will be explored too.

The analysis of droughts through NDVI is associated with the assumption that vegetation is related to strong environmental gradients of moisture availability and lengths of dry season (Krishnaswamy et al., 2009), then NDVI values of various vegetation types across a precipitation gradient should indicate different levels of seasonal variation in NDVI. Therefore, research questions arise from this. Will VI time series analysis be able to detect long periods of lack of precipitation and moisture across a precipitation gradient? Will the response be equal in different vegetation types? How do you define a drought when combining meteorological and remotely sensed data? Is there any correlation between vegetation productivity and quantity of precipitation? How much variance in vegetation productivity could be explained by precipitation and droughts? Answering these questions will be possible with the availability of different sources of data such as climate records and remote sensing data. The case study will be the Yucatan Peninsula, where an interesting vegetation and climatological northwest-east gradient is represented and its geographical location between the Atlantic and Gulf of Mexico makes it vulnerable to extreme events (see chapter 2).

In this research, an analysis of vegetation productivity change and vegetation recovery after droughts in the Yucatan Peninsula, Mexico, will be conducted using remote sensing and climatological data.

Hence, the principal aim and objectives for this project are:

Aim

- Develop an understanding of how the vegetation of the Yucatan Peninsula responds to droughts.

Objectives

- Analyse available climatological data (i.e., precipitation) and identify droughts that have occurred in the Yucatan Peninsula during the period 1982 to 2011.

- Explore and apply appropriate remote sensing data to detect vegetation changes caused by droughts.

- Analyse and characterise drought impact on different vegetation types and analyse their resistance and resilience.

- Understand how vegetation productivity is linked to climatological processes using vegetation indices and climatological data.

- Identify spatial variability in the relationship between vegetation productivity and precipitation.

1.10 Thesis outline

The structure of this thesis is formed into six chapters and it is schematically represented in Figure 1-3. After the introduction and the extensive review of the literature of what has been done in regard to how remote sensing observations have been used to monitor drought-related variables from a climatological point of view and how to assess and quantify droughts impact on ecosystems given in chapter 1, chapter 2 illustrates a complete overview of the Yucatan Peninsula physical setting and vegetation. Chapters 3, 4, and 5 are the main research chapters and each of them comprise the methodology and the obtained results. Finally, chapter 6 summarises the discussion, conclusion and future work.

Chapter 1 reviews the principal concepts to understand droughts, the impacts they have on vegetation, to follow with a review of how droughts have been analysed from the remote sensing perspective.

Chapter 2 provides a detailed description of the physical features of the Yucatan Peninsula, including the geological setting, the climatology and hydrology of the area. In addition, a description of the different types of vegetation is provided. Finally, a brief description of the principal human activities that has taken place in the Peninsula is presented.

Chapter 3 analyses the precipitation patterns in the Yucatan Peninsula through cluster analysis and kriging. These methodologies are described and the analysis of the results are presented. In addition, a drought detection analysis is made for the area on an annual and monthly basis. The methods are also described and the results of drought detection are addressed and analysed.

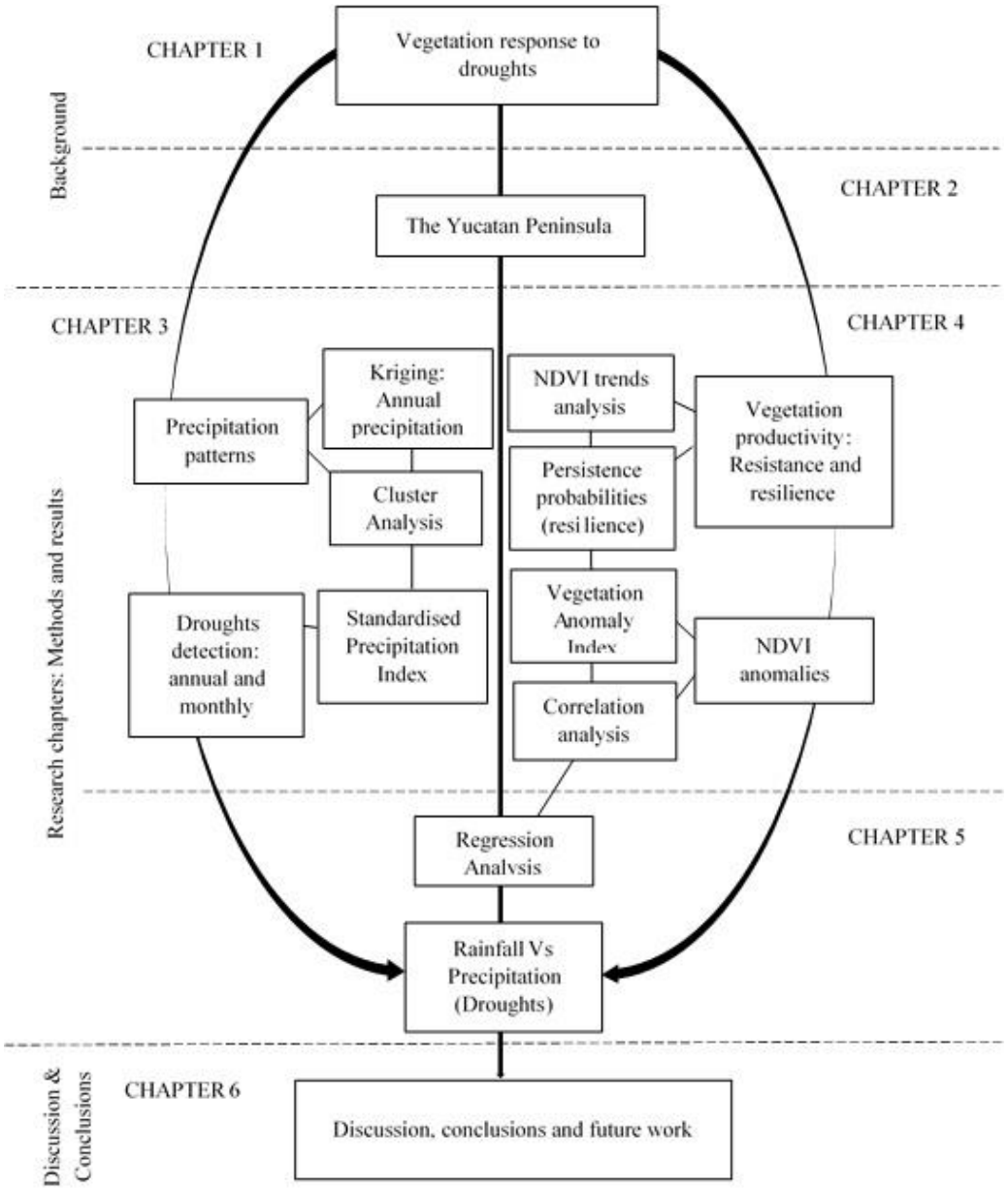


Figure 1-3. Thesis structure

Chapter 4 explores and quantifies vegetation dynamics, resistance and resilience across the Yucatan Peninsula between 1982 and 2011 using NDVI from AVHRR data in order to understand the vulnerability to environmental changes

of the different types of vegetation. This analysis is followed by the exploration of anomalies in vegetation productivity using the same vegetation index. Finally, a correlation analysis is presented in order to understand the relationship between precipitation and vegetation productivity.

Chapter 5 attempts to examine the relationship through regression analysis between vegetation productivity, using NDVI (AVHRR) and MTCI (MERIS), with precipitation data in order to identify and explain how much variance in the NDVI and MTCI is explained by the variance of rainfall and the lack of it (i.e. droughts). An analysis of the spatial variability of this relationship is also presented for the period 1982-2011.

Chapter 6 discusses and concludes the results of this thesis and provides suggestions for future research that could be developed based on the contribution of this work.

CHAPTER 2. **SITE DESCRIPTION: PHYSICAL SETTING, VEGETATION, AND HUMAN ACTIVITIES AT THE YUCATAN PENINSULA, MEXICO**

This chapter aims to provide a description of the Yucatan Peninsula and put in context the importance of studying droughts in this area. A broad overview of the Peninsula is presented, following by an outline of its physical settings: geology, hydrology, and regional climatology. In addition, it includes an overview of the vegetation distribution and the principal human activities in the area.

2.1 **Overview**

The Yucatan Peninsula is located in southeast Mexico (Figure 2-1) surrounded by two seas: the Gulf of Mexico and the Caribbean Sea (Gómez Ramírez, 1998) with 65 million years of history (Vázquez-Domínguez and Arita, 2010). From a geographical perspective this region includes the Mexican states of Campeche, Yucatan and Quintana Roo, the north parts of Belize and Guatemala. For this thesis the Mexican part of the Peninsula is the case study. The reason behind this is because the data collection and policies are different in the three countries, thus, selecting one country will allow us to assure consistency on the data. The Mexican portion of the Yucatan Peninsula covers approximately 145,000 km^2. However, most of the physical features described in this chapter are applicable for the whole Peninsula (i.e. including Belize and Guatemala portions).

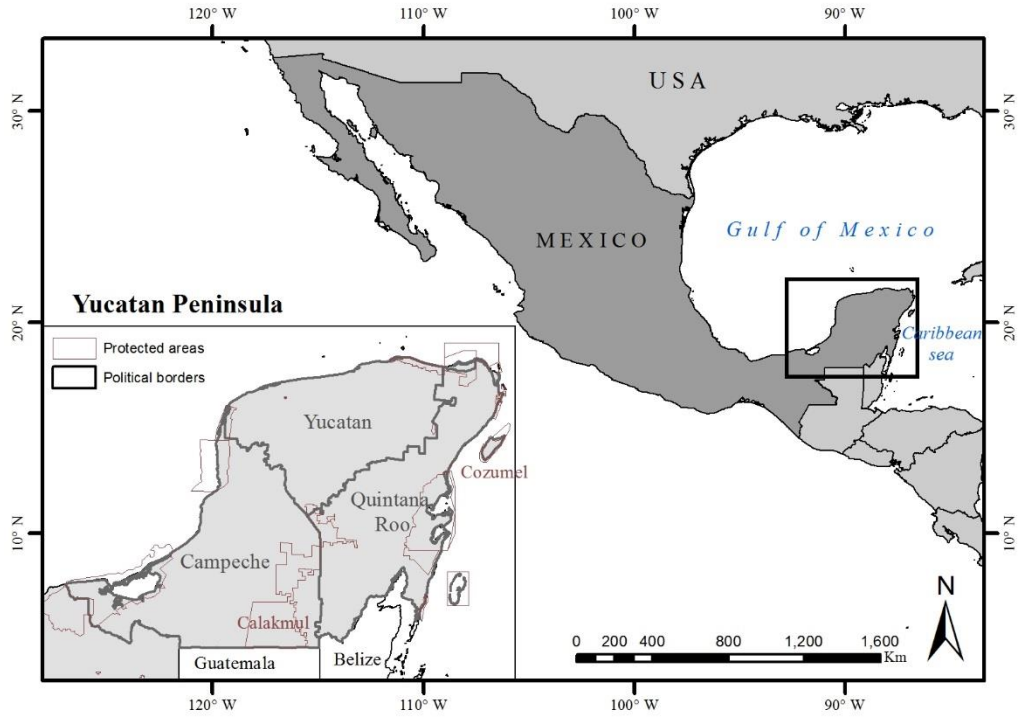


Figure 2-1 Location of the Yucatan Peninsula (21 - 17° N; 91 -87° W) with the political division which includes the states of Yucatan, Campeche and Quintana Roo and the two adjacent countries (Guatemala and Belize). Red borders in inset map show the Natural Protected Areas.

The Yucatan Peninsula is one of the fifteen physiographic provinces present in Mexico; the country was divided in these regions according to their geological origin, their landscapes, types of rock and similar geomorphologies (Ordonez, 1936). The Yucatan Peninsula is an unique and complex area due to the geomorphological, hydrological, and edaphic factors that have helped develop this particular region (Wilson, 1980) and thus also have a significant effect on its biota; it has a variety of flora, fauna, and landscapes associated evidently with its climatology and geographic features. The Peninsula is considered by some authors as a single biogeographic province within Mexico as it is distinctive from the rest of the country; it shares larger number of species with the Caribbean and it has a geological identity, as it is a single calcareous platform. Although the Yucatan Peninsula shows the same wet (summer) and dry (winter) precipitation pattern from the rest of the country, it has its own heterogeneity and its location make it a complex climatic area where different teleconnections and climatic events take place. Thus, the Peninsula has its own temperature and precipitation gradient (Florescano and Swan, 1995; Mendez Perez, 2003; Méndez and Magaña, 2010) and the precipitation anomalies in this area are often different

from the rest of the country. The vegetation in this area follows this moisture gradient (Dirzo and Gil, 1996) and the forests of the Peninsula have been deforested for centuries, with a maximum deforestation rate occurring in the late 1960s (Turner et al., 2001). Because of its great biodiversity and because of being threatened this area has been target of conservation policies and it has one of the largest tropical natural reserves in Mexico with an extension of 7,231 km^2 (Calakmul, see Figure 2-1). The following subsections outline the general features of the Peninsula. First an overview of the geological and physical setting is given, following with the climatic characteristics of the area and the vegetation distribution. Finally, a general description of the principal human activities is presented. Knowing these general features allow us to put into context the importance of the possible droughts impacts in this area.

2.2 **Geology and hydrology**

This area is a ~350,000 km^2 marine limestone platform (including the part under modern sea level) which originated from tectonic movements during the Miocene and Plio-Pleistocene (Wilson, 1980; Whitmore et al., 1996), of which half is submerged under the Gulf of Mexico. It has not been affected by subsequent tectonic uplift or orogenic events making this area predominantly flat (Collins et al., 2015).

The main physiographic features of the Peninsula are the Sierra de Ticul, with an elevation of 275 m, and San Felipe, which is located in the south and has an elevation of 400 m (Barber et al., 2000). The former divides the Peninsula into two main regions the central-south, which has hills up to 275 m, and the north, which is flat (Barber et al., 2000) and generally less than 50 m.a.s.l (see Figure 2-2).

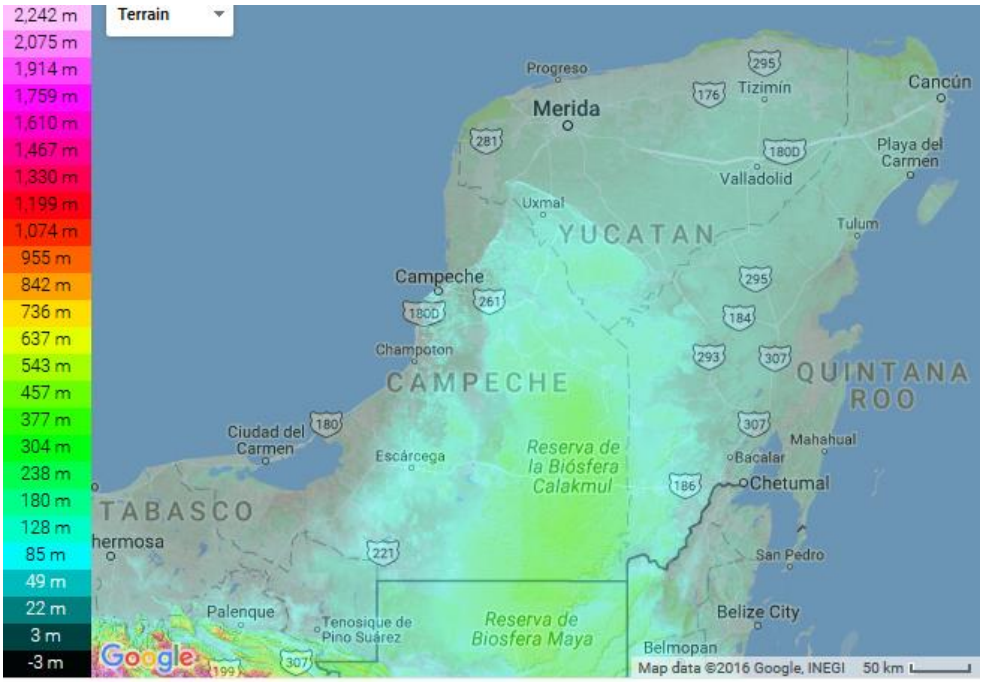


Figure 2-2. Topography of the Yucatan Peninsula. Image taken from: http://en-ca.topographic-map.com/places/Yucatan-Peninsula-8159035/

The Yucatan Peninsula has a complex geology in terms of its evolution and has contributed to the origin of the Gulf of Mexico and the Caribbean. The metamorphic platform is characterised by a sedimentary structure of 3000 meters thick from the Jurassic (Lugo Hubp et al., 1992). In the Cretaceous period the sedimentation changed, thus the centre part of the platform emerged and was exposed. The Peninsula has reduced soil thickness, evolving in a karst aquifer system. The limestone platform in this area has an important role in the Peninsula hydrology, since this platform is highly porous allowing fast penetration of rainfall through it occasioning a lack of superficial hydrology (i.e. rivers or lakes) (Collins et al., 2015). This permeability results also in the development of sinkholes or *cenotes* (from the Mayan word *ts'onot*) which have water circulation below surface (Stringfield and LeGrand, 1976; Wilson, 1980). Is in the north-western part of the Yucatan Peninsula where the presence of *cenotes* characterised this area. *Cenotes*, as aforementioned, are caves or sinkholes distributed as a ring and are related to the Chicxulub crater impact (Marin et al., 2004), which in turn is associated with the extinction of many species at the end of the Cretaceous period (Marin et al., 2004). The central-south part of the

Peninsula is distinguished as the region with the greater elevation and topographic structures and has both karst formations and tall vegetation.

The Yucatan Peninsula aquifer has great importance since it is the primary source of fresh water for human activities and due to the lack of drainage system and the rapid population growth, the aquifer is vulnerable to pollution (Marin et al., 2004). The aquifer is composed of water derived mainly from precipitation from the surface and saline water underneath, the latter comes from the coast through the porous limestone (Collins et al., 2015). The aquifer consists of a 60 m thick fresh water lens from near the city of Merida, in the state of Yucatan, to Quintana Roo, where it is only 15 m thick. Water table depth across the Peninsula is variable, increasing the depth inland, in the cost the depth is few meters and in the centre (close to the highest part, Ticul) the depth is approximately of 125 m.

2.3 **Climatology**

The Peninsula generally has a tropical climate (average annual temperature 26°C) with a subhumid moisture regime and maximum precipitation during summer in common with most of Mexico. There is a generally dry period from November to May and a rainy period from June to October (Barber et al., 2000; Smart et al., 2006). According to the Köppen system modified by García Amaro and García (1973), the Peninsula has three climate types: Bs (Semi-arid), Aw (Tropical Savanna), Am (Tropical Monsoon) (Figure 2-3). The Bs occurs in the extreme northwest coast (Yucatan State) with a temperature range of 24°C to 27°C and annual precipitation between approximately 500 to 610 mm with high evaporation. Aw is the dominant type across the Peninsula in the states of Yucatan, Quintana Roo and Campeche; this climate is characterised by drier months which could have 60 mm of rainfall, however the range of precipitation in this type of climate is from 940 - 1600 mm and a temperature range of 26°C - 27°C. Two Am areas with heavy summer rains and a higher percentage of winter rain are present, one in the southwest of Campeche and the other one on the island of Cozumel (Figure 2-3). It should be noted that there is another climate area (Af, not shown in figures) which includes Belize, Guatemala, and the

Tabasco state which is next to Campeche. This area is characterised by high rainfall amounts (more than 1600 mm), in fact this area receives the highest rainfall amount in the whole of Mexico (García, 1965; Wilson, 1980; Barber et al., 2000).

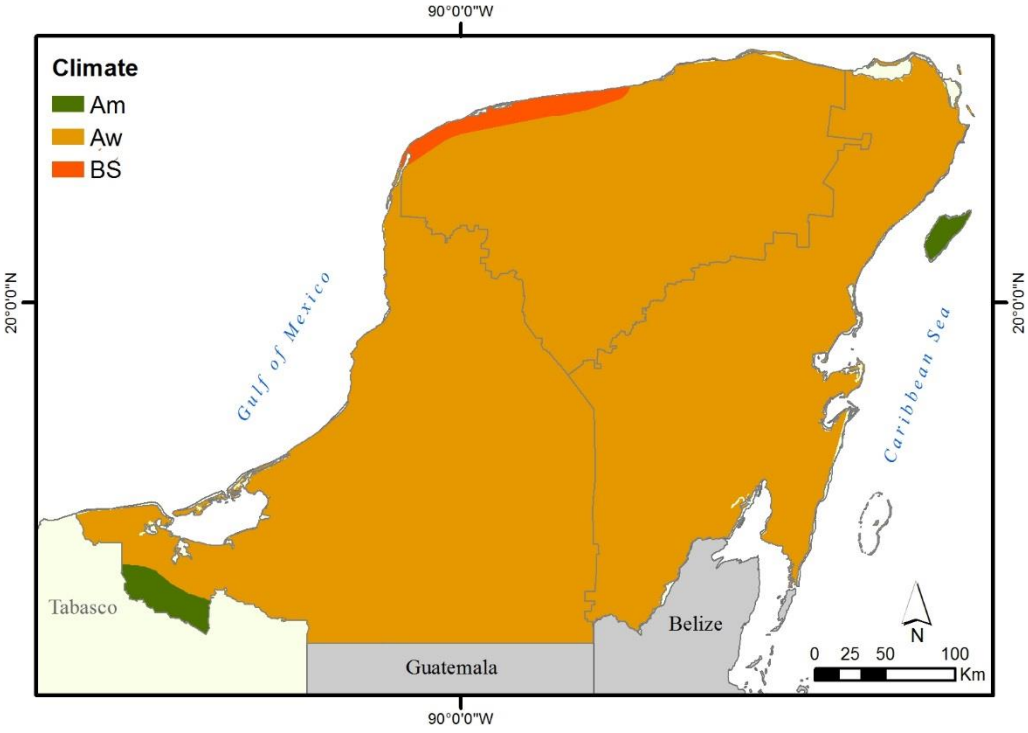


Figure 2-3. Climates types present in the Yucatan Peninsula according to the Köppen system modified by García (1998a).

2.3.1 Spatial and temporal precipitation variability

The primary source of seasonality in the Yucatan Peninsula is the distribution of precipitation. Precipitation in the Yucatan Peninsula is variable in terms of space and time (Hodell et al., 2005) and is characterised by convective rainfall as there is no real complicated orography. Temporal precipitation variability is driven principally by the position and movement of the Intertropical Convergence Zone (ITCZ) and other meteorological mechanisms such as the Azores-Bermuda (A-B) subtropical system (Hodell et al., 2005), Mexican monsoon, easterly waves and hurricanes in the Caribbean Sea and Gulf of Mexico.

The ITCZ is a zone where the trade winds converge near the Equator creating low atmospheric pressure or cyclone areas (Metcalfe et al., 2015). During the

boreal summer the ITCZ migrates to the north in comparison to its position during winter, bringing rain to this area between May and October. Cloud structures and high sea surface temperatures (SSTs) in combination with trade winds cause this rainy season (Metcalfe et al., 2015), then easterly winds (trade winds) carry moisture to the Peninsula (Torrescano-Valle and Islebe, 2015). At the end of the summer, the ITCZ moves to the south (Figure 2-4) thus bringing high pressure during winter producing descending air over the Yucatan which diminishes cloud formation through evaporation of the cloud moisture and results in the dry season of the boreal winter (Wilson, 1980; Giddings and Soto, 2003; Torrescano-Valle and Islebe, 2015).

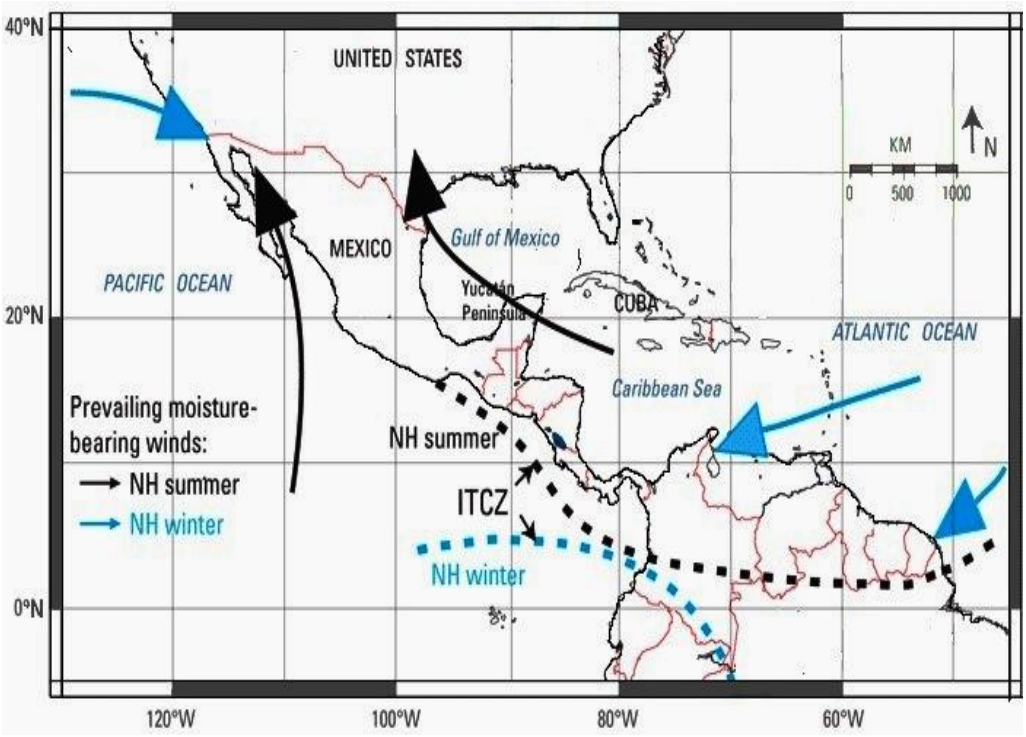


Figure 2-4. Position and movement of the ITCZ (dashed lines) for boreal hemisphere during summer (black) and during winter (blue). Arrows represent the direction of the prevailing moisture-bearing winds in summer (black) and in winter (blue). Modified from: http://soundwaves.usgs.gov/2008/04/

In terms of spatial variability, the Yucatan Peninsula presents a precipitation gradient from northwest to southeast (Figure 2-5) (Hodell et al., 2005) (300 mm to 2500 mm respectively) in approximately 350 km distance. For example, the Caribbean coast receives in excess of 1500 mm per year, 80% of which falls during the wet season, in summer (Smart et al., 2006). Also, there is a

precipitation increase from west (~ 1000 mm/yr) to east (~1400 mm/yr) in the northern part of the Peninsula driven by the prevailing easterly winds (Hodell et al., 2005). According to Márdero et al. (2012), this area is more exposed to the influence of the trade winds that carry warm moist air masses, especially in the summer time. Gradually the amount of precipitation decreases toward the centre-west of the Peninsula.

The map shown in Figure 2-5 shows the precipitation gradient in the Yucatan Peninsula and it is before this thesis the most updated map for the area. It was created with orography and wind direction data for the whole country. In chapter 3 a detailed creation of new maps are presented.

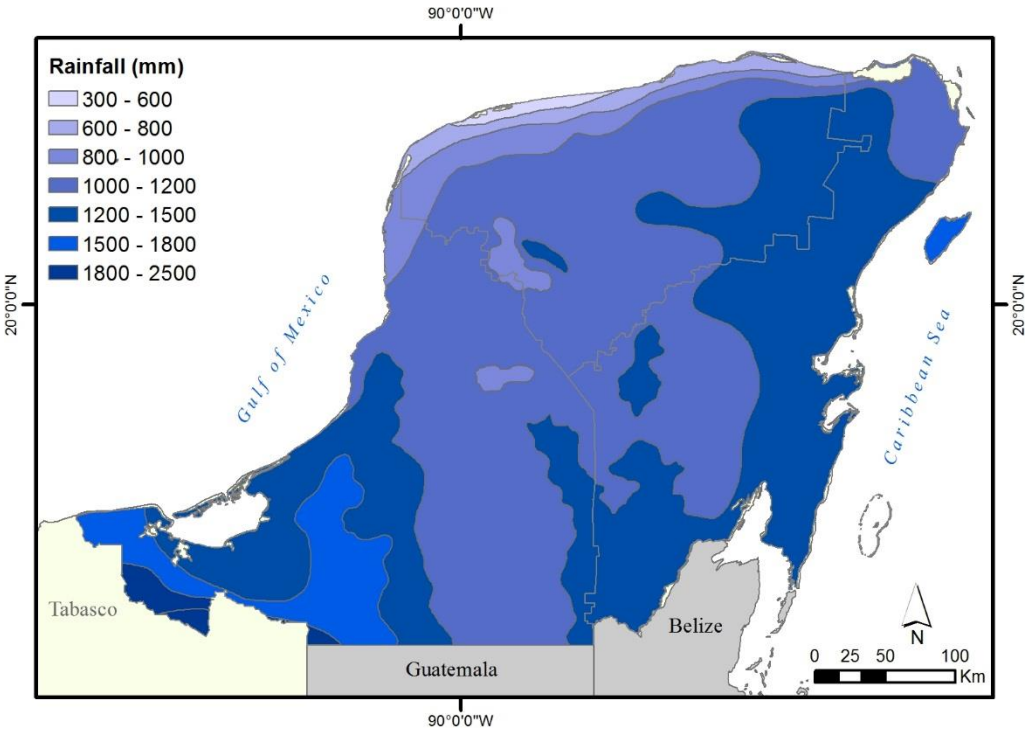


Figure 2-5. Annual precipitation map across the Yucatan Peninsula. Data from (García, 1998b). Note: The dates used by García (1998b) for the creation of this map are not reported and was constructed taking into account orography and wind direction. The source can be found in: http://www.conabio.gob.mx/informacion/metadata/gis/isoyt1mgw.xml?_httpcache=yes&_xsl=/db/metadata/xsl/fgdc_html.xsl&_indent=no

As a part of the annual cycle, the summer rainy season presents two maximum values of precipitation: one in June, and the other in September (during the hurricane season, see 2.3.3); therefore, there is a relative minimum between July and August known as the *canícula*, *sequía intraestival* or summer drought

(Figure 2-7). This phenomenon could be explained by the meridional migration of the ITCZ and its double crossing over Central America and the Caribbean and by diminution of deep convective clouds producing a higher solar radiation and therefore an increase of surface temperatures (Liverman, 1999; Magaña, 1999; Magaña et al., 1999; Orellana et al., 2009).

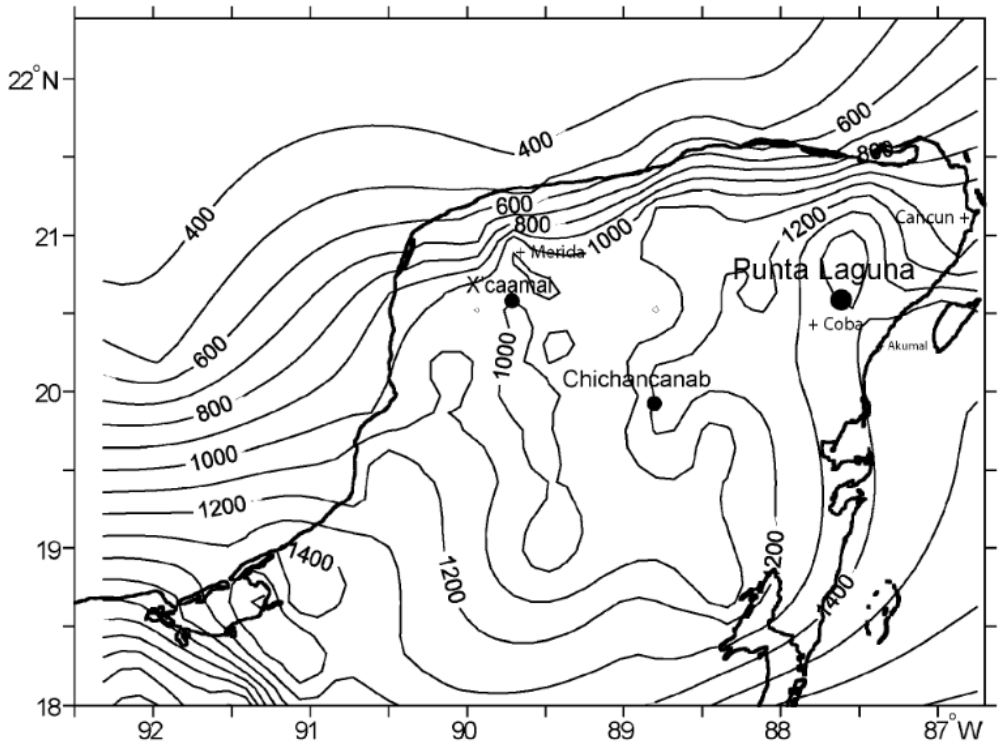


Figure 2-6. Map of the Yucatan Peninsula with contours of mean annual precipitation in millimetres. Taken from Hodell et al. (2007)

On the other hand, the highest amount of rain is related to tropical low pressure troughs called easterly waves, which are masses of thunderstorm clouds moving into the Peninsula (Caribbean coast) during the summer. These easterly waves are associated with hurricanes and tropical storms, which hit the Peninsula almost every year during summer and autumn causing extremely heavy rainfall.

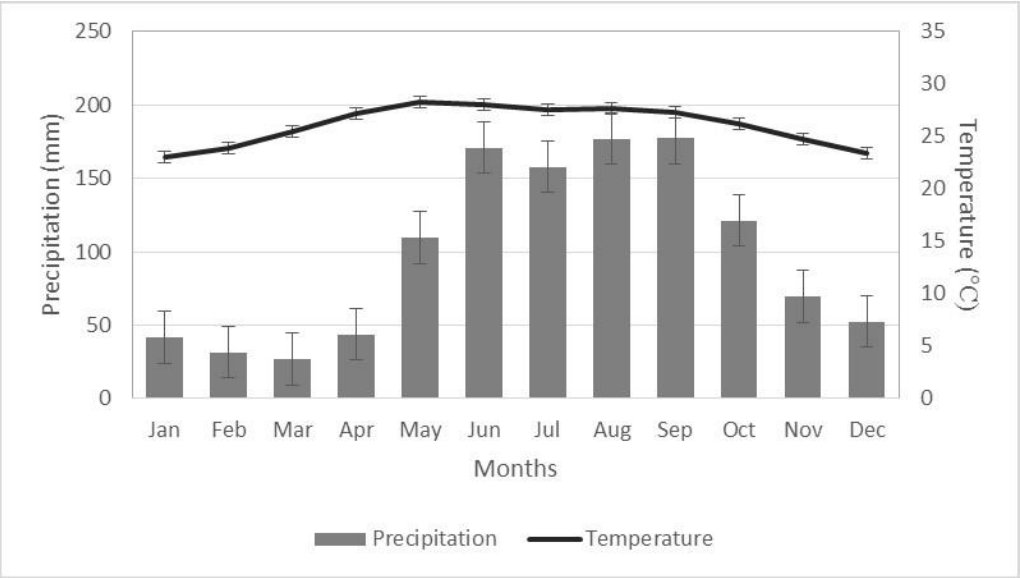


Figure 2-7. Average annual precipitation (1941-2010) and temperature (1971-2010) at the Yucatan Peninsula (CONAGUA, 2010b).

During winter (from October to May), *nortes* play an important role in the Peninsula. These are low pressure systems from the accumulation of cold air in mid-latitudes causing outbreaks of cold air towards the tropics; when this cold air collides with warm and humid air it produces clouds which in its turn generates rain. If the position of the cold front is such that the wind blows strongly from north to south over the Yucatan Peninsula, then it is called a *norte*. *Nortes* can last from one day to two weeks and they can occasionally bring more rain than the normal during winter (Mendoza et al., 2007) and cold weather for some days.

Summarising, in order to understand the precipitation gradient in the Peninsula it is important to take into account the different factors that are involved on this. First, the ITCZ which dictated the wet/dry seasons. Secondly, ENSO which creates anomalies in the precipitation patterns; thirdly, the *nortes* bringing more rain during winter and it is related to the *canicula*. Finally, the fluctuations and interactions associated with tropical depressions and trade winds. As a result of all these interactions the Yucatan Peninsula presents this gradient and make this area rather complex for studying. The climatology in the Peninsula has changed in history and droughts have been documented as an important part of this history (Hodell et al., 2005).

2.3.2 Temperature across the Peninsula

High temperatures predominate in the Yucatan Peninsula due its location (21 - 17° N) and low elevation; the annual mean average is 26 °C. The temperature range during the year is approximately ~7 °C. The high temperatures in the Peninsula during summer are also due to the warm maritime currents which are formed from the North Equatorial Current, which in turn generates the Caribbean current and the one in the Yucatan trough; these currents maintain warm temperatures in summer and later help to generate tropical storms. Conversely, in winter, there are some days with low temperatures due to the *nortes* (Herrera-Silveira and Ramirez-Ramirez, 1996).

According to Orellana et al. (2009) and Giddings and Soto (2003) temperature presents a subtle spatial gradient across the Peninsula, where the highest temperatures occur in the west part (the Gulf of Mexico coast in Campeche) and decrease to the east portion in the State of Yucatan and in the south of Quintana Roo. However, as mentioned above, the temperature is really stable during all seasons, except with the occurrence of *nortes*.

2.3.3 Extreme meteorological events

Timing and distribution of precipitation is an important issue in the Yucatan Peninsula since it is exposed to three main climate hazards: tropical storms, hurricanes and droughts and as indicated by the IPCC (2013) climate changes have resulted in extreme meteorological events which have been changing in frequency (i.e., more often) and intensity (i.e., more intense). Life and economic losses, as well as ecosystem damage, are some of the consequences caused by the extreme meteorological events, and thus it is of much importance that we have a better understanding of extreme meteorological events and their impacts. Mexico and in particular the Yucatan Peninsula and Central America are catalogued as vulnerable areas for climate change consequences (Orellana et al., 2009).

The Yucatan Peninsula is located on one of the main hurricane paths in the North Atlantic and, therefore, tropical storms and hurricanes occur every year here (see

chapter 3, Figure 3-18 and Table 3-4). According to the IPCC (2013) the intensity (wind speed and heavy precipitation) will increase by 2020 in 20% (Curry et al., 2009). Between 1980 and 2011, sixteen hurricanes and tropical storms hit the Peninsula (NOAA, 2016) causing material damage, life and economic losses.

The Peninsula, in particular the northeast region, is catalogued as one of the five areas in Mexico which has severe droughts (Márdero et al., 2012). According to Hernandez Cerda et al. (2000), who catalogued the whole Mexico in different levels of drought severity calculating a severity drought index which measures the deviations of precipitation from the normal, found that the states of Campeche and Quintana Roo present are affected by strong droughts and the state of Yucatan was catalogued as affected by very strong and severe droughts for the year 2000. In the future scenario, Hernández Cerda et al. (2000) reported an increase of droughts in the whole Peninsula. For instance, it was reported that the states of Quintana Roo and Campeche are the most vulnerable, where 99% and 75% respectively of their territories will be more affected by droughts (Márdero et al., 2012). Moreover, it is reported that Calakmul Natural Reserve (seen in Figure 2-1) rainfall has decreased by 16% in the last 50 years and the whole reserve is catalogued vulnerable to severe droughts. In general, in the Yucatan Peninsula, droughts tend to be more intense than the wet periods (Giddings and Soto, 2003).

The droughts in the Yucatan Peninsula have been associated with different meteorological processes and sea surface temperature anomalies (i.e. ENSO, AMO, and PDO) as well as to the characteristics and conditions of this area. ENSO refers to the variations in the sea surface temperatures, convective rainfall, surface air pressure, and atmospheric circulation at the equatorial Pacific Ocean. AMO (Atlantic Multidecadal Oscillation) refers to a long duration changes in the sea surface temperature for the North Atlantic Ocean. PDO is the Pacific Decadal Oscillation and it refers to the internal changes between two circulation patterns that take place approximately every 30 years in the North Pacific Ocean.

Few studies (Magaña, 1999; Magaña et al., 2003; Salas et al., 2014) have focused on understanding these relationships, however the results in the literature are varied. For instance, some studies Mendoza et al. (2005) and 2007 Márdero et al. (2012) stated that droughts are associated with El Niño; in the contrary, Giddings and Soto (2003) found that this association is not always positively correlated. Mendoza et al. (2007) who furthermore showed a relationship between El Niño and 25 severe droughts detected in a period of 365 years; they also found that drought frequency was lower in the twentieth century than in the nineteenth century. Márdero et al. (2012) analysed the spatial and temporal variability of precipitation across the southern part of the Peninsula, addressing the anomalies and trends of annual and seasonal precipitation as well as the occurrence of meteorological droughts and they also found that drought events in the Yucatan Peninsula coincide with El Niño years. However, Audefroy (2015) pointed out that between 1970 and 2011 eight droughts were reported in the State of Yucatan and they indicate, contrarily, that drought frequency increased at the end of the twentieth century and in the early twenty first century. The Disaster Information Management System shows in its website information system (http://www.desinventar.net/) a total of 109 records of droughts between 1970 and 2011.

Droughts in this area also are expected to increase in frequency (i.e. more often) and intensity (i.e. intense). This is one of the reasons why Yucatan Peninsula has been a target place to study droughts from a climatological perspective. As mentioned before, the occurrence of droughts are related to meteorological conditions (i.e. the position of the ITCZ, easterly waves, tropical storms) but to get a better understanding of droughts and how they could affect a specific area, it is important to understand the physiography characteristics of the area

2.4 **Vegetation**

Precipitation is the most important limiting factor for primary production of vegetation and this is reflected in the floristic composition of ecosystems. Thus,

in the Yucatan Peninsula the vegetation type location is linked to the gradient of precipitation; for instance, in the eastern part the rainfall is approximately 1400 mm, where the semi-evergreen tropical rain forest occurs, whilst in the central portion, where the transition from semi-deciduous to tropical dry forest occurs, the rain is about 1000 mm. The western portion receives approximately 500-1000 mm in the transition of semi-deciduous tropical dry forest to the tropical dry forest (Flores-Guido and Espejel, 1994).

The soils in this area are mostly Rendzina and Lithosol types; Arenosol, Cambisol, Gleysol, Histosol, Regosol, Solonchak and Vertisol types are also important (Flores-Guido and Espejel, 1994). Some research affirms that differences in vegetation over large areas are linked to regional climatic gradients or to local differences in parent materials. White and Hood (2004) analysed the links between soils and vegetation distribution and found that topographic and substrate attributes affect distribution and abundance of woody species in the Peninsula forests. In this heterogeneous vegetated area, the principal vegetation types are (i) evergreen tropical rain forest; (ii) semi-evergreen tropical rain forest; (iii) tropical dry forest; (iv) semi-deciduous tropical dry forest and (v) mangroves (Figure 2-8) (Miranda, 1964; Pennington and Sarukhan, 1998). Vegetation in this area of Mexico is really important because these ecosystems are located in the transition areas between the west to east movement of tropical development (Turner et al., 2001), in addition, the vegetation in this area has extreme relevance in terms of the ecosystem services that it provides to the society, the role it plays for climate regulation, for the aquifer functioning; it hosts the biggest carbon stock in the country and also harbours great biodiversity (Rada et al., 2015)

The evergreen forest is present in the south of the Peninsula in the State of Campeche and Quintana Roo. It is characterised by dense, tall trees more than 30m tall and green during all seasons. This type of vegetation develops in warm, wet weather (temperature is higher than 20°C and average annual precipitation is more than 1500mm) and the dry season is short or absent. As being present in the Yucatan Peninsula, this vegetation is also present in neighbouring Belize and

Guatemala (Miranda and Hernández, 1963; Vázquez, 1999; Challenger and Soberón, 2008).

The semi-deciduous forest consists of some trees that lose their leaves in the dry season. They are present where the temperature is more than 20°C and sub-humid with more than 1200 mm of annual precipitation. This vegetation occurs in the States of Campeche and Quintana Roo (Miranda and Hernández, 1963; Rzedowski, 1978).

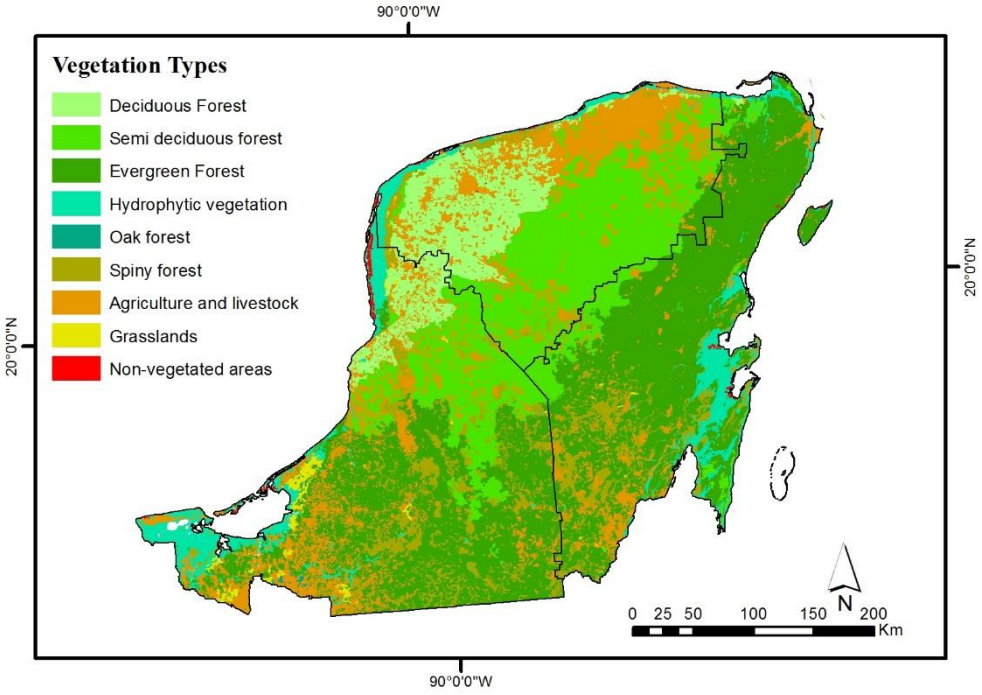


Figure 2-8. Vegetation types across the Yucatan Peninsula. The colours of each class are grouped according to the same type of vegetation including secondary vegetation and some perturbed areas. Data from the National Forest Inventory (INEGI, 2010).

In the semi-deciduous forest, more than half of the trees lose their leaves in the dry season, which it is important to mention for understanding the spectral response of this type of vegetation at different times of the year. Normally such forests are located in lowlands and are present in the Yucatan State. Annual average temperature is approximately more than 20°C with 1200 mm of annual precipitation and the dry season is longer than the semi-evergreen tropical rain forests (Miranda and Hernández, 1963; INEGI, 2010).

The tropical dry forest or deciduous forest is characterised by short trees of less than 15 m and a climate with a very clear contrast between the wet and dry seasons; normally the dry season lasts seven or eight months and during this time the trees lose their leaves (Rzedowski, 1978). This vegetation is developed in semidry and warm areas which have an annual average temperature of more than 20°C and annual precipitation between 500 mm to 1200 mm. This forest covers the north part of the state of Yucatan and the north of Campeche (see Figure 2-8) (Miranda and Hernández, 1963).

Mangroves, represented as hydrophytic vegetation in Figure 2-8, are species that live primarily in saltwater; they develop in intertidal areas of sheltered coastlines (Kaplowitz, 2000) and develop best in marshes and estuaries. They are characterised by their air roots and for the presence of the *Rhizophora mangle* (with heights up to 25 m), *Laguncularia racemosa* and *Avicennia germinans* species. The mangroves in the Yucatan Peninsula are located all around the coastline (Figure 2-8) (Miranda and Hernández, 1963).

In the last decades some protection programmes have been developed in order to preserve the vegetation of the Yucatan Peninsula region. The Peninsula has 39 protected areas, which six are catalogued as Biosphere Reserves: Calakmul, Sian Ka'an, Ria Celestun, Banco Chinchorro, Ria Lagartos and Los Petenes; seven as National Parks: Arrecife Alacranes, Isla Contoy, Xcalak, Arrecifes de Cozumel, Tulum, Isla Mujeres and Puerto Morelos; and three as fauna and flora protected areas: Yum Balam, Bala'ank'aax and Otoch Maax Yete lKo oh (CONANP, 2010). The rest are catalogued as National Parks. These areas make a genetic flow biological corridor which connects to the Biosphere Reserves in Guatemala and Belize –El Peten Guatemalteco and Chiquilub in Belize (see Figure 2-9) (Tetetla-Rangel et al., 2012).

According to Chiappy and Gama (2004) the state of conservation in the Peninsula is shown as follows. In the state of Yucatan, 10% of its vegetation is primary vegetation, 68% is secondary vegetation and 22% is anthropogenic vegetation, i.e. crops, meadows and plantations. In contrast with this, the state of Campeche has 60% of primary vegetation, 34% secondary vegetation and 6%

anthropogenic vegetation. Finally, Quintana Roo presents 74%, 23% and just 3% respectively (Valdez-Hernández et al., 2014).

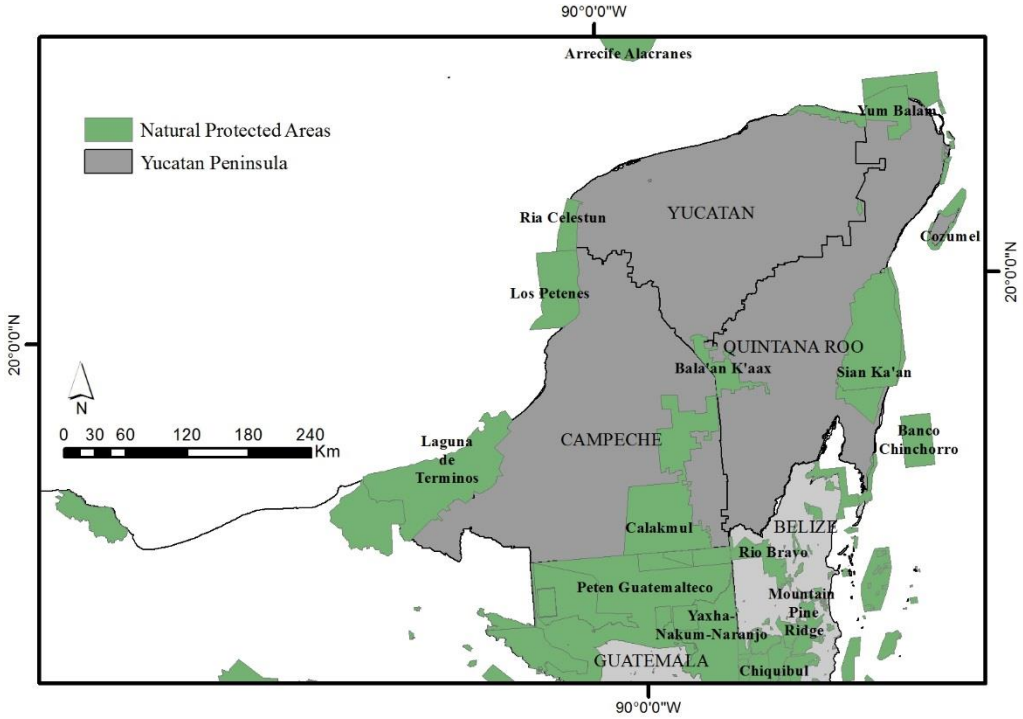


Figure 2-9. Natural protected areas in the Yucatan Peninsula including Belize and Guatemala. Data from (CONANP, 2010) and http://www.protectedplanet.net/

2.5 **Principal human activities in the Peninsula**

The Yucatan Peninsula has been occupied by humans for thousands of years (approx. 3000 years) and human activity has been an important driver of forest composition and extent (Valdez-Hernández et al., 2014). It is well documented that Mayan practices have impacted forests in the Peninsula. Pollen evidence shows major losses of forest cover during the Maya period, followed by recovery post 'collapse' and the major drought periods that also seem to have occurred in the terminal Classic period. The subsequent recovery of the forest suggests that it can be quite resilient to the impact of both climate and people (Rosenmeier et al., 2002; Hodell et al., 2007). Today, the Yucatan Peninsula's natural diversity presents considerable fragmentation mainly due to anthropogenic activities such as traditional slash and burn method for clearing agricultural land, seasonal agriculture, irrigated agriculture, pasture, timber extraction and agriculture

associated with forest activities due to both industrial and domestic causes (Chiappy and Gama, 2004; Valdez-Hernández et al., 2014).

Tourism is another important factor that has modified coastal areas in particular areas close to Cancun and the Riviera Maya (principal touristic destinations) and it is one of the causes behind demographic growth since migration to these areas grew especially in the last decades. In the coastal region the principal human activities include fishing, hunting, tourist services, salt extraction and agriculture. The increase in these activities caused significant migration into these areas (Cancun and the Riviera Maya); in the 1970's the population grew up to 300% (Batllori-Sampedro et al., 2012).

Chiappy and Gama (2004) report that the newest activities in the Peninsula are pig farming, *maquila* (manufacturing companies which import products as a free trade zone) industry, and the construction and renovation of roads. In accordance with this, Quintana Roo is the part of the Peninsula which has the least human impact due to the presence of some natural protected areas, however those areas close to Cancun and the Riviera Maya are the exception. The next is Campeche which has the Calakmul Reserve; although this protected area has been modified in its surroundings. In contrast, the State of Yucatan is the one that presents the most perturbation in the Peninsula due to a number of factors including the growth of the urban areas (principally Merida), industrial and mining activity, cattle, poultry and swine farming, and tourism activity. Furthermore, wood extraction and *chicle* (gum) extraction have been other causes of deforestation (Turner et al., 2001; White and Hood, 2004).

The vegetation in the Peninsula has undergone significant alteration and recovery over time. One of the most important problems in the Peninsula is agricultural land clearance which has been practiced for more than 2000 years since the Mayan civilization, which has led to severe erosion of the Yucatan Peninsula soils (Whitmore et al., 1996; Aguilar and Domínguez, 1999).

This chapter provides a full description of the Yucatan Peninsula and showed the unique features that this part of Mexico presents. The Yucatan Peninsula has

been target of many studies for its great ecological importance in (i.e. biodiversity) and its physical characteristics. Also, and in the context of this thesis, droughts have been a major concern in this area. For instance, the ongoing scientific debate about the climatological changes in this area and the collapse of the Mayan culture due to a drought has attracted the attention for many years. The Yucatan Peninsula is a vulnerable area to droughts due to its physical and climatic characteristics such as the highly seasonal rainfall regimen, the lack of available surface water, the presence of thin soils across the area and the variable access to groundwater. Vegetation in the area has been changed and has been under pressure since Mayan period and it is reported to be resilient to these changes. However, there is a lack of studies in terms of the actual climatology and the detection of droughts in the area. Therefore, next chapter is focused on this last point in order to analyse the general patterns of precipitation in the Peninsula from 1980 to 2011 and the detection of droughts in the same period.

CHAPTER 3. **PRECIPITATION PATTERNS AND DROUGHTS ACROSS THE YUCATAN PENINSULA**

3.1 **Introduction**

This chapter aims to analyse and understand precipitation patterns and their spatio-temporal variability at the Yucatan Peninsula, Mexico. In addition, droughts during the period of 1982-2011 are detected. The analysis in this chapter will help, first, to understand the link between precipitation and vegetation productivity, and second, to understand how droughts could impact vegetation. In addition, the most reliable spatial distribution maps of precipitation and droughts to date have been produced in order to understand precipitation variability in the Yucatan Peninsula. The current understanding of climatology in the area needs investigation in order to fill a gap in the knowledge, since there have not been any climatological studies conducted for the entire Peninsula based on the precipitation data provided by meteorological stations. An overview of the climatology of the Yucatan Peninsula was described in section 2.3. The following sections, precipitation pattern analysis and droughts detection using meteorological stations' data across the Yucatan Peninsula is performed and discussed.

Precipitation across the Peninsula exhibits both spatial and temporal variability and there are no continuous and updated rainfall maps available. First, an exploratory analysis of the data was carried out and long-term and annual precipitation maps created. Second, precipitation anomalies and droughts were detected and analysed. A few studies have been done (Magaña et al., 2003; Márdero et al., 2012; Salas et al., 2014) with some of the meteorological data available in the Peninsula. However, this chapter will provide a comprehensive precipitation study which is based on all the data sets available to date and covering the entire Peninsula.

3.2 Dataset and methods

3.2.1 Precipitation dataset

The main data used for climatological studies, and principally for drought analysis, is precipitation data, for this reason it is crucial to gather long term, uninterrupted and spatially continuous precipitation data (Easterling, 2013). In these terms, Mexico has been making a major effort gathering rain gauge data all over the country, with a meteorological station network which has been established since 1901. At that time the network was formed by 31 meteorological stations (one per state), 18 observatories and a few independent stations. The goal since the beginning of this network was to establish an institution (*Servicio Meteorológico Nacional* (SMN)) responsible for the compilation, processing and analysis of the climatological data in the country. Unfortunately, throughout Mexican history the collection of meteorological data has been started and stopped as a result of political and economic problems in the country (CONAGUA, 2012). In the 1950s and 1960s the network was incorporated into the former institution of the National Water Commission in Mexico (CONAGUA) and the number of stations across the country increased considerably. Unfortunately, in the 1980s many stations were disrupted due to socio-political issues in the country (e.g. cutback in science sector, economic crisis, etc.), thus there is a decline of data from that period and less number of stations kept running without interruption.

Currently, the SMN has as its main goal atmospheric monitoring in order to identify weather events that can affect various economic activities and especially cause loss of human lives (e.g. droughts, major tropical storms). The SMN is also in charge of the collection of national climatological information and updating of the National Climate Data Bank. This data bank includes historical records of approximately 5000 stations – in some cases since the nineteenth century to-date (CONAGUA, 2010a). Each station gathers daily information about precipitation, temperature and evaporation.

In the Yucatan Peninsula, the first station was established in 1921 and the number of stations has been increasing through time. Currently, the Yucatan Peninsula has data from 229 meteorological stations: 89 in the State of Yucatan, 59 in Quintana Roo, and 81 stations in Campeche (Figure 3-1).

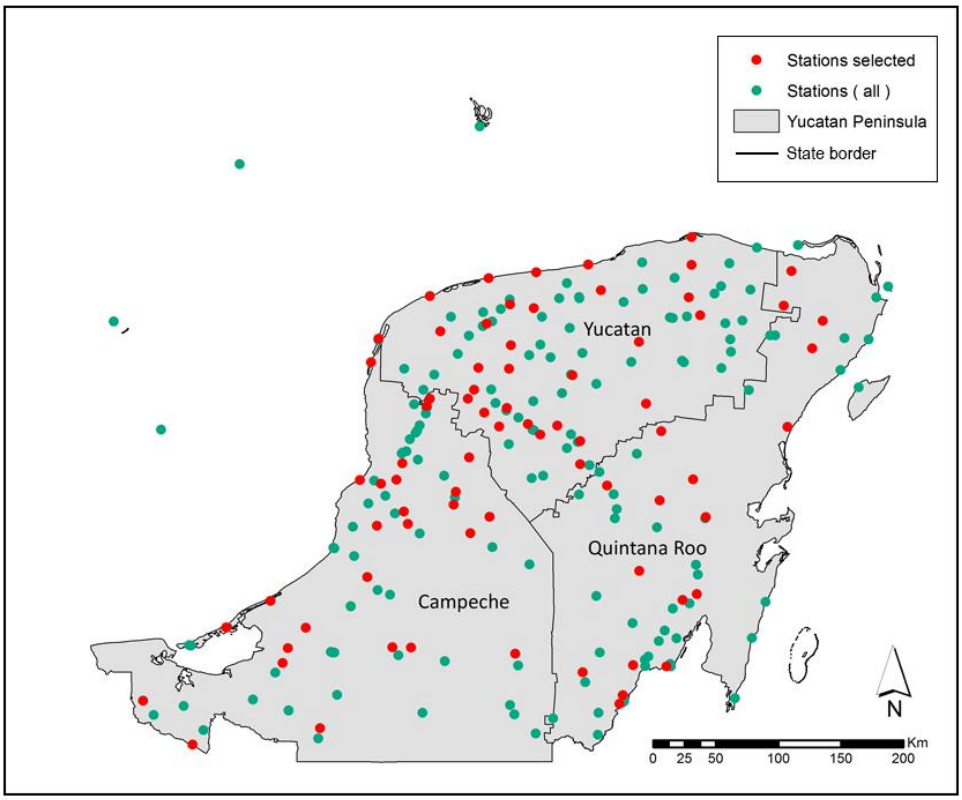


Figure 3-1. Spatial distribution of the 229 existing meteorological stations in the Yucatan Peninsula. Red points represent the stations selected with more than 60% of reliable data. The points on the sea are stations located in small land areas called *cayos*.

As shown in Figure 3-2, half of the current stations were set up in the 1960s and by the 1990s the number of meteorological stations had doubled across the Peninsula. However, the records of all these stations are not continuous in terms of time and just one station has data for a substantial period, and that is 85 years (*Champoton* station, in the state of Campeche) (Figure 3-3).

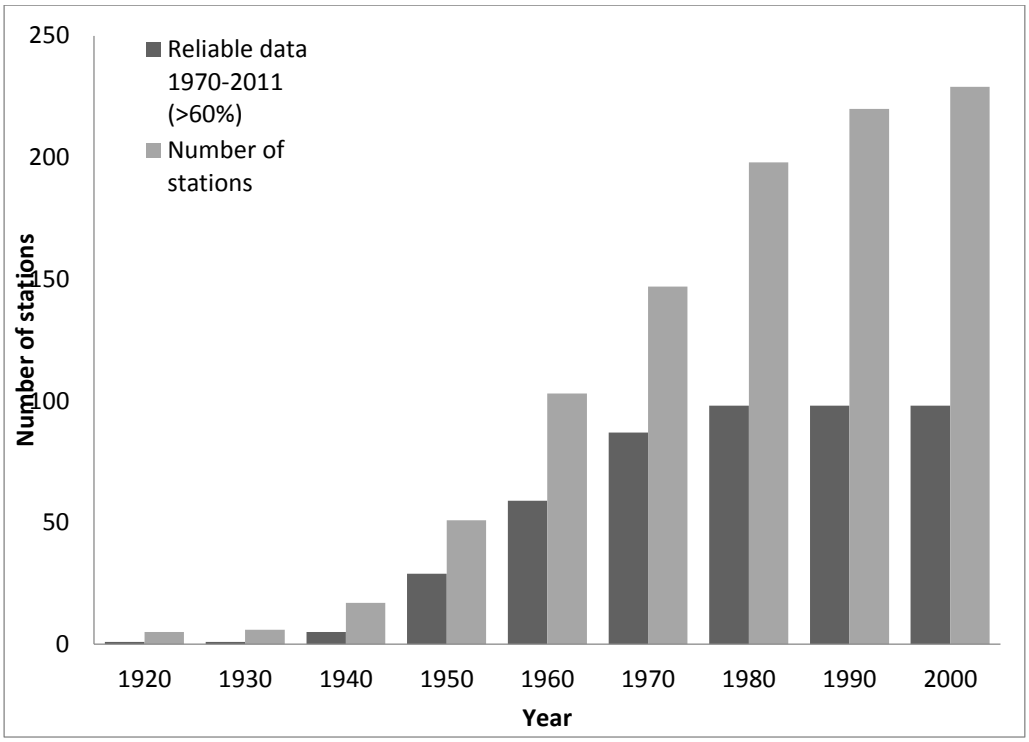


Figure 3-2. Number of meteorological stations in the Yucatan Peninsula through time. Bars show the number of stations set up in each decade. Darker bars show the stations with more than 60% reliable data and lighter bars show the total number of station in the current year.

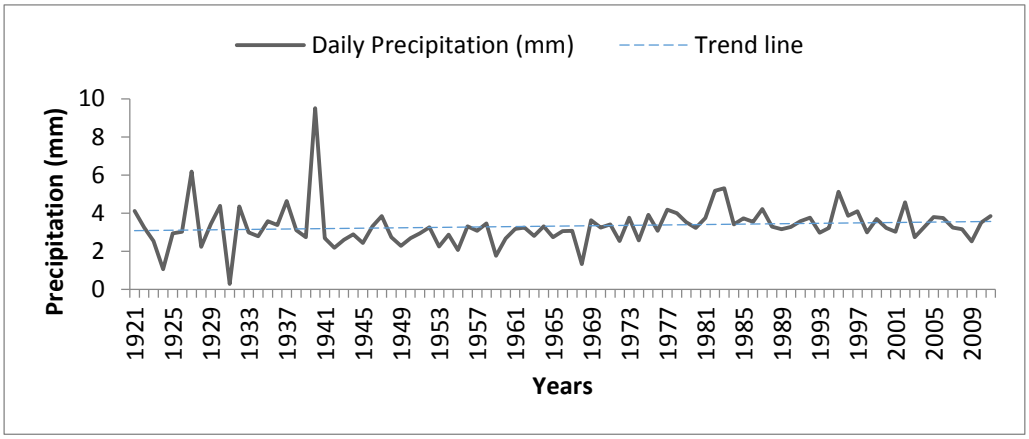


Figure 3-3. Champoton station (in the east of Campeche). This is the station with the longest period of data. The black solid line represents the daily precipitation for this station; the blue dashed line represents the trend line.

The lack of continuity, in addition to the political and economic crises in the country, is related to the occurrence of human errors and the lack of clear guidelines for gathering the information. Furthermore, a few stations have been deactivated and others were activated, bringing discontinuity to the data. This

means that the number of years and months with available data varies considerably from station to station.

3.2.1.1 Precipitation data cleaning

Hence, data preparation is not trivial in this study as there is no unique national climatic database published and accepted in Mexico. Moreover, the data are spread across different departments of the same Institution and every state is responsible for the administration of their own stations, so, the lack of suitable and uniform data is a problem. For example, in the Yucatan State the stations are not automated yet, hence, from 2007 the meteorological data are not available on-line (as the other data) and the data available for this state is spread over two different institutions (i.e. SMN and the water commission of the state of Yucatan). Moreover, between the two data sets there are some records with inconsistences, for example some records in one dataset are zeros and in the other one are recorded as "no data". Moreover, there are periods without any data; this is the case for 1997, 1998, 2008 and 2009 where there are a few stations with periods (more than three consecutive months) of no data.

There are also spatial gaps in the meteorological data since the stations are not present all over the Yucatan Peninsula and most of them are located in or close to urban areas. There are areas in the centre and east portion of the Peninsula where the stations are sparsely scattered or where no stations exist (Figure 3-1). In order to understand the precipitation patterns in the region it is necessary to select the stations carefully in terms of completeness, amount of data and a suitable period of time (Bravo Cabrera et al., 2012). According to the World Meteorological Organization (WMO, 1989) any climatological study needs its data analyses to be undertaken over a minimum period of 30 years, as it is this period required to detect interannual variations and long term climatological trends. As shown in Figure 3-2, the largest number of stations (60 - 70) with daily precipitation records was in the period from 1980s to 2000s; so, 1980 was chosen as the start of the period to study. Since this data will be compared with remote sensing images and the last remote sensing images available are from 2011; this year was selected as the end of the analysis period.

In the area, a total of 229 stations have data for at least one year; however, in this study after the cleaning process, 98 stations were left for annual and monthly analyses. The reasons for choosing these stations are based on (1) the quality of data, (2) the length of rainfall records and (3) the percentage of data in each station in the period from 1980-2011. Appendix 1 (Table A- 1) summarises the details of each station and the period of time when they have data available that it is reliable. For annual analysis, a "complete station" was demarcated when it had at least 60 % of data in the whole year, regardless of when the missing data occurred. For monthly analysis, each station was selected following the same rule but monthly. This means a complete month must have at least 60 % data capture. Other studies (e.g. Bravo Cabrera et al. (2012) used more rigorous rules, they defined a full year of observations if it had complete 12 months of observations during 35 years. In this study, however, in order to take advantage of the data available and in order to increase the spatial distribution of the stations, the data cleaning was less strict.

In order to make the most of the potential of the data available and depending on the temporal scale used for the different analysis, the precipitation data was used in some cases with a slightly different criteria. For instance, for creating the annual precipitation surfaces (section 3.3.2), the meteorological stations were used differently. As every yearly map was independent from the other, all meteorological station with data available (> 60% of the data) for that year were used for the creation of the map. For example, it is possible that one station was not selected for the cluster analysis due to the lack of data (less than 60%) for the whole period (1980-2011), but it was used for creating an annual map because in that specific year that station fulfil the condition of more than 60% of the data (see Table 3-1).

Table 3-1. Number of stations used for each annual kriging map. Results of these maps are shown in section 3.3.2.

Year	Number of stations used
1980	111
1981	111
1982	147
1983	144

1984	142
1985	146
1986	151
1987	147
1988	140
1989	137
1990	138
1991	131
1992	133
1993	133
1994	133
1995	130
1996	131
1997	133
1998	142
1999	144
2000	147
2001	143
2002	132
2003	143
2004	145
2005	148
2006	138
2007	144
2008	114
2009	106
2010	109
2011	108

3.2.2 Methods

Once the meteorological data were cleaned, three different analyses were performed to analyse the precipitation trends. First of all, a cluster analysis was made in order to see general patterns in the data. Second, yearly precipitation maps were created using kriging interpolation. Finally, a monthly precipitation analysis was done for each cluster in order to understand better the seasonality

of the area. Following the analysis of precipitation, a drought detection and precipitation anomalies analysis was performed in both the clusters and the krigged maps.

3.2.2.1 Cluster analysis

Cluster analysis is a methodology that uses multivariate techniques which classify data and/or reduce large amounts of data into subgroups or clusters that are easier to manage (Bravo Cabrera et al., 2012). This methodology does not need previous knowledge about the groups. As mentioned in section 2.3.1, the study area presents a spatial precipitation gradient; this means that if regions have similar rainfall amounts, then, cluster analysis could group these sites. A few studies (Fovell and Fovell, 1993; Unal et al., 2003; Bravo Cabrera et al., 2012) have used this technique to analyse the climatological patterns across regions or countries.

With the purpose of understanding the precipitation data, grouping the stations and analysing if the patterns of these clusters follow any spatial pattern, a hierarchical clustering technique was performed using RStudio data analysis software. In this case, the cluster objects are the meteorological stations and the variables are the long-term precipitation data. This means that a 98 x 31 matrix is being analysed; where 98 rows correspond to the stations and 41 columns are the mean precipitation for each year between 1980 and 2011.

The hierarchical cluster analysis is an agglomerative statistical technique which repeatedly classifies the data into groups or clusters based on different variables (precipitation through time) until it creates a final dendrogram, where the different groups are shown (Olson, 1995) and where every branch of the tree represents a step of the process. First of all, a dissimilarity matrix is created; then, each station is assigned to its own cluster, and next and based on the distance matrix, the two most similar objects get joined and so forth until create a single cluster including all objects (Murtagh and Legendre, 2011). Within this technique there are different methods such as single linkage, complete linkage, average linkage, centroid method, Ward's method, etc. In this case, since the

data contain a significant number of NA's (no data), the complete linkage method was selected principally because it allows the 'no data' in the matrix. Concurrently, the distance matrix could be calculated by different methods, for this analysis the Euclidian distance, the arithmetic difference between two precipitation values, was used as it is the most straightforward and accepted method to compute distances and it is useful to handle raw data.

One of the advantages of using hierarchical clustering is that the number of clusters is defined by the user, then it is necessary to analyse the clusters' characteristics at every step and decide when the number of clusters has an interpretable solution and homogenous groups. However, in hierarchical cluster analysis it is also possible to set the number of clusters by plotting the distance between clusters, which is a powerful and simple way to visualise the optimal number of clusters.

In order to assess the clusters quality, a silhouette width method was computed. This is a graphical display to help the cluster analysis interpretation and its goal is to show which objects fit strongly within their cluster, and which objects could belong to either one or other cluster (Rousseeuw, 1987). The computation of this plot uses dissimilarities between the objects, this is how far two objects are; and conversely similarities, which measures how much an object resembles another (Rousseeuw, 1987).

3.2.2.2 Interpolation analysis (Kriging)

Climatological stations produce *in situ* data recorded through time, however these data are not available in a continuous precipitation surface for every year; it is therefore necessary to create these surfaces in order to understand the spatial distribution of precipitation across an area. Geostatistics is a tool which allows physical variables to be estimated across the space. With the purpose of creating reliable precipitation maps across the Yucatan Peninsula, a Kriging analysis was performed. Kriging technique provide reliable estimations of climatological variables when it is used in homogeneous topographic surfaces (Marquínez et al., 2003). Thus, this analysis was possible since the precipitation data is based

on meteorological stations which are distributed across the study area and the region is predominantly flat so that orographic effects are not likely to be significant.

The assumptions for using kriging as an interpolation technique are the following:

- The variation of the points to be interpolated should be random;
- Data points must be spatially dependent; and
- The random process should be stationary with constant mean and the variance depending on the distance between points. This indicates homogeneity across the space.

Within the advantages of using kriging are: i) it aids in minimising the cluster effects that the data could present. This is possible by assigning less weight to those points that could belong to a cluster in the data, thus assuming clusters as single points instead of isolating points; ii) it allows the creation of kriging variance maps or error estimated maps (see Figure C-1, Appendix 4) which show which areas have better estimation of the data. There are no models able to describe exactly what is happening in the terrain, thus any interpolation technique produce error in the estimations, for this reason it is important the incorporation of uncertainties in the model (Bohling, 2005; Kaymaz, 2005); iii) it produce more reliable predictions since the spatial correlation is considered from the semivariogram.

Kriging is an interpolation technique based on a regression model which uses irregular spatial data as coordinates and the steps or requirements to perform the analysis are the following: (1) exploratory analysis of the data; (2) estimation of the spatial correlation function; (3) apply the estimated function to calculate the linear equations for the best kriging estimator (see Figure 3-4); finally (4) generate the estimated values for each cell. The first step was to create matrices with the accumulated precipitation per year per station, where the rows were the stations and the columns were the precipitation data for each station in a given year plus coordinates and altitude of the location. Secondly, the data were tested

for having a normal distribution since kriging estimators are sensitive when the data is not normal distributed. Finally, the semivariograms were computed in RStudio and the kriging interpolation was done in ArcGIS 10.2.2 software to create long term and annual rasters from 1980-2011.

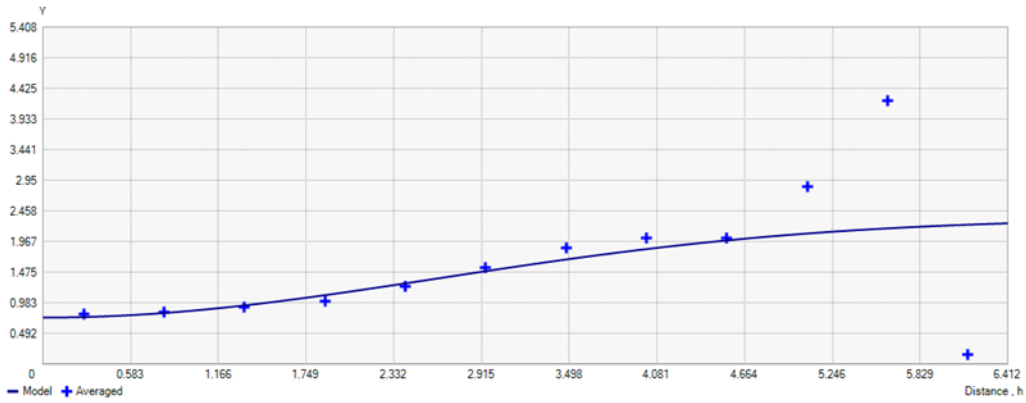


Figure 3-4. Semivariogram with the fitted model for the estimation of kriging as an example for the year 2005. Parameters: Nugget = 0.74; sill = 1.59; range: 6.4. Parameters estimated in RStudio and semivariogram created in ArcGIS.

3.2.2.2.1 Kriging validation

Precipitation studies are mostly based on point-based measures and rainfall surfaces are needed to improve the understanding of rainfall spatial distribution. However, kriging interpolation could bring some problems due the distribution of these points (gauge stations) since they are sparse and not uniformly distributed. To avoid creating rainfall surfaces with estimated data, the broader use of remote sensing data and the development of different Earth observing missions, which provides necessary data to address different types of research (such as the Precipitation Estimation from Remotely Sensed Information Using Artificial Neural Networks (PERSIANN), the Tropical Rainfall Measuring Mission (TRMM) and the Multisatellite Precipitation Analysis (TMPA) (Huffman et al., 2007) have become important for precipitation research. However, none of these products are completely ideal for this and they have important disadvantages in terms of spatial and temporal resolution. PERSIANN has data available from March 2000 and at 0.25 x 0.25 degrees spatial resolution and it is not available for all areas on Earth. The TRMM data also has 0.25 x 0.25 degrees latitude-longitude spatial resolution, but it has better coverage and

different types of products; its data is available from the end of 1997. The TMPA products have been broadly used for its better accuracy in terms of variable estimation. In this study, the use of TRMM satellite data, particularly a product called 3B42 version 7, which is a TRMM TMPA product was used for validating kriging maps over the Yucatan Peninsula.

The 3B42 product provides precipitation data from the very end of 1997 to the present with 0.25 x 0.25 degrees latitude-longitude spatial resolution, 3-hour temporal resolution (Huffman and Bolvin, 2013) and covers the entire study area. In order to validate the kriging maps, the TRMM 3B42 product was used as reference data for the period 1998-2011. The validation process was made in three stages. The first step was to download the TRMM data; which was obtained in both NetCDF and ASCII formats from the TRMM Online visualisation and Analysis System (TOVAS) available in http://disc.gsfc.nasa.gov /precipitation/tovas. The images obtained were the latitude-longitude map time-averaged. This means that the final downloaded images were maps which average daily precipitation per year. These products could therefore be compared with the kriging maps. However, the spatial resolution between these two datasets was different (krigged maps are at 1.5 km spatial resolution) and it was necessary to make them comparable. Hence, in the second stage, new reduced-resolution kriging maps were generated using the Aggregate mean function in ArcGIS 10.2.2. Then, the third stage of the process was to export these images in an ASCII format, so that there are two forms of precipitation data –one from TRMM data and another from kriging- for each pixel. The validation analysis between the two datasets could then be performed.

3.2.2.3 Monthly precipitation in clusters

In order to have a better understanding of the climatological trends and drivers of precipitation across the Peninsula, a monthly analysis of the clusters was done based on the average data per month per cluster. Bar plots were created to see the monthly distribution of precipitation, Afterwards matrix plots were generated in order to visualise and understand the seasonality for each cluster. Matrices are a powerful way to represent the amount of rain, and the dry/wet periods in a time

series. It is also possible to see single extreme events such as hurricanes and they are good way to visualise the differences between clusters.

3.2.2.4 Precipitation Anomalies

The Standardized Precipitation Index (see section 1.5.1) was used in order to detect droughts as this Index a) uses a rolling mean in its calculation b) is standardized, it controls for the different variances and, c) it is accepted and recommended by the World Meteorological Organization (WMO). It is as well the most common and widely used index to monitor meteorological droughts. It was developed by McKee et al. (1993) in order to determine over different time scales (1 month, 3 months, 9 months, etc.) when there is an abnormally dry period at a given time scale –selected by the user. SPI is based on probabilities taking the monthly precipitation data as the unique input. The mathematics behind this index are explained in McKee et al. (1993). The result of this index is a number for the given period of time that goes from -2 to 2, where values close to -2 are the periods when there is a water deficit, while values above zero represent more rain than the long term (the time scale given) precipitation. According to McKee et al. (1993) and as recommended by the World Climate Programme (WCP) it is necessary to analyse 30 years of monthly precipitation data for calculating the SPI.

SPI time scales are important for understanding the dry or drought periods. The 1-month SPI values represent the percent of normal precipitation for a month; this SPI time scale reflects short term conditions (monthly). Due to this, this time scale does not reflect drought periods persistence and according to the National Drought Mitigation Center it is rather related with short term soil moisture and crop stress during the growing period. Large negative or positive SPI values at this monthly scale are still very similar to those for annual average precipitation in the current time.

The 3-month SPI takes three month averages and compares the same three months over the long-term (1980-2011 in this case) and reflects short and medium term moisture conditions. It may therefore provide a better

understanding of seasonality, however the 3-month SPI may be misleading in areas where it is normally dry during that 3-month period. However, the sensitivity of 3-month SPI to precipitation deficit has been reported to be better at this time scale (Hayes et al., 1999; Wu et al., 2001). On a different time step, the 6-month SPI values represent that period of time in comparison with the 6-month long term record. At this time scale it shows medium term precipitation tendencies and it is better to show the precipitation patterns at the different seasons, being that 6 months is a period that covers a complete season even at low and mid latitudes. This time scale also gives important information on the water deficit at different levels. 9-month and 12-month SPI values reflect long term precipitation patterns and these SPI values are better indicators of drought periods since a drought normally takes some months to develop (Svoboda et al., 2012). According to the National Drought Mitigation Center, values below -1.5 are indicators of a drought since at this point some impacts on agriculture and other sectors are possible.

In order to detect droughts conditions in each cluster, the SPI was calculated for each cluster for 1, 3, 6, 9, and 12 month with the Program to Calculate SPI available in the National Drought Mitigation Center website (NDMC, 2015).

Following the SPI clusters analysis, yearly anomalies maps were created in two different ways. First of all, precipitation anomalies were computed in ArcGIS with raster calculator, the inputs were 1) yearly krigged maps and 2) the long term precipitation average map resulting from the interpolation analysis (see 3.2.2.2). The anomalies were computed as the difference between the long term mean maps and each year total precipitation map. Secondly, for every station the 12-month SPI was computed and krigged maps were generated, in this way, the results are SPI maps for every year.

3.3 Results

3.3.1 Cluster precipitation trends

A cluster analysis was run on 98 stations, each with precipitation data from 1980 to 2011 (32 variables to analyse corresponding to 32 years). A hierarchical cluster analysis using the complete linkage method (see section 3.2.2.1) produced five clusters (Figure 3-5).

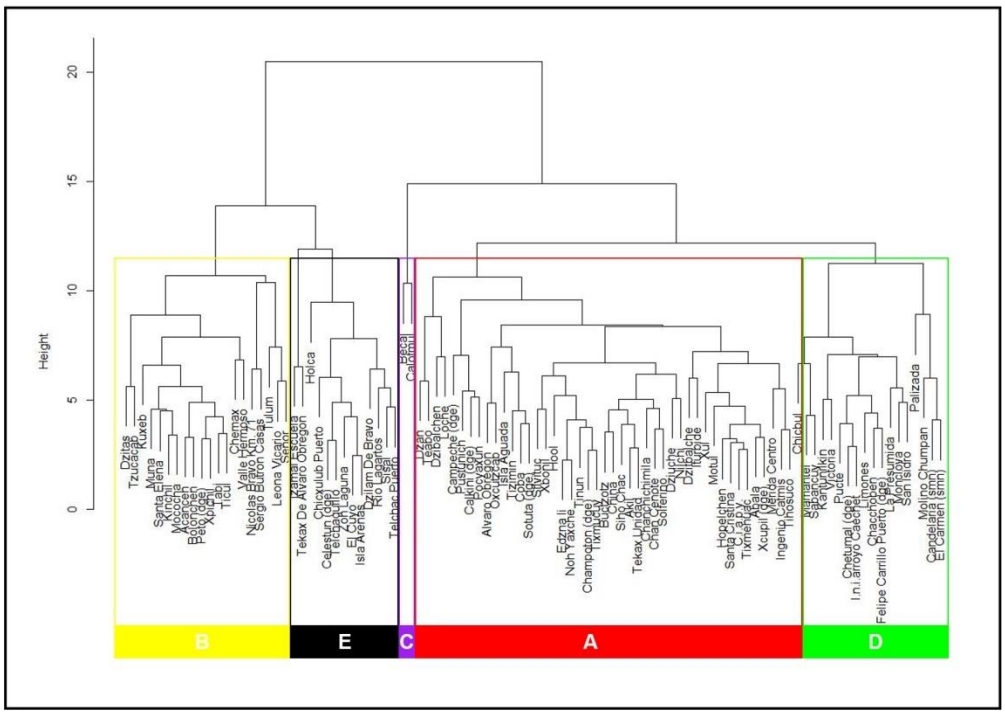


Figure 3-5. Meteorological station dendrogram resulting from cluster hierarchical analysis. Each rectangle represents each cluster. Yellow: Cluster B; Black: Cluster E; Purple: Cluster C; Red: Cluster A; Green: Cluster D

The resulting dendrogram (Figure 3-5) shows the clusters and the dissimilarity (or similarity) between them and how the algorithm grouped them step by step, this is represented on the y-axis in the dendrogram, which denotes a measure of closeness of either individual data points or clusters. The order on the x-axis is insignificant; each branch on the dendrogram represents an identified group when objects were joined together into clusters. As the y-axis represents the observations closeness when they were agglomerated into clusters, clusters whose branches are very close together are probably not very significantly

different among them. In contrast, if the branches show more difference in height between one cluster and the new one, this indicates a better separation (more significance) between clusters. As shown in the Figure 3-5, the branches with height (y-axis) from 10 to 0 are close together and the clusters formed are for individual stations rather than group of them, it seems that there are two big clusters in the data (B/E and C/A/D) which would be more significant.

In order to decide the optimal number of clusters, a dissimilarity matrix was created and the results of this are plotted in Figure 3-6. This plot represents the number of clusters on the x-axis and the distance between clusters (similarity) on the y-axis represents and indicates the similarity between the data of each possible cluster in relation to the distance between clusters. In order to set the number of clusters to be used, the idea is to identify when the curve is stable or when the distance range between the points is minimised. In this case the optimal solution would be six or eleven clusters, as there is a big jump in similarity values. However, it is better for interpreting the results and for analysing the patterns not to have clusters formed by one or two stations. If we had chosen 6 or more clusters there were more than 3 clusters formed by 2 stations. In this case 5 clusters were selected as the optimal solution although there is one cluster (C) formed by two stations.

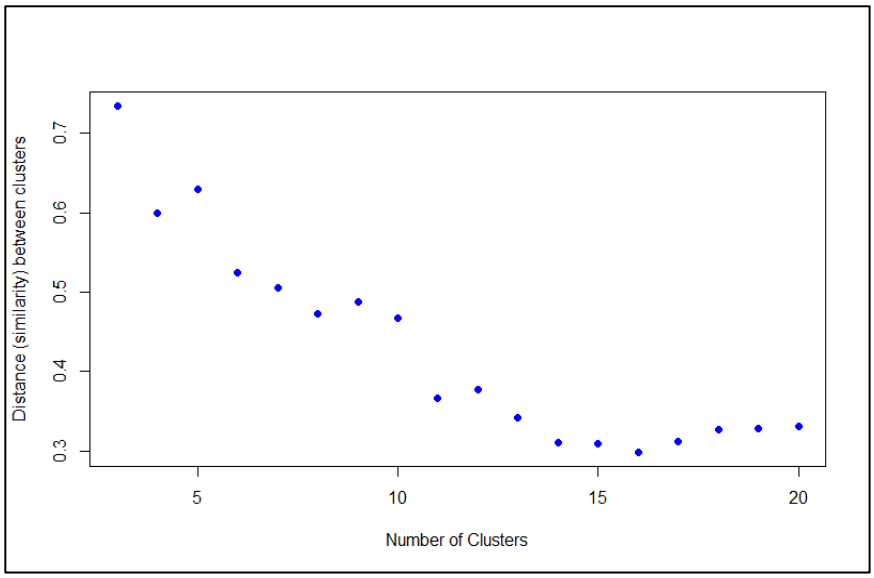


Figure 3-6. Dissimilarity plot shows the distance between clusters. In the x-axis the ideal number of clusters is represented according to the dissimilarity between them (y-axis).

The silhouette plot (see section 3.2.2.1) shown in Figure 3-7 shows the accuracy of the cluster analysis based on the model and the variables used, where every bar plotted represents the stations and the clusters formed (each silhouette). There are three measures represented in this plot: 1) a measure that calculates how well each observation (meteorological station) fits in the cluster it is assigned to; this value is shown on the x-axis and the members of each cluster are arranged from the biggest number to the lowest, according to their silhouette width, meaning that values closer to one indicate that the station belongs strongly to that cluster, while values closer to zero represent that the station could belong to one or another cluster; 2) the significance value for each cluster; and 3) the average silhouette width for all clusters. This plot exhibits that differences between the variables in each cluster were not significantly different from the overall mean silhouette width of 0.1.

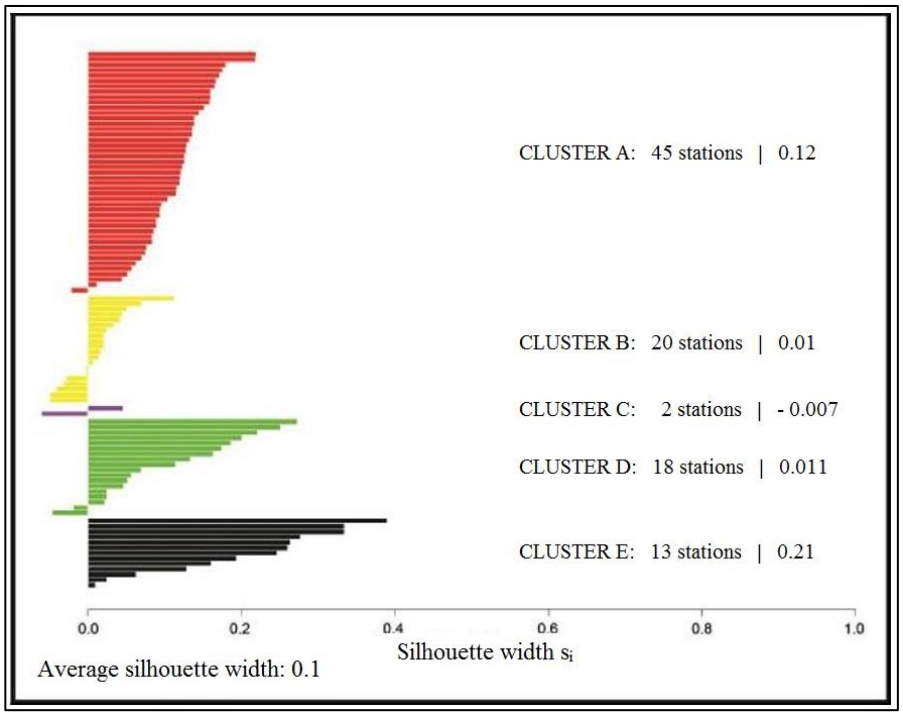


Figure 3-7. Silhouette plot analysis. It shows the separation significance between clusters. Each colour represents each cluster. Yellow: Cluster B; Black: Cluster E; Purple: Cluster C; Red: Cluster A; Green: Cluster D. In the right margin it also shows (right hand column) the strength of the affinity of each cluster within cluster. The overall significance in the bottom left corner (average silhouette width).

None of the clusters have substantial natural structure as they present values below 0.25. However, silhouette widths indicate that the distances within

clusters are big in comparison to the distances between clusters. Hence, the dataset has a structure containing two compact clusters (E and D) with the others not showing a strong structure with silhouette width values less than 0.2. Moreover, there is no strong separation between clusters. Values on the left normally are referred to outliers or misclassified in the dataset not detected by the cluster analysis. For instance, in cluster A, there is just one station (Alvaro Obregon) at the south (see Figure 3-8) which is represented in Figure 3-7 by the red line at the left of the plot (i.e. an outlier).

The cluster distribution it is represented on Figure 3-8 in order to explore whether the resulting groups follow any particular spatial pattern and if they show to some extent, the precipitation gradient in the Yucatan Peninsula.

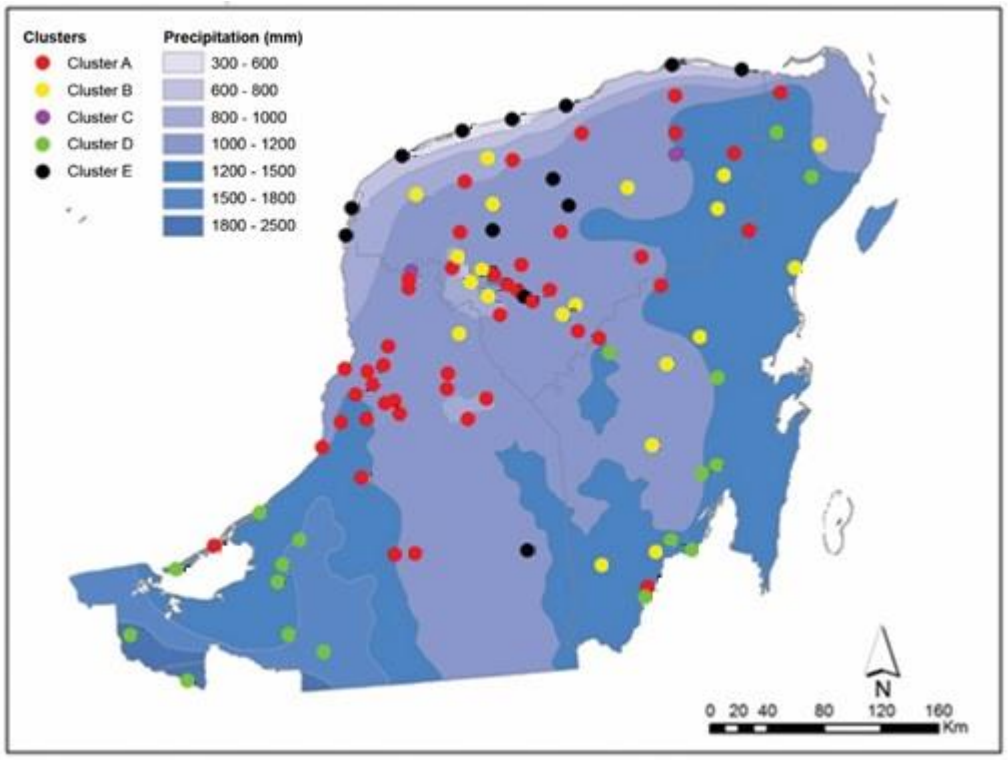


Figure 3-8. Spatial distribution of the clusters (A-E) resulting from the hierarchical cluster analysis on a map that represents the annual precipitation totals across the Yucatan Peninsula.

As the silhouette results show, there are two clusters which are more separated from the others (clusters E and D). The spatial distribution shows that the clusters are spatially coherent, and that the two clusters with higher values of significance are those located in the north (E) and southeast and southwest (D) of the

Peninsula. There is an overlapping of the other three clusters in the centre. The northern coast is composed principally of one cluster (E) and as is shown in Figure 3-9, is the driest part of the Peninsula.

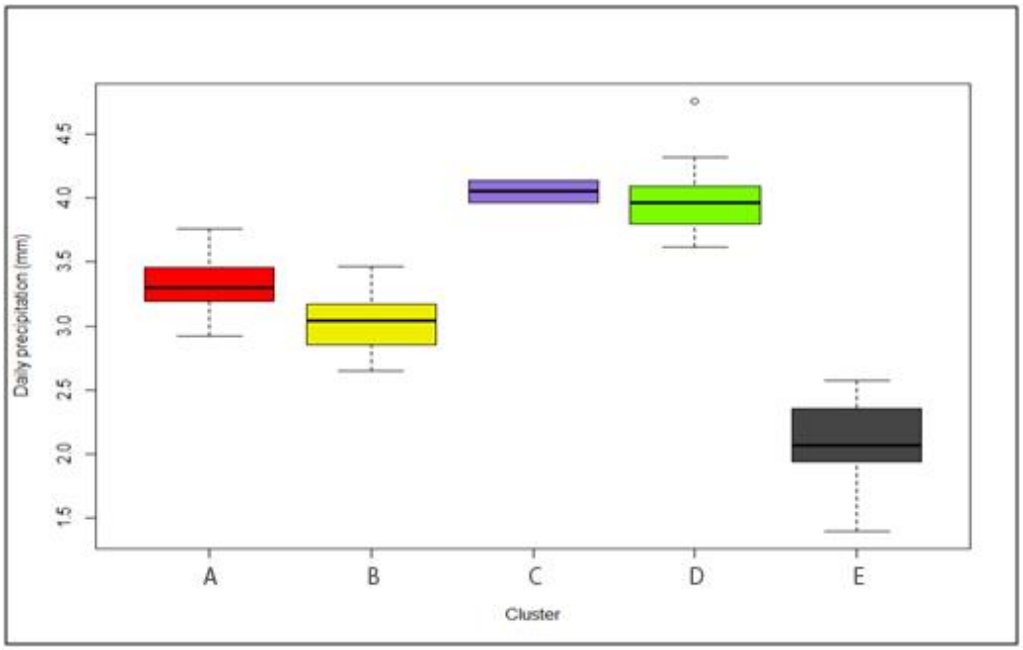


Figure 3-9. Daily precipitation average data grouped in clusters. The bars represent the standard deviation for each cluster. Each colour represents each cluster. Yellow: Cluster B; Black: Cluster E; Purple: Cluster C; Red: Cluster A; Green: Cluster D

The central part of the Peninsula has three (A, B and C) fuzzy and overlapping clusters; the clusters A and B have the biggest number of stations, while C is formed by only two stations and is the cluster with the lowest value of significance. For this reason, from now on, cluster C will not be discussed, as it has a really negative value of significance (-0,007) based on the silhouette analysis and it is formed by two stations which had a lot of no data records.

However, it is important to point out that in general terms, the clusters follow the precipitation gradient across the Peninsula as mentioned in section 2.3.1. Figure 3-9 exhibits also the precipitation gradient. For instance, one cluster (E) is located in the driest part (north) while another one (D) is located in the wettest area (southeast and southwest). The overlapping clusters are in the most homogenous region in terms of precipitation values (Figure 3-8) and this might be the reason why the clusters are similar. Despite of this overlapping, cluster B

has some sites in the west part; these stations (Muca, Tzuzacab, Santa Elena, Valle Hermoso, Chemax and Peto, see appendix 3, Figure A - 1) could form another cluster if more clusters were selected for the analysis as they group in a branch of the dendrogram with the same height (Figure 3-5). Regarding daily precipitation for each cluster, in Figure 3-9 is shown that cluster A has more rainfall than cluster B and this is coherent with the location; for instance, most of the stations from cluster A are a bit northern than cluster B (Figure 3-8).

Figure 3-10 shows the daily precipitation average every year for each cluster. This plot summarises a lot of information for those clusters with many stations. The wettest cluster (D) is represented by the green line, and it is shown that in all years the daily average precipitation is above all clusters and most of the stations of this cluster receive 1200 – 1800 mm precipitation per year. In summary, the grouping shows areas of low rainfall in the north part of the Peninsula and more rainfall in the central part, more or less at the borders of the three states (Yucatan, Quintana Roo, Campeche). These results show some features of the climate of the Peninsula and in general terms the precipitation gradient is reflected.

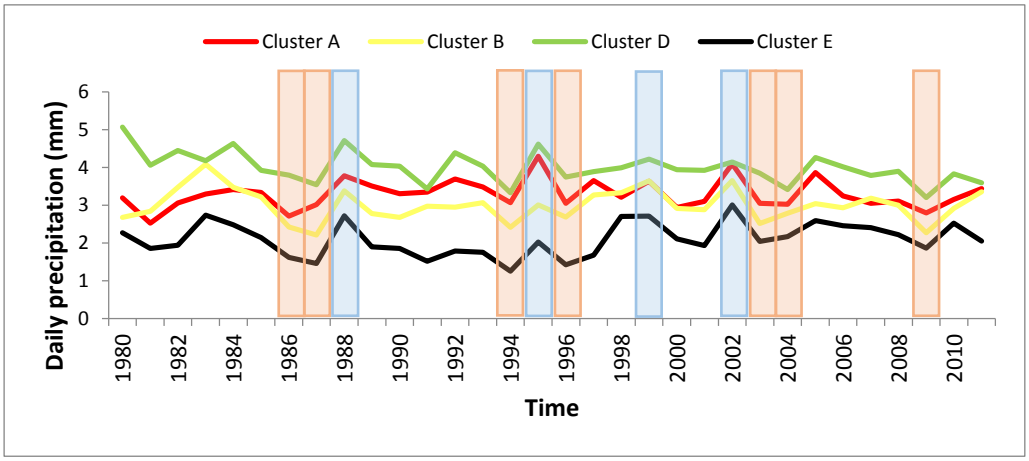


Figure 3-10. Cluster daily precipitation average (in mm) from 1980 to 2010. Each line represent the time series of each cluster. Red bars indicate the dry years and blue bars the wet years for all clusters.

In order to understand the clusters' distribution in more detail, in Figure 3-11 the resulting clusters (A-E) were mapped and overlapped with vegetation types, temperature and altitude across the Yucatan Peninsula and in Table 3-2 the

correspondence of each cluster with these layers is summarised. Temperature does not show any real pattern; however, it is interesting how vegetation types follow, to some extent, the cluster distribution. For instance, Cluster E is associated with mangroves, aquatic vegetation and tropical dry forest; there is one station in E in the south where the high perennial forest is, this point is located in the highest point of the Peninsula (Figure 3-11c) which is the station with less affinity in cluster E (see Figure 3-7).

Table 3-2. Table to show the distribution of cluster with different features in the Yucatan Peninsula

Cluster	Location	Vegetation types	Altitude (m.a.s.l.)	Mean Annual Temperature °C
A	Central part	Mainly medium semi-deciduous forest with some stations located in tropical dry forest, grasslands and agriculture	0 – 153	26-28
B	Central and northeast	Mainly tropical dry forest with various stations located in medium and high forest.	0 – 153	24-28
D	Southeast and southwest	Manly in high evergreen forest with some stations in the southwest in grasslands	0-71	24-28
E	North with one station in the south	Mainly tropical dry forest and aquatic vegetation	0-71 One station at the highest point (318)	24-28

The cluster analysis was useful to identify patterns in the data, and the results showed clearly coherent behaviour in terms of the north-south rainfall gradient and clustering. The area could be divided into three principal areas: the northern (cluster E); the middle part (clusters B and A); and the southern region (cluster D). Regionalising the precipitation in the Yucatan Peninsula is a valuable piece of research since there are no other studies of this type. The previous studies regionalised the Peninsula as a whole area, whereas the analysis done here shows the climatic variation across the Peninsula. However, the climatic variation is not completely detected just by a cluster analysis. Instead, it is possible to improve these results in combination with geostatistical methods.

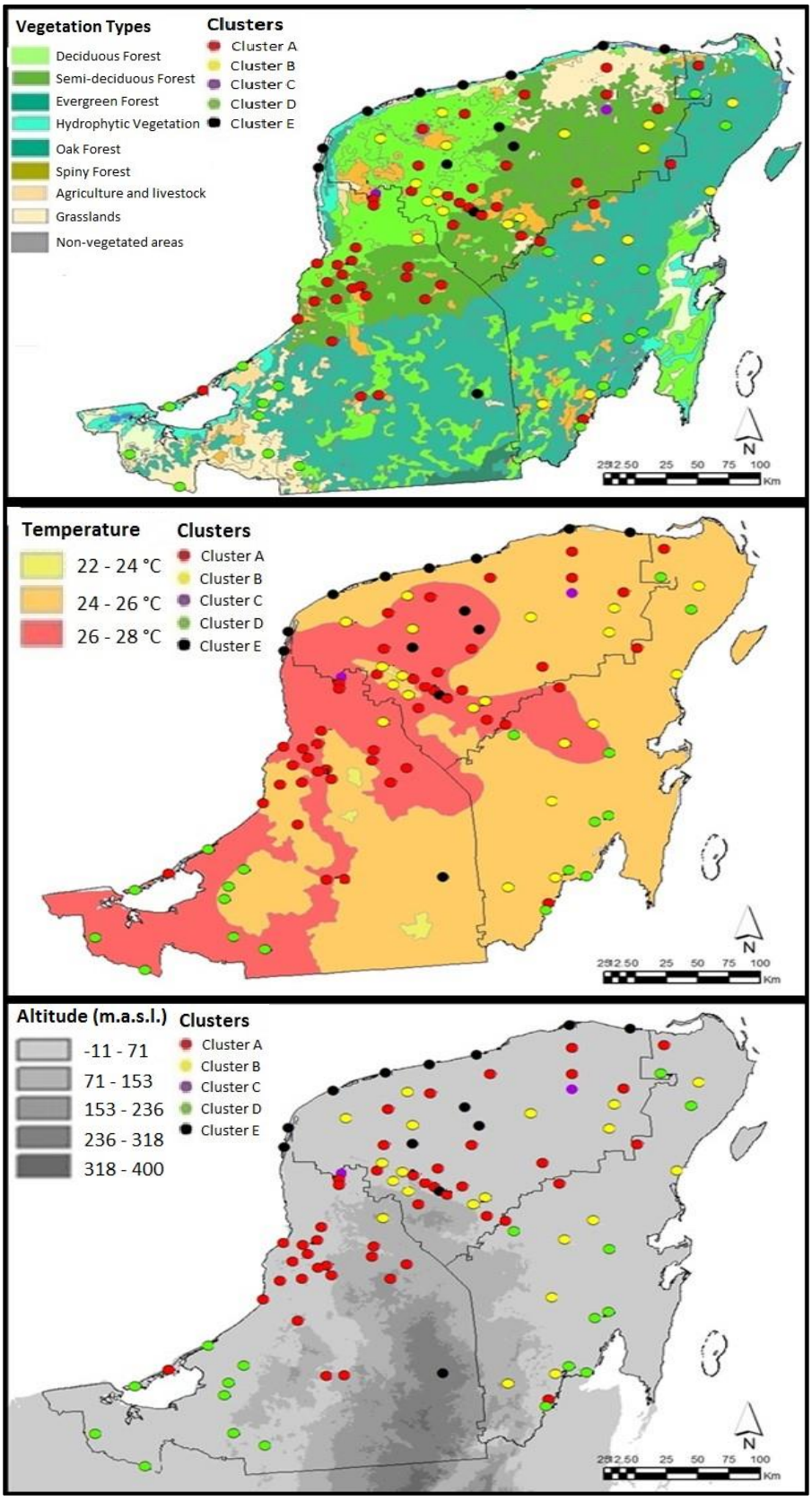


Figure 3-11.a) Vegetation types map overlapped with the five clusters (A-E) across the Yucatan Peninsula; b) Temperature ranges map overlapped with the five clusters (A-E) across the Yucatan Peninsula; c) Altitude in m.a.s.l overlapped with the five clusters (A-E) across the Yucatan Peninsula.

3.3.2 Kriging

Two long term precipitation maps were created; one using daily mean precipitation and the second one using the annual total rainfall. Both figures (Figure 3-12a and b) are the results for long term (1980-2011) precipitation. Both maps show the same precipitation pattern across the Peninsula, and these results are similar to those published by (García, 1998b) and Hodell et al. (2007) (Figure 2-5 and Figure 2-6 respectively) where the same gradient is shown: the northern part receives the least amount of rainfall, while the southern receives the most and the gradient of precipitation goes from northwest to the southeast. These results also are coherent with the cluster results discussed above.

The annual Kriging maps were created with the daily precipitation data in order to maximise the amount of data used and avoid the biases that NoData (NAs) bring to the study. In this case, a yearly matrix was created with the stations which have available data for the given year and the kriging maps were generated. The results are shown in Figure 3-13, where each map represents the average daily precipitation in each year from 1980 to 2011. The maps show that in the state of Campeche and in the south of Quintana Roo (see Figure 3-13) it rains more than the other regions and in the northern part rains less. However, there are changes in the spatial precipitation distribution; the general behaviour is less rain in the north and more rain in the south. There are some years (i.e. 1981, 1986, 1987, 1994, 1996, 2003, 2004, and 2009) showing clearly less rainfall than others and these years are reflected as well in every cluster (see Figure 3-10). 1998 in Figure 3-10 shows a different pattern from normal with a decrease in cluster A, but in contrast, cluster E (the northern and drier part) shows a peak; this could be reflected in the krigged map where the northern part of the Peninsula unusually has the same rain as the southern, which means more rain than the average for the northern part.

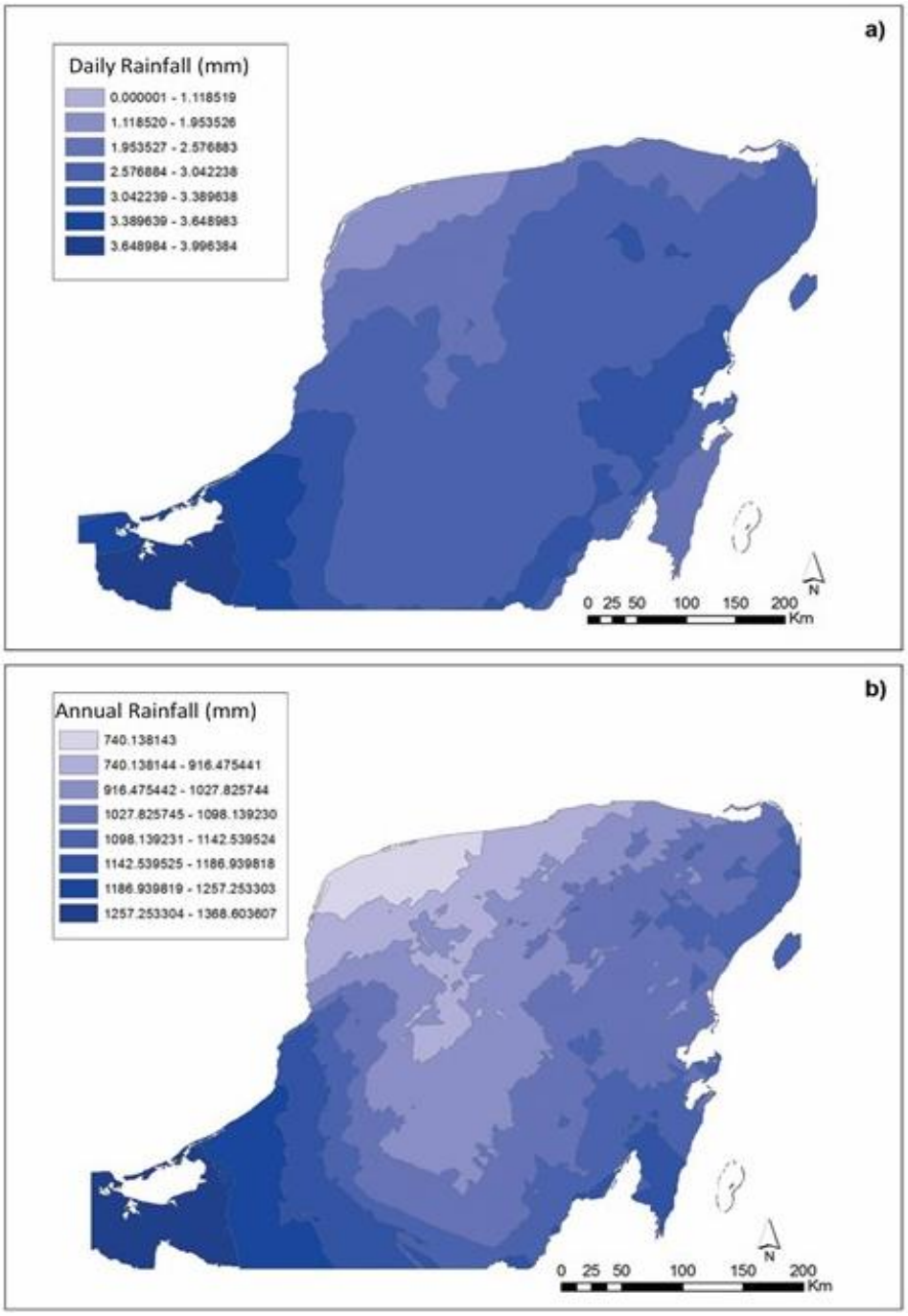


Figure 3-12. Long-term average (1980-2011) maps resulted from Kriging analysis. a) Long-term precipitation average from daily data. b) Long-term accumulated precipitation.

Wet years, are also coherent in both the annual krigged maps and the cluster results (Figure 3-10). For instance, in 1988, 1995 and 2002 were years with more rainfall than the other years. Despite the different amount of rainfall falling every year, there are no systematic trends towards drier or wetter conditions, this opens the research question of which are the processes involved in these wet and dry conditions.

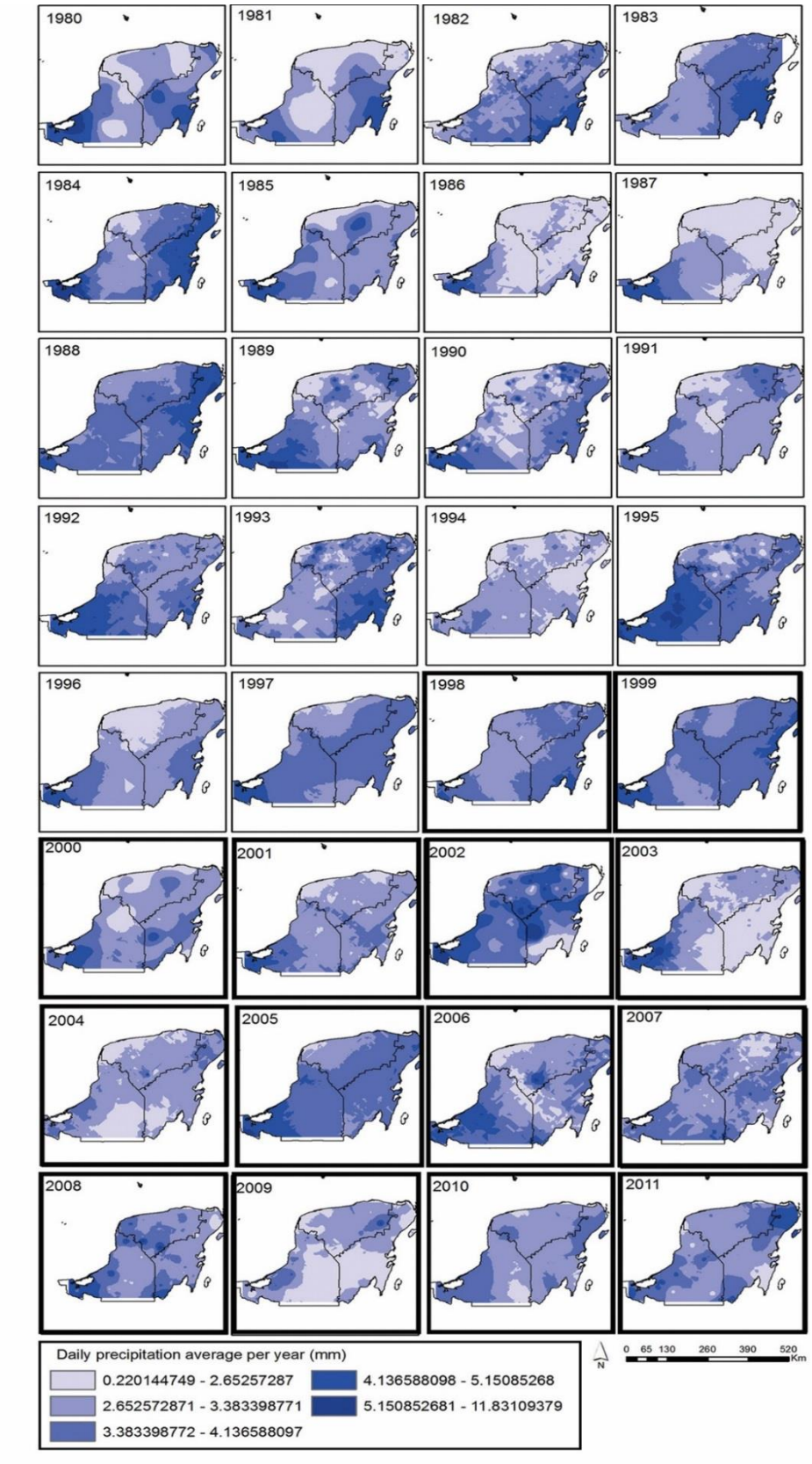


Figure 3-13. Maps (1980-2011) resulting from Kriging analysis. Each map represents the average daily precipitation for a given year in millimetres across the Yucatan Peninsula. Highlighted maps were validated with TRMM data. The number of stations used for creating each map are shown in Table 3-1.

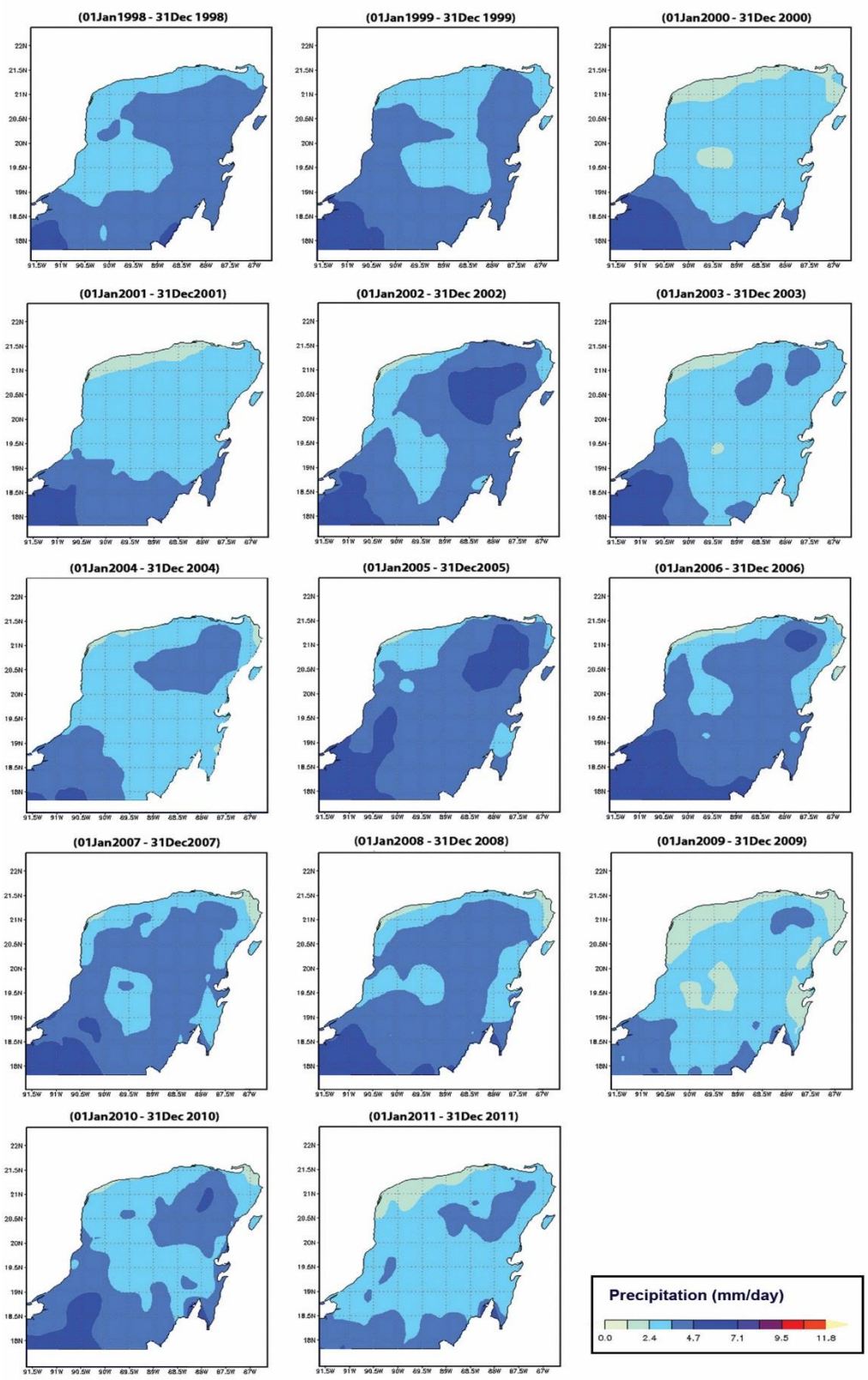


Figure 3-14. TRMM 3B42 v7 precipitation data (1998 – 2011). All maps were created with the TRMM Online Visualization and Analysis System (TOVAS) and they are a product from daily TRMM and Other Rainfall Estimate (3B42 V7) derived.

The TRMM 3B42 maps downloaded from the TRMM Online visualisation and Analysis System (TOVAS) are shown in Figure 3-14. These maps represent the average daily precipitation per year, which are comparable with those highlighted in Figure 3-13 (1998-2011). In general terms coherent patterns in precipitation regimes are exhibited. For example, 2003, 2004 and 2009 are in both datasets years with less precipitation than other years; whereas in 2002 and 2005 both datasets show strong blue colours (more rainfall) across the Peninsula.

The krigged maps validation results are summarised in both Figure 3-15 and Table 3-3. In Figure 3-15 the correlation results between TRMM 3B42 data against reduced-resolution krigged maps per year are plotted as a scatterplots. The reduced-resolution maps were done by resampling to a coarser resolution. Each graph represents each year from the period 1998 to 2011. In the x-axis the precipitation values derived from the TRMM 4B42 v7 are plotted and the kriging data is represented on the y-axis. From these scatterplots we can see that the relationship between the two datasets is linear and therefore the appropriate measure to describe their dependence is the correlation coefficient.

In Table 3-3, the correlation results are summarised. First column presents the Pearson correlation coefficients, second column the p-values for the test of statistical significance and in the last two columns the 95% confidence intervals. All correlation coefficients are positive and statistically significant and show a good match between kriging and TRMM maps. Correlation was stronger in the years 2000, 2001, 2003, 2005 and 2006; whereas moderate correlation values occur in 2004, 2007 and 2008. Finally, the 1998, 1999, 2002, and 2009-2011 showed the smallest values of correlation. It is interesting to point out that those years with higher correlation are significant spatially coherent.

Table 3-3. Correlation values between the TRMM data and the resulting Kriging data per each year (1998-2011). First column presents the Pearson correlation coefficients, second column the p-values for the test of statistical significance and in the last two columns the 95% confidence intervals

Year	Pearson correlation coefficient (r)	Regression coefficient (R^2)	2-tailed p value	Confidence interval for r	
1998	0.355334748	0.126262783	0.00000098	0.518856192	0.476816736
1999	0.280659884	0.078769971	0.00013552	0.140149749	0.410088949
2000	0.703262807	0.494578576	0.00000000	0.620862355	0.77029263
2001	0.720449845	0.519047979	0.00000000	0.641818387	0.784089437
2002	0.204728428	0.041913729	0.00583617	0.060269847	0.340787127
2003	0.70676979	0.499523537	0.00000000	0.625128852	0.773112948
2004	0.380396965	0.144701851	0.00000014	0.24792789	0.498902295
2005	0.699639492	0.489495419	0.00000000	0.616459453	0.767376001
2006	0.587254343	0.344867664	0.00000000	0.48242864	0.675496703
2007	0.453546059	0.205704028	0.00000000	0.329115315	0.562495057
2008	0.45300014	0.205209126	0.00000000	0.328502513	0.562025184
2009	0.343627458	0.11807983	0.00000233	0.207808622	0.466447101
2010	0.309116018	0.095552713	0.00002419	0.170564312	0.435681173
2011	0.375582388	0.14106213	0.00000020	0.242648718	0.49467146

It is important to remember that the kriging maps were aggregated, and so some information could be lost. In almost all years (except 2003 and 2007), as a general pattern, the TRMM data underestimates the values in comparison with the kriging maps. Some findings in the literature have shown that TRMM data underestimates precipitation values. However, in 2003 and 2007 in the north of the Peninsula, the kriging maps underestimate amount of rainfall as it is also shown in the scatterplots (Figure 3-15). It should be mentioned that the two datasets are different, the krigged maps are interpolated and the TRMM data uses passive microwave (PMW)-calibrated and IR to estimate precipitation, thus the reliability of the data should be treated carefully. However, still both datasets are coherent in almost all years.

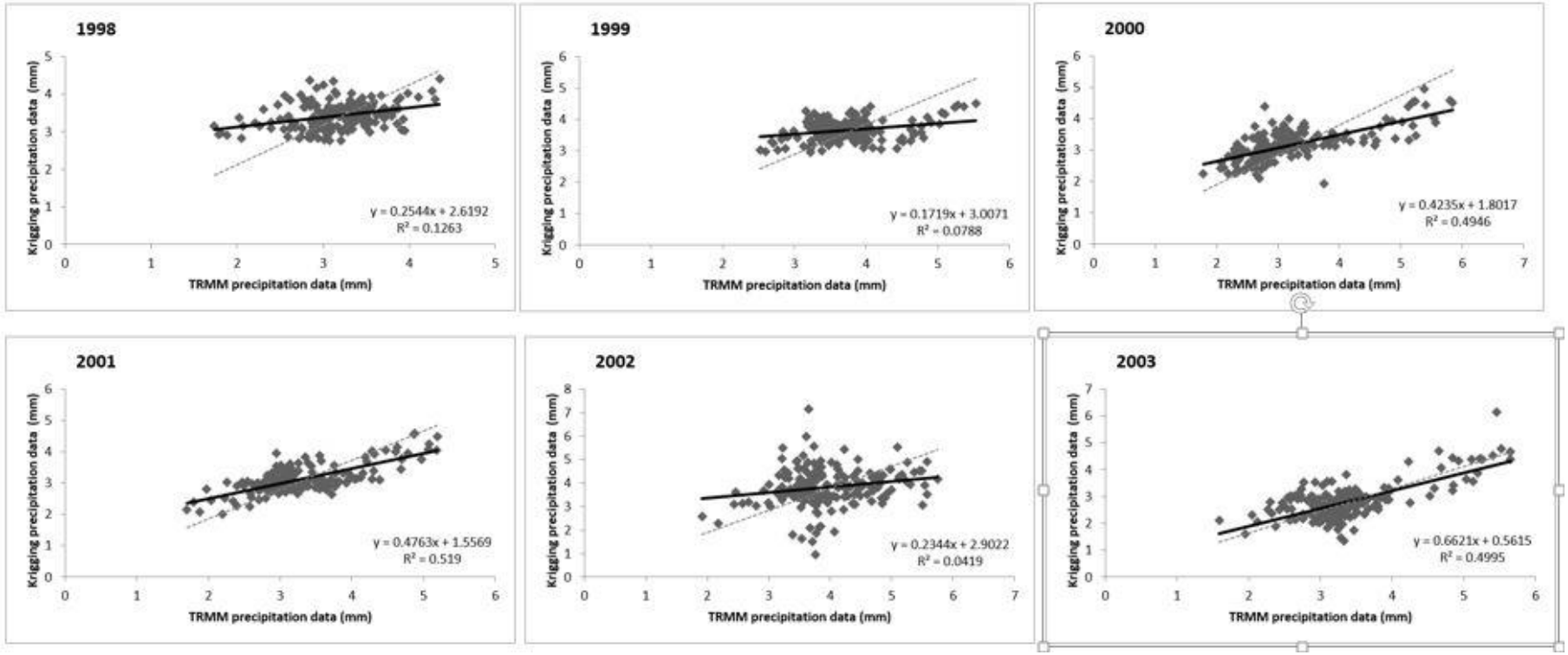


Figure 3-15. Relationships between resulting kriging maps and precipitation from TRMM 3B42 product. Every plot represent each year from 1998-2011. R^2 shows the square root of Pearson correlations

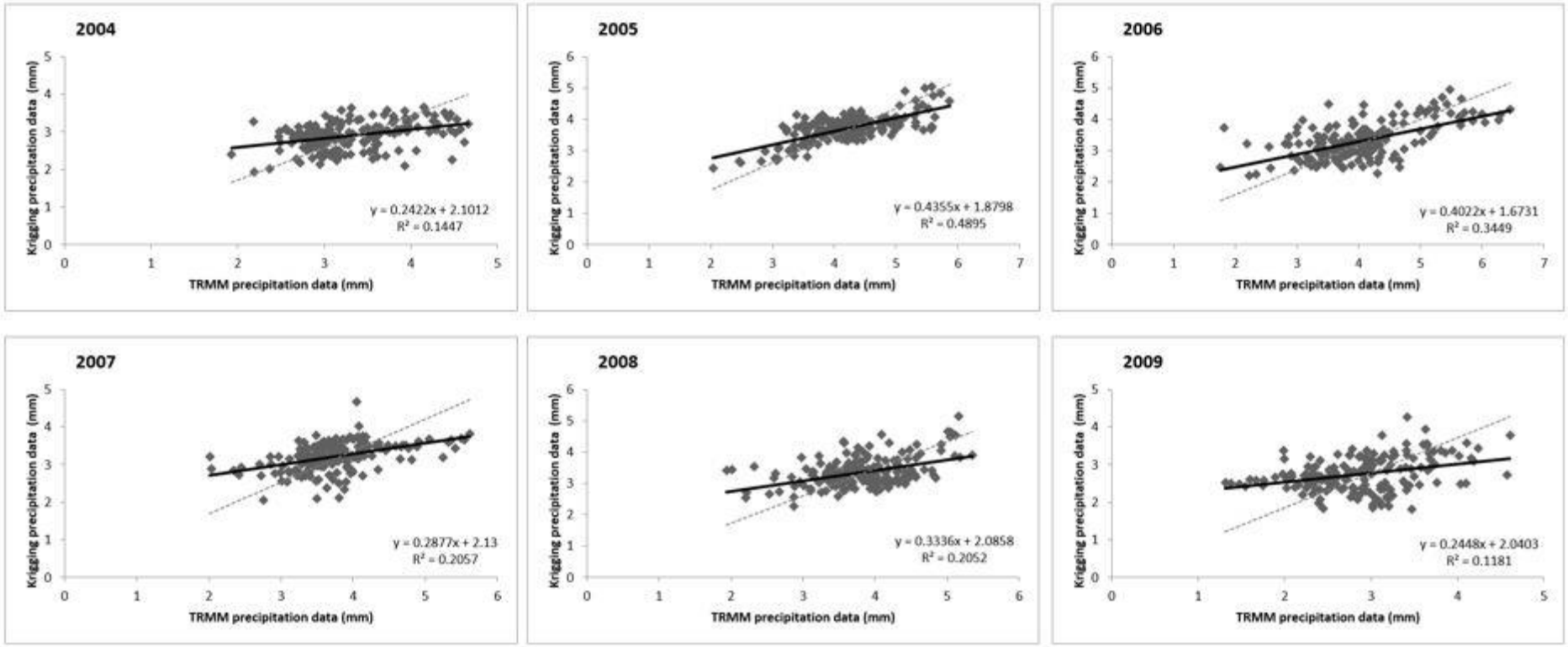


Figure 3-15 (cont.). Relationships between resulting kriging maps and precipitation from TRMM 3B42 product. Every plot represent each year from 1998-2011. R^2 shows the square root of Pearson correlation

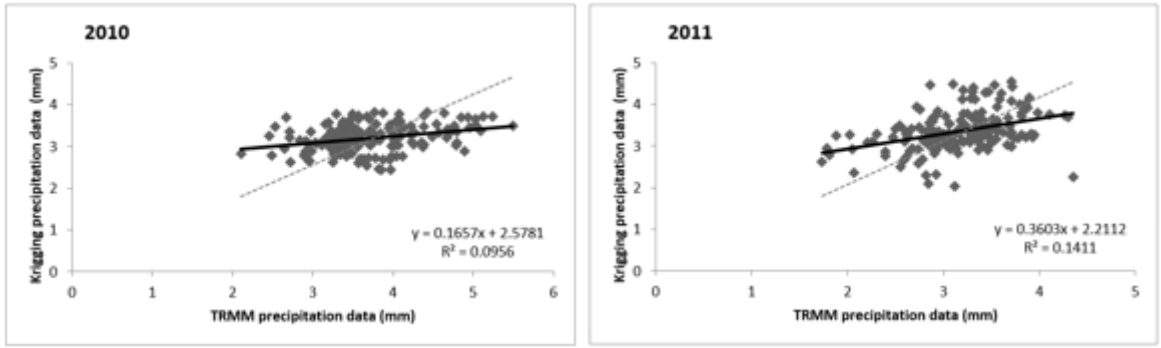


Figure 3-15 (cont.). Relationships between resulting kriging maps and precipitation from TRMM 3B42 product. Every plot represent each year from 1998-2011. R^2 shows the square root of Pearson correlation.

3.3.3 Monthly analysis

As has been mentioned before, the Peninsula has a rainy period and a dry period every year, making this area strongly seasonal. For this reason is important to understand and analyse the rainfall on a monthly basis and see what mechanisms could be detected in this time scale.

Figure 3-16 shows the long term monthly precipitation for each cluster. The first notable feature, as pointed out before, is the clear dry and wet periods in winter and summer respectively. The rainy period is from June to October, and the dry period starts in November and lasts until May, when the rainfall starts increasing. The lowest amount of rainfall is during February and March, while the highest amount of rainfall in the Peninsula occurs in September (Figure 3-16). Despite this dry season, it is interesting to point out that there are always rain events during the dry season across the Peninsula and they are related also with cold fronts as mentioned in section 2.3.1. In the boxplots (Figure 3-16) it is possible to identify the midsummer drought (*canicula*) which occurs during July and start increasing during August.

The boxplot figures (Figure 3-16) show the variability of the data for each cluster and this reveals that the variance between clusters is not uniform; instead, it seems that more variance is present where rainfall amounts are higher (cluster D); while lower amounts of precipitation show less variance in the data (cluster E).

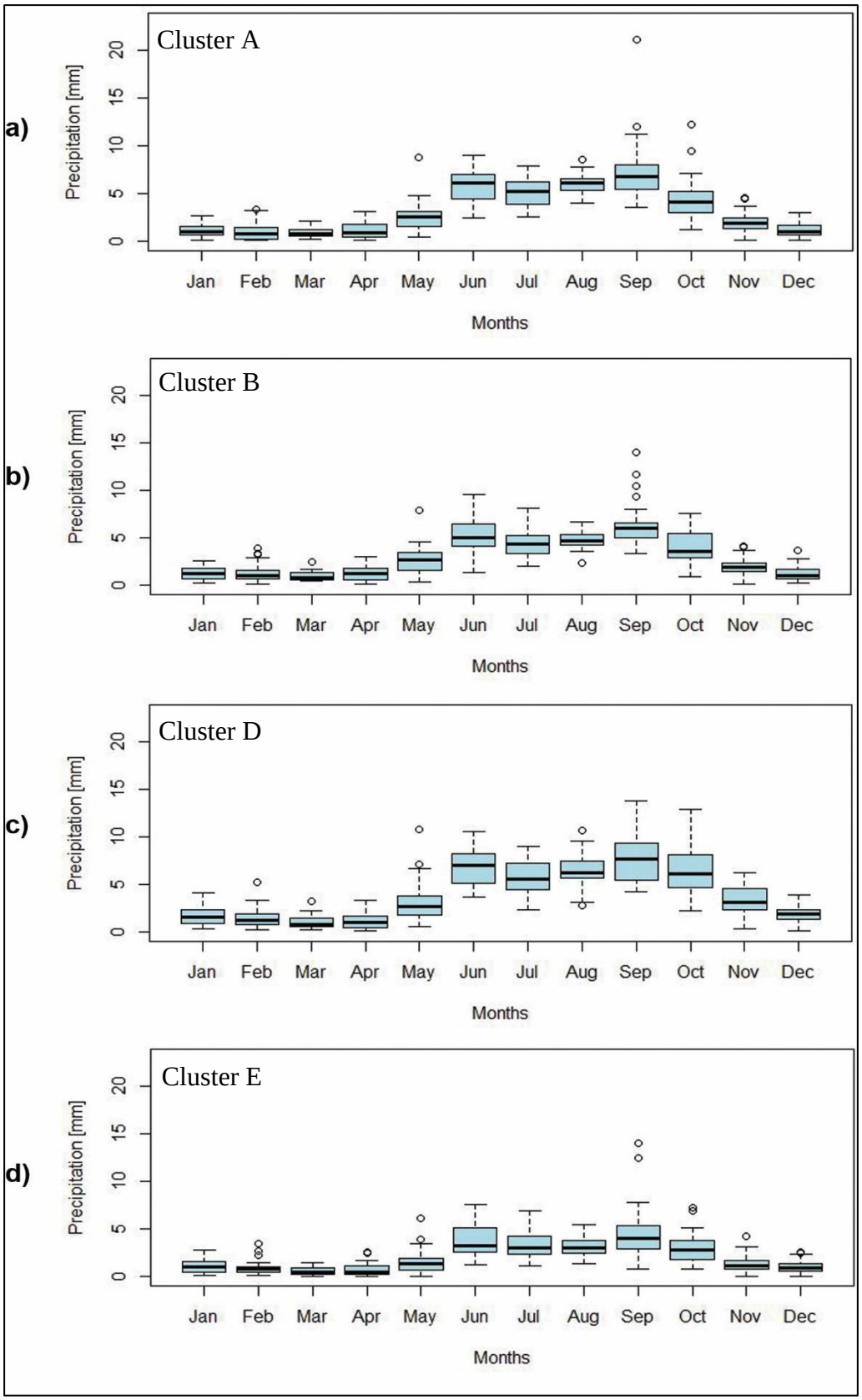


Figure 3-16. Boxplots of daily average precipitation by month. X-axis represents the months and y-axis represent the daily precipitation average. The lines in the middle of the boxes represent the mean and the whiskers represent the standard deviation, while the points represent outliers. a) Cluster A; b) Cluster B; c) Cluster D; d) Cluster E

In the coloured matrices shown in Figure 3-17 the seasonality pattern can be seen as well. These figures represent the average daily precipitation in each month and year. On the x-axis every year is represented and the months are represented on the y-axis. The colours represent the amount of rainfall in the given month and year. Therefore, it is easy to compare visually between months and years in these plots. For instance, all the matrices change colour during the rainy season and the dry season, showing the basic seasonality pattern. However, the total amount of rain between the different clusters is different. For example, it is evident that cluster E is the driest and it is marked by a predominance of red colour (Figure 3-17d), while cluster D (Figure 3-17c) is the wettest and it has most rainfall events even during winter, in particular during November and December and a smaller amount, but still with some rainfall, in January and February (Figure 3-17c). This latter cluster is the least seasonal cluster as it is a region where more rain falls in winter and summer. It is located in the southern part of the Peninsula closer to the area where the highest precipitation falls in all Mexico (49.6% of the total amount of the country) (Esparza, 2014). Monthly analysis coincides with the yearly cluster analysis (section 3.3.1). Clusters A and B are between clusters D and E in terms of rainfall amount and they are located in the north and central part of the Peninsula. The amount of precipitation in each cluster varies, for instance, in cluster E rainfall does not exceed 7 mm per day. In contrast, clusters D and A have maximum values in almost 10 mm a day.

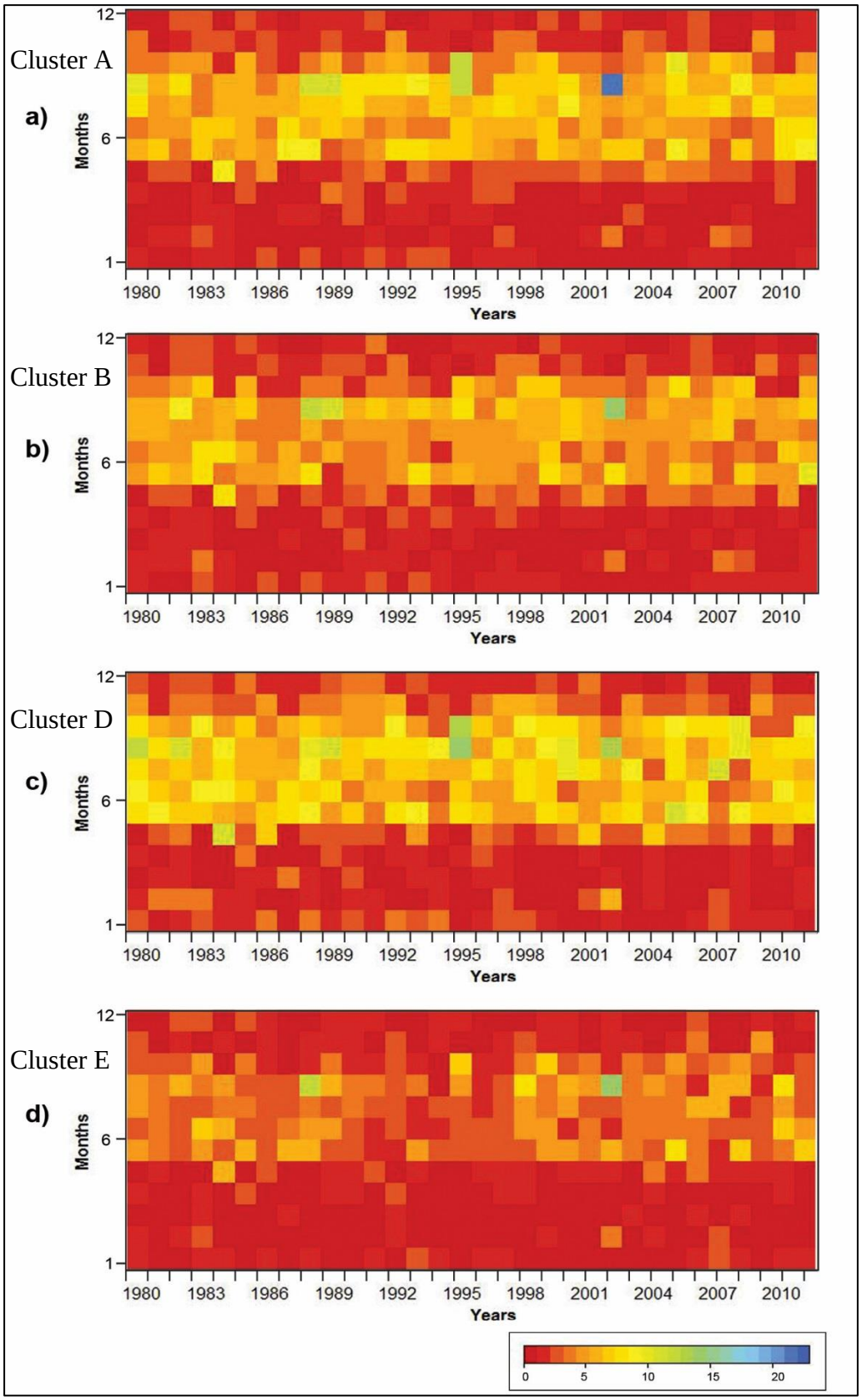


Figure 3-17. Matrix plots of daily average precipitation by month. X-axis represent the years (1980-2011) and y-axis are the months. a) Cluster A; b) Cluster B; c) Cluster D; d) Cluster E. Different colours represent the amount of precipitation in mm.

Other special events that can be seen in all matrices are the highest amount of rainfall in a given year and month, these are represented by the blue squares in the matrix. Hurricanes and tropical storms (Table 3-4), as mentioned in section 2.3.3, are important events that hit the Peninsula every year, with the highest activity during September and October; some of these hurricanes can be seen in all the matrices. For example, the highest amount of rainfall recorded for all clusters and almost for all individual stations was in September 2002, which was the month that hurricane *Isidore* (category III), hit the Mexican coast producing a large amount of rainfall over two days (Hodell et al., 2005) and causing major social and economic impacts (the government declared a disaster area). Similarly, in 1988, the clusters show an increase in rainfall amount coinciding with hurricane *Gilbert* (category V); in 1995 with the tropical storm named *Opal*, and in 2007 hurricane *Dean*. However, there are some other hurricanes (Table 3-4), such as *Katrina* and *Mitch*, which are not reflected in the cluster data matrices but some individual stations record high amounts of rainfall and it is reported that they caused lot of material damage across the Peninsula. Some hurricanes in the Peninsula just hit the area for some hours others stay longer bringing more rainfall (Figure 3-18). The amount of rainfall they bring depends on both the path they take and the time they take. It is important to mention as well that the hurricanes season could be delayed as it was in 1988 and 2009; this could also affect the general pattern of precipitation.

Table 3-4. Tropical depressions (TD), tropical storms (TS), and hurricanes (categories I to V) at the Yucatan Peninsula from 1980-2011.

Date	Wind (Km/hr)	Category	Name
07/08/1980	190	V	*Allen*
22/09/1980	50	TS	*Hermine*
02/06/1982	20	TD	*Alberto*
02/09/1986	20	TD	*Unnamed*
14/09/1988	167	V	*Gilbert*
21/11/1988	69	TS	*Keith*
04/08/1990	45	TS	*Diana*
18/09/1993	35	TS	*Gert*
04/06/1995	58	TS	*Allison*
30/09/1995	35	TS	*Opal*
11/10/1995	115	III	*Roxanne*
20/08/1996	65	TS	*Dolly*

04/11/1998	35	TS	*Mitch*
01/01/1999	25	TS	*Katrina*
17/09/2000	65	TS	*Gordon*
03/10/2000	30	TS	*Keith*
21/08/2001	45	TS	*Chantal*
21/09/2002	127	III	*Isidore*
29/06/2003	20	TD	*Bill*
11/07/2003	58	TS	*Claudette*
29/09/2003	20	TD	*Larry*
04/07/2005	25	TD	*Cindy*
21/10/2005	138	IV	*Wilma*
02/10/2005	46	TS	*Stan*
18/07/2005	132	IV	*Emily*
15/12/2007	30	TD	*Olga*
21/08/2007	150	H5	*Dean*
31/05/2007	25	TD	*Barry*
21/07/2008	52	TS	*Dolly*
31/05/2008	40	TS	*Arthur*
08/11/2009	98	II	*Ida*
27/06/2010	55	TS	*Alex*
15/09/2010	55	TS	*Karl*
25/10/2010	40	TS	*Richard*
13/10/2010	98	II	*Paula*
23/08/2011	50	TS	*Harvey*
27/10/2011	50	TS	*Rina*

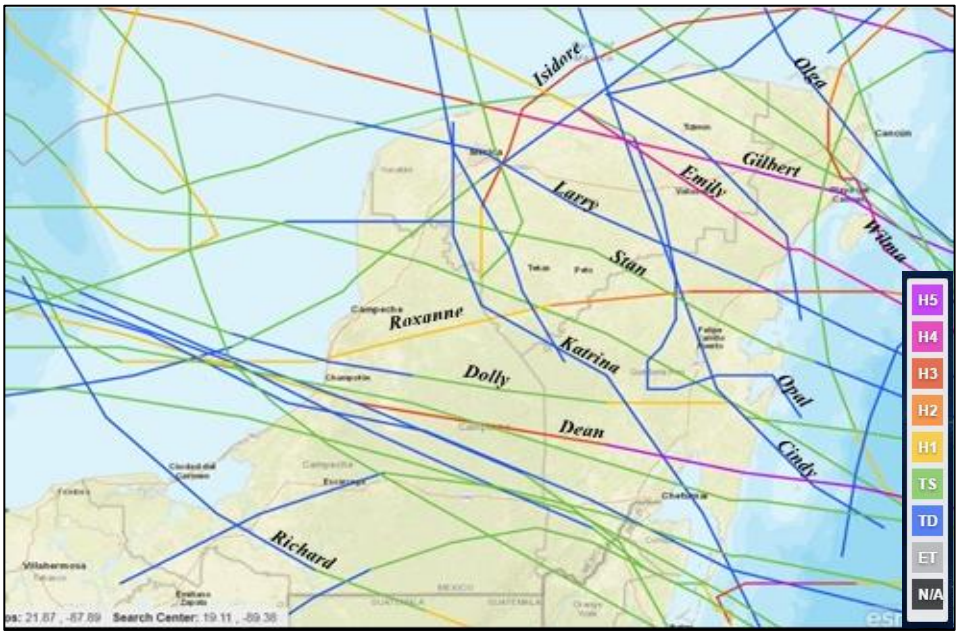


Figure 3-18. Routes of hurricanes and tropical storms from 1980 – 2011. Different colours represent the hurricane category (Taken from: NOAA (2016)). Strongest hurricanes are labelled.

3.4 Precipitation anomalies

3.4.1 Drought detection in clusters

SPI was computed and analysed for each cluster and the results are summarised in the Figure 3-19. It shows the SPI computed for each cluster at different time scales (1 to 12 months). Years (from 1980 – 2011) are on the x-axis and the y-axis represents the time scale (months). All clusters show a pronounced recurrence of dry periods (red/orange colours) in 1980, 1986-1987, 1994 (see also Figure 3-10 and Figure 3-13), and 2009 especially in the longer time scales of SPI and some wet periods such as in 1983 (blue/green colours). This figure exhibits that when analysing droughts with longer SPI time scale, stronger droughts can be detected (from orange to red colours in the verticals). It is interesting to point out that there are some years (e.g. 1988, 1995, and 2004) when the dry and wet periods do not behave the same in all clusters.

Different values of SPI between both time scale and years indicate the spatial variability of droughts across the area. For example, as mentioned above, 2004 presents different values between clusters; in cluster E (northern) conditions were wetter, whereas cluster D, B and in lesser extent A present dry conditions. These findings are coherent with some patterns that could be seen in Figure 3-13 and Figure 3-10, where the northern part of the Peninsula seems to have normal conditions, while the southern part has less amount of rainfall per year.

SPI was calculated for 1 (SPI-1), 3 (SPI-3), 6 (SPI-6), 9 (SPI-9), 12 (SPI-12) month period. The time scale showed in the following figures will be just for 3, 6 and 12 months to try to focus on water deficit that does not reflect the normal rainfall variability and focus more on drought periods.

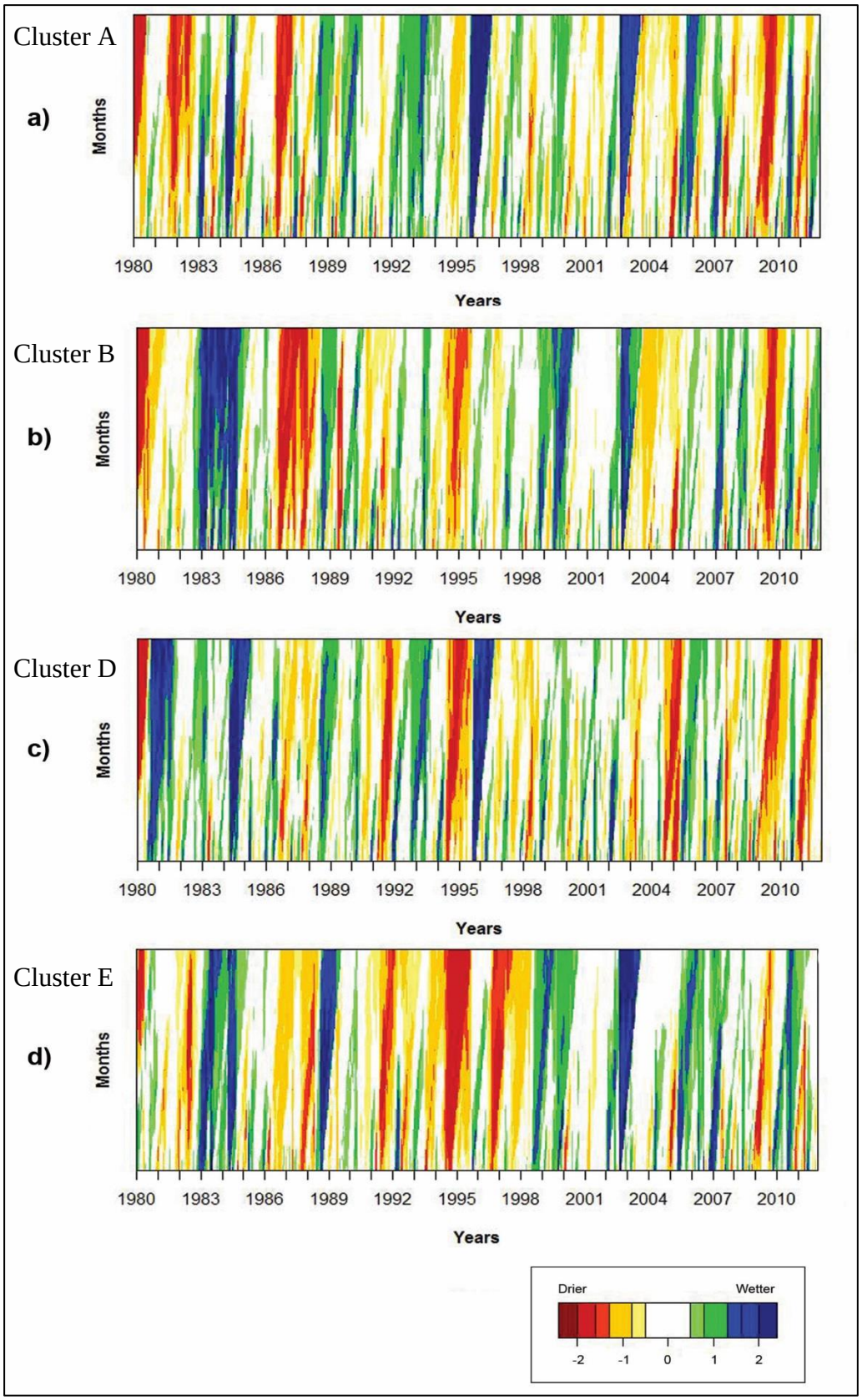


Figure 3-19. Standardized Precipitation Index (SPI) computed for each cluster at different time scales (1 to 12 months). Year from 1980 – 2011 on x-axis and y-axis represents the SPI time scale (months) from SPI-1 to SPI-12 for each cluster.

In the following figures (Figure 3-20 to Figure 3-23) the time series of SPI-3, SPI-6, and SPI-12 for clusters is shown in the period 1980-2011. Same plots are shown in appendix 2 (Figure B - 1, Figure B - 2, and Figure B - 3) but by SPI period rather than by cluster. Different time scales show different patterns. For instance, in SPI-3 figures (Figure 3-20a to Figure 3-23a) the *canicula* can be seen during June and July as this period of time reflects rainfall seasonality and medium term moisture conditions (see circles in Figure 3-20a to Figure 3-23a). In the 6-month SPI figures (Figure 3-20b to Figure 3-23b) the precipitation in different seasons is shown, for instance, SPI positive values increase around May and June and decrease in November in almost all years, showing the wet season.

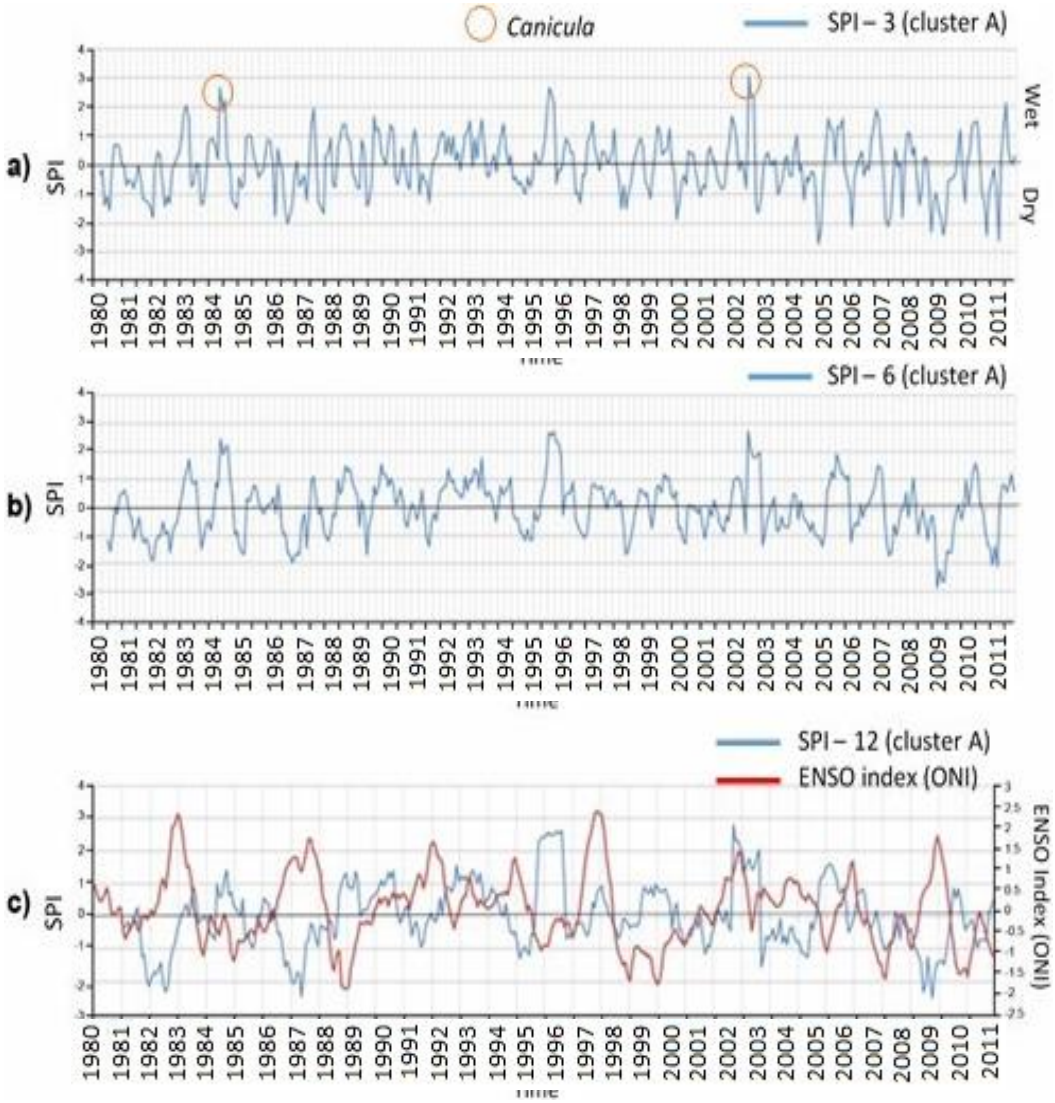


Figure 3-20. 3, 6, and 12-month SPI values for cluster A. c) shows the 12-month SPI in the primary axis and the Oceanic Niño Index in the secondary axis

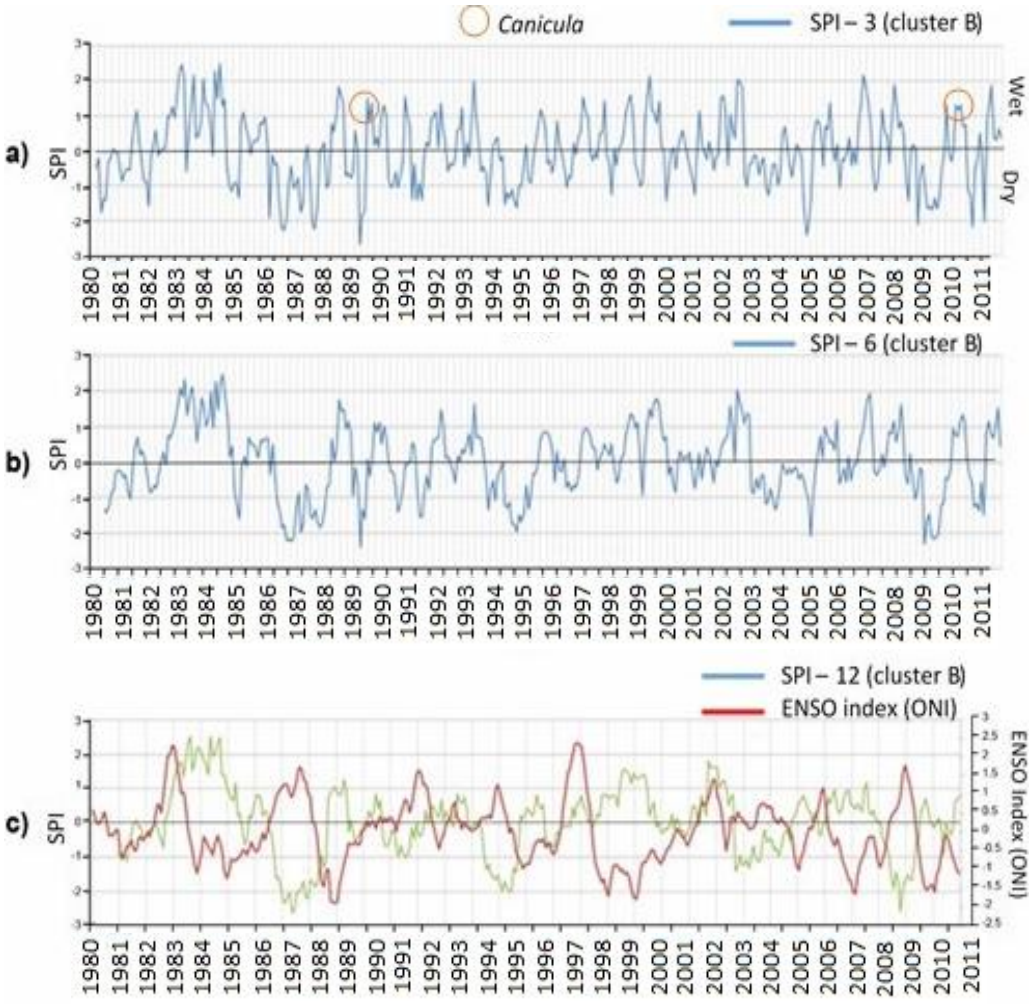


Figure 3-21. 3, 6, and 12-month SPI values for cluster B. c) shows the 12-month SPI in the primary axis and the Oceanic Niño Index in the secondary axis

The SPI-12 (Figure 3-20c to Figure 3-23c) shows both drought events and extreme wet periods for each cluster between 1980 and 2011. It can clearly be seen that some years present SPI values less than -1.5. However, not all the clusters present these values in the same years. The only two years that coincide in all clusters are 1994 and 2009; the latter is a year that CONAGUA declared as one of the strongest droughts in some parts of the Peninsula principally in the state of Yucatan (north part) (Estrada Medina and Cobos Gasca, 2014). On the contrary, and as shown in the same plots, they reported 1995 as a period with higher rainfall, which could be due to the high amount of rainfall during

September. Conversely, the data in this study do not coincide with the report in Márdero et al. (2012) where 1995 is a drought year.

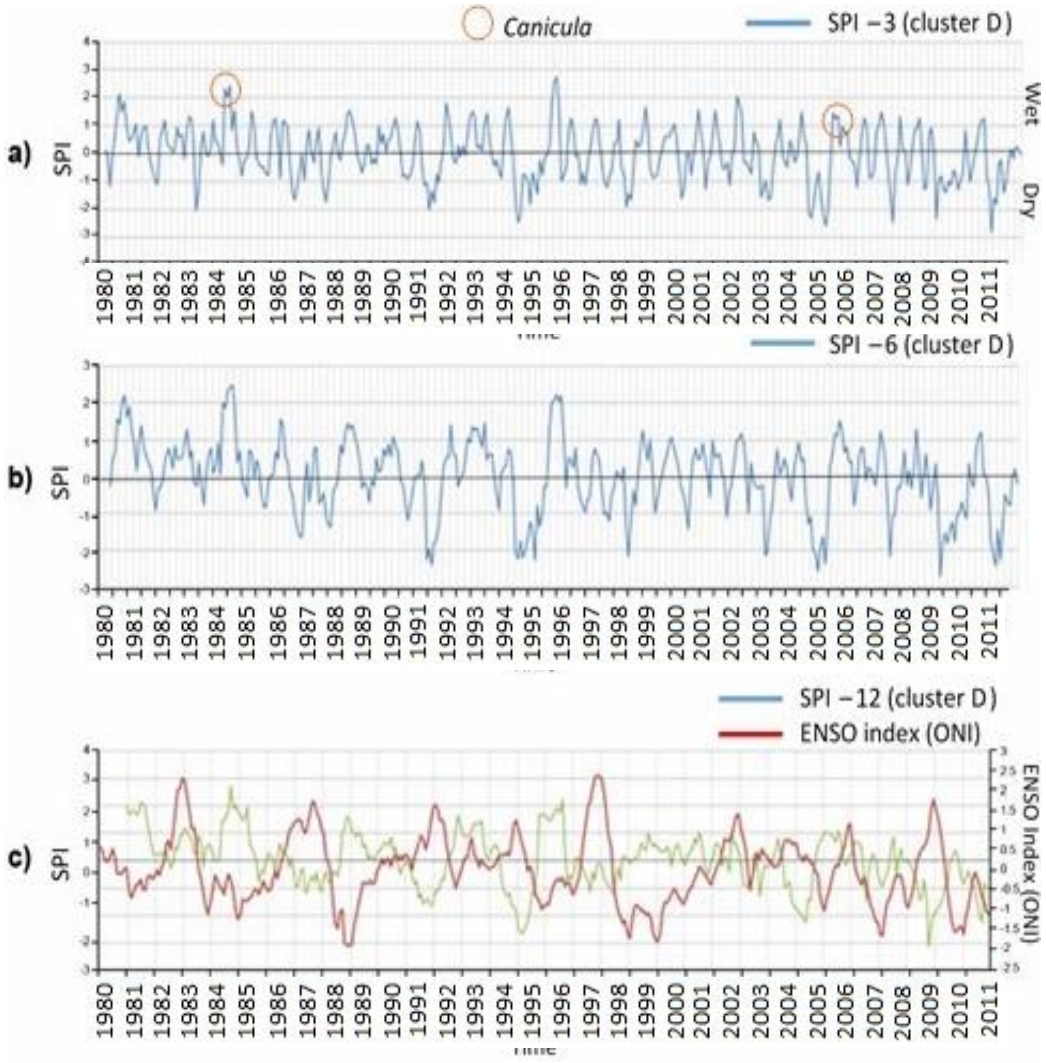


Figure 3-22. 3, 6, and 12-month SPI values for cluster D. c) shows the 12-month SPI in the primary axis and the Oceanic Niño Index in the secondary axis

In the north part of the Peninsula, cluster E presents SPI values less than -1.5 (Figure 3-23) in 1992, 1994, 1997 and 2009; whereas, in the southern part (cluster D) (Figure 3-22), where more rain falls, the driest years are 1991, 1994, 2005, 2009 and 2011 as seen also in Figure 3-10. In addition, clusters A and B had drought periods during 1987, 1995 and 2009. On the contrary, the wet periods vary between clusters; the northern cluster E (Figure 3-23) is wetter in 1983, 1984, 1988-89, 2002 and 2010. Two of these years coincide with two

important hurricanes (*Gilberto* and *Isadore*). Cluster D (southern) instead has wet periods during 1981, 1984 and 1996. It is important to mention that the SPI values show if a station or cluster (in this case) is wet or dry relative to the historical average for the same station or cluster and not the total rainfall amount, which is an advantage as every cluster is analysed against itself long term and not against the other clusters (Giddings et al., 2005).

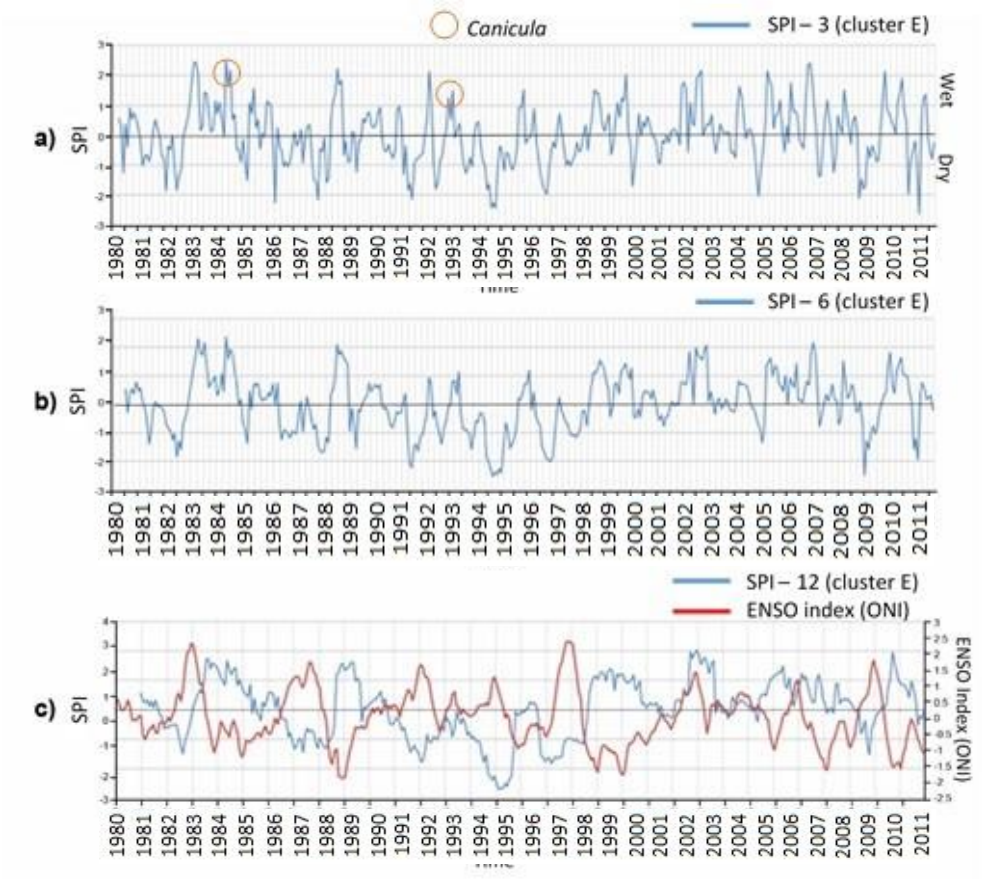


Figure 3-23. 3, 6, and 12-month SPI values for cluster E. c) shows the 12-month SPI in the primary axis and the Oceanic Niño Index in the secondary axis

3.4.2 Precipitation anomalies maps

To analyse and understand more deeply the spatial and temporal variability in the Yucatan Peninsula, the rainfall anomalies (the difference between the long term average and individual year) were mapped. In Figure 3-24 every map represents the results for each year and it exhibits deviations from the mean (two standard deviations for every change of colour). It is clear that the anomalies spatial distribution is not equal across the entire Peninsula, there is no year which presents just a negative or positive anomaly across the Peninsula. Every year has both negative and positive anomalies. However, it is shown that some years present bigger areas with negative anomalies (drier) such as 1987, 1991, 1992, 1994, 1999, and 2009.

If we compare these anomaly maps with the previous results (section 3.4.1), it is possible to see some coherent patterns within the wettest and driest clusters. For example, in 1982, 1988, 1992, 1994, and 1997 the northern part of the Peninsula is drier than the normal (Figure 3-24), and in cluster E the driest years present SPI values below -1.5 (Figure 3-23). In contrast, the south and east of the Peninsula (cluster D) present negative anomalies in 1991, 1994, 2005, and 2009. The same pattern is exhibited in 1987 and presents negative SPI values in cluster A and B (Figure 3-20 and Figure 3-21).

Estrada Medina and Cobos Gasca (2014) reported 2002 as the wettest year in the period 1982-2012; during this year in September a hurricane (*Isidore*) hit the Peninsula (see blue squares in Figure 3-17), bringing with it great amounts of rain, reflected in the centre part of the Peninsula in 2002 (Figure 3-24). There are however a few years without any agreement with the data reported in the literature; for example, as stated before and reported by Estrada Medina and Cobos Gasca (2014), 2009 was declared as one of the driest years for the state of Yucatan (north) and the results presented here (Figure 3-24, Figure 3-10, Figure 3-13, and Figure 3-14) do not show dry conditions in the north, instead it seems to be wetter than normal.

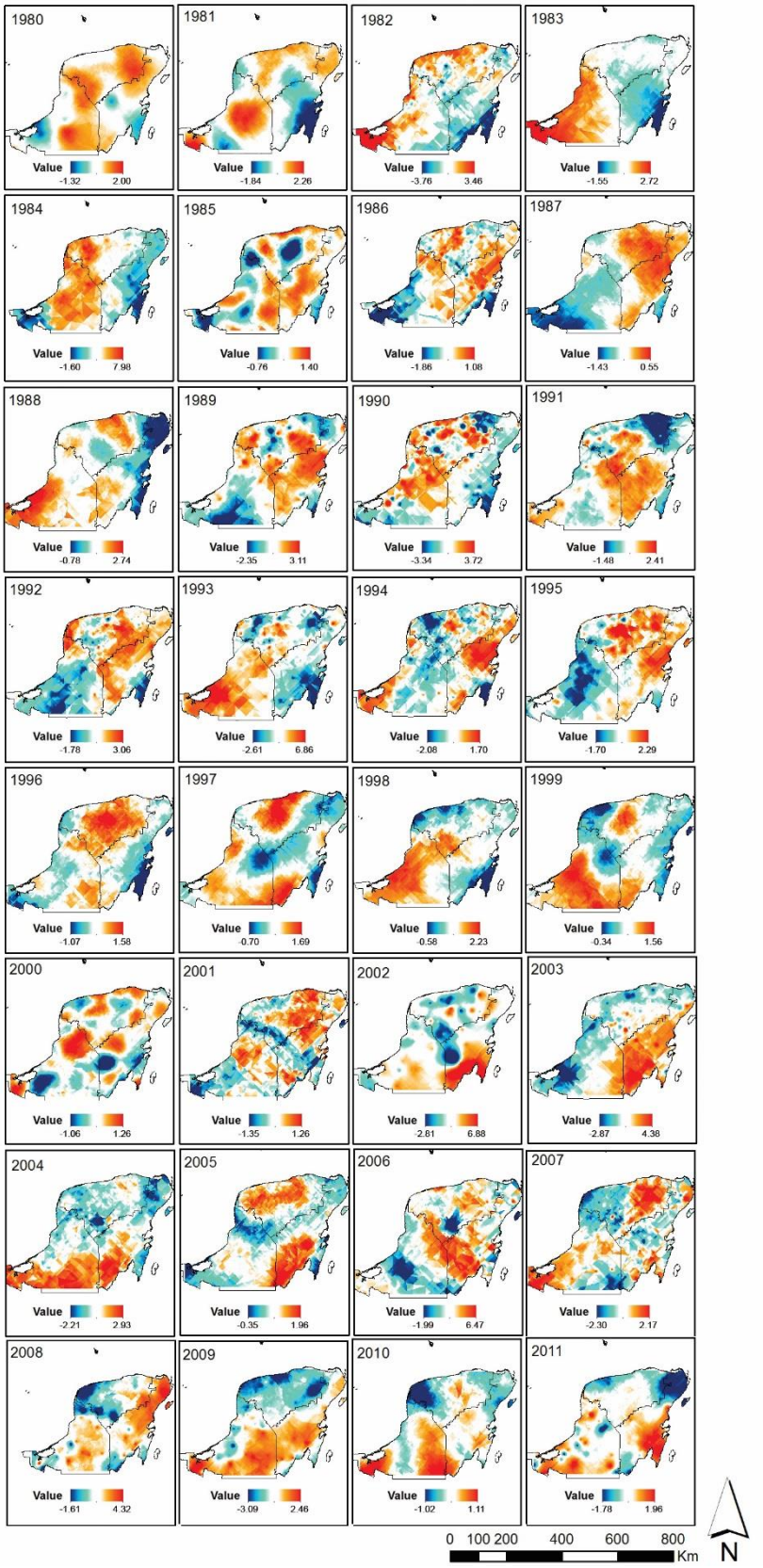


Figure 3-24. Maps showing the difference between the long-term average precipitation and annual average precipitation in mm. Each map represent each year from 1980-2011.

These previous results are based on a method with several pronounced drawbacks which may result in misleading conclusions. Subtracting a common mean in time does not seem realistic because there are several affects which span across long periods or short periods of time. The latter refers to global phenomena, for example ENSO years, hurricanes, etc. could bring more or less precipitation during winter or summer and this could be reflected in the annual mean. Furthermore, the previous method does not control for the variance of the above anomalies; the mean could be affected by extreme values and the strong seasonality in this area. Thus, major rainfall events (e.g. tropical storms) could affect the annual average precipitation, and then in annual maps some results could be hidden and misinterpreted. In other words, the long-term precipitation average in reality is moving year by year, taking 32 year averages these movements on the mean could not be seen. Therefore, a method which captures these seasonal effects would be a more accurate method of measuring dry or wet periods through time.

3.4.3 Kriging SPI

In order to improve and complement the previous analysis, SPI surfaces were created with the same technique as the precipitation dataset. For this analysis, results concerning the 12-month time scale are presented. Figure 3-25 shows the spatial and temporal variability of drought events for the period of 1980 – 2011. The results show that the severe drought years were 1981, 1986, 1987, 1994, 1996, 2004 and 2009 (Figure 3-25). These findings are coherent with those resulting from the cluster analysis showed in Figure 3-10. Also, these results coincide with some reported in the literature. For instance, Giddings and Soto (2003) reported 1986 and 1987 as dry years in the central and north part of the Peninsula, and Márdero et al. (2012) reported 1986 and 1994 as the years with largest negative anomalies during the period of 1953 – 2007; and 1987 with weaker negative anomalies.

On the other hand, Figure 3-25, also shows those year with wetter conditions. Results show that 1983, 1984, 1988, 1992, 1995, 2002, and 2005 are years with positive SPI values (wetter years). In these maps could be identified some facts already discussed in previous sections (see sections 2.3 and 3.4.2). For instance, in 2002 when the hurricane *Isidore* hit the Peninsula, it is reported that *Isidore* brought great amounts of rain in the north part and it is also reflected in Figure 3-25. In addition, Salas et al. (2014) found that during El Niño years 1982-83 and 1997-98 the conditions on the Yucatan Peninsula were wetter than the normal which are also coherent with our results. The highest values of SPI in some years (1983, 1984, 1997, and 1999) are registered in the east coast, which is more exposed directly to trade winds as noted also by Márdero et al. (2012).

SPI kriging maps in combination with the analysis of precipitation variability (section 3.3.2) and the cluster analysis (section 3.3.1) give valuable information about the occurrence of droughts in the Peninsula, which afterwards would be useful to understand the relationship between droughts and their impact on vegetation.

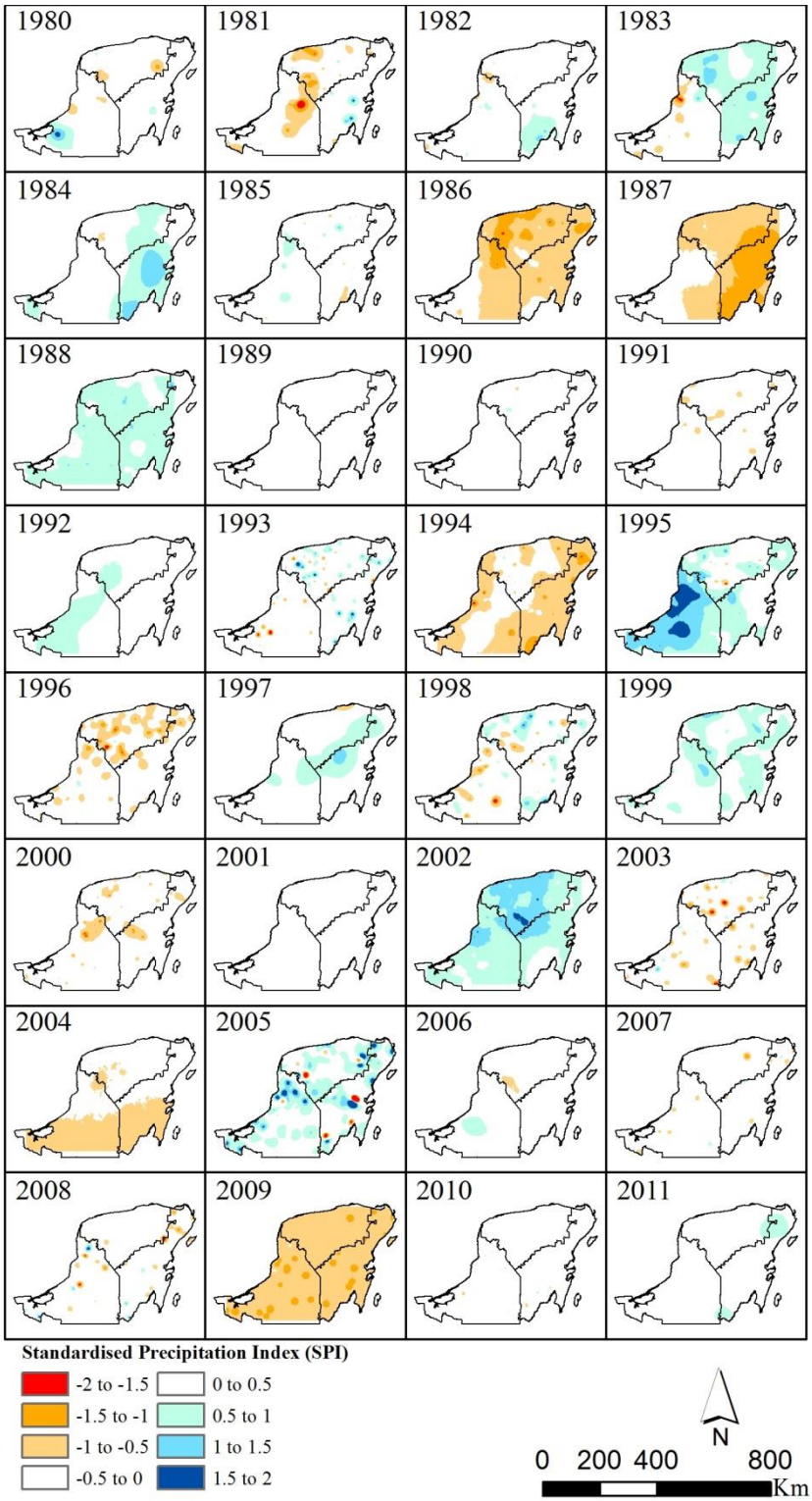


Figure 3-25. Maps showing the krigged annual SPI. Each map represent each year from 1980-2011. The scale is based on the North American Drought Monitor (NADM): i) closer to -2: low precipitation over 12 months; ii) approximately 0: normal precipitation over 12 months; iii) closer to 2: heavy precipitation over 12 months.

3.5 Chapter summary

This chapter is a contribution and a step towards the better understanding of the spatial and temporal variability of precipitation in the Yucatan Peninsula, which will help to provide a benchmark to understand the link between the climate and vegetation productivity and how vegetation is impacted by droughts. Also, this chapter provided evidence on what have been reported in the literature regarding precipitation patterns across the Peninsula (see section 2.3.1).

An initial objective of this thesis was to identify precipitation variability across the Yucatan Peninsula. To understand if the precipitation data had any spatial structure, a cluster analysis was performed. Cluster analysis does not use station location data, and thus it is more general and it shows how the data are distributed and structured. Four distinct clusters were found. One (cluster E) is located in the northern coast, two of them (clusters A and B) are entwined towards the central part of the Peninsula and a fourth one (cluster D) contains stations which are located in the southwest and east part where more rainfall occurs. The clusters, as expected, correspond with the precipitation gradient. Maps which compare these clusters with altitude, vegetation and temperature data show that the clustering is coherent with the vegetation map but not with the temperature and the altitude map. This finding shows vegetation type is closely related to precipitation as has been reported previously in the literature (Flores-Guido and Espejel, 1994; Valdez-Hernández et al., 2015). Precipitation is not linked with altitude or temperature since the Peninsula does not present much variability in these features.

Within the objectives of this chapter was to develop the most reliable and up to date rainfall surfaces across the Yucatan Peninsula. This analysis was using more stations and more recent data than those reported in the literature. However, our findings are similar to earlier compilations, which suggests that precipitation in the Peninsula has not changed in rainfall amount and spatial variability. As has been mentioned in the literature, there is a precipitation gradient across the Peninsula which goes from northwest to southeast and from west to east in the northern part. Kriging interpolation was employed, a technique which is able to

interpolate point-based data into a surface and thus create a map of the precipitation in the study area. The analysis was carried out for both long term and annual averages. The aim of this part was to assess the validity and accuracy of an existing map frequently encountered in the literature and used as a basis of other analyses (García, 1998b). The kriging analysis, which is a formal statistical technique based on detailed data of 99 stations, provided a more detailed map of the precipitation patterns in the area. Overall the two maps (long term precipitation from daily data and accumulative annual data, see Figure 3-12) agree on the general precipitation gradient but the kriging map, because of the larger number of stations available during the period of study, provides greater accuracy on precipitation amounts in smaller geographical locations. It is important to mention that the map published by García (1998b) (see Figure 2-5) used fewer stations and the stations she used are from the period 1920 to 1960; moreover, the number of meteorological stations in 1960 was half that of the period used here (1980 to 2011). Hence, the number of stations used in this analysis was more representative of the Yucatan Peninsula as a whole.

Annual maps were also created for the years 1982 – 2011 and some changes year by year were detected and some changes in the normal patterns of precipitation could be related to different atmospheric mechanisms such as ENSO (see sections 1.6.2.3 and 1.7). In the last decades, much research has been done in understanding the relationship between droughts and teleconnections (Caviedes and Waylen, 1998; Anyamba et al., 2001; Boyd et al., 2006; AghaKouchak et al., 2015), and in some regions a strong relationship between the occurrence of droughts and ENSO has been found. These results show some years that present droughts coincide with years of El Niño or La Niña. For instance 1986, 1987, 1994, 2003, and 2009 coincide with an increase of sea temperature caused by El Niño. Although the aim of this thesis is not related with the analysis of this relationship, these results can help for further research in the area.

The maps created in this chapter give us the opportunity to see how rain was distributed in each year and are necessary for the analysis of vegetation presented in the following chapters. The validation of the kriging maps indicates that the technique used has reasonable skill in the interpolation of precipitation data.

However, there are years where the NoData is reflected in the results and these years are underestimating the results compared with the remotely sensed data (TRMM). However, the kriging maps have better spatial resolution (1.5 km spatial resolution); therefore a lot of information has been aggregated in the comparison of maps which could bias the results. Thus, the krigged maps created in this chapter are important results and new data which has important advantages in comparison with the TRMM data, within this advantages are: i) spatial resolution (1.5 km); ii) temporal resolution (1980-2011); iii) they were created with accurate data recorded in all meteorological stations.

This study set out also with the aim of assessing the climatological anomalies, specifically droughts in the Yucatan Peninsula. In order to detect droughts, deviations from the mean were taken and the results indicate that precipitation anomalies in the Yucatan Peninsula are variable in terms of space and time. That is, the driest/wettest areas in the Peninsula change almost every year. Some of these results are different from those published in the literature and even from the cluster analysis. These results are likely to be related to the methodology used and they may partly be explained by the strong precipitation seasonality in the area. Therefore, these findings must be interpreted with caution because using the simple difference between the long term average and the current year average could be hiding some seasonal processes such as hurricanes, droughts, extreme rainfall, etc.

CHAPTER 4. **VEGETATION PRODUCTIVITY DYNAMICS AT THE YUCATAN PENINSULA**

The previous chapter aimed to understand the spatio-temporal patterns of precipitation and droughts in the Yucatan Peninsula. This chapter aims to understand vegetation productivity trends focusing on the persistence and resilience of the different vegetation types present over the Yucatan Peninsula using remotely sense data, specifically, the Normalised Difference Vegetation Index (NDVI) from the NOAA-AVHRR (National Oceanic and Atmosphere Administration Advanced Very High Resolution Radiometer) as a proxy for productivity for the period 1982 to 2011. The research draws attention to the Normalized Difference Vegetation Index (NDVI) multi-temporal series analysis as a proxy to detect anomalies and to understand trends on vegetation productivity. Anomalies in vegetation productivity will lead us to try to understand vegetation resilience and resistance and its response to climate events associated with droughts across the Yucatan Peninsula, Mexico.

4.1 **Introduction**

Studying and understanding vegetation response to droughts has great importance since this will allow better understanding of environmental disturbance and the possible effects of extreme climatological events in the future that have been predicted to be more frequent and extreme (Orellana et al., 2009; IPCC, 2013). Moreover, the study of the response and recovery times after these extreme events (i.e. droughts) is important in order to understand the rates (time) of ecosystem change. In other words, how resistant and resilient each vegetation type is to an event (MacGillivray et al., 1995; Coppola et al., 2009; Harris et al., 2014). Specifically, vegetation resilience can be defined as the ability of the vegetation to tolerate and then recover after disturbances and return to its original state. Resilience can be measured as a function of the time that vegetation takes to return to its original state (Harris et al., 2014; Poorter et al., 2016). Resilience and parameters of vegetation response are important measures which allow the monitoring of vegetation dynamics in a more accurate way and

is therefore a realistic approach (Simoniello et al., 2008) to analyse extreme climatological events' impact.

Having described the spatial and temporal patterns of rainfall in the Yucatan Peninsula (chapter 3), the following sections present a vegetation analysis using remote sensing data from the NOAA-AVHRR (National Oceanic and Atmosphere Administration Advanced Very High Resolution Radiometer), for a time period of nearly 30 years, between 1982 and 2011. This is the first analysis of this type using remotely sensed data at the Yucatan Peninsula. The NDVI derived from AVHRR instruments has been an important tool for monitoring vegetation processes and study changes over time (Pinzon and Tucker, 2014). First of all, an annual analysis of the vegetation productivity is presented, followed by the study of anomalies; subsequently, and using the results from chapter 3, the relationship between productivity and rainfall will be evaluated. Finally, a spatial and temporal analysis of persistence and resilience of vegetation is presented. Thus, affording a better understanding of how different types of vegetation (from tropical dry forest to semi-evergreen forest) respond to rainfall anomalies.

4.2 Datasets and pre-processing

4.2.1 Normalised Difference Vegetation Index (NDVI) dataset

NDVI3g (third generation GIMMS NDVI from AVHRR sensors) data was generated by the radiation acquired in channels 1 (0.58 - 0.68 um) and 2 (0.725 - 1.00 um) of the Advanced Very High Resolution Radiometer (AVHRR) instrument aboard the NOAA-series of satellites. The available NDVI3g product for the period January 1982 to December 2011 was downloaded from the Global Inventory Modelling and Mapping Studies (GIMMS) website. The dataset is an improved 8-km NDVI from NOAA 7 to 18 satellites (Tucker et al., 2005) which has better calibration and post processing normalisations than the previous version. Each NDVI image presents the Maximum Value Composite (MVC) with fifteen days temporal resolution; this is a bi-monthly NDVI product (thus there are 24 images per year). The dataset has been improved, by the same

institution, through a series of corrections for residual sensor degradation, removal of volcanic aerosols, distortions caused by cloud cover, and viewing geometry (Pinzon and Tucker, 2014).

The period of time selected matches that with the precipitation data available (see chapter 3) and it is long enough to capture rainfall variability occurring in the area. From the data downloaded (NDVI3g), NDVI yearly averages (using the mean values) were computed in order to analyse the data in a yearly basis and make it comparable with the yearly precipitation data presented in chapter 3. Precipitation maps (1.5 km spatial resolution) were resampled to match the spatial resolution of NDVI images

4.2.2 Vegetation types

As stated in chapter 2, the Yucatan Peninsula is covered with many different vegetation types. The classification of vegetation was the one provided by INEGI (2010) also shown in chapter 2. The INEGI vegetation map contained different classification for land cover and use. The classification used in this thesis was based on the deciduousness of forests in order to delimit areas with similar climatic, seasonal and ecological conditions (INEGI, 2010). Figure 4-1 shows this classification and through this, the vegetation gradient (from tropical dry forest to evergreen forest) present in the Peninsula.

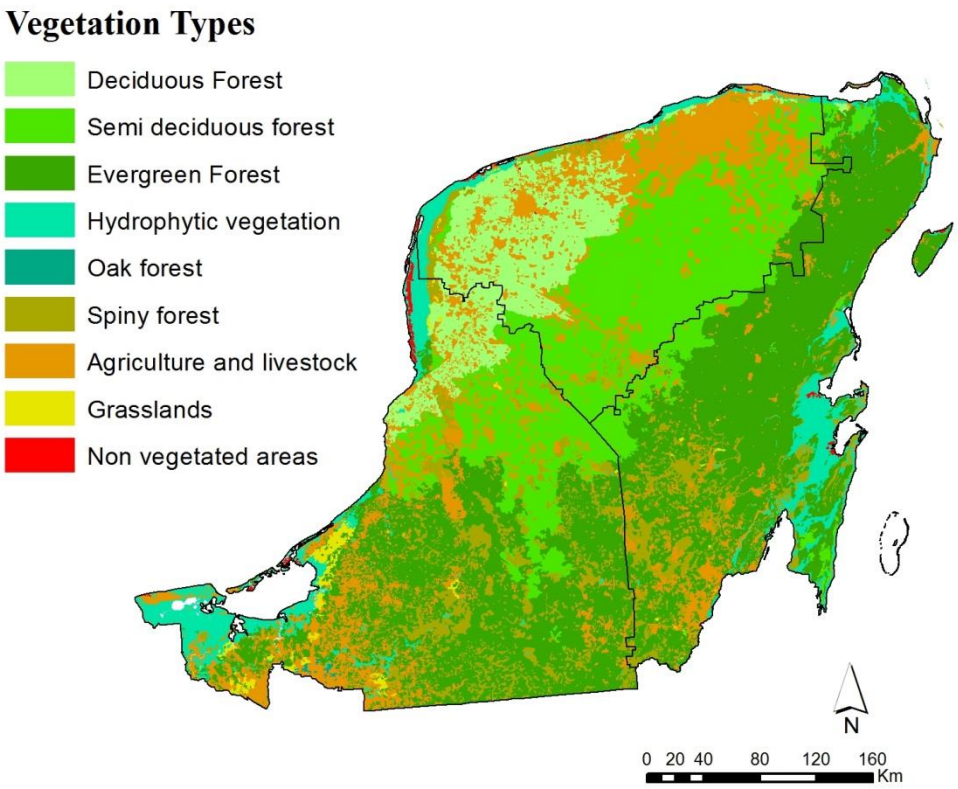


Figure 4-1. Forest classification according to its deciduousness in the Yucatan Peninsula. Data obtained by INEGI (2010).

4.2.3 Precipitation dataset

The precipitation data used is the one created in chapter 3. A kriging approach was used to calculate annual precipitation surfaces based on rain gauge data for each of the 99 stations. The precipitation data pre-processing consisted of resampling of the kriging maps (1.5 km spatial resolution) in order to make them with the same spatial resolution and extent as the NDVI data, thus affording per-pixel analyses and comparison both within and between vegetation types.

4.3 Methodology

4.3.1 NDVI Smoothing and extraction of metrics: TIMESAT

The NDVI time-series (24 images per year) was smoothed in order to remove outliers and reduce noisy data and any contamination caused by clouds and atmospheric variability (Atkinson et al., 2012). Here the TIMESAT software

was used as one of its many functions is to smooth time-series data. TIMESAT was specifically created for the purpose of using NDVI time-series data and it has proved popular (Jönsson and Eklundh, 2004; Boyd et al., 2011; Atkinson et al., 2012; Chunqiao et al., 2012; Eklundh and Jönsson, 2015). One advantage of this software is the visualisation facility that it offers, affording a more flexible, intuitive and appropriate approach to selecting a method. Here, after analysing the three methods that TIMESAT provides, it was found that Savitzky–Golay filtering was the most suitable fitting method for the data. Savitzky–Golay smoothing method uses moving average filtering and preserves important patterns in the seasonal peaks, since this method does not distort the data and adjusts the data to the upper NDVI envelope, which helps in maintaining the NDVI pattern of change (Jönsson and Eklundh, 2004). Since the Yucatan Peninsula is extremely seasonal and it has a heterogeneous environment (i.e. different types of vegetation) and it has been shown that TIMESAT is able to smooth the data without distorting it, and thus in this study it was decided to use TIMESAT for smoothing the data.

This TIMESAT software also allows for the extraction of metrics, such as those illustrated in Figure 4-2. The metrics that can be computed are: start of season, end of season, length of season, maximum value, base value, time of middle of season, amplitude, small integrated value and large integrated value. Extracting seasonal parameters from vegetation is helpful to improve the understanding of vegetation phases, such as start and end of the growing season, its length and amplitude. Also, as stated by Wei et al. (2012), these metrics can be used as indicators for drought impacts on vegetation, and they have been used in many studies regarding vegetation trends (Piao et al., 2004; Eklundh and Jönsson, 2015).

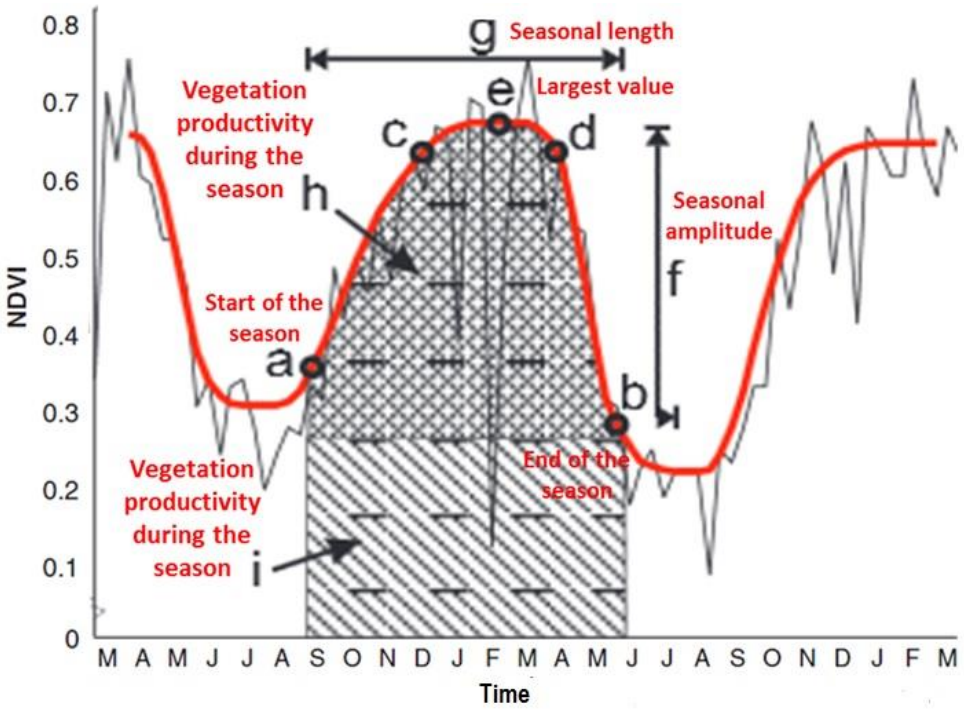


Figure 4-2. Possible seasonality parameters derived in TIMESAT. (a) start of season, (b) end of season, (e) maximum value, (g) length of season, (h) small integrated value, (i) large integrated value. Figure modified from Jönsson and Eklundh (2004).

In order to understand how vegetation productivity varies in time and space across the Yucatan Peninsula during the study period (1982 - 2011), the small integral was extracted from TIMESAT and it is calculated as the area under the curve created by the NDVI function having the base level when the start of the season occurs. This metric is an indicator of the seasonal vegetation productivity and allows understanding of the vegetation productivity patterns as a measure of the accumulative annual NDVI across the Peninsula. The extraction of this metric will allow us to understand seasonality patterns in the area and understand how NDVI data behaves in terms of productivity.

4.3.2 Persistent and resilient vegetation behaviour analysis

In order to understand the persistence and resilience of vegetation, a persistence analysis was performed across the Yucatan Peninsula using the NDVI yearly average maps for the period 1982-2011. The vegetation persistence analysis was based in the methodology used by Lanfredi et al. (2004); Simoniello et al. (2008); Harris et al. (2014). This methodology is based on the occurrence of

NDVI positive or negative trends over time. Using trends instead of deviations of the mean is important in order to minimise as much as possible any remaining noise in NDVI data and minimise the influence of other factors such as land cover types (Coppola et al., 2009) which is an important when the main objective is to understand how persistent and resilient is the vegetation rather than changes in land cover type. Thus, these methodologies measure persistent trends year by year following a base period.

The principal idea of this methodology is to create trend surfaces $s(x, y; t)$; where *x* and *y* are the coordinates of the pixel, and *t* represents the time step. Afterwards, every pixel is reclassified as +1 when the pixel shows positive trends or -1 when showing a negative trend. The first surface $s(x, y, t_i)$ is the reference period, constructed with a long enough sample to make sure it includes climatic variability; in this case the base period selected was for 10 years (1982 - 1991) as proposed by (Harris et al., 2014). Then, subsequent years are added to create a new surface and compared with the previous one. Every new surface is constructed as follows:

$$P(x, y, t) = s(x, y, t) \quad t = t_i$$

$$P(x, y, t) = \begin{cases} P(x, y, t-1) & if\ s(x, y, t) = P(x, y, t-1) \\ 0 & if\ s(x, y, t) \neq P(x, y, t-1) \end{cases} \quad t > t_i$$

At the end of the whole period (*T*), in this case 1982 - 2011, a cumulative map (persistence map) is constructed as $P_{t_i}^{T}(x, y) = \sum_{t=t_{ti}+1}^{T} P(x, y, t)$. Hence, at any (x, y), the magnitude on the final surface (persistence map) indicates the number of years in which that trend has persisted as the trend has not been cleared or changed sign (i.e. persistence time). The sign represents the direction of the trend (Lanfredi et al., 2004; Harris et al., 2014).

4.3.2.1 Persistence probabilities: recovery times

After obtaining the persistence map for the whole region, it is possible to calculate the persistence probability or the first-passage probability $p(q)$ for each of the vegetation types. Vegetation type were extracted from the persistence

map (previous section, 4.3.2) according to the vegetation map presented in Figure 4-1. Posteriorly, each vegetation type was rasterise and persistence probabilities were calculated. Table 4-1 shows the number of pixels that each class represent.

Table 4-1. Number of pixels for each vegetation type (sample size).

Vegetation type	**Number of pixels (n)**
Hydrophytic vegetation	113
Agriculture and livestock	292
Deciduous forest	141
Spine forest	144
Evergreen forest	636
Grasslands	17
Semi-deciduous forest	382
Oak forest	4

The persistence probability is the probability that a given fluctuating field deviates from a reference level for a time interval *t* before returning to it (Lanfredi et al., 2004; Harris et al., 2014). The persistence probability is defined as follows:

$$p(q) = \frac{N(t)}{N(t_i)}$$

Where, $N(t)$ is the number of pixels with the same sign in each time step, for $t > t_i$; and $N(t_i)$ is the number of pixels with the same sign for the base period. In other words, those are the number of pixels with non-cleared (they do not change the sign) trends with the same sign (Lanfredi et al., 2004; Harris et al., 2014).

In order to estimate the recovery time, an exponential decay function was used to fit the persistence probability $p(q) = e^{-\frac{t}{\tau}}$. The estimation of the mean lifetime (t) represents the average time (*T*) during which a trend (both positive and negative) persists before it decays (Lanfredi et al., 2004).

Therefore, we hypothesise with this resilience and resistance analysis that vegetation with higher resilience will present shorter recovery times and resilience should be reduced in those areas affected by any environmental shock (Lanfredi et al., 2004; Harris et al., 2014) (i.e. droughts). Conversely, healthy vegetation is expected to be persistent for longer periods of time and resistant vegetation should show shorter recovery times. It is important to emphasise that pixels with positive/negative persistence for the whole period should not be related necessarily to an increase/decrease of vegetation productivity in the future. Instead, it should be read as a probability that "shocked" vegetation will not return to the initial (base period) trend (Simoniello et al., 2008).

4.3.3 NDVI anomalies

Climate events such as droughts can affect vegetation dynamics, then NDVI variation from the mean could be analysed as a proxy to measure droughts (Peters et al., 2002; Amri et al., 2011; Fensholt et al., 2013). Thus, it is interesting to measure NDVI anomalies year by year during the period (1982 - 2011). In order to explore the occurrence of any extreme event or any significant NDVI deviation from the long-term mean, NDVI anomalies were computed.

The anomalies were calculated with two different approaches. First as proposed by Amri et al. (2011) the anomalies were computed with the Vegetation Anomaly Index (VAI). The index is calculated as follows:

$$VAI_i = \frac{NDVI_i - (NDVI_i)_{mean}}{\sigma_i}$$

Where $NDVI_i$ is the NDVI for a given year *i*, $(NDVI_i)_{mean}$ is the long term average NDVI, in this case representing the NDVI average from 1982-2011; and σ_i is the standard deviation of the NDVI values estimated for the year *i* (n=24, corresponding to 24 images per year).

This NDVI index shows the deviations from the mean, however it does not show which of these anomalies are statistically significant. Therefore, the analysis of significant anomalies was carried out. For this, a T test was applied to every VAI

map and reclassified according to the confidence levels; then, pixels outside the confidence interval (values between -1.96 and 1.96) were masked as zeros and all others were considered significant anomalies.

4.3.4 Understanding the relationship with precipitation

As mentioned in previous chapters, precipitation patterns are dynamic in terms of time and space and changes on them result in impacts on terrestrial biosphere (Boyd et al., 2006). In the Neotropics, it has been established that rainfall is a principal cause for vegetation phenology, thus changes in precipitation patterns and the occurrence of natural disturbances have a response in vegetation (Sánchez-Azofeifa et al., 2005). In addition, droughts are ecosystem drivers and impact vegetation in terms of biomass decrease, vegetation cycles, growth and vitality. Therefore, if there is a change in precipitation patterns, a change in vegetation productivity would also be expected. The study of the relationship between NDVI and rainfall is therefore crucial (Nicholson et al., 1990; Herrmann et al., 2005).

To accomplish this and in order to find the relationship between vegetation and rainfall for every single pixel, a pixel-wise regression was computed between annual rainfall and annual NDVI. The result is a map showing the R^2 value for every pixel in the area. This was computed in RStudio software with a linear regression model. The magnitude of R^2 will show what percentage of the vegetation productivity variance is explained by rainfall. In other words, which is the impact of precipitation in vegetation productivity.

4.4 Results

4.4.1 Small integral analysis

Figure 4-3 shows the spatial distribution of the annual vegetation production during the growing season (small integral metric obtained in TIMESAT) per year for the period of 1982-2011. As shown in Figure 4-3 the small integral varies both spatially across the Yucatan Peninsula and through time. The green gradient represents the active vegetation production over the growing season, that is, darker green values indicate major active vegetation production during the growing season for the current year. Overall, the highest values are in the southern part of the Peninsula, especially in the State of Yucatan. For several years the amount of "no information" (zeros) is concentrated in the southern part of the Peninsula; these pixels denote that a growing season was not detected. It is important to point out that the southern part of the Peninsula is the area that has more evergreen and less deciduous vegetation and where the values of NDVI are larger.

However, the general pattern of the small integral which increases towards the north follows the north-south rainfall gradient mentioned several times before. Similarly, vegetation shifts from tropical dry forest to evergreen forest following the same north-south pattern (Figure 4-1). The highest integral values are concentrated in the north where there is deciduous forest; whereas the lower values are in the southern part where there is evergreen forest. The lack of vegetation productivity in the growing season in the southern part could be due to the small changes in greenness that evergreen forest presents. These forests have high values of NDVI through the year so it is not possible to observe big changes that would signal a growth period. It is important to mention that these results are obtained with TIMESAT, which was designed for higher latitudes and this is one of the drawbacks of using it in lower latitudes.

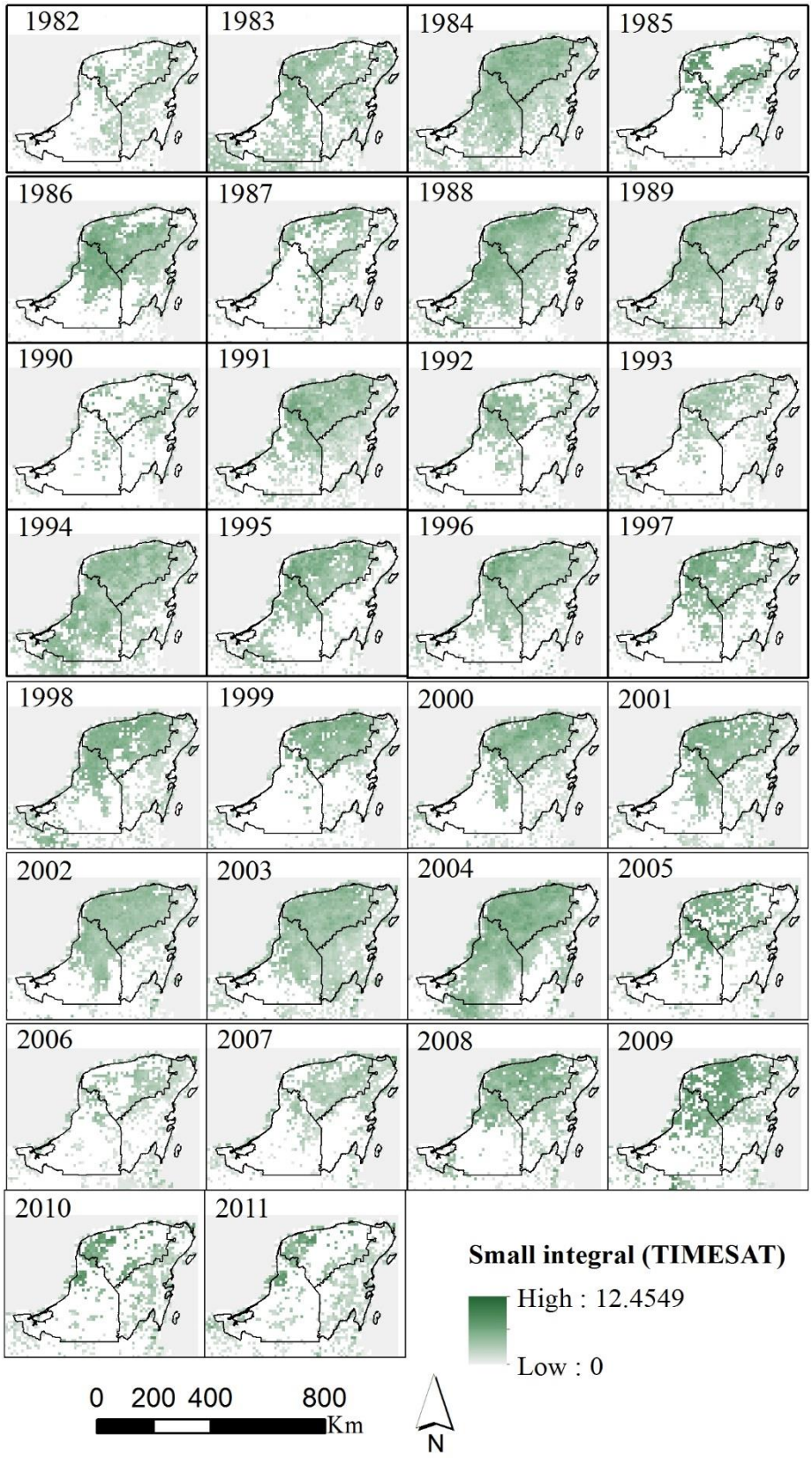


Figure 4-3. Normalized difference vegetation index (NDVI) based on growing season NDVI integral. Data resulting from TIMESAT.

In Figure 4-2 it is shown that TIMESAT in some years (1984, 1988, 1989, 1994, and 2004) are greener in the whole Peninsula. This suggests that in those years all these green areas, even in the south part of the Peninsula, present a marked greening period. Whereas in almost all the other years, in the southern part of the Peninsula the missing data is caused by low seasonal integral of NDVI. This analysis give us information about the seasonality of the area and the evidence that results from TIMESAT shall be treated carefully since analysing productivity in areas with different patterns of seasonality (deciduous forest and evergreen forest) (Fensholt and Rasmussen, 2011). Therefore, in this study, the small integral was no longer used. Instead MVC of NDVI were used for the following analysis.

4.4.2 Vegetation persistence

The persistence map (Figure 4-4) shows the total persistence $\sum_{1992}^{2011} P\,(x, y)$ of NDVI trends for the period 1992-2011, with a base period from 1982-1991. It shows the number of years that a trend persists across time and space. Blue colours represent persistent positive trends; conversely, the reddish colours symbolise persistent negative trends in the area. In general the results show spatial coherence and positive persistence pixels are predominant. For instance 50 % of the pixels persisted positively for 20 years and just 0.77 % pixels had negative trends during the 20 years. On the other hand, 6% of pixels cleared their trend (changed sign) in the first year; those are the less persistent pixels.

Positive persistence trends are dispersed across the Peninsula with a big cluster located in the centre-south, two in the south of Yucatan State and a small one in the west part of Quintana Roo. On the other hand, negative persistence trends are not that frequent and appear mostly around the main cities, in the north-east where Cancun is located, in the west close to Campeche City and some others close to the north coast. Long term persistence trends are those that persist negatively or positively for the whole period (20 years) and the positive ones dominate almost all the Peninsula. The short persistence trends are represented by yellowish colours and almost all of them are located in the west of Campeche

and persisted for less than two years. On the contrary, short negative trends are concentrated in southern of Quintana Roo and the Campeche coast.

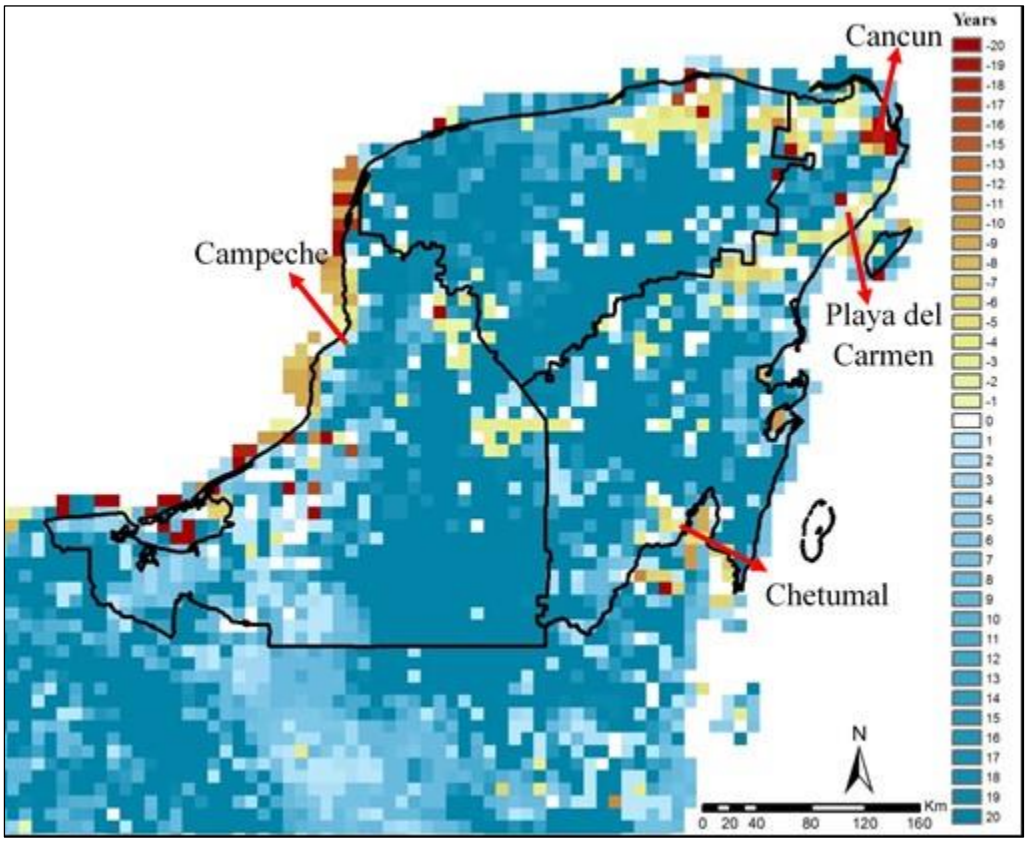


Figure 4-4. Cumulative persistence map $P_{t_i}^{T}(x, y)$ for the period 1992-2011. Base period is from 1982-1991. Persistence values are expressed in number of years from 1992-2011 (20 years). Sign indicates the trend tendency (positive or negative). Yucatan Peninsula is demarcated with the black line.

Those areas with negative persistent trend for the whole period of time describe areas where vegetation is stressed and the length of persistence could be related more to vegetation degradation than climate variables. On the contrary, blue colours (positive trends) describe healthy vegetation for the whole period of time. Those areas where the trend is cleared in both ways (positive to negative or negative to positive) describe more unstable vegetation conditions. Overall, the vegetation status of the Yucatan Peninsula seems to be stable for the period of 1991-2011. However, to understand the impacts on each type of vegetation and how different vegetation would respond to droughts or other impacts; the analysis of the persistence probabilities as a measure of resilience is necessary and this is presented in the following section.

4.4.2.1 Persistence probabilities (resilience): recovery times in each type of vegetation

The plots shown in Figure 4-5 represent persistence probabilities for each vegetation type. Persistence probability, as stated by Lanfredi et al. (2004), is a measurement of a given fluctuation that deviates from the reference period (1982 - 1991) and the time that takes it to return back to the initial state. Hence, this approach is a proxy to measure vegetation resilience and the tendency of trends, both negative and positive, in each vegetation type. The fitted line is an exponential decay curve which shows the estimation of negative and positive trend lifetimes (t). For healthier vegetation it is expected negative trends decline faster than the positive ones, which is seen in the majority of the plots. The decay period is related to the recovery of vegetation; thereby, a short period of decay is related to rapid recovery ability.

Table 4-2 presents an overview of the results from the persistence probabilities for each vegetation type. Positive and negative lifetime trends (t) are presented in the first two columns. The last columns of Table 4-2 contain the R-squared of the regressions which show how well the exponential model fits the data. In most of the cases the R-squared is very high which supports the use of the exponential model in explaining the data. The exponential model cannot capture abrupt and short lived changes in the probabilities well, as in the cases of positive trends for the grasslands and negative trends for deciduous and spiny forest.

In most cases positive trends persist for a much longer time than negative ones. Positive trends on average last between 20 and 70 years with the exceptions of the grasslands whose mean life is three years. In contrast, negative trends in general are much less persistent with mean lifetimes between 4 and 16 years, with the exception of the deciduous forest areas where negative trends last for approximately 30 years. Coppola et al. (2009); Harris et al. (2014) also found that positive trends are more persistent than negative trends for all vegetation types. In this study, however the positive trends are much stronger than negative ones indicating higher resistance and more persistence for positive trends than negative trends.

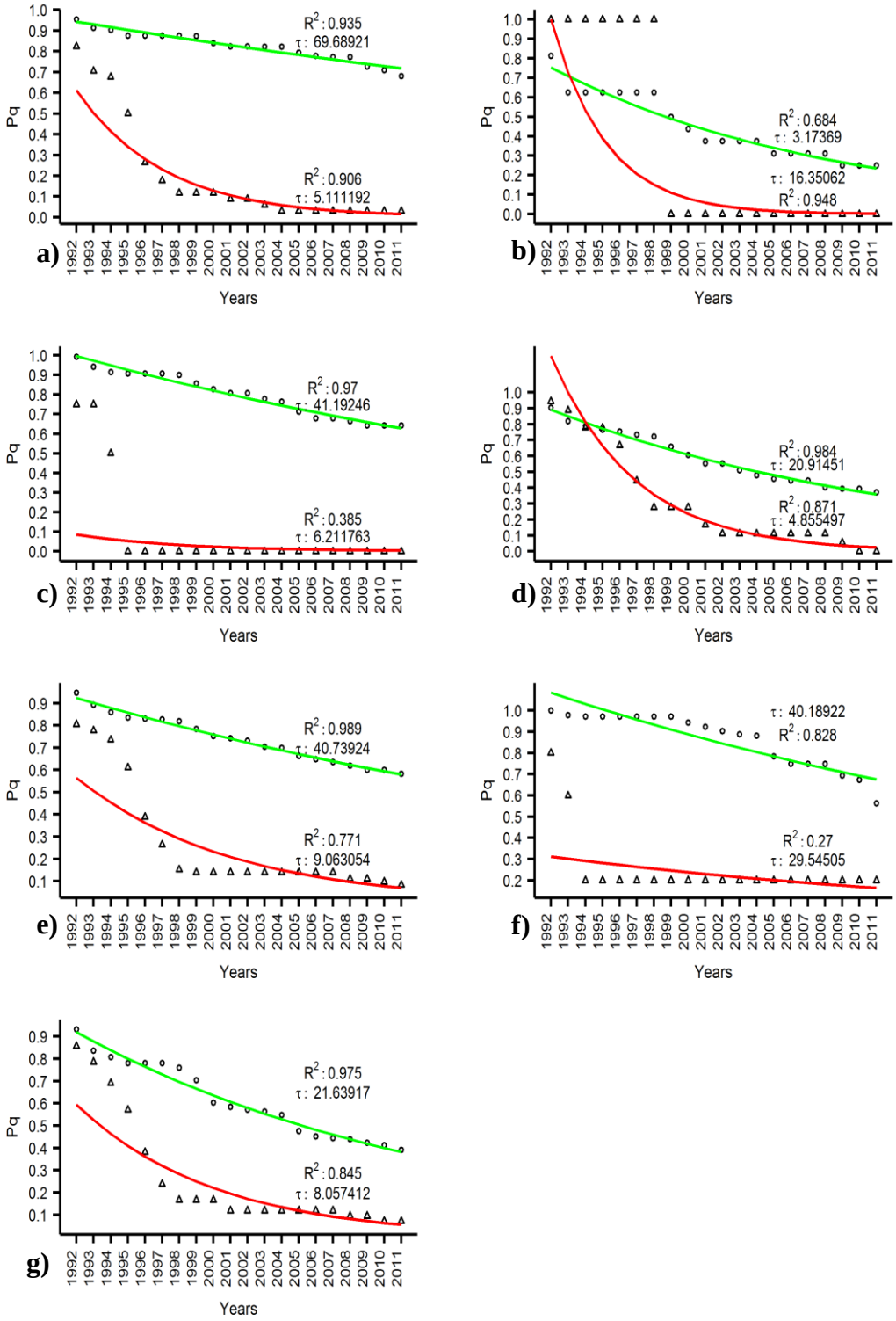


Figure 4-5. Positive (○) and negative (Δ) persistent probability plots for different vegetation type fitting an exponential decay. Each plot represents different vegetation type; a) Semi-deciduous forest, b) Grasslands, c) Spiny forest, d) Hydrophytic vegetation, e) Evergreen forest, f) Deciduous forest , g) Agriculture and livestock. The estimation of τ represents the mean time life and the R^2 the goodness of fit of the exponential model to the data. Red and green lines represent the best persistence probability fit (exponential model) for negative and positive trends respectively.

Table 4-2. Summary of the results obtained from the persistence probabilities for each vegetation type. Mean life times (in years) of positive and negative trends (t); R-squared for the negative and positive fitted exponential model.

Vegetation type	Positive trends		Negative trends	
	τ (years)	**R^2**	**τ (years)**	**R^2**
Semi-deciduous forest	69.69	0.935	5.11	0.906
Grasslands	3.17	0.684	16.35	0.948
Spiny forest	41.19	0.97	6.21	0.385
Hydrophytic vegetation	20.91	0.984	4.85	0.871
Evergreen forest	40.74	0.989	9.06	0.771
Deciduous forest	40.19	0.828	29.55	0.27
Agriculture and livestock	21.64	0.975	8.06	0.845

As is illustrated in Figure 4-1 evergreen forests inhabit the southern part of the Peninsula where rainfall is higher and seasonality is not as marked as in the northern part of the area as explained in 4.4.1 and shown in Figure 4-2. The trend analysis shows a strong asymmetry between negative (~ 9 years) and positive (~ 40 years) mean life times (Table 4-2). Evergreen forest has a long persistence period and a short recovery period. The same response is shown by the semi-deciduous forest with positive trends of ~ 69 years and ~ 5 years for recovering after negative disturbances. These results suggest that evergreen and semi-deciduous forests are on average highly resilient vegetation types and NDVI values in these areas tend to be positive for longer periods of time. Thus, it would be expected that these areas were not affected as much by droughts, and if they are affected the time of recovery would be faster than others areas such as tropical dry forest.

The same asymmetry is shown for hydrophytic vegetation (~ 20 and ~ 4 years respectively) and for the spiny forest (~ 41 years and ~ 6 years). However, this vegetation is represented by few pixels in most of these areas; in particular the hydrophytic vegetation shows a large number of pixels with negative persistent trends. Spiny forest is also represented by few pixels; moreover, its negative trends decline in the second year to zero. This abrupt decrease is not well captured by the exponential model ($R^2 = 0.3$).

Deciduous forests have lasting positive and negative trends. Since the mean recovery time for negative trends is really high (~ 29 years), these results suggest that this vegetation is less resilient and it presents signs of stress. This vegetation type is located in the north part of Yucatan state (Figure 4-1) and it has been reported as an area with extreme forest decrease due to forest clearance between 1980 and 2000 (Miles et al., 2006). However, these forests have a marked seasonality and it has been proposed that the NDVI signal in dry seasons could result in non-vegetated signals in trend analysis (Fensholt et al., 2015). This could be a bias which causes the long persistence in negative trends.

For agriculture and livestock, the positive mean life (~ 21 years) is not that long and the difference with the negative trends (~ 8 years) is smaller in comparison with the other cases. There are different types of agriculture in this area: seasonal, permanent and irrigated agriculture. However, the largest areas in this classification are occupied by pastures for livestock. As a result there are more stable decay curves for this class.

In contrast, grasslands present the opposite behaviour; positive trends decay faster than the negative trends. The mean life time for positive trends is ~ 3 years and the negative trend life is ~ 16 years, thus, indicating that this vegetation has low level of resilience or it could be a sign of stressed vegetation. However, it is important to note that grasslands have a small representation on number of pixels in the areas that could bias these results.

From the above it is clear that the persistence of trends depend on the type of vegetation which in fact is interrelated with the climatic conditions of the area. Further analysis is needed in order to investigate which are the determinants of positive and negative trends and in particular the latter. Prime candidates include precipitation and its seasonality. As was discussed in chapter 2, the precipitation gradient and different climatic events such as droughts, or global cycles as El Niño could affect trends in vegetation productivity. Another important factor is human activity and land use change. As can be seen in Figure 4-4, the most persistent negative trends are located by the coast, with more intense agriculture activity, and where the bigger cities are. The causes behind vegetation

productivity changes are very active and challenging area of research and part of the topic of next chapter.

4.4.3 Evaluation of the NDVI anomalies

The study of variability in NDVI patterns can reveal extreme events which may have detrimental effects on the vegetation of an area. An interesting problem is how to identify these rare events and how to link them to underlying causes. The main method of identifying extreme NDVI variation is by calculating deviation from the long-term mean; these deviations can be used as a proxy to measure drought events.

Figure 4-6 shows the result of the significant anomalies which have 5% probability of occurrence. Blue colours represent positive productivity anomalies and red colours exhibit negative anomalies. A negative anomaly implies a NDVI deviation from the normal behaviour (long-term average); in the contrary, positive anomalies represent those pixels where the productivity of vegetation increase from the long-term average. Throughout time, 1982, 1984, 1993 are the years with highest negative anomalies and with the greatest coverage across the Peninsula. The negative anomalies are mostly represented in the south-east part of the area and in some areas around the coast, with the exception of 1984, in which negative anomalies appear in the north part of the Peninsula.

On the contrary, numerous positive anomalies occurred in 1990 and 1996. NDVI positive anomalies in these years are distributed across all the study area. In other years (2008, 2009 and 2010) positive anomalies are confined to small areas. In 2008 positive anomalies are distributed in the south-west part, whereas in 2009 and 2010 they are localised in the eastern part of the Peninsula.

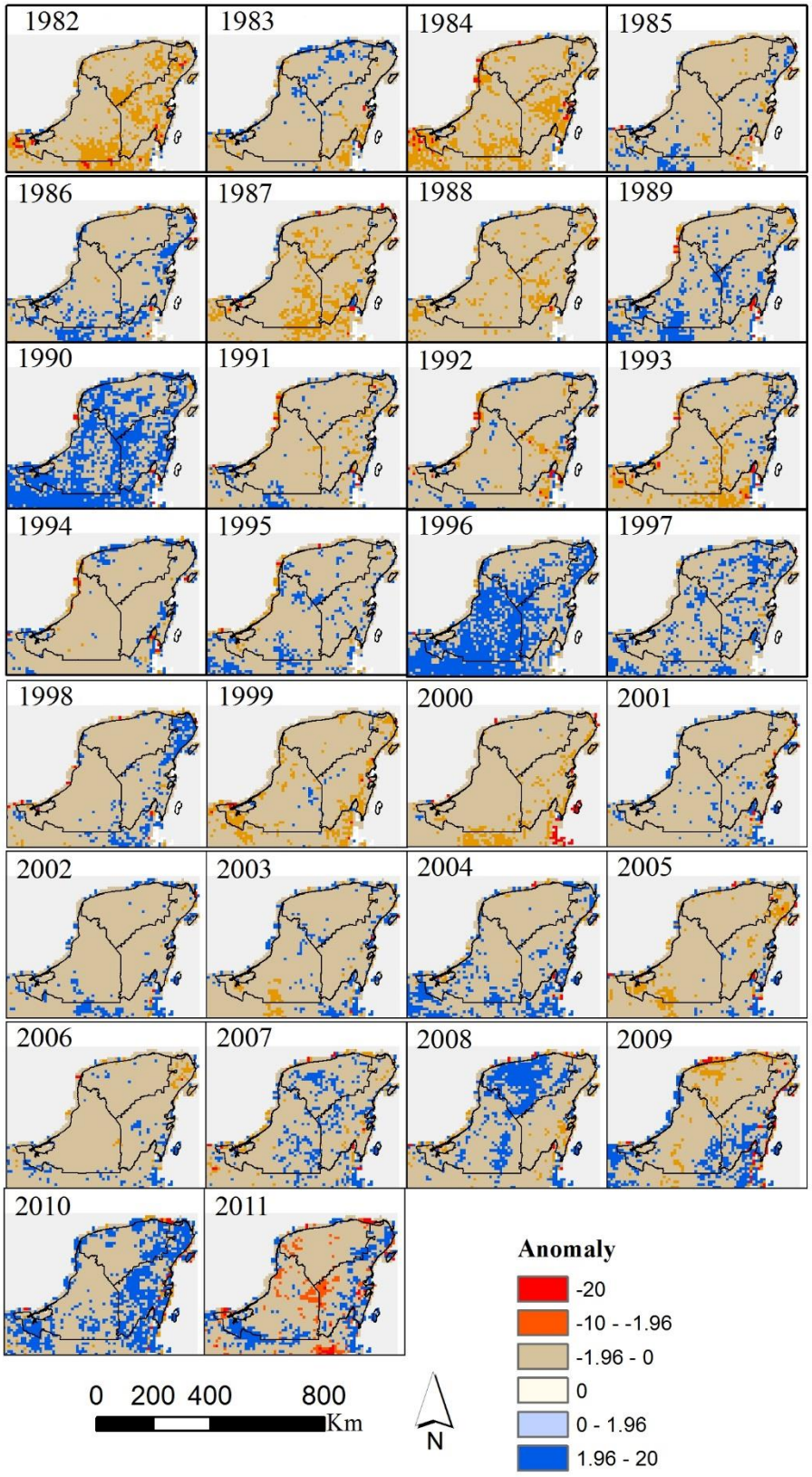


Figure 4-6. NDVI annual anomalies in the Yucatan Peninsula for the period 1982-2011. Coloured pixels represent those anomalies that are significant and have 5% probability of occurrence. Negative values (red colours) represent negative anomalies and positive values denote positive anomalies (blue colours).

These results can be compare to those described in the analysis of the persistence of vegetation. It was found there that the central area of the Peninsula is characterised by long persistent trends and same areas do not exhibit anomalies in almost all years. This suggests that this area could be more resistant and resilient than other parts of the study area. Thus resilient areas will not show great changes in NDVI, therefore, extreme climatological events could be more difficult to detect in these types of vegetation.

It would be expected that significant negative anomalies (values below -1.96, significance of 0.025) are coherent with the occurrence of droughts since in a drought event, productivity of vegetation will be affected negatively. However, not all the years are consistent with the results shown in sections 3.3.2 and 3.4.2. NDVI significant negative anomalies are present in 1982, 1984, 1987, 1988, and 2009. Only 1982, 1987, and 2009 are years that coincide with those reported in Figure 3-13 and Figure 3-24. Incoherent results show that vegetation productivity not only depends on rainfall during the same period of time, also it is affected by previous precipitation events. Hence, it is crucial to understand how NDVI depends on rainfall variations. The next section and next chapter address this topic

4.4.4 Correlation between NDVI and precipitation

In this section a short, preliminary, investigation of the relationship between precipitation and vegetation productivity is conducted. The method of choice is correlation analysis.

The per-pixel correlation between NDVI and interpolated rainfall maps for annual observations from the period 1982-2011 are shown in Figure 4-7. The figure represents R-squared values. A dark brown colour denotes a higher R-squared, whereas a beige colour symbolises a lower one.

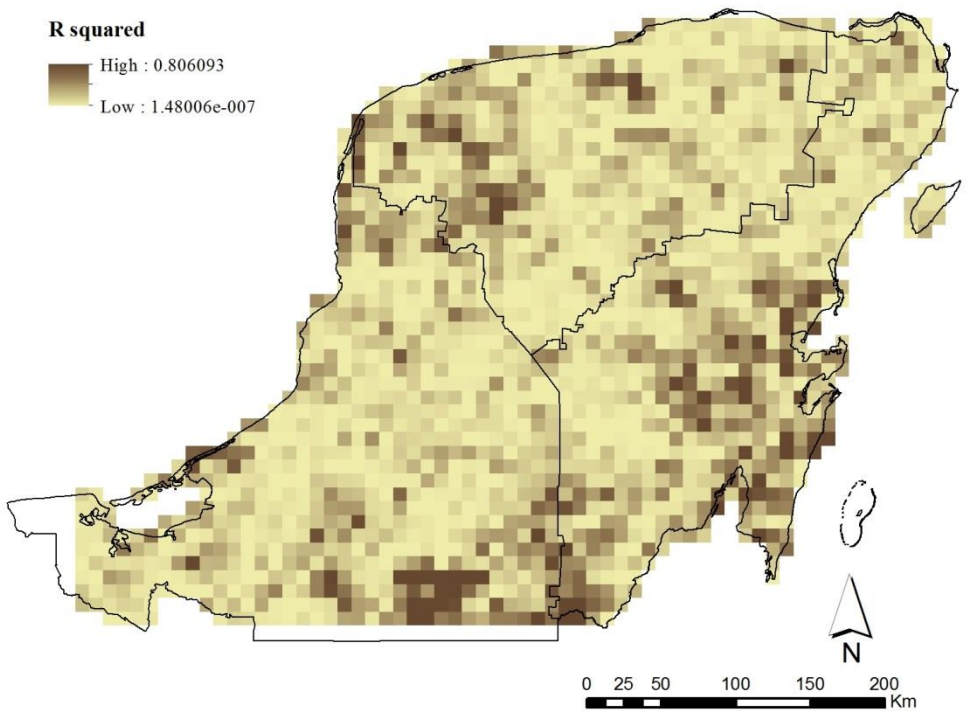


Figure 4-7. R-squared annual NDVI and annual rainfall krigged maps from the period 1982-2011 for the Yucatan Peninsula.

The results from the correlation reveal only a weak association between precipitation and vegetation productivity. Most of the map is of beige colour. The highest R-squared values are located in the north-west, in the south part close to Guatemala, and in the east part of Quintana Roo state. Several high R-squared values appear in various places but this information is not useful because these pixels lack spatial coherence. It is expected that in the north part of the Peninsula rainfall explains the behaviour of NDVI better, as vegetation is extremely deciduous. Interestingly, in terms of seasonality and greenness, the southern part of the Peninsula, where vegetation is evergreen, presents less amplitude. However, evergreen forests have been reported as being less sensitive to climatic variability (Udelhoven et al., 2009). However, it is important to mention that NDVI saturates in high biomass conditions as reported by Huete et al. (1997) and as explained in 4.4.1 and shown in Figure 4-3, then, the higher values of NDVI in this area could impact the regression results.

This preliminary analysis shows that there is a relationship between annual precipitation and vegetation productivity. The R-squared values, although small, indicate that precipitation amount is related to vegetation growth. High values of R-squared appear in areas with more water-dependent vegetation types. Other factors which drive vegetation dynamics, and which could be the subject of future research, are soil water and nutrients content, evapotranspiration rates, rainfall, temperature, among others.

4.5 Chapter summary

One of the objectives of this thesis is to study extreme climatological events, especially droughts through vegetation indices (in this chapter using NDVI). This chapter attempts to analyse vegetation dynamics in the Yucatan Peninsula and to isolate whether these dynamics are related to precipitation patterns, in particular drought. First, an analysis of the small integral metric was computed to understand the phenology of vegetation in the area. Second, a trend analysis was developed to understand how persistent vegetation productivity trends across the Yucatan Peninsula are. Next, a detailed analysis of resilience for each type of vegetation was completed in order to understand how different types of vegetation recover after stressed conditions. Third, NDVI anomalies were helpful to understand that the relationship between vegetation and precipitation is not direct and at the same time. Therefore, and finally, a correlation analysis between yearly NDVI and yearly precipitation was performed as a preliminary analysis for understanding this relationship that will be object of the next chapter.

In order to understand and analyse the spatio-temporal patterns of productivity across the Yucatan Peninsula, an analysis of the small NDVI integral was made using TIMESAT software from 1982-2011. The small integral is an indirect technique to see in which areas vegetation productivity is higher and it gives information about seasonality. In general more vegetation productivity in the growing season is concentrated in the north part of the Peninsula where the deciduous forest is. The blank data resulting from this analysis is located in the south of the Peninsula where evergreen vegetation is located, thus the problem of the saturation of NDVI in more vegetated areas seems to arise in this area of

the Yucatan Peninsula which is one of the shortcomings of using NDVI. Moreover, these results suggest that no growing season was detected for those areas. It is important to stress that these results were computed in TIMESAT, which is software that has been used mostly in higher latitudes and was developed for that type of environments.

Calculation of lifetime positive and negative trends is proposed as a good method to understand the resilience of vegetation. This methodology gives us the opportunity to understand how resilient and resistant the different types of vegetation are and this could increase our understanding of how extreme climatological events, in particular, those that cause stress in vegetation (i.e. droughts) will affect the vegetation. Persistent positive trends were found to be more predominant across the region. However, it is interesting that persistent negative trends are located in areas with more human perturbation,

In order to evaluate the capacity of the vegetation to return to the original state (resilience), persistence probabilities and the mean life time of trends were estimated for each vegetation type. In Figure 4-5 it can be seen that few temporal deviations are present in the positive trends. In contrast, abrupt negative trends changes in most vegetation types are shown in the first two or four years after the base period. This would be really interesting if these years are comparable with the anomalies. For instance, in 1993 –two years after the base period–, the 1999 and 2000 the anomaly maps show negative anomalies (Figure 4-6) which coincide with the negative trend decays in the persistent plots. These results suggest that the most resilient vegetation types in the area are the semi-deciduous forest and evergreen forest. Similar results were found by (Saleska et al., 2007) where Amazon forest (evergreen forest) seems to be more resilient in response to short-term climatic anomalies.

Persistence probability plots show a rapid decay in 1994 in most of all vegetation types. Abrupt changes are congruent with the results shown in chapter 3 (Figure 3-12) which shows negative anomalies in precipitation maps for the years 1994 and 1996. The rainfall data presented in the previous chapter show drier conditions in 1994 in the north, 1996 in the south, 2000 in the central part, 2004

in the south, and 2009 in almost all the Peninsula. By 1995 most of the negative trends have cleared (return to the base period) and this is visible in the steep changes in the probability maps in Figure 4-5. However after a trend clears there is a possibility that another one begins, i.e. after a negative trend clear in 1994 it might be that a new positive or negative trend begins there or shortly after. These new trends cannot be captured by the current method.

Significant anomalies indicate that deviations of NDVI values were coherent in some cases with the precipitation anomalies presented in chapter 3. Significant negative NDVI anomalies in 1982, 1987, 2000, 2009 and 2011 match negative rainfall anomalies in the same years (Figure 3-13). In contrast, wet years do not coincide with the findings in the precipitation data. It is possible that the incoherent results are due to the temporal scale. Yearly analyses can miss changes in vegetation during the growing season. Moreover, these result indicate that NDVI is not only affected by precipitation. However, per-pixel linear regression analysis of NDVI against precipitation showed that there is a relationship in the data. This evidence motivates the more comprehensive and detailed analysis of the factors which drive the NDVI and which is the subject of the following chapter.

CHAPTER 5. **RELATIONSHIP BETWEEN VEGETATION PRODUCTIVITY AND PRECIPITATION**

5.1 **Introduction**

The previous two chapters aimed to analyse both precipitation patterns and vegetation productivity trends across the Yucatan Peninsula. In the third chapter, detection of droughts and precipitation patterns were analysed. The fourth chapter aimed to analyse vegetation productivity trends focusing on the persistence and resilience of the different vegetation types present over the Yucatan Peninsula in order to understand seasonality, vegetation trends and quantify which are the less resilient and resistant vegetation types in the area. This chapter aims to bring these two together in order to understand any relationship between vegetation productivity and rainfall and the deficit of it (i.e. droughts) at a more detailed temporal scale (monthly). With the premise that if a relationship does exist, then any alteration in rainfall patterns as a result of climate variability will result in impact on vegetation in those locations where the vegetation was shown to be less resilient. In this context, we know that precipitation is a limiting factor for plant development and growth in the tropics (Karnieli et al., 2010; Wardlow et al., 2012b; Barnes et al., 2016), therefore having a better understanding of how this relationship behaves in this area could contribute in evaluating how the Yucatan Peninsula may change or may be affected under future scenarios of extreme climatic events (Li et al., 2015). Furthermore, it is important for assisting in effective resource management in terms of food security, water supply, and even in agricultural activity.

Broadly speaking, as Hielkema et al. (1986) observed, the response of vegetation productivity depends on the distribution of precipitation, principally during the growing season and also in the individual rain events throughout the whole year. Also, as stated by Fang et al. (2005) and Gaughan et al. (2012) this relationship depends on the different storage capacities of each vegetation type as well as other factors such as geographical region and topography, soil types, soil fertility and management practices (i.e. agriculture and stocking). Thus, there are good

justifications as to why studying this relationship should be explored: first, studying how vegetation productivity is affected by rain at a finer temporal scale is important to gain a better understanding of how environmental systems work in relation to climate variability. Second, these findings can be used for climatological models and drought early warning and monitoring. Finally, it could help in understanding how the lack of rain could affect vegetation productivity and subsequently assist in drought mitigation in terms of reduction of vulnerability and impacts, improving for instance forecasts and drought planning.

In this chapter we use two different vegetation indices (NDVI and MTCI, see section 1.6.2) as a proxy of vegetation productivity and rainfall data to study this relationship. Moreover, the standardised precipitation index (SPI), as a drought index, is used to assess how droughts can impact vegetation. The use of vegetation indices for assessing droughts is based on the premise that vegetation productivity and vigour are strongly related to moisture condition. Thus, changes in precipitation regimens such as lack of water (i.e. droughts) will impact vegetation productivity.

5.2 Correlation analysis between vegetation productivity and precipitation

In the last section of the previous chapter a pixel-wise correlation between NDVI and precipitation was shown. We found low values of correlation across the Peninsula. In this regard, many studies (Nicholson et al., 1990; Ichii et al., 2002) have used the correlation coefficient (ρ) in order to quantify the relation between these two time series data types (Herrmann et al., 2005). This is a numerical indicator which indicates the relationship between two variables. The correlation between NDVI and precipitation at time t is given by:

$$\rho(y_t, x_t) = \frac{\sum(X - \overline{X})(Y - \overline{Y})}{\sqrt{[\sum(X - \overline{X})^2][\sum(Y - \overline{Y})^2]}}$$

Where y_t denotes the vegetation index and x_t the rainfall data. This expression describes how much one variable (vegetation index) will change at a month *t*, in terms of standard deviations, when the other variable (rainfall) changes by one standard deviation at time also *t*.

A correlation model has a considerable drawback as it does not explain how vegetation productivity at time *t* is affected by precipitation at time *t* - 1, i.e. by the previous month's precipitation. The only way to consider this option in a correlation model would be as following:

$$\rho(y_t, x_{t-1})$$

However, this is not helpful because the contemporaneous effect is lost. Furthermore, it might be important to incorporate the effect of other periods. Literature shows that precipitation from previous months (e.g. $t-3$, $t-2$ and $t-1$) affect NDVI at time *t*. For instance, Herrmann et al. (2005) took into account the three month accumulated rainfall as $k_{t-1} = x_{t-1} + x_{t-2} + x_{t-3}$ and with that they calculated the correlation between those three months and NDVI data as:

$$\rho(y_t, k_{t-1})$$

This method has severe limitations: a) it does not explain why only three months back were chosen and not two or four; b) it does not show what the effect of each past month's precipitation is; finally, c) this methodology cannot be used to capture other factors which affect the NDVI, such as seasonality, severe droughts, etc. These shortcomings can be overcome by using regression analysis.

5.3 **Regression analysis between vegetation productivity and rainfall**

The linear regression model gives the possibility to assess the relative impact of a predictor variable on a particular outcome. This is how one variable (vegetation productivity) varies with changes in the other variable (rainfall) (Wooldridge, 2012). Also, it gives the possibility to integrate more than two variables in a

model and it allows the effect of each variable on the independent variable to be quantified. For example and using the same data a linear regression model could be constructed as follows:

$$y_t = a + \beta_1 x_t + \beta_2 x_{t-1} + \ldots + \varepsilon_t$$

Where y_t denotes the vegetation index at time *t*; a is the intercept on *y* axis; β are the slopes of the regression line; and ε_t is the random error. In this model the effect of every month's precipitation is captured by every β in the equation. For example, an increase in rainfall one month ago x_{t-1} will increase the NDVI by β_2. This model would then be really useful to understand the effect of rainfall in vegetation productivity. Furthermore, hypothesis testing will allow seeing how many months back precipitation is important (i.e. statistically significant).

Another powerful characteristic of regression analysis is that it is possible to incorporate qualitative data into the model using dummy variables. For example, it would be possible to take into account seasonality, drought periods or other important qualitative variables.

There are some assumptions that data should follow for using linear regression as a method to explain the variables. The assumptions are the following:

- The independent and dependent variables should have a linear relationship
- The residuals of the regression should be normally distributed
- The errors should be statistical independent
- There should be little or no autocorrelation of the data

It has been found that precipitation and vegetation productivity have a linear relationship (Nicholson et al., 1990; Li et al., 2002; Wang et al., 2003; Herrmann et al., 2005), however, it has been also found that this relationship is much more complex (Nicholson et al., 1990; Ji and Peters, 2003) and many other factors play an important role (i.e. soil, climate, vegetation cover type). Nevertheless, using a linear regression model gives a first approach and it is important for

understanding better this relationship. Moreover, this method will give the opportunity to incorporate lag, seasonality and the droughts effects. In this respect, it is important to emphasise that this Chapter aims to understand the relationship between vegetation productivity and precipitation in a time series analysis, including the effects of droughts (lack of precipitation measured by SPI). Thus, it is assumed that for each location (where a meteorological station is located) other factors are temporally constant. In order to accomplish the other assumptions the data was tested for autocorrelation as explain in section 5.4.4.

5.4 Datasets and Methodology

This chapter focuses on understanding the relationship between rainfall and vegetation productivity and to improve an understanding of how useful satellite imagery could be to detect droughts. Thus, the data collected consisted of ground measured rain gauge data (see section 3.2.1), NDVI from AVHRR for the period 1982-2011 (see section 4.2.1), MTCI from MERIS for the period 2002-2011, and SPI for measuring droughts.

5.4.1 Rainfall dataset

Time-series of monthly cumulative rainfall data were constructed from daily precipitation of 122 meteorological stations for the analysis with NDVI data, and 93 with the MTCI data. In chapter 3, 98 stations were selected. However, for the NDVI analysis 122 were selected since monthly temporal resolution allows us the use more data. On the other hand, 93 stations were used for MTCI analysis. The reason for the difference of stations used is due to the different spatial and temporal resolution of the data. The dataset covers two periods: one from January 1982 to December 2011 to be analysed with the NDVI dataset. The second one covers the period from June 2002 to December 2011 for comparison with the MTCI dataset.

5.4.2 Normalised Difference Vegetation Index dataset (NDVI) and MERIS Terrestrial Chlorophyll Index (MTCI)

NDVI data were downloaded and pre-processed as described in chapter 4. However, in this chapter, instead of yearly data, monthly data were used. In addition, 1 km reduced spatial resolution MTCI data from the MEdium Resolution Imaging Spectrometer (MERIS) sensor was downloaded from the NERC Earth Observation Data Centre (NEODC) website (http://www.neodc.rl.ac.uk). These data are a composite from MERIS L2 product which uses a monthly arithmetic mean. This data covers the period from June 2002 to December 2011. MTCI advantages are described in section 1.6.2.2. MTCI is the ratio of the difference in reflectance between band 10 and band 9 and the difference between band 9 and band 8 of the MERIS band setting:

$$MTCI = \frac{(R_{band10} - R_{band9})}{(R_{band9} - R_{band8})}$$

NDVI monthly time-series data from 1982 to 2011 were constructed based on the location of each meteorological station. That is 122 time-series data were extracted for the 122 pixels within which a meteorological station was located. These time-series data were retrieved from the biweekly MVC NDVI averaging the two images available for each month. The same procedure was made for the MTCI dataset; that is the average monthly MTCI of all 93 pixels where a meteorological station is located were extracted.

5.4.3 Standardised Precipitation Index (SPI)

1-, 3-, 6-, and 12-month SPI was calculated for the 122 stations with the SPI_SL_6.exe World Meteorological Organization program (McKee et al., 1993) which calculates the SPI for any location based on the long-term (30 years minimum is recommended) rainfall records for different time scales (see section 3.2.2.4). The use of SPI has a few advantages compared to other precipitation indices. First, SPI computation needs only precipitation data. Secondly, it can be calculated for different time scales; and thirdly, it is reported as a good indicator for meteorological drought (McKee et al., 1993; AghaKouchak et al., 2015). SPI

is used rather than other indices due to the data availability and because it meets the requirements to detect the lack of rain across time and space.

As explained in chapter 3, measuring and detecting a drought is a complex task due to the difficulties of establishing the start, the ending and exact location of a drought event. However, for practical reasons, different institutions and studies define a drought in different ways. For instance, according to the WMO and taking in account SPI as a drought indicator, a drought is detected and starting when SPI values are equal or below -1 (see chapter 3). The period of a drought is considered finished when the values become positive again. For this chapter, a drought is defined when 3-month SPI values are below -0.5 and it continues being a drought until the values become positive as recommended by the WMO. This threshold will allow us to detect few meteorological drought events at different times of the year and in all locations during studied period. The selection of 3-month SPI was based on the fact that this time scale resulted as the most accurate detection of lack of water in both wet and dry seasons and it has been reported as the best time scale for detecting seasonal drought occurrence and persistence (Meng et al., 2016).

5.4.4 Regression analyses

A regression analysis was carried out at 122 locations across the Yucatan Peninsula in order to investigate the relationship between vegetation productivity and precipitation. Moreover, with the aim to establish whether vegetation productivity is affected by droughts and investigate their persistence and impact on vegetation, other variables were included one by one in the regression analysis. Thus, four regression models were created in order to include seasonality, droughts and vegetation productivity decay rate. Slopes, statistical significance and R-squares were computed for each regression model.

The regression analysis took into account the vegetation productivity (NDVI or MTCI) as the dependant variable and accumulated monthly rainfall as the predictor variable. In all regressions the coefficient of determination (R-square) and the *p*-value were calculated to assess the significance of the model of each

variable. The *p*-value of the regression analysis shows the probability of rejecting the null hypothesis, indicating in this case that there is no relationship between the variables. For all regressions, $\alpha = 0.05$ was used as the threshold of significance.

Four regression models were computed in order to understand each variable and the lag effects that they have in vegetation productivity. It is necessary to find first if the data present autocorrelation, as proposed by Ji and Peters (2003) the Durbin-Watson statistic was calculated and no autocorrelation was found. In order to find whether the coefficients were statistically significant or not, every variable with different lags was added step by step to see when significance was dropping down (larger p-values), and consequently to find the variables that should be eliminated and those that improve the model.

5.4.4.1 Precipitation lags

The first regression model was computed taking in account rainfall and vegetation productivity. It was based on the evidence that vegetation productivity will be affected by variation in precipitation and on the fact that vegetation productivity has a lagged response to rainfall events. There is some evidence (Nicholson et al., 1990; Schultz and Halpert, 1993; Wang et al., 2001) in the Sahelian region in Africa that NDVI and precipitation variance have 1-3 months of time-lag; in South Africa it was found to be between 1 and 2 months (Gaughan et al., 2012) and in Spain between 1-3 months (Udelhoven et al., 2009). Therefore, and in order to detect how long vegetation productivity takes to respond, the first regression was expressed as:

$$y_t = a + \beta_1 x_t + \beta_2 x_{t-1} + \beta_3 x_{t-2} + \beta_4 x_{t-3} + \beta_5 x_{t-4} + \beta_5 x_{t-5} + \varepsilon_t$$

Where y_t represents the NDVI or MTCI in the current time; x_t is the rainfall in the current time, x_{t-i} is the rainfall in the previous months; $\beta_0, \beta_1, \ldots,$ are the regression coefficients, and ε is random error.

5.4.4.2 Vegetation productivity decay

A second analysis was done by adding one-month lagged vegetation productivity (either NDVI or MTCI) in order to capture the vegetation greenness decay rate. The regression model looks as:

$$y_t = a + \beta_1 x_t + \beta_2 x_{t-1} + \beta_3 x_{t-2} + \beta_4 x_{t-3} + \beta_5 x_{t-4} + \beta_5 x_{t-5} + \boldsymbol{\beta_6 y_{t-1}} + \varepsilon_t$$

Where all variables are the same as in the previous regression, but y_{t-1} represents the NDVI or MTCI in the previous step (i.e. the previous month). Adding the lagged dependent variable captures the rate of decay of vegetation, or in other words its resistance to lack of rain.

5.4.4.3 Seasonality

Thirdly, a model regression analysis was computed adding seasonality as a dummy variable. Dummy variables are indicator variables which take the values either 0 or 1 to designate the presence or absence of a categorical variable. According to Ji and Peters (2003) seasonality is a variable that should be included in this type of analysis to get accurate results due to the variation of precipitation within the growing season. Moreover, taking seasonality into account will allow us to understand better the effects of droughts by eliminating the seasonality factor, which is strong in the Yucatan Peninsula. Seasonality was established in this model according to the precipitation data and was divided in two seasons: the rainy period from June to October, and the dry period from November to May. The selection of these two periods was based on the historical precipitation data and from the results in the curves for the long term average of vegetation productivity. The regression is expressed as:

$$y_t = a + \beta_1 x_t + \beta_2 x_{t-1} + \beta_3 x_{t-2} + \beta_4 x_{t-3} + \beta_5 x_{t-4} + \beta_5 x_{t-5} + \beta_6 y_{t-1} + \boldsymbol{\beta_7 S_t} + \varepsilon_t$$

Where $\beta_7 S_t$ represents the seasonality dummy variable and the binary values were assigned as follows:

S_t	
0	If observation at time *t* is rainy season
1	If observation at time *t* is dry season

5.4.4.4 Drought detection

Finally, the last regression was computed taking in account the SPI as a dummy variable. This analysis was based on the assumption that lack of precipitation will be reflected in vegetation productivity. Monthly temporal resolution could give us the opportunity to see the effects of droughts in vegetation productivity at a finer temporal resolution. Some studies revealed that droughts affect vegetation productivity which is reflected in the vegetation greenness (Zhao and Running, 2010; Kattelus et al., 2015; Barnes et al., 2016), thus could be captured by vegetation indices. Therefore, in the last and final regression the equation is expressed as:

$$y_t = a + \beta_1 x_t + \beta_2 x_{t-1} + \beta_3 x_{t-2} + \beta_4 x_{t-3} + \beta_5 x_{t-4} + \beta_5 x_{t-5} + \beta_6 y_{t-1} + \beta_7 S_t + \boldsymbol{\beta_8 SPI_t} + \boldsymbol{\beta_9 SPI_{t-1}} + \varepsilon_t$$

Where SPI_t represents a drought and SPI_{t-1} represents a drought in the previous month. The dummy variables were taken into account as follows:

SPI_t	SPI_{t-1}	
0	0	If observation is not in drought
1	1	If observation presents a drought

5.5 Results and discussion

5.5.1 Precipitation lags

The relationship between precipitation and vegetation productivity was explained in a deeper way by using a regression model rather than a simple correlation analysis. The correlation analysis (chapter 4, section 4.4.4, Figure 4-7) shows that correlation coefficients between rainfall and NDVI are low in almost all parts of the Peninsula. However, regression analysis indicates that precipitation is a key factor for vegetation productivity across the Peninsula. The next figures contain the estimations of the regressions. Every map has 122 points for NDVI and 93 for MTCI. These points show the coefficient of a specific variable when the regression is run in that pixel. In total every regression has been run 122 and 93 times respectively. Having confidence level $\alpha = 0.05$, the critical values are -1.64 and 1.64.

Figure 5-1 is composed of six maps; the top left map contains the values of the t-statistics of $\hat{\beta}_1$ in the first regression. Similarly, the rest of the maps contain the rest of the precipitation coefficients t-statistics.

Precipitation is a dominant ecological driver for plant growth and reproduction. In general, results show that vegetation productivity and monthly rainfall have a strong relationship and this relationship seems strongest in the Northwest part of the Peninsula. In Figure 5-1 the results of the first regression using NDVI are shown. It can be seen that some of the coefficients are positive, proving positive relationship between rain and greenness with statistical significance up to 4 month lags with rain. The most important rainfall lags are *t - 1* and *t - 2* and not the current time as some works assumed (Nicholson et al., 1990). These results support the fact that with a simple correlation analysis the effect of each month cannot be captured. The significance in almost all locations drops in the 5^{th} lag (green, blue and black points) and further rain lags were not statistically significant.

The northwest part of the Peninsula seems to respond faster to precipitation or it is more sensitive to rain events than other areas in the Peninsula. As stated by Murphy and Lugo (1986) the relationship between water availability and vegetation growth is stronger with aridity. Our results confirm that this relationship is stronger in areas with less rainfall and where more seasonal patterns are present. Statistical significance from the contemporaneous rain until the 4th lag was found. Thus, these results support the importance of precipitation in the growing period.

R-square values follow an interesting spatial pattern, where the highest values are in the north and lower in the south (Figure 5-2). R-squares are between 0.11 and 0.78; these relationships are strong in general. However, there are several cases in the southern part with considerably lower values. This might be due to the presence of evergreen forest which is not as responsive as tropical dry forest to rainfall variations.

Figure 5-3 shows the same regression using MTCI and it can be seen that again, the resultant coefficients are positive. However, there are two main differences from NDVI. First, the *t - 2* and *t - 3* lags seem to be more important in comparison with NDVI which could indicate that the greenness continues to increase but NDVI does not capture it because of its problem of saturation at high levels of green vegetation. Second, in this regression model R-squared values are larger even in places where NDVI has lower values (Figure 5-4). An explanation of this could be that MTCI captures the effects of the rain better.

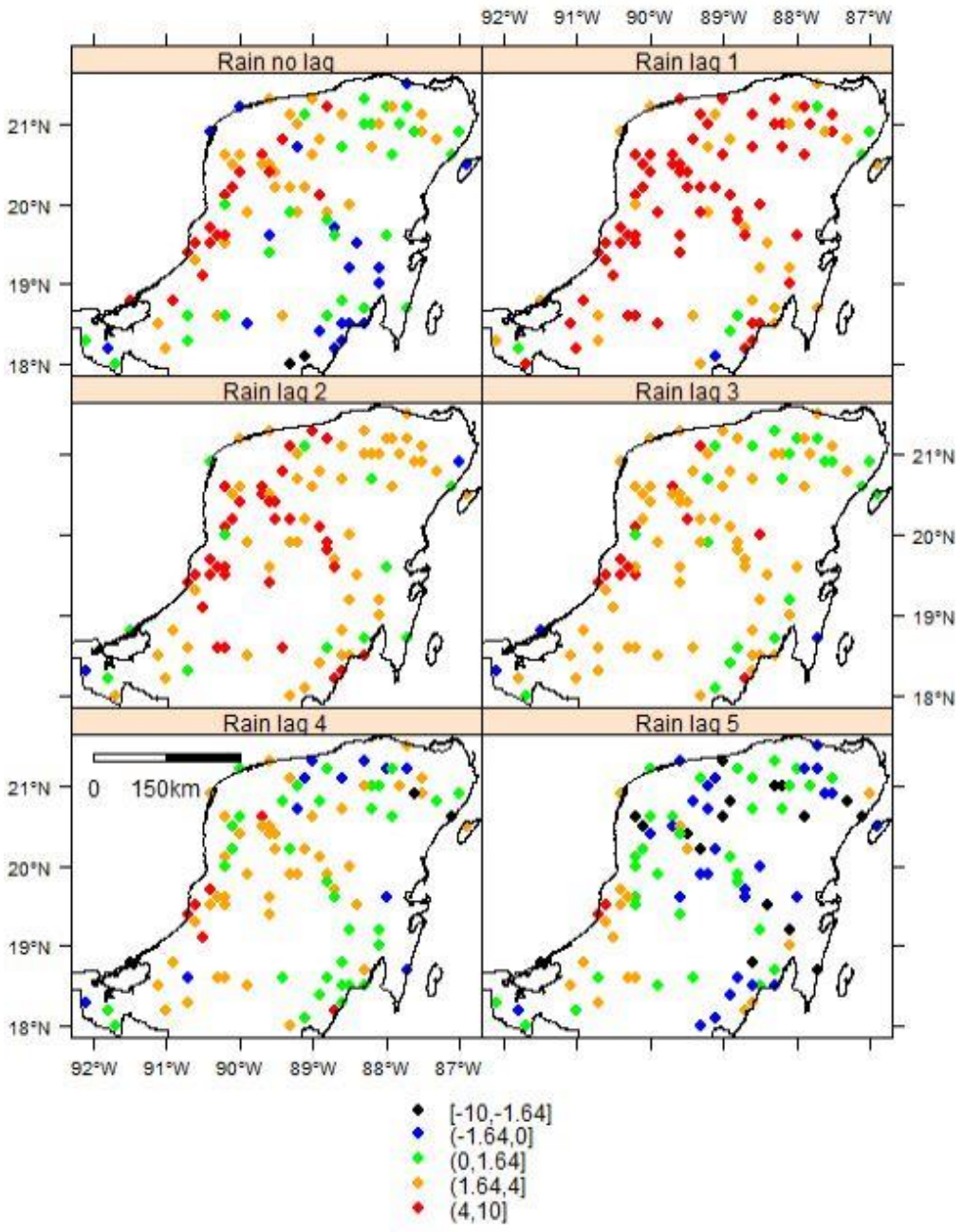


Figure 5-1. Estimations of the regressions. Every map has 122 points showing the significance of the coefficient of a specific variable when the regression is run in that pixel. Having confidence level $\alpha = 0.05$, the critical values are -1.64 and 1.64, the scale is constructed to show them. Each map contains the values of the t-statistics of $\hat{\beta}_1$ in the following regression:

$$y_t = a + \beta_1 x_t + \beta_2 x_{t-1} + \beta_3 x_{t-2} + \beta_4 x_{t-3} + \beta_5 x_{t-4} + \beta_5 x_{t-5} + \varepsilon_t$$

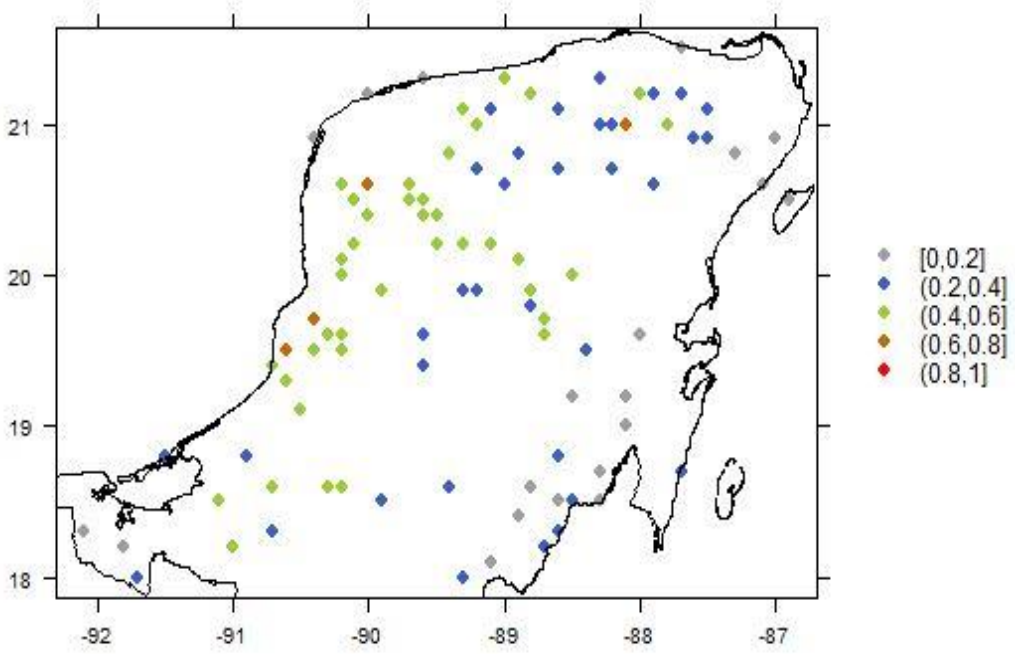


Figure 5-2. R-squares resultant from the first regression model. Each point represent the R-squares for every regression

$$y_t = a + \beta_1 x_t + \beta_2 x_{t-1} + \beta_3 x_{t-2} + \beta_4 x_{t-3} + \beta_5 x_{t-4} + \beta_5 x_{t-5} + \varepsilon_t$$

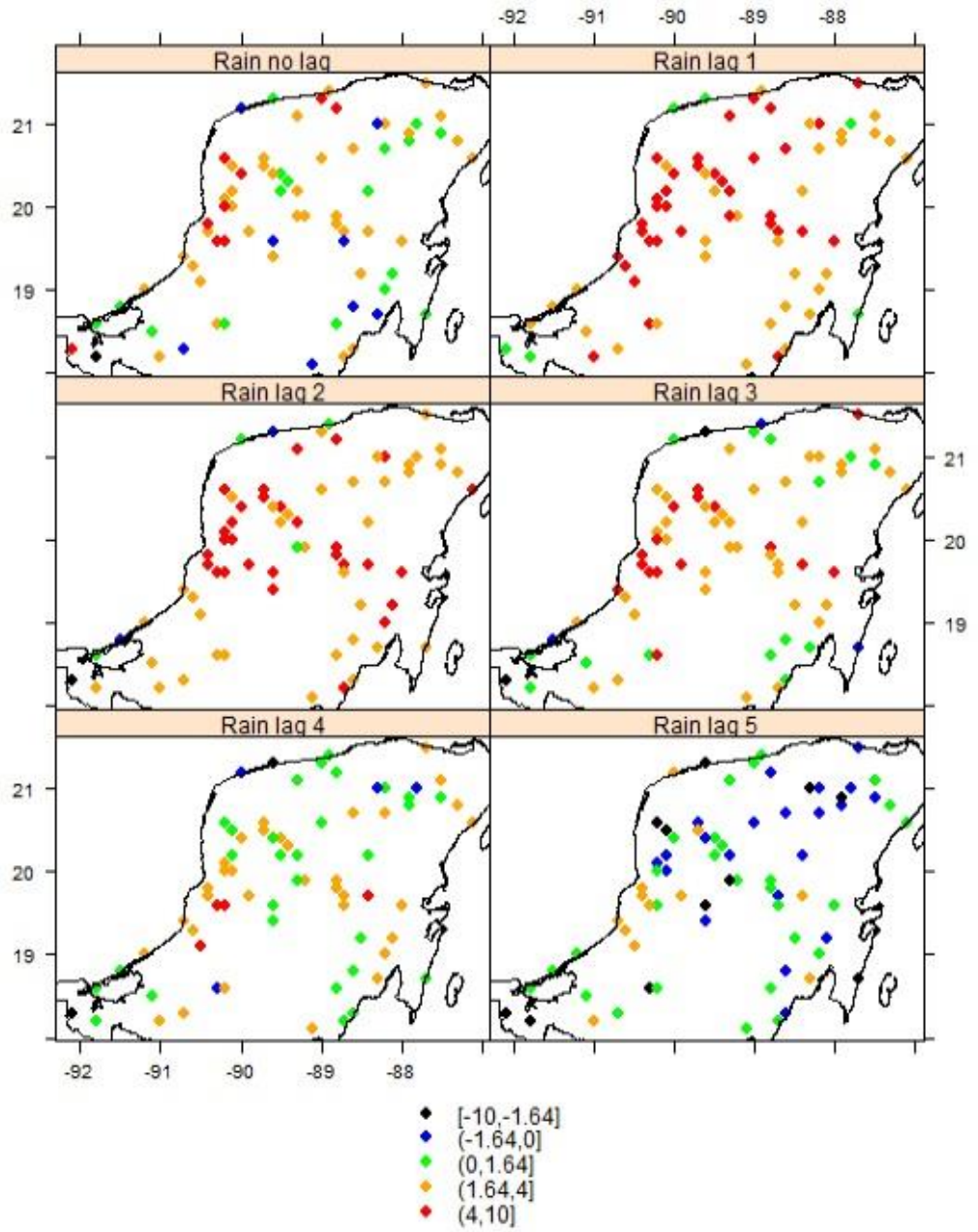


Figure 5-3. Estimations of the regressions (MTCI). Every map has 93 points showing the coefficient of a specific variable when the regression is run in that pixel. Having confidence level $\alpha = 0.05$, the critical values are -1.64 and 1.64, the scale is constructed to show them. Each map contains the values of the t-statistics of $\hat{\beta}_1$ in the following regression model:

$$y_t = a + \beta_1 x_t + \beta_2 x_{t-1} + \beta_3 x_{t-2} + \beta_4 x_{t-3} + \beta_5 x_{t-4} + \beta_5 x_{t-5} + \varepsilon_t$$

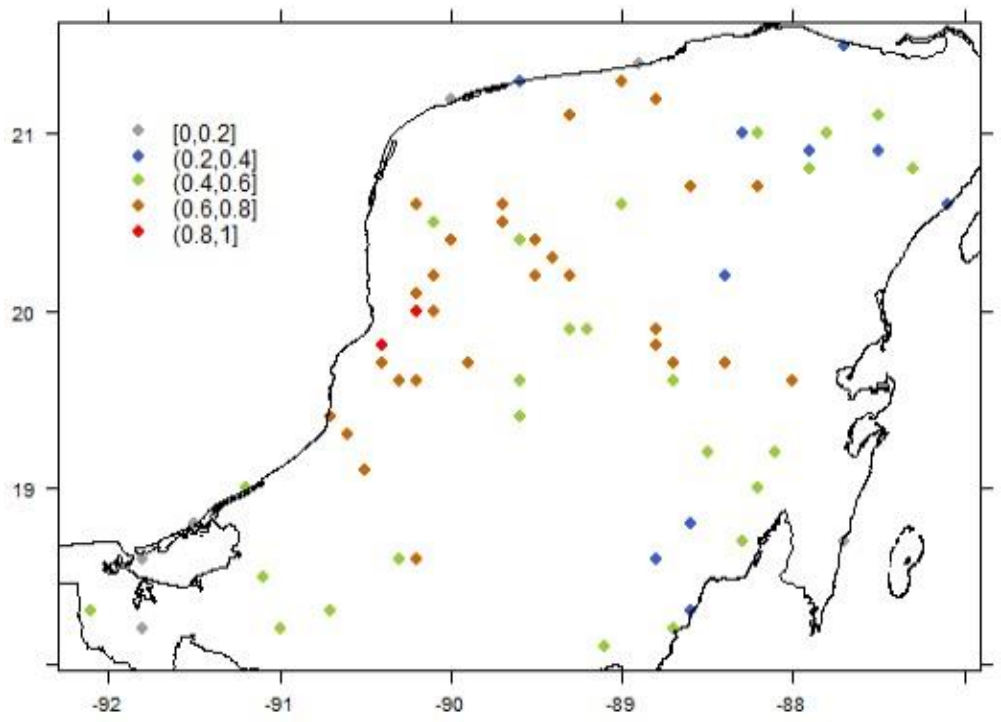


Figure 5-4 R-squares resultant from the first regression model (MTCI). Each point represent the R-squares for every regression.

$$y_t = a + \beta_1 x_t + \beta_2 x_{t-1} + \beta_3 x_{t-2} + \beta_4 x_{t-3} + \beta_5 x_{t-4} + \beta_5 x_{t-5} + \varepsilon_t$$

5.5.2 Vegetation productivity decay

To the best of our knowledge, this model has not been used before in the literature. Here, in the right hand side of the regression a lagged dependent variable i.e. NDVI *t - 1* was introduced. The coefficient of NDVI *t - 1* captures the resistance of vegetation productivity to rain. For example in the scenario when no rain falls in a month, vegetation productivity will not sharply drop, but it will decay slowly over the following months and the rate of decay is characterised by this coefficient. This parameter is extremely important for high frequency data (weekly or monthly data) as it is important to take into account that productivity in the current moment it is dependent on the previous time step.

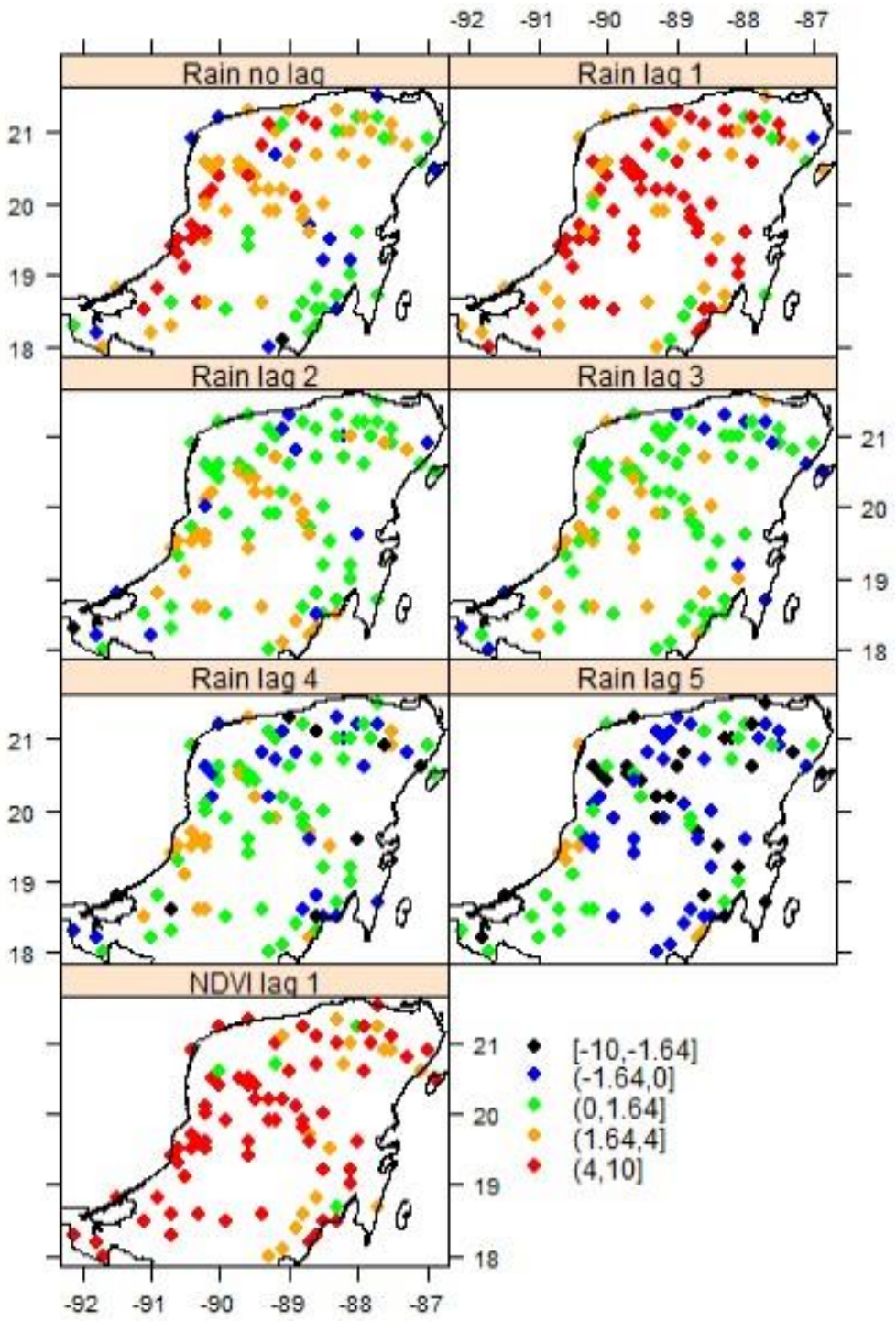


Figure 5-5. Estimations of the regressions. Every map has 122 points showing the coefficient of a specific variable when the regression is run in that pixel. Having confidence level α = 0.05, the critical values are -1.64 and 1.64, the scale is constructed to show them. Each map contains the values of the t-statistics of $\hat{\beta}_1$ in the following regression model:

$$y_t = a + \beta_1 x_t + \beta_2 x_{t-1} + \beta_3 x_{t-2} + \beta_4 x_{t-3} + \beta_5 x_{t-4} + \beta_5 x_{t-5} + \boldsymbol{\beta_6 y_{t-1}} + \varepsilon_t$$

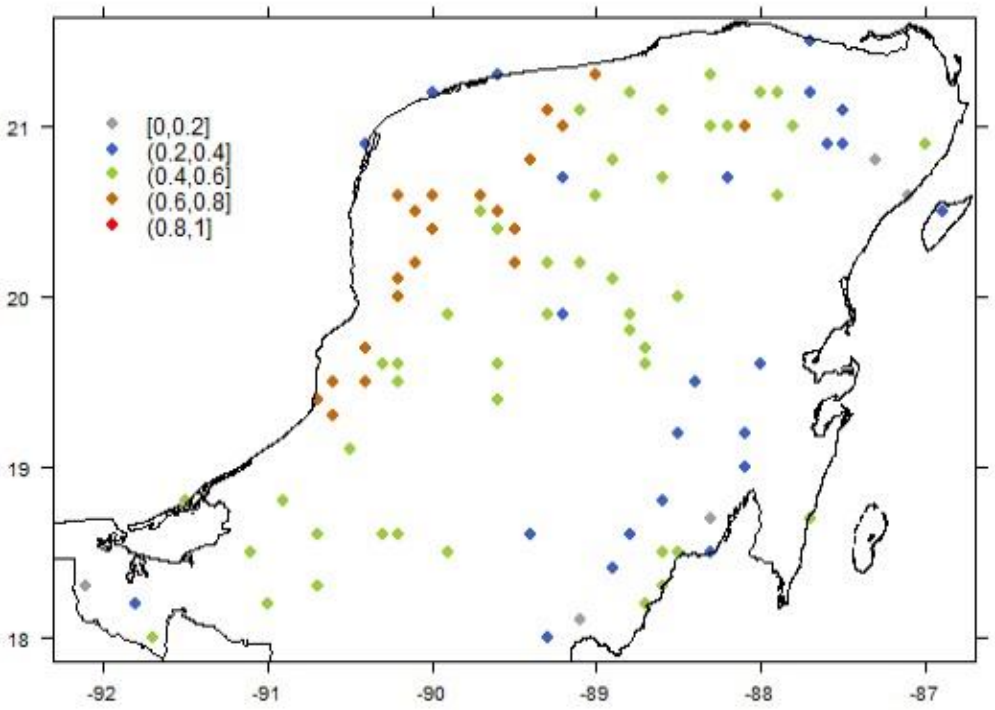


Figure 5-6 R-squares resultant from the second regression model. Each point represent the R-squares for every regression.

$$y_t = a + \beta_1 x_t + \beta_2 x_{t-1} + \beta_3 x_{t-2} + \beta_4 x_{t-3} + \beta_5 x_{t-4} + \beta_5 x_{t-5} + \boldsymbol{\beta_6 y_{t-1}} + \varepsilon_t$$

Vegetation productivity in the current time step is influenced by the vegetation productivity in the previous time. Including this variable improves the model as NDVI or MTCI depends evidently of how were these indices in the previous steps, thus changes in the decay rate of vegetation productivity

When this last component is included it can be seen that only the rain in the current time and *t - 1* affect vegetation (Figure 5-5). Therefore, it seems that this decay effect is part of the model; the lag of NDVI was captured before by the others rain lags coefficients (Figure 5-5) and this is the reason why they were larger in the precious regression. Based on R-squares (Figure 5-6), this model explains the data better. With MTCI data the results are similar (Figure 5-7) but again with higher R-squares (Figure 5-8).

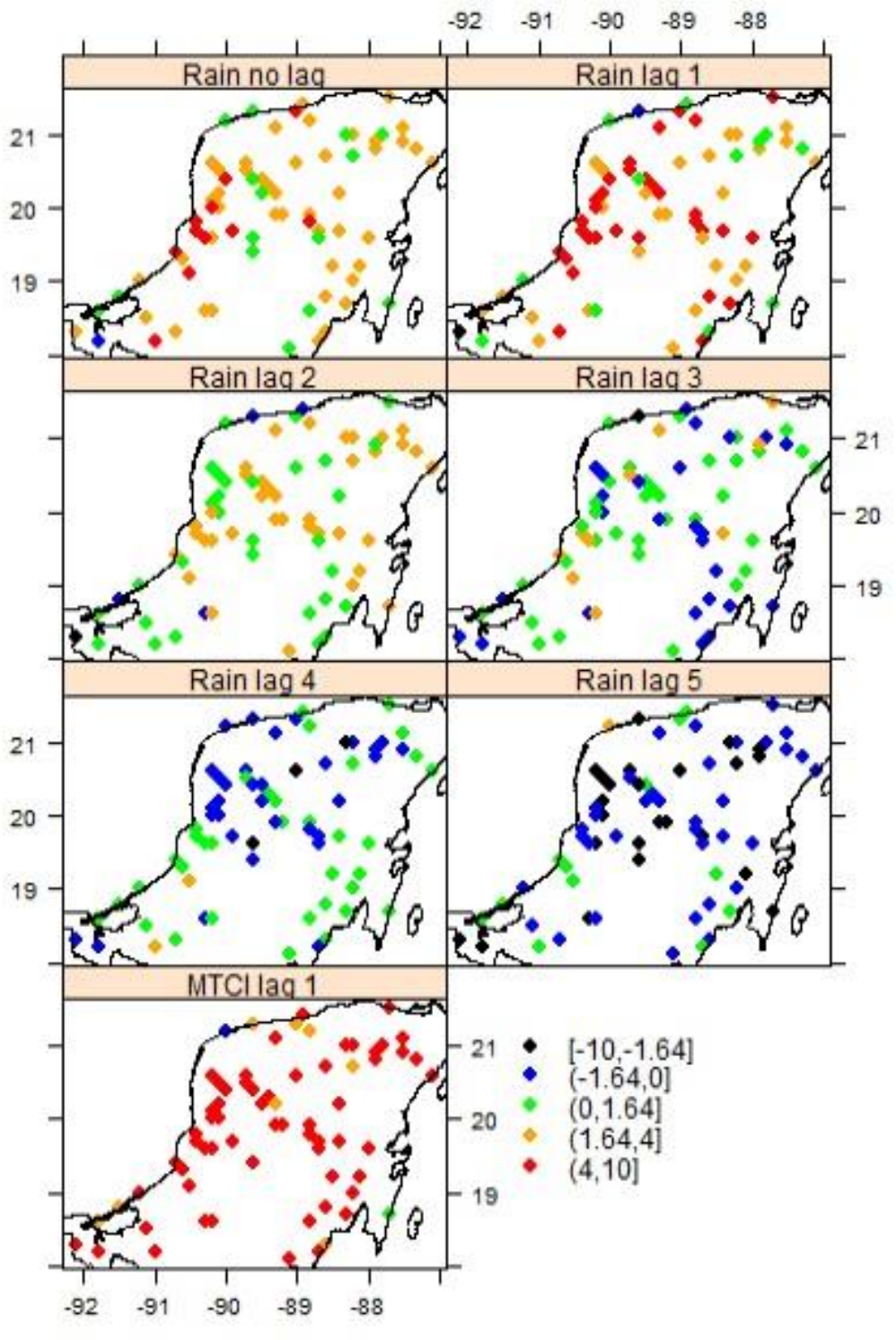


Figure 5-7. Estimations of the regressions (MTCI). Every map has 122 points showing the coefficient of a specific variable when the regression is run in that pixel. Having confidence level $\alpha = 0.05$, the critical values are -1.64 and 1.64, the scale is constructed to show them. Each map contains the values of the t-statistics of $\hat{\beta}_1$ in the following regression:

$$y_t = a + \beta_1 x_t + \beta_2 x_{t-1} + \beta_3 x_{t-2} + \beta_4 x_{t-3} + \beta_5 x_{t-4} + \beta_5 x_{t-5} + \boldsymbol{\beta_6 y_{t-1}} + \varepsilon_t$$

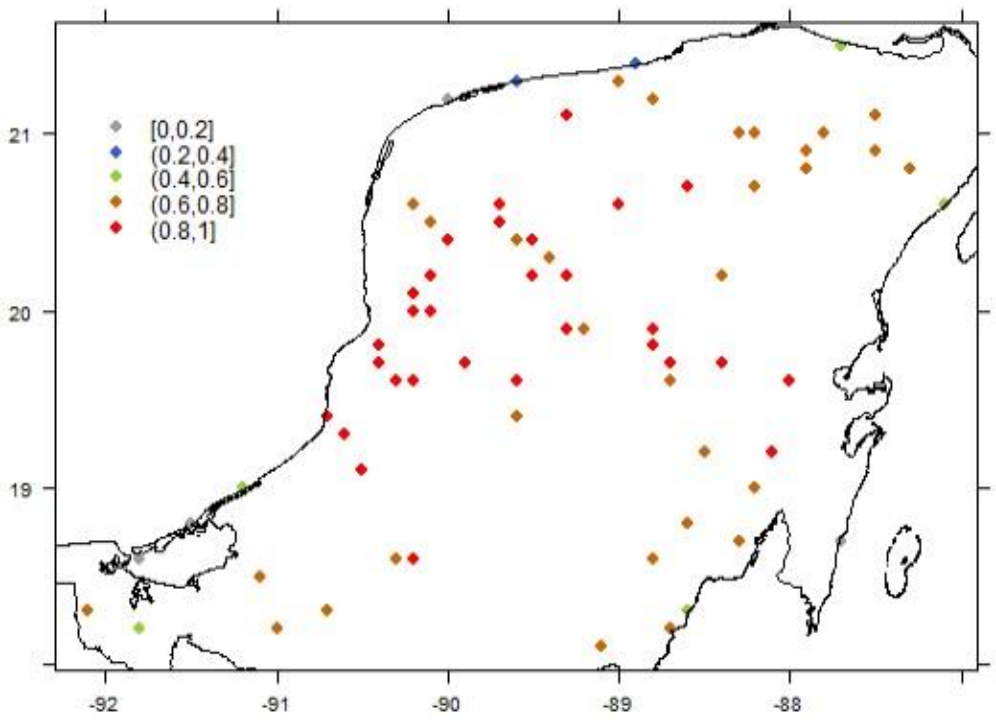


Figure 5-8 R-squares resultant from the second regression model (MTCI). Each point represents the R-squares for every regression.

$$y_t = a + \beta_1 x_t + \beta_2 x_{t-1} + \beta_3 x_{t-2} + \beta_4 x_{t-3} + \beta_5 x_{t-4} + \beta_5 x_{t-5} + \boldsymbol{\beta_6 y_{t-1}} + \varepsilon_t$$

5.5.3 Seasonality

In this model seasonality was incorporated. The results show in Figure 5-9 that seasonality is statistically significant in almost all areas of the Peninsula but it is more important in the northwest part. This result was expected as in the north part, vegetation productivity follows these dry/wet cycles. Introducing seasonality to the model allow us to capture other seasonal factors related with the effect of water availability on vegetation vigour (Ji and Peters, 2003). As shown in Figure 5-9, incorporating seasonality as a categorical variable lowers the effect of the actual rain, but R-squares are a bit higher (Figure 5-10) which indicates that the effect of rainfall on vegetation productivity does not occur instantaneously and it seems to be an accumulative process. This could also be a reason why the first lag drops when seasonality is taking into account. Our results show that the seasonal factor is also very important for vegetation productivity.

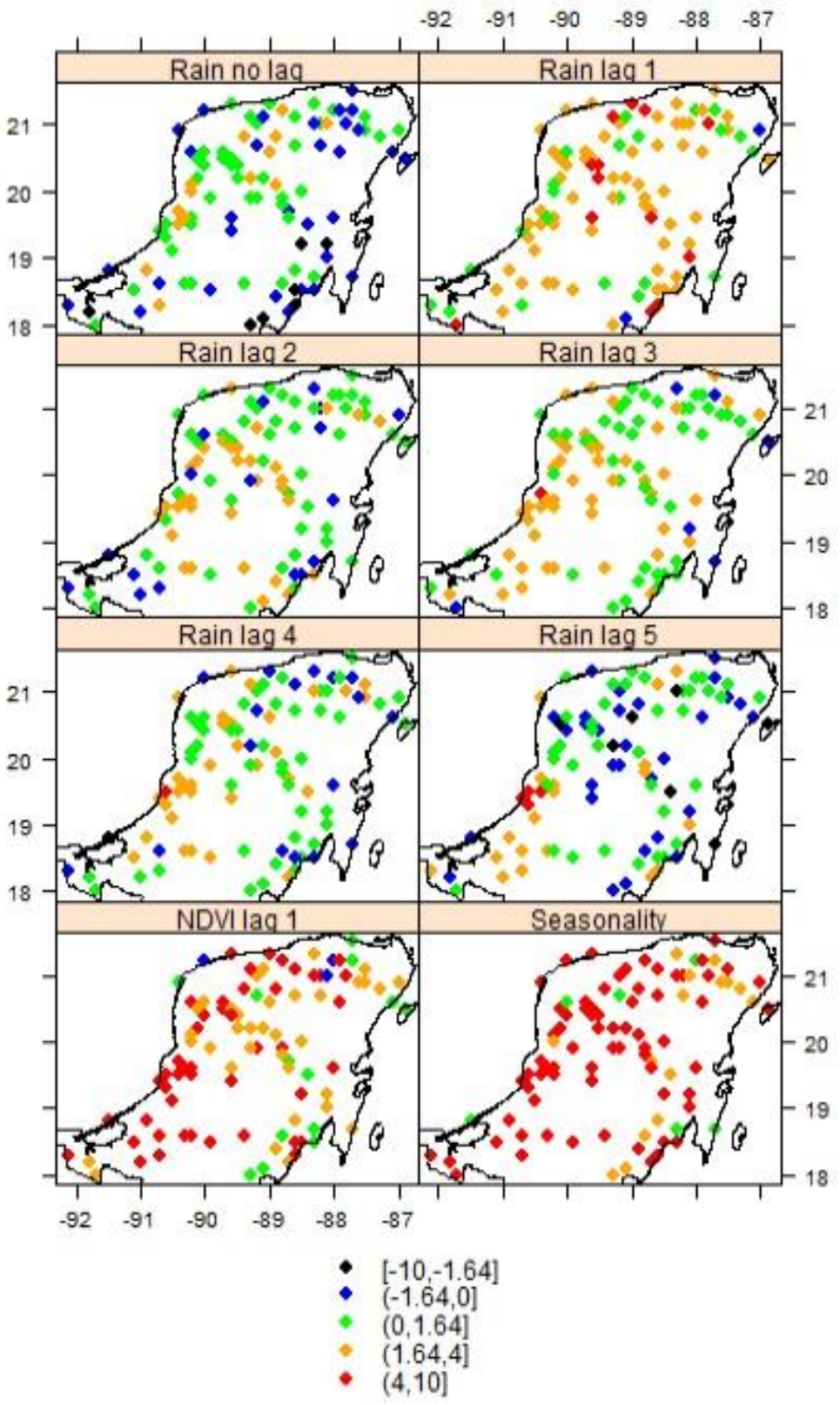


Figure 5-9 Estimations of the regressions. Every map has 122 points showing the coefficient of a specific variable when the regression is run in that pixel. Having confidence level $\alpha = 0.05$, the critical values are -1.64 and 1.64, the scale is constructed to show them. Each map contains the values of the t-statistics of $\hat{\beta}_1$ in the following regression:

$$y_t = a + \beta_1 x_t + \beta_2 x_{t-1} + \beta_3 x_{t-2} + \beta_4 x_{t-3} + \beta_5 x_{t-4} + \beta_5 x_{t-5} + \beta_6 y_{t-1} + \boldsymbol{\beta_7 S_t} + \varepsilon_t$$

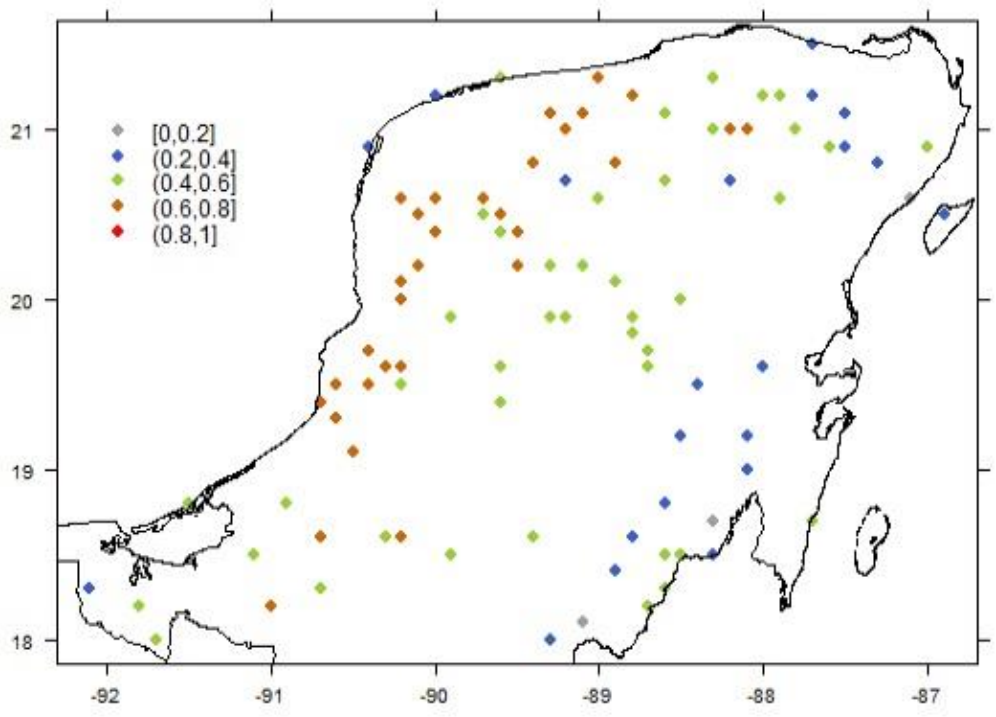


Figure 5-10 R-squares resulting from the third regression model. Each point represents the R-squares for every regression.

$$y_t = a + \beta_1 x_t + \beta_2 x_{t-1} + \beta_3 x_{t-2} + \beta_4 x_{t-3} + \beta_5 x_{t-4} + \beta_5 x_{t-5} + \beta_6 y_{t-1} + \boldsymbol{\beta_7 S_t} + \varepsilon_t$$

MTCI shows (Figure 5-11) the same effect when seasonality is added. However R-squares are again higher for MTCI (Figure 5-12). It is seen overall that the inclusion of lagged MTCI affects past rainfall lags, particularly the 3rd, 4th and 5th month's lags as indicated in Figure 5-11; and the inclusion of seasonality affects more than current rain.

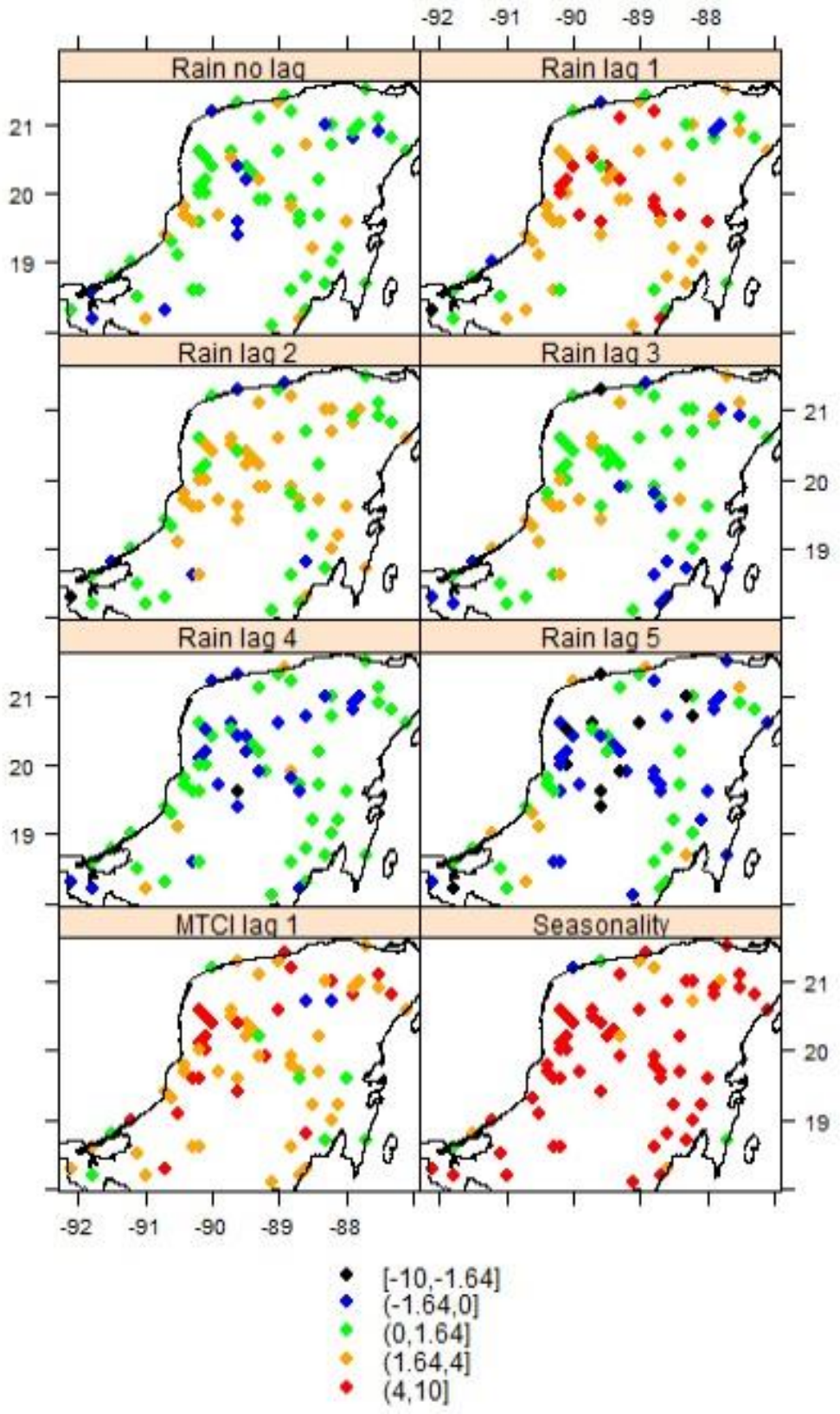


Figure 5-11. Estimations of the regressions (MTCI). Every map has 93 points showing the coefficient of a specific variable when the regression is run in that pixel. Having confidence level α = 0.05, the critical values are -1.64 and 1.64, the scale is constructed to show them. Each map contains the values of the t-statistics of $\hat{\beta}_1$ in the following regression:

$$y_t = a + \beta_1 x_t + \beta_2 x_{t-1} + \beta_3 x_{t-2} + \beta_4 x_{t-3} + \beta_5 x_{t-4} + \beta_5 x_{t-5} + \beta_6 y_{t-1} + \boldsymbol{\beta_7 S_t} + \varepsilon_t$$

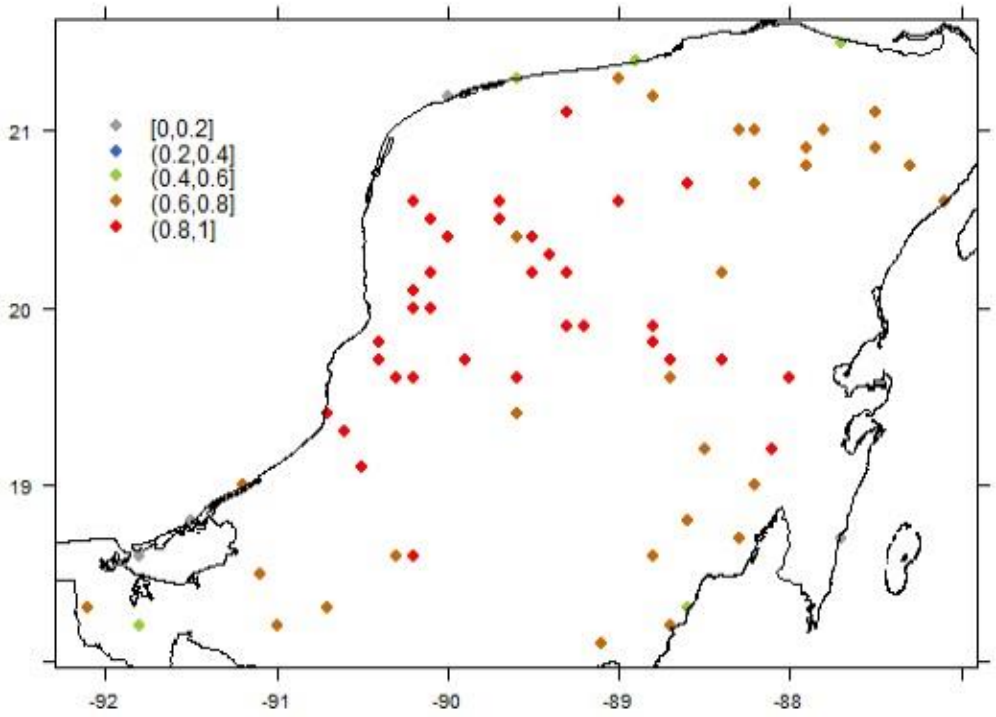


Figure 5-12 R-squares resulting from the third regression model (MTCI). Each point represents the R-squares for every regression.

$$y_t = a + \beta_1 x_t + \beta_2 x_{t-1} + \beta_3 x_{t-2} + \beta_4 x_{t-3} + \beta_5 x_{t-4} + \beta_5 x_{t-5} + \beta_6 y_{t-1} + \boldsymbol{\beta_7 S_t} + \varepsilon_t$$

5.5.4 Drought detection

As our interest in this thesis is to understand how droughts affect vegetation, a drought was added as a dummy variable to the regression model as the last step. SPI with 3-months temporal scale (see section 1.5.1) has been found to be better correlated with NDVI (Ji and Peters, 2003). In order to assure including drought periods a threshold of -0.5 of SPI was selected and including in the regression as a dummy variable. It was found, as shown in Figure 5-13, that drought has a very strong immediate impact, however, it lasts for a short period of time as is shown in the lag *t - 1* of SPI where almost all coefficients are not significant anymore in comparison with the SPI at the current time. It is widely known that water is one of the most important factors for vegetation growth; lack of water will alter vegetation productivity and, therefore, it is expected that lack of water (i.e.

droughts) will be detected in the model. As expected, SPI coefficients resulting from the regression were negative in almost all areas of the Peninsula, demonstrating that an occurrence of a drought promoted negative changes in vegetation productivity.

However, it is interesting to note that the effects of droughts are statistically significant mostly in the north and northwest part of the Peninsula where deciduous vegetation is located. It has been reported (Boyer, 1996; Ji and Peters, 2003) that the onset period or early reproduction stages are most susceptible to droughts and as a mechanism some plants avoid the lack of water by maturing faster. Moreover, deciduous vegetation presents a higher hydraulic conductivity which is reduced in a drought event, whereas evergreen forest has a constant conductivity of water. This plant physiology and behaviour in a limited water scenario is a probable explanation of why tropical dry forest productivity is more affected by droughts than evergreen forest or other types of vegetation presented in the Peninsula. Likewise, Murphy and Lugo (1986) reported that evergreen tropical forest can endure drought periods of up to 2.5 months; whereas tropical dry forest is more vulnerable to these events. These patterns are reflected in the results where the impact of droughts is reflected in the northern part of the Peninsula and less significance was found in the southern part. On the contrary, the south east part of the Peninsula does not present a negative relationship with the occurrence of droughts. This area is a region with high agricultural and livestock activity. Regarding the MTCI dataset, same patterns were captured (Figure 5-15). Conversely, fewer pixels were significant in the occurrence of a drought and as in the other regressions, the R-squares are higher (Figure 5-16) than NDVI.

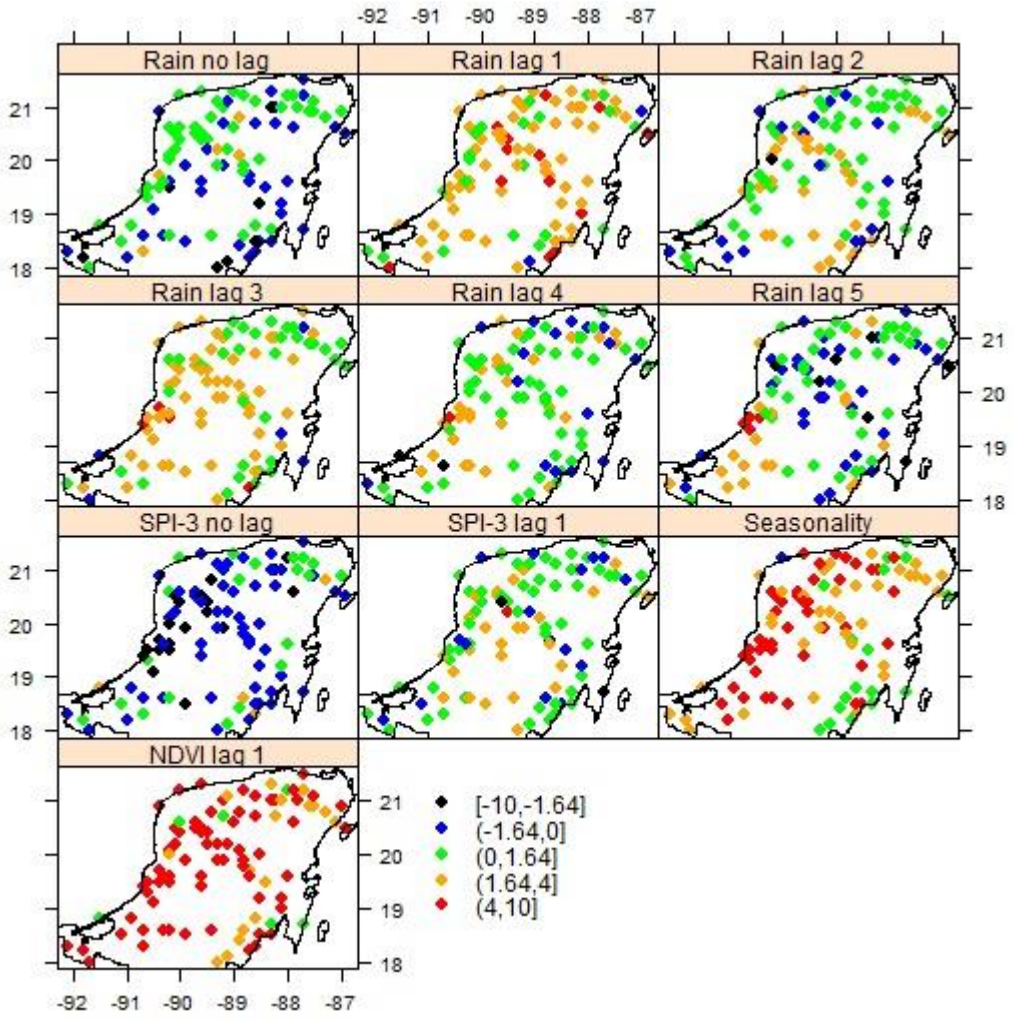


Figure 5-13 Estimations of the regressions (NDVI). Every map has 122 points showing the coefficient of a specific variable when the regression is run in that pixel. Having confidence level $\alpha = 0.05$, the critical values are -1.64 and 1.64, the scale is constructed to show them. Each map contains the values of the t-statistics of $\hat{\beta}_1$ in the following regression: $y_t = a + \beta_1 x_t + \beta_2 x_{t-1} + \beta_3 x_{t-2} + \beta_4 x_{t-3} + \beta_5 x_{t-4} + \beta_5 x_{t-5} + \beta_6 y_{t-1} + \beta_7 S_t + \boldsymbol{\beta_8 SPI_t} + \boldsymbol{\beta_9 SPI_{t-1}} + \varepsilon_t$

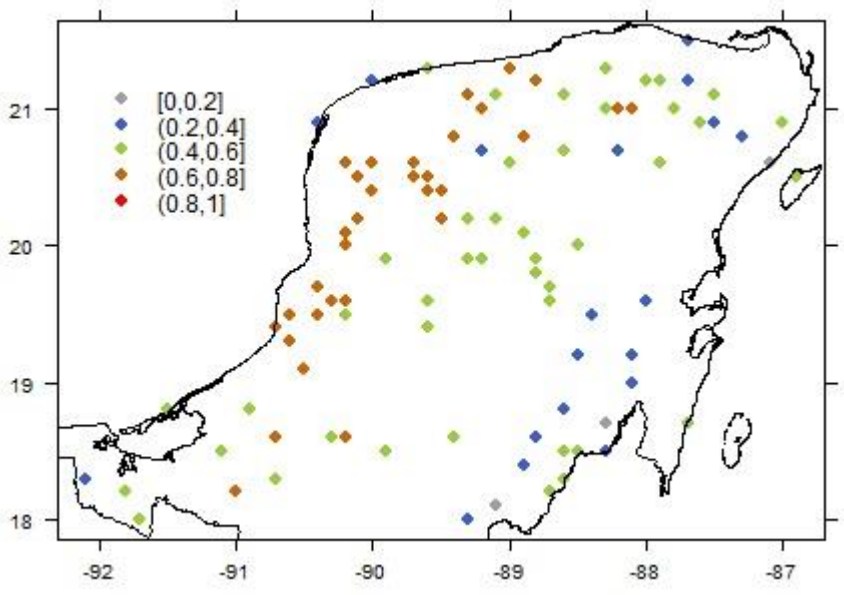


Figure 5-14 R-squares resulting from the fourth regression model. Each point represents the R-squares for every regression.

$$y_t = a + \beta_1 x_t + \beta_2 x_{t-1} + \beta_3 x_{t-2} + \beta_4 x_{t-3} + \beta_5 x_{t-4} + \beta_5 x_{t-5} + \beta_6 y_{t-1} + \beta_7 S_t + \boldsymbol{\beta_8 SPI_t} + \boldsymbol{\beta_9 SPI_{t-1}} + \varepsilon_t$$

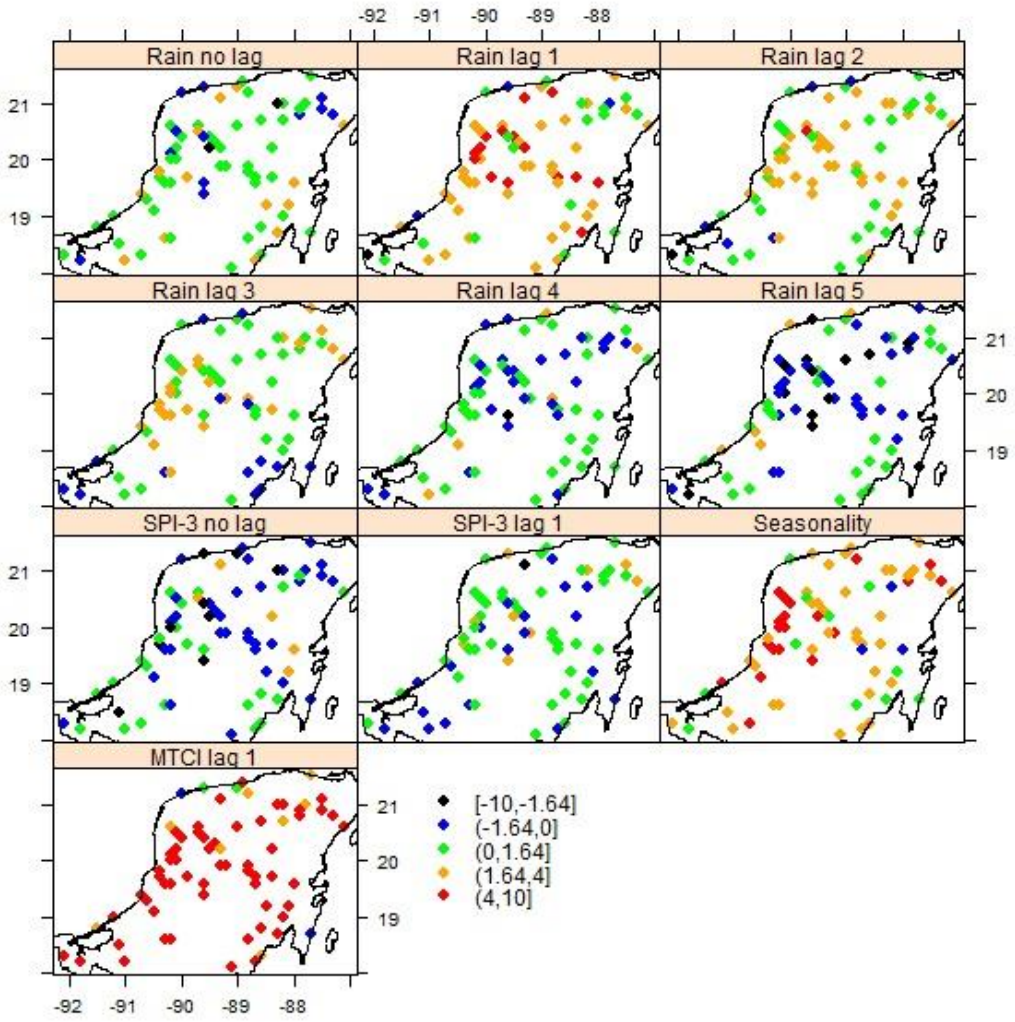


Figure 5-15 Estimations of the regressions (MTCI). Every map has 122 points showing the coefficient of a specific variable when the regression is run in that pixel. Having confidence level $\alpha = 0.05$, the critical values are -1.64 and 1.64, the scale is constructed to show them. Each map contains the values of the t-statistics of $\hat{\beta}_1$ in the following regression: $y_t = a + \beta_1 x_t + \beta_2 x_{t-1} + \beta_3 x_{t-2} + \beta_4 x_{t-3} + \beta_5 x_{t-4} + \beta_5 x_{t-5} + \beta_6 y_{t-1} + \beta_7 S_t + \boldsymbol{\beta_8 SPI_t} + \boldsymbol{\beta_9 SPI_{t-1}} + \varepsilon_t$

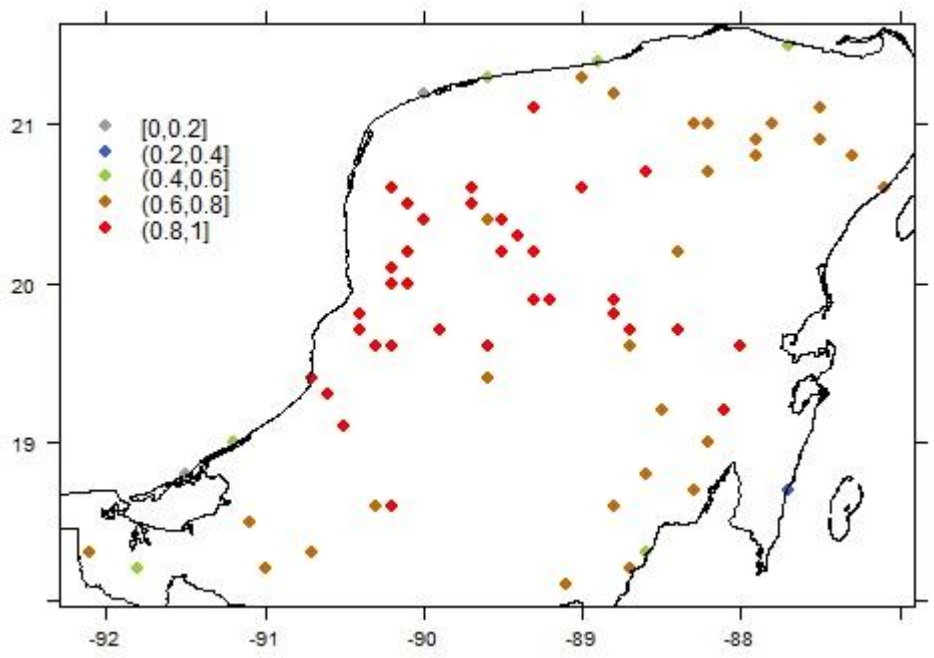


Figure 5-16 R-squares resulting from the fourth regression model (MTCI). Each point represents the R-squares for every regression.

$$y_t = a + \beta_1 x_t + \beta_2 x_{t-1} + \beta_3 x_{t-2} + \beta_4 x_{t-3} + \beta_5 x_{t-4} + \beta_5 x_{t-5} + \beta_6 y_{t-1} + \beta_7 S_t + \boldsymbol{\beta_8 SPI_t} + \boldsymbol{\beta_9 SPI_{t-1}} + \varepsilon_t$$

5.6 Chapter summary

Returning to the aims presented at the beginning of this chapter, it is now possible to state that the relationship between vegetation productivity and precipitation in the Yucatan Peninsula is significant and regression analysis gave us the tools to analyse this relationship in a better way than a simple correlation. In addition, we found that including categorical variables was helpful to understand the spatial and temporal patterns of this relationship.

This chapter has also shown that vegetation productivity is affected by the lack of rain (i.e. droughts). The percentage of pixels which show impact of droughts may seem surprising at first sight; however, it is in line with our findings in our trend analysis results of chapter 4. Tropical dry forests are more affected by the lack of water than evergreen forests and according to the findings in the previous chapter tropical dry forest is the least resistant and resilient vegetation type.

However, seasonality in this area is stronger, thus this vegetation responds faster to precipitation changes. Therefore, vegetation is more responsive to changes and perhaps to climatic variations. Nevertheless, as shown in Figure 5-13 vegetation productivity does not show negative response after a month of the drought period.

In general, vegetation productivity responds principally in the first and second lags, being more significant for both MTCI and NDVI. However, MTCI shows that the third month lag of rain also affects vegetation productivity and this difference between the two indices could be related to the already discussed saturation drawback of NDVI. R-squares in all models were higher for MTCI, which could indicate that MTCI is more sensitive to rain.

It was novel to incorporate the lag of NDVI/MTCI and it seems important for high frequency data. Results showed that this variable was positive and statistically significant in all regressions. Similarly, vegetation productivity was also affected greatly by seasonality.

The use of vegetation indices seems to be a good approach to detect droughts and understand the impacts they have on vegetation productivity. In addition, the regression model as a technique is extremely flexible and could be used for improving inferences in the future adding other variables such as soil moisture, monthly dummies variables, vegetation categories, ENSO effects or by using other indices for both droughts and productivity. Thus, different questions arise from this analysis and open the possibility to understand better how vegetation is impacted by droughts and its relationship with other climatic or anthropogenic factors. The next chapter presents a discussion of the key findings and propose some research lines for future work.

CHAPTER 6. **DISCUSSION, CONCLUSIONS AND SUGGESTIONS FOR FUTURE WORK**

This chapter presents a discussion of the main research findings and outlines the contribution of this thesis to current research. Further, it provides a link between the theoretical and experimental aspects of the research and suggests possible directions for future research. Conclusions are then stated.

The research is based on the premise that remote sensing for Earth Observation is a useful approach for monitoring vegetation dynamics, thus allowing for follow up of possible impacts of events on vegetation. This thesis focuses on the extreme climatological event of drought. In chapter 1, the lack of understanding of how vegetation responds to droughts in the Yucatan Peninsula was described. This limited understanding is a result principally of the complexities surrounding the topic, which is related to different types of factors such as regional climatology, land use and cover change, ecology and species interaction, and the difficulty of detecting droughts (i.e., threshold and timing to define a drought) and isolating their impacts. Moreover, previous studies in the Yucatan have been focused principally on the impacts of both deforestation and human activities (particularly urbanisation) (Geoghegan et al., 2001; Turner et al., 2001; Turner II et al., 2004; García-Frapolli et al., 2007; Ellis and Porter-Bolland, 2008; Colditz et al., 2015). Much less effort has been focussed on trying to understand the impacts of drought in this geographical area, yet it is an area which experiences much variability in precipitation (see section 2.3.1).

The main contributions of the research contained within this thesis have, therefore, been to: i) develop an understanding of how vegetation responds to droughts; ii) understand the precipitation variability in the Yucatan and when droughts have occurred (during the period 1980-2011) (see chapter 3); iii) assess vegetation productivity across the Yucatan Peninsula and quantify resilience and resistance of the different types of vegetation to variability in precipitation amount (see chapter 4); iv) understand how the above is contingent on the remote

sensing data used, in this case through the production of vegetation indices (see chapter 5).

Understanding the responses of vegetation to droughts is imperative since it will help to explain the implications that droughts have for human subsistence (Wilhite, 2000; 2012). Moreover, understanding vegetation dynamics at a regional scale will help to create a baseline for further studies and, therefore advance research for decreasing the potential vulnerability of the Yucatan Peninsula.

6.1 Discussion of key findings

In reference to the thesis' aims outlined in section 1.9, the key findings are summarised below:

Precipitation in the Yucatan Peninsula increases in magnitude from the northwest to southeast. Annual precipitation totals can range from ~ 1500 mm to ~ 1800 mm in the south eastern part, and ~ 300 mm to ~ 600 mm in the north western part (Figure 2-5). This gradient is closely related with the different vegetation types in the area following the same gradient from north (deciduous forest) to south (evergreen forest). Although this pattern has reported in the literature (García, 1998b; Torrescano-Valle and Folan, 2015), this research is based on more updated data at spatial and temporal resolutions not previously seen. Moreover, with climate change being linked to change in precipitation (Villers-Ruiz and Trejo-Vázquez, 1997; Orellana et al., 2009; IPCC, 2013), ongoing studies to understand the patterns of precipitation are important, particularly to understand how resistant and resilient the vegetation in the area is as precipitation scenarios in the Peninsula indicate a decrease in precipitation, especially in the northern part (Orellana et al., 2009). It is demonstrated that precipitation patterns in the Peninsula have not changed in terms of the general gradient (Figure 2-5) if these results are compared with those reported by Garcia (1998b) and Hodell et al. (2007).

Yearly precipitation maps were created for the whole Peninsula (Figure 3-13). Although the same precipitation gradient as previously seen in the literature was evident, these maps illustrate when the wettest years (1988, 1995, 2002 see section 3.3.1, Figure 3-10 and Figure 3-13) and the driest years occurred (1986, 1987, 1994, 1996, 2003, 2004, 2009) in the period 1980-2011 and the spatial severity of these extremes. Although excess of rain was not an aim for this thesis, wet-dry patterns in precipitation are important to understand in terms of vegetation recovery.

With respect to the extremes of precipitation leading to a drought, the precipitation data were used in two ways to detect where and when droughts had occurred across the Yucatan Peninsula, during the period 1980 – 2011. Maps of SPI and precipitation anomalies were generated and showed that the years of 1981, 1986, 1987, 1994, 1996, 2003, and 2009 were those that could be described as having had a drought. 2009 is reported widely as having been one of the driest years in the history of the Mexico (Esparza, 2014). Moreover, these results are similar to those reported by Márdero et al. (2012) where 1986, 1987 and 1994 are reported as years with negative rainfall anomalies in 7 out of the 9 meteorological stations used located in the south part of the Peninsula. As there is a lack of these type of studies, unfortunately, it is difficult to compare the results obtained in this work with other findings. However, the findings of this investigation complement those of earlier studies and also this research provides a framework for the exploration of how drought events impact on vegetation.

Via the use of the NDVI (from the AVHRR sensor), spatial and temporal patterns of vegetation dynamics across the Yucatan Peninsula for the period of study illustrated a dominance of positive NDVI trends, covering almost all the Peninsula (see Figure 4-4). Fewer areas with negative persistent trends were observed; these are located close to some of the principal cities (i.e. Cancun, Chetumal, and Campeche, excluding Merida), across the Riviera Maya and in the northeast of the Peninsula. This could be concomitant with human activities such as mass tourism, population growth, and agricultural intensification in these regions (García-Frapolli et al., 2007; Ellis and Porter-Bolland, 2008). Negative trends in these areas are related to more unstable vegetation conditions with

lower levels of recovery ability and can be related to a preliminary sign of stressed conditions. In contrast, positive trends do not necessarily imply that vegetation trends are increasing through time, instead they describe more stable vegetation.

As a "picture" of the state of the vegetation across the Peninsula across the time period of study the use of the NDVI data within an analysis of resilience allowed us to understand how each vegetation type recovers from a disturbance. Persistence probabilities (i.e. resilience) and NDVI decay times plots (i.e. recovery) (see section 4.4.2.1) showed that all vegetation types, with the exception of deciduous forest and grasslands, had longer lifetimes for positive trends than those for negative trends. In contrast, deciduous forest and grasslands have longer persistent negative trends. This means that deciduous forest and grasslands are much less resilient (i.e. longer recovery periods) than the other types of vegetation and the recovery of these two types of vegetation is longer than with the other ones. Estimating the resilience and resistance of vegetation provides realistic information of the dynamics of vegetation and the status of it. This information could be related cautiously to structural, anthropogenic and climatic features in the Yucatan Peninsula. Isolating the impacts of a drought on vegetation is challenging due to the complexity of both. However, understanding patterns and timings of the occurrence of droughts and vegetation is a benchmark for further studies. Thus, it is important to understand also the relationship in this area between vegetation productivity and precipitation.

It was observed that a strong statistical association exists between precipitation and vegetation productivity in the Yucatan Peninsula. Regression analysis showed that vegetation productivity variance could be explained by rainfall variance. The spatial patterns between these two variables are remarkably similar and the vegetation cycles (i.e. phenology) are closely related to the precipitation seasonality. The best association between rainfall and NVDI and MTCI was found with a lag of one to two months between precipitation and vegetation response. However, the strongest relationship between these two variables seems to be in the northwest part of the Peninsula. The regression models developed show that including seasonality and a lagged dependent

variable (i.e. NDVI or MTCI) improves the r-squared coefficient suggesting that these variables should be included in these type of analysis to get better results as suggested by Ji and Peters (2005). Including a lagged dependent variable it is helpful to understand the resistance of vegetation productivity.

Regarding droughts, they have an immediate negative impact on vegetation productivity across the Peninsula (see section 5.5.4), in contrast with the lagged response to rainfall; thus, droughts impact vegetation in the next month after their occurrence and they do not last longer than a month in most of the locations in the Peninsula. However, stronger negative effects were found in the north part where the vegetation is less resistant. On the contrary, in the southern part of the Peninsula droughts have less impact on vegetation productivity and following the results of resistance and persistence, it is in these places where vegetation is more resilient and resistant (see section 4.4.2).

In summary, precipitation analysis and drought detection (chapter 3) allow us to understand the spatial and temporal variability of rainfall and the occurrence of droughts. Afterwards, vegetation productivity analysis (chapter 4) aided in understanding vegetation persistence trends and which vegetation types are more or less resilient under stress conditions. Despite using a methodology which aims to diminish land cover changes, thus expecting climatological variations to be shown, the results do indicate that negative trends are located in areas where more human disturbances have occurred. Therefore, and with the premise that rainfall is the main driver for vegetation in this area, the analysis of the relationship between precipitation and vegetation productivity (chapter 5) allowed us to understand in which areas of the Peninsula the effects of droughts are more significant and we found that in the north part of the Peninsula vegetation productivity and rainfall have a stronger association, thus the occurrence of a drought is more evident there. Regarding the methodologies used in this thesis, it can be confirmed that the methodologies selected in chapters 3, 4 and 5 were appropriate for developing a better understanding of how droughts can impact vegetation in the Yucatan Peninsula as discussed in each chapter.

6.2 **Knowledge gaps addressed and thesis novelty**

The Yucatan Peninsula has great importance due to its biodiversity and the ecosystem services it provides to society (Turner et al., 2001; Islebe et al., 2015). One of the main efforts to understand and preserve this area has been concentrated on ecological studies and on the absolute changes that vegetation has suffered (i.e. land use and land cover changes). However, less effort has been made in understanding the responses of vegetation to the different effects that climate change is having on the natural environment and on human well-being. The Yucatan Peninsula is vulnerable to natural disasters due to its location and its climatology. This vulnerability is more relevant in areas where the development level is low, poverty is high and no pertinent programmes for these weather events are a priority (Boyd and Ibarrarán, 2009). Therefore, this research is not only important in terms of the physical impacts, it is also valuable for using it for further studies including society impacts.

To my knowledge, this study presents the largest dataset analysis to-date with a comprehensive analysis of precipitation, droughts and vegetation productivity and the relationship between them in the Yucatan Peninsula. Previous analyses have been focused either on exploring patterns of precipitation in specific areas of the Peninsula (Márdero et al., 2012) (Neeti et al., 2012) or in the analysis of historic droughts (Mendoza et al., 2005; Mendoza et al., 2006; Mendoza et al., 2007) (i.e. climatological reconstruction) or vegetation dynamics in terms of deforestation (Geoghegan et al., 2001; Colditz et al., 2008; Ellis and Porter-Bolland, 2008).

A particular contribution of this study is the extended geographical range (Mexican part of the Peninsula) of analysis from the driest part of the Peninsula to the wettest area, covering all vegetation types from tropical dry forest to evergreen forest. It is the first study which analyses vegetation sensitivity in terms of resistance and resilience using remote sensing data in this area. These analyses and their relation to droughts are an important insight as they could be really powerful to understand how different impacts would result in different vegetation types and therefore their application can be extended to ecosystem

services for society. Furthermore, quantifying recovery times of vegetation is novel and it can be a powerful tool for conservation policies and warning/response programmes in case of extreme climatological events (i.e. droughts, not excluding others such as hurricanes).

6.3 Reflections on datasets and methods

Traditionally, climatic analyses are based on meteorological data (i.e. precipitation, temperature, evapotranspiration) collected *in situ*. Networks of meteorological stations are absolutely valuable as the data collected is the most accurate measures we can have. In Mexico, despite the efforts and the investment for maintaining this network, there are many problems related to data continuity (i.e. no data available for all time periods), to geographical distribution (i.e. sparsely distributed), and to data consistency (i.e. different institutions manage the same data in different ways) (see section 3.2.1). Meteorological stations result in high-cost maintenance and there are still inaccessible or rural areas without information. In this thesis, this was a major challenge. The gathering of data from the meteorological stations was not trivial as the data are dispersed and inconsistent through the institutions in charge of them, thus, making this task challenging. In this regard, homogenisation of the data is needed in order to progress and avoid duplicating efforts between researchers and institutions, this will allow progress towards deeper climatology analysis, droughts and modelling scenarios.

In terms of drought detection, drought indices are used to quantify the severity (i.e. intensity), location, and duration (i.e. start and end timing) of droughts (see section 1.5.1). However, it is well known that different results are obtained depending on the type of drought index and the way to compute them. For instance, one of the most widely used indices is the Palmer Drought Severity Index (PDSI), however, this index requires complex calculations, is not spatially comparable (cannot be comparable between regions), and needs a complete series of data of precipitation, temperature and available water content, thus its application to the Yucatan Peninsula is not possible. Some institutions have tried to calculate it, but it is just available for middle and high latitudes. Therefore,

the SPI was selected for this research and as recommended by the WMO (see section 1.5.1). Although this index does not require data other than precipitation, there are still some problems in the computation of it. It was found in this thesis that different programs (i.e. software) give different results. The official program that the WMO recommends is available in the National Drought Mitigation Center (http://drought.unl.edu/monitoringtools/downloadablespiprogram.aspx). The results from this program differ from, for example, three available R packages: package "SPI", package "SPEI", and package "SCI". Therefore the results obtained for any of these software packages should be analysed carefully. In addition, it was found that in Mexico, the SPI data available on the CONAGUA website is similar to the results calculated in the R program. However, the North American Drought Monitor, which includes Mexico, uses the SPI from the WMO software (Figure 6-1).

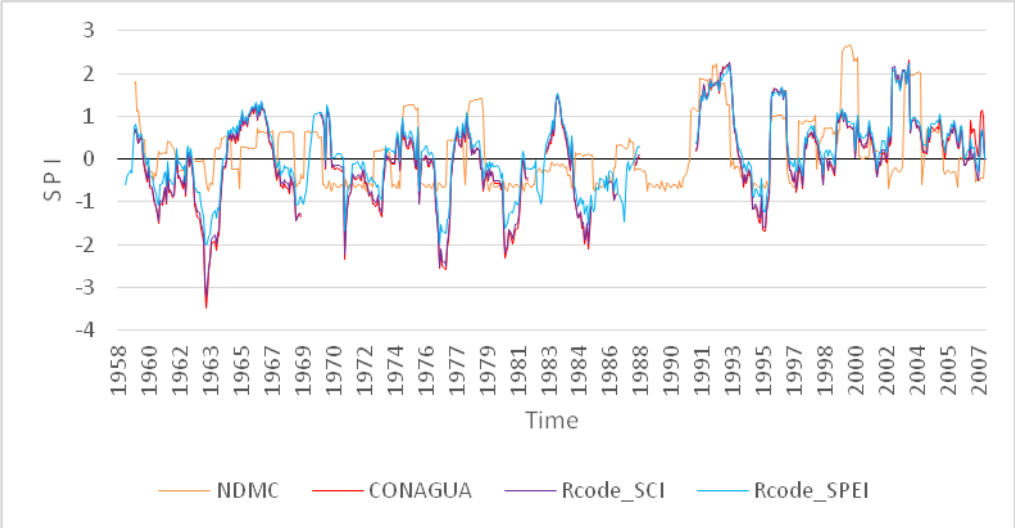


Figure 6-1. SPI computation from different software and sources of information.

Current research of drought includes remote sensing observations to assess drought vegetation impacts with the premise that droughts affect vegetation in terms of health and growth. In other words, the photosynthetic activity of plants is affected by the lack of water, thus vegetation indices have been broadly used (see section 1.6.2). The remote sensing arena is growing in terms of the number of products available and the improvements in spatial, temporal and spectral resolution. However, there are still some considerations that we need to take into account for using remote sensing observations. For instance, the oldest products

available are those from AVHRR and Landsat which go back in time to the 1970s. In this thesis NDVI from AVHRR was selected for this reason as this index cover the period of time necessary for study droughts in a climatological perspective (30 year period). However, there is always a trade-off between spatial, spectral or temporal resolution for selecting the best product to accomplish the objectives of the study.

NDVI has important drawbacks as mentioned in section 1.7. These disadvantages are related to the saturation of NDVI in areas with higher biomass (i.e. dense forested areas), thus changes in productivity in these areas is difficult to detect. Therefore, using this index in tropical environments becomes more challenging. Other indices have been developed to overcome these drawbacks, one is the MTCI (see section 1.6.2.2). The results from chapter 5 shows that MTCI seems to be more sensitive to changes in the southern part of the Peninsula where evergreen forest is present. However, MTCI is only available for the period 2002-2011. This period of time is not long enough, for example, for performing the resistance and resilience analysis for the area. However, the development of new products and the launch of new missions (i.e. Sentinels) has brought and opened new research insights to develop better results regarding droughts and other environmental studies. Sentinels, for instance have new spectral bands across the visible, VNIR and SWIR spectrum and the new bands centred around 1600 nm and 2200 nm will be suitable for analysing content of water and stress detection in vegetation. New challenges are coming and the use of these data will open new research lines. Nevertheless, for now, the historical data available from satellite imagery and climatological data provides a real opportunity to test, quantify and detect the impacts of droughts on vegetation.

Developing models, especially for complex problems or locations such as the relationship between vegetation productivity, droughts and precipitation in the Yucatan Peninsula, necessarily involves a simplification of the heterogeneity of problem. For instance, in chapter 5, it was assumed that the relationships are linear, however, they might not be linear, but as a first approach to understand the variability of vegetation productivity in the Peninsula caused by rain or the lack of it (i.e. droughts) it is novel in the area even though many studies have

been done elsewhere, principally in the Sahel area. Also, it is important to mention that many non-linear relationships can be approximated well by linear models as other studies have shown (Nicholson et al., 1990; Ji and Peters, 2005).

6.4 Monitoring droughts and conservation implications

This study is one of a handful of environmental studies of the Yucatan Peninsula that have investigated the spatial and temporal variability of the precipitation in the area, the sensitivity of vegetation in terms of resilience and resistance and the spatial understanding of how droughts impact vegetation productivity. It provides evidence and quantifies times that would be really useful for: i) detecting and monitoring droughts; ii) understanding trends in vegetation dynamics; iii) prioritising conservation efforts on less resistant and resilient vegetation; iv) creating programmes for warning and response in case of droughts and v) estimates of recovery times could be really useful for monitoring and mitigation of droughts. For instance the results in this thesis show that tropical dry forest is the type of vegetation which seems more vulnerable since recovery times are longer and it is less resistant than other types of vegetation and it is in this area where drought impact seems to be more pronounced than in others. Therefore, it is important to understand that there are multiple stressors in this area. The major impacts on the Yucatan Peninsula appear to be in areas where anthropogenic pressures have been stronger, i.e. coastal environments, close to cities and where there is more agriculture and livestock. Also, it is important in the evaluation of climate change and water resources in the region, and serves as a basis for various study disciplines associated with activities such as agriculture, resource conservation, and adaptation of the population to the occurrence of droughts. Thus, more research is needed and multidisciplinary studies would enrich this research.

The results of this thesis are valuable for decreasing the vulnerability of the Yucatan Peninsula and will help to have better records and data that could be related to climate and environmental changes, allowing us to increase our understanding of the area and go further to create warning and conservation programmes.

6.5 Future work

This study has aimed to develop an understanding of how the vegetation of the Yucatan Peninsula responds to droughts. However, some future work is still needed to deepen understanding. Also, this thesis is intended as a benchmark for further studies. This is expanded below along with some suggestions of future work.

The creation of annual precipitation maps and its anomalies (chapter 3) of the Yucatan Peninsula can be really useful as a baseline to understand and analyse the impacts of other types of natural hazards such as hurricanes. For instance, these maps (Figure 3-13, Figure 3-24, and Figure 3-25) show areas where hurricanes have hit the Peninsula. Having the spatial distribution and the time of these two extreme events (hurricanes and droughts) are valuable information for going further in some analysis and try then to identify the drivers of these events. There are some gaps in knowledge and contradictions in the literature regarding the relationship between droughts (or hurricanes) and ocean-atmosphere processes such as ENSO (El Niño, La Niña), the *nortes*, AMO, among others (Caviedes and Waylen, 1998; Magaña et al., 2003; Mendoza et al., 2005; Peralta-Hernández et al., 2008; Salas et al., 2014). In addition, it has been found that analysing droughts and vegetation productivity separately during the wet and dry season would be powerful for understanding both the drivers and the patterns of droughts in the Yucatan Peninsula.

Climate change is altering the hydrological cycle, and the intensity and frequency of droughts will increase (Orellana et al., 2009) (Giddings and Soto, 2003) (IPCC, 2013), therefore the analysis of vegetation sensitivity in terms of resilience and resistance should be updated to the present and improved using other resources from remote sensing data (i.e. Sentinels) that afford more detail in terms of spatial and spectral resolution.

The quantification (i.e. timing) of the vegetation response after the occurrence of a drought event it is also a great opportunity to continue this research, thus creating a good background for decision makers and conservation policies in

vulnerable ecosystems such as tropical dry forest across the Yucatan Peninsula. More research avenues could be explored to improve the understanding of vegetation impacts. Among these lines are: i) study the relationship between carbon, water and energy between the atmosphere and the vegetation; ii) modelling climate events and changes; iii) social impacts of droughts such as food security and natural resources management. Thus outcomes of this thesis reinforce that further research needs to be more focused on a deeper understanding on how systems will respond to changes in different climate change scenarios and environmental variations especially in the Yucatan Peninsula where lack of research in this arena is evident.

6.6 **Conclusions**

The impacts of droughts on the Yucatan Peninsula have been documented back to the Mayan period. Climate change scenarios forecast more frequency and intensity of extreme climate events and the Yucatan Peninsula has been identified as a vulnerable area. This is also likely to hold true for other tropical regions facing similar combination of climatic, social and economic problems such as poverty and low development as Mexico. Human impacts on the Peninsula are one of the major drivers of environmental impact in this area. However, the effects of climatological variations such as droughts are also important drivers in vegetation and they also have important impacts on society. For instance, the World Bank estimates that the recovery from these events in developing countries could be even more than their own GDP. In Mexico, according to the health, social development, and security federal offices the cost for events related to excess of rain, droughts and hurricanes has been 284.351 billion of Mexican pesos (approximately £11,374,040,000) in the last 12 years (Rueda and García, 2002).

The combined impacts of these extreme events remain uncertain and a need for a full understanding of such phenomena is urgent. Insights from this thesis can be used to prioritise management and responses efforts, which is vital in a megadiverse and developing country. This thesis shows that the most vulnerable region in the Yucatan Peninsula is located in the north part, however, areas where

human development is increasing and agricultural activity is concentrated are also vulnerable. Further studies at finer resolutions are imperative to identify the possible impacts on these areas in the face of extreme climatological events, and more studies are needed to better understand their drivers. Resilience to environmental hazards and resource management plans should be robust and interdisciplinary to create this. This thesis is a benchmark and the methodologies used can be implemented for further studies and in other areas of the Earth. Also, these analyses can be applied for specific areas such as agriculture.

In a country like Mexico, where ground monitoring data availability at appropriate temporal and spatial scales is difficult to afford, the use of other tools such as remote sensing to cover the gaps is needed. However, in this thesis it was shown that the combination of both *in situ* meteorological data and remotely sensed data are a valuable combination for greater accuracy and reducing uncertainty of what is happening on Earth. Thus, creating a great opportunity for further research in measuring the effects of droughts on vegetation and relating these results with other physical and social processes, without excluding decision making strategies.

REFERENCES

AghaKouchak, A., Farahmand, A., Melton, F. S., Teixeira, J., Anderson, M. C., Wardlow, B. D. & Hain, C. R. 2015. Remote sensing of drought: Progress, challenges and opportunities. *Reviews of Geophysics,* 53**,** 452-480.

Aguilar, R. L. S. & Domínguez, S. R. 1999. Deforestación en la Península de Yucatán, los retos que enfrentar. . *Madera y Bosques,* 5**,** 3-17.

Akinremi, O., McGinn, S. & Barr, A. 1996. Evaluation of the Palmer drought index on the Canadian prairies. *Journal of Climate,* 9**,** 897-905.

Alley, W. M. 1984. The Palmer drought severity index: limitations and assumptions. *Journal of climate and applied meteorology,* 23**,** 1100-1109.

Amri, R., Zribi, M., Lili-Chabaane, Z., Duchemin, B., Gruhier, C. & Chehbouni, A. 2011. Analysis of Vegetation Behavior in a North African Semi-Arid Region, Using SPOT-VEGETATION NDVI Data. *Remote Sensing,* 3**,** 2568-2590.

Anderson, L. O., Malhi, Y., Aragão, L. E. O. C., Ladle, R., Arai, E., Barbier, N. & Phillips, O. 2010. Remote sensing detection of droughts in Amazonian forest canopies. *New Phytologist,* 187**,** 733-750.

Anyamba, A. & Eastman, J. 1996. Interannual variability of NDVI over Africa and its relation to El Niño/Southern Oscillation. *Remote Sensing,* 17**,** 2533-2548.

Anyamba, A., Tucker, C. & Eastman, J. 2001. NDVI anomaly patterns over Africa during the 1997/98 ENSO warm event. *International Journal of Remote Sensing,* 22**,** 1847-1860.

Anyamba, A. & Tucker, C. J. 2012. Historical Perspectives on AVHRR NDVI and Vegetation Drought Monitoring. *Remote Sensing of Drought.* CRC Press.

Atkinson, P. M., Jeganathan, C., Dash, J. & Atzberger, C. 2012. Inter-comparison of four models for smoothing satellite sensor time-series data to estimate vegetation phenology. *Remote Sensing of Environment,* 123**,** 400-417.

Audefroy, J. F. 2015. Potential effects of climate change on the habitat in Mexico. *Disaster Prevention and Management,* 24**,** 249-262.

Bachmann, M., Tungalagsaikhan, P., Ruppert, T. & Dech, S. 2015. Calibration and Pre-processing of a Multi-decadal AVHRR Time Series. *Remote Sensing Time Series.* Springer.

Barber, A., Tun, J. & Crespo, M. 2000. A new approach on the bioclimatology and potential vegetation of the Yucatan Peninsula (México). *Phytocoenologia,* 31**,** 1-32.

Baret, F., Guyot, G. & Major, D. TSAVI: a vegetation index which minimizes soil brightness effects on LAI and APAR estimation. Geoscience and Remote Sensing Symposium, 1989. IGARSS'89. 12th Canadian Symposium on Remote Sensing., 1989 International, 1989. IEEE, 1355-1358.

Baret, F. & Guyot, G. 1991. Potentials and limits of vegetation indices for LAI and APAR assessment. *Remote sensing of environment,* 35**,** 161-173.

Barnes, M. L., Moran, M. S., Scott, R. L., Kolb, T. E., Ponce-Campos, G. E., Moore, D. J., Ross, M. A., Mitra, B. & Dore, S. 2016. Vegetation productivity responds to sub-annual climate conditions across semiarid biomes. *Ecosphere,* 7.

Batllori-Sampedro, E., González-Piedra, J. I., Díaz Sosa, J. & Febles-Patrón, J. L. 2012. Caracterización hidrológica de la región costera noroccidental del estado de Yucatán, México. *Investigaciones Geográficas, Boletín del Instituto de Geografía***,** 74.

Bayarjargal, Y., Karnieli, A., Bayasgalan, M., Khudulmur, S., Gandush, C. & Tucker, C. 2006. A comparative study of NOAA–AVHRR derived drought indices using change vector analysis. *Remote Sensing of Environment,* 105**,** 9-22.

Bohling, G. 2005. Kriging. *Kansas Geological Survey, Tech. Rep*.

Boyd, D. S., Foody, G. M. & Phipps, P. C. 2006. Dynamics of ENSO drought events on Sabah rainforests observed by NOAA AVHRR. *International Journal of Remote Sensing,* 27**,** 2197-2219.

Boyd, D. S., Almond, S., Dash, J., Curran, P. J. & Hill, R. A. 2011. Phenology of vegetation in Southern England from Envisat MERIS terrestrial chlorophyll index (MTCI) data. *International Journal of Remote Sensing,* 32**,** 8421-8447.

Boyd, R. & Ibarrarán, M. E. 2009. Extreme climate events and adaptation: an exploratory analysis of drought in Mexico. *Environment and Development Economics,* 14**,** 371-395.

Boyer, J. S. 1996. Advances in drought tolerance in plants. *Advances in agronomy,* 56**,** 187-219.

Bravo Cabrera, J., Azpra Romero, E., Zarraluqui Such, V., Gay García, C. & Estrada Porrúa, F. 2012. Cluster analysis for validated climatology stations using precipitation in Mexico. *Atmósfera,* 25**,** 339-354.

Bréda, N. & Badeau, V. 2008. Forest tree responses to extreme drought and some biotic events: Towards a selection according to hazard tolerance? *Comptes Rendus Geoscience,* 340**,** 651-662.

Breshears, D. D., Cobb, N. S., Rich, P. M., Price, K. P., Allen, C. D., Balice, R. G., Romme, W. H., Kastens, J. H., Floyd, M. L., Belnap, J., Anderson, J. J., Myers, O. B. & Meyer, C. W. 2005. Regional vegetation die-off in response to global-change-type drought. *Proc Natl Acad Sci U S A,* 102**,** 15144-8.

Caviedes, C. & Waylen, P. 1998. Respuestas del clima de América del Sur a las fases de ENSO. *Bulletin de l'Institut francais d'études Andins,* 27**,** 613-626.

Challenger, A. & Soberón, J. 2008. Los ecosistemas terrestres. *Capital natural de México,* 1**,** 87-108.

Chen, J., Jönsson, P., Tamura, M., Gu, Z., Matsushita, B. & Eklundh, L. 2004. A simple method for reconstructing a high-quality NDVI time-series data set based on the Savitzky–Golay filter. *Remote sensing of Environment,* 91**,** 332-344.

Chiappy, C. & Gama, L. 2004. Modificaciones y fragmentación de los geocomplejos tropicales de la Península de Yucatán. *Universidad y Ciencia***,** 17-25.

Chunqiao, S., Bo, H. & Songcai, Y. Comparison of three time-series NDVI reconstruction methods based on TIMESAT. Geoscience and Remote Sensing Symposium (IGARSS), 2012 IEEE International, 2012. IEEE, 2225-2228.

Chuvieco, E. Aportaciones de la Teledetección espacial a la cartografía de ocupación del suelo. Anales de Geografía de la Universidad Complutense, 1985. 29.

Colditz, R. R., Conrad, C., Wehrmann, T., Schmidt, M. & Dech, S. 2008. TiSeG: A flexible software tool for time-series generation of MODIS data utilizing the quality assessment science data set. *Geoscience and Remote Sensing, IEEE Transactions on,* 46**,** 3296-3308.

Colditz, R. R., Llamas, R. M., Mascorro, V. S. & Ressl, R. A. Land cover change analysis of the Yucatan Peninsula using landsat data from 1985 to 2010. 2015 IEEE International Geoscience and Remote Sensing Symposium (IGARSS), 2015. IEEE, 4621-4624.

Collins, S., Reinhardt, E., Rissolo, D., Chatters, J., Blank, A. N. & Erreguerena, P. L. 2015. Reconstructing water level in Hoyo Negro, Quintana Roo, Mexico, implications for early Paleoamerican and faunal access. *Quaternary Science Reviews,* 124**,** 68-83.

CONAGUA. 2010a. *Historia del Servicio Meteorológico Nacional* [Online]. Available: http://smn.cna.gob.mx/index.php?option=com_content&view=article&id=19&Itemid=22 [Accessed 2014].

CONAGUA. 2010b. Temperatura y precipitacion. *Comision Nacional del Agua* [Online]. Available from: http://smn.cna.gob.mx/index.php?option=com_content&view=article&id=12&Itemid=112.

CONAGUA 2012. *Servicio Meteorológico Nacional: 135 años de historia en México*, Secretaría de Medio Ambiente y Recursos Naturales.

CONANP. 2010. Areas Naturales Protegidas decretadas. *Comision Nacional de Areas Naturales Protegidas* [Online]. Available from: http://www.conanp.gob.mx/que_hacemos/.

Coppola, R., Cuomo, V., D'emilio, M., Lanfredi, M., Liberti, M., Macchiato, M. & Simoniello, T. 2009. Terrestrial Vegetation Cover Activity as a Problem of Fluctuating Surfaces. *International Journal of Modern Physics B,* 23**,** 5444-5452.

Curry, J., Jelinek, M., Foskey, B., Suzuki, A. & Webster, P. 2009. Potential economic impacts of hurricanes in Mexico, Central America, and the Caribbean ca. 2020–2025. *Assessing the Potential Consequences of Climate Destabilization in Latin America*.

Dai, A. & NCAR. 2016. *The Climate Data Guide: Palmer Drought Severity Index (PDSI)* [Online]. Available: https://climatedataguide.ucar.edu/climate-data/palmer-drought-severity-index-pdsi [Accessed].

Dash, J. & Curran, P. J. 2004. The MERIS terrestrial chlorophyll index. *International Journal of Remote Sensing,* 25**,** 5403-5413.

Dash, J., Jeganathan, C. & Atkinson, P. 2010. The use of MERIS Terrestrial Chlorophyll Index to study spatio-temporal variation in vegetation phenology over India. *Remote Sensing of Environment,* 114**,** 1388-1402.

Di, L., Rundquist, D. C. & Han, L. 1994. Modelling relationships between NDVI and precipitation during vegetative growth cycles. *International Journal of Remote Sensing,* 15**,** 2121-2136.

Dirzo, R. & Gil, P. R. 1996. *Diversidad de flora mexicana*, CEMEX Corporation.

Duncan, J., Biggs, E. M., Dash, J. & Atkinson, P. M. 2013. Spatio-temporal trends in precipitation and their implications for water resources management in climate-sensitive Nepal. *Applied Geography,* 43**,** 138-146.

Easterling, D. R., Meehl, G. A., Parmesan, C., Changnon, S. A., Karl, T. R. & Mearns, L. O. 2000. Climate extremes: observations, modeling, and impacts. *Science,* 289**,** 2068-2074.

Easterling, D. R. 2013. Global data sets for analysis of climate extremes. *Extremes in a Changing Climate.* Springer.

Eastman, J. R., Sangermano, F., Machado, E. A., Rogan, J. & Anyamba, A. 2013. Global trends in seasonality of normalized difference vegetation index (NDVI), 1982–2011. *Remote Sensing,* 5**,** 4799-4818.

Eklundh, L. & Jönsson, P. 2015. TIMESAT: A Software Package for Time-Series Processing and Assessment of Vegetation Dynamics. *Remote Sensing Time Series.* Springer.

Ellis, E. A. & Porter-Bolland, L. 2008. Is community-based forest management more effective than protected areas?: A comparison of land use/land cover change in two neighboring study areas of the Central Yucatan Peninsula, Mexico. *Forest ecology and management,* 256**,** 1971-1983.

Esparza, M. 2014. La sequía y la escasez de agua en México: Situación actual y perspectivas futuras. *Secuencia***,** 193-219.

Estrada Medina, H. & Cobos Gasca, V. 2014. Programa de Medidas Preventivas y de Mitigación de la Sequía de la Cuenca Península de Yucatán. *Informe Final. Programa Nacional contra la sequía PRONACOSE Versión 2***,** 297.

Evans, J. & Geerken, R. 2004. Discrimination between climate and human-induced dryland degradation. *Journal of Arid Environments,* 57**,** 535-554.

Fang, J., Piao, S., Zhou, L., He, J., Wei, F., Myneni, R. B., Tucker, C. J. & Tan, K. 2005. Precipitation patterns alter growth of temperate vegetation. *Geophysical research letters,* 32.

Fensholt, R. & Rasmussen, K. 2011. Analysis of trends in the Sahelian 'rain-use efficiency'using GIMMS NDVI, RFE and GPCP rainfall data. *Remote Sensing of Environment,* 115**,** 438-451.

Fensholt, R., Rasmussen, K., Kaspersen, P., Huber, S., Horion, S. & Swinnen, E. 2013. Assessing Land Degradation/Recovery in the African Sahel from Long-Term Earth Observation Based Primary Productivity and Precipitation Relationships. *Remote Sensing,* 5**,** 664-686.

Fensholt, R., Horion, S., Tagesson, T., Ehammer, A., Grogan, K., Tian, F., Huber, S., Verbesselt, J., Prince, S. D. & Tucker, C. J. 2015. Assessing Drivers of Vegetation Changes in Drylands from Time Series of Earth Observation Data. *Remote Sensing Time Series.* Springer.

Flores-Guido, J. S. & Espejel, I. 1994. Tipos de Vegetación de la Península de Yucatán. *Etnoflora Yucatanense. Fascículo III, Ediciones de la Universidad Autónoma de Yucatán, Yucatán, México*.

Florescano, E. & Swan, S. 1995. *Breve historia de la sequía en México,* Universidad Veracruzana Direccion Editorial.

Forkel, M., Carvalhais, N., Verbesselt, J., Mahecha, M. D., Neigh, C. S. & Reichstein, M. 2013. Trend change detection in NDVI time series: effects of inter-annual variability and methodology. *Remote Sensing,* 5**,** 2113-2144.

Fovell, R. G. & Fovell, M.-Y. C. 1993. Climate zones of the conterminous United States defined using cluster analysis. *Journal of Climate,* 6**,** 2103-2135.

Gallo, K., Daughtry, C. & Bauer, M. E. 1985. Spectral estimation of absorbed photosynthetically active radiation in corn canopies. *Remote Sensing of Environment,* 17**,** 221-232.

Gao, B.-c. 1996. NDWI—A normalized difference water index for remote sensing of vegetation liquid water from space. *Remote Sensing of Environment,* 58**,** 257-266.

García-Frapolli, E., Ayala-Orozco, B., Bonilla-Moheno, M., Espadas-Manrique, C. & Ramos-Fernández, G. 2007. Biodiversity conservation, traditional agriculture and ecotourism: Land cover/land use change projections for a natural protected area in the northeastern Yucatan Peninsula, Mexico. *Landscape and urban planning,* 83**,** 137-153.

García Amaro, E. & García, E. 1973. Modificaciones al sistema de clasificación climática de köppen para adaptarlo a las condiciones de la república mexicana.

García, E. 1965. *Distribución de la precipitación en la República Mexicana*, Instituto de Geografía, UNAM.

García, E. 1998a. Comisión Nacional para el Conocimiento y Uso de la Biodiversidad (CONABIO). 1998. Climas. Clasificación de Köppen, modificado por García. Escala 1: 1000000. México.

García, E. 1998b. Precipitación total anual.

Gaughan, A. E., Stevens, F. R., Gibbes, C., Southworth, J. & Binford, M. W. 2012. Linking vegetation response to seasonal precipitation in the Okavango–Kwando–Zambezi catchment of southern Africa. *International journal of remote sensing,* 33**,** 6783-6804.

Geoghegan, J., Villar, S. C., Klepeis, P., Mendoza, P. M., Ogneva-Himmelberger, Y., Chowdhury, R. R., Turner, B. & Vance, C. 2001. Modeling tropical deforestation in the southern Yucatan peninsular region: comparing survey and satellite data. *Agriculture, Ecosystems & Environment,* 85**,** 25-46.

Giddings, L. & Soto, M. 2003. Rhythms of precipitation in the Yucatan Peninsula. *The lowland Maya area: three millennia at the human-wildland interface. Haworth Press, Binghampton***,** 77-90.

Giddings, L., SOTO, M., Rutherford, B. & Maarouf, A. 2005. Standardized precipitation index zones for Mexico. *Atmósfera,* 18**,** 33-56.

Gillespie, T. W., Foody, G. M., Rocchini, D., Giorgi, A. P. & Saatchi, S. 2008. Measuring and modelling biodiversity from space. *Progress in Physical Geography,* 32**,** 203-221.

Gitay, H., Suárez, A., Watson, R. & Dokken, D. 2002. Cambio climático y biodiversidad. *Documento Técnico V, IPCC.*

Gómez Ramírez, M. 1998. Ciclones Tropicales que Entraron a la Península de Yucatán de 1970 a 1995. *Revista Geográfica***,** 153-171.

Hardisky, M. A., Michael Smart, R. & Klemas, V. 1983. Growth response and spectral characteristics of a short Spartina alterniflora salt marsh irrigated with freshwater and sewage effluent. *Remote Sensing of Environment,* 13**,** 57-67.

Harris, A., Carr, A. & Dash, J. 2014. Remote sensing of vegetation cover dynamics and resilience across southern Africa. *International Journal of Applied Earth Observation and Geoinformation,* 28**,** 131-139.

Hayes, M., Svoboda, M., Wardlow, B., Anderson, M. & Kogan, F. 2012. Drought Monitoring. *Remote Sensing of Drought.* CRC Press.

Hayes, M. J., Svodoba, M. D., Wilhite, D. A. & Vanyarkho, O. V. 1999. Monitoring the 1996 drought using the standardized precipitation index. *Bulletin of the American Meteorological Society,* 80**,** 429.

Heim Jr, R. R. 2002. A review of twentieth-century drought indices used in the United States. *Bulletin of the American Meteorological Society,* 83**,** 1149.

Hernández Cerda, M., Tapia, L. T. & Madero, G. V. 2000. Sequía meteorológica; México: una visión hacia el siglo XXI. *El cambio climático en México*.

Herrera-Silveira, J. A. & Ramirez-Ramirez, J. 1996. Effects of natural phenolic material (tannin) on phytoplankton growth. *Limnology and Oceanography,* 41**,** 1018-1023.

Herrmann, S. M., Anyamba, A. & Tucker, C. J. 2005. Recent trends in vegetation dynamics in the African Sahel and their relationship to climate. *Global Environmental Change,* 15**,** 394-404.

Heumann, B. W., Seaquist, J., Eklundh, L. & Jönsson, P. 2007. AVHRR derived phenological change in the Sahel and Soudan, Africa, 1982–2005. *Remote Sensing of Environment,* 108**,** 385-392.

Hickler, T., Eklundh, L., Seaquist, J. W., Smith, B., Ardö, J., Olsson, L., Sykes, M. T. & Sjöström, M. 2005. Precipitation controls Sahel greening trend. *Geophysical Research Letters,* 32.

Hielkema, J., Prince, S. & Astle, W. 1986. Rainfall and vegetation monitoring in the savanna zone of the Democratic Republic of Sudan using the NOAA Advanced Very High Resolution Radiometer. *International Journal of Remote Sensing,* 7**,** 1499-1513.

Hird, J. N. & McDermid, G. J. 2009. Noise reduction of NDVI time series: An empirical comparison of selected techniques. *Remote Sensing of Environment,* 113**,** 248-258.

Hodell, D. A., Brenner, M., Curtis, J. H., Medina-González, R., Ildefonso-Chan Can, E., Albornaz-Pat, A. & Guilderson, T. P. 2005. Climate change on

the Yucatan Peninsula during the little ice age. *Quaternary Research,* 63**,** 109-121.

Hodell, D. A., Brenner, M. & Curtis, J. H. 2007. Climate and cultural history of the northeastern Yucatan Peninsula, Quintana Roo, Mexico. *Climatic Change,* 83**,** 215-240.

Holben, B. N. 1986. Characteristics of maximum-value composite images from temporal AVHRR data. *International Journal of Remote Sensing,* 7**,** 1417-1434.

Hostert, P., Griffiths, P., van der Linden, S. & Pflugmacher, D. 2015. Time Series Analyses in a New Era of Optical Satellite Data. *Remote Sensing Time Series.* Springer.

Huete, A., Didan, K., Miura, T., Rodriguez, E. P., Gao, X. & Ferreira, L. G. 2002. Overview of the radiometric and biophysical performance of the MODIS vegetation indices. *Remote sensing of environment,* 83**,** 195-213.

Huete, A. R. 1988. A soil-adjusted vegetation index (SAVI). *Remote sensing of environment,* 25**,** 295-309.

Huete, A. R., Liu, H. & Van Leeuwen, W. J. The use of vegetation indices in forested regions: issues of linearity and saturation. Geoscience and Remote Sensing, 1997. IGARSS'97. Remote Sensing-A Scientific Vision for Sustainable Development., 1997 IEEE International, 1997. IEEE, 1966-1968.

Huffman, G. J., Bolvin, D. T., Nelkin, E. J., Wolff, D. B., Adler, R. F., Gu, G., Hong, Y., Bowman, K. P. & Stocker, E. F. 2007. The TRMM multisatellite precipitation analysis (TMPA): Quasi-global, multiyear, combined-sensor precipitation estimates at fine scales. *Journal of Hydrometeorology,* 8**,** 38-55.

Huffman, G. J. & Bolvin, D. T. 2013. TRMM and other data precipitation data set documentation. *NASA, Greenbelt, USA***,** 1-40.

Ichii, K., Kawabata, A. & Yamaguchi, Y. 2002. Global correlation analysis for NDVI and climatic variables and NDVI trends: 1982-1990. *International journal of remote sensing,* 23**,** 3873-3878.

INEGI. 2010. *Conjunto Nacional de Uso del Suelo y Vegetación a escala 1:250,000, Serie IV, DGG-INEGI, México.* Mexico: INEGI.

IPCC 1997. Estabilización de los gases atmosféricos de efecto invernadero: implicaciones físicas, biológicas y socioeconómicas.

IPCC, C. C. 2013. The Physical Science Basis. Working Group I Contribution to the Fifth Assessment Report of the Intergovernmental Panel on Climate Change. *Cambridge, United Kingdom and New York, USA*.

Islebe, G. A., Schmook, B., Calmé, S. & León-Cortés, J. L. 2015. Introduction: Biodiversity and Conservation of the Yucatán Peninsula, Mexico. *Biodiversity and Conservation of the Yucatán Peninsula.* Springer.

Jackson, R., Slater, P. & Pinter, P. 1983. Discrimination of growth and water stress in wheat by various vegetation indices through clear and turbid atmospheres. *Remote sensing of environment,* 13**,** 187-208.

Jain, V. K., Pandey, R. P., Jain, M. K. & Byun, H.-R. 2015. Comparison of drought indices for appraisal of drought characteristics in the Ken River Basin. *Weather and Climate Extremes,* 8**,** 1-11.

Jeganathan, C., Dash, J. & Atkinson, P. 2014. Remotely sensed trends in the phenology of northern high latitude terrestrial vegetation, controlling for land cover change and vegetation type. *Remote Sensing of Environment,* 143**,** 154-170.

Ji, L. & Peters, A. J. 2003. Assessing vegetation response to drought in the northern Great Plains using vegetation and drought indices. *Remote Sensing of Environment,* 87**,** 85-98.

Ji, L. & Peters, A. J. 2005. Lag and seasonality considerations in evaluating AVHRR NDVI response to precipitation. *Photogrammetric Engineering & Remote Sensing,* 71**,** 1053-1061.

Jolly, W. M. & Running, S. W. 2004. Effects of precipitation and soil water potential on drought deciduous phenology in the Kalahari. *Global Change Biology,* 10**,** 303-308.

Jönsson, P. & Eklundh, L. 2004. TIMESAT—A program for analyzing time-series of satellite sensor data. *Computers & Geosciences,* 30**,** 833-845.

Justice, C. O. & Hiernaux, P. 1986. Monitoring the grasslands of the Sahel using NOAA AVHRR data: Niger 1983. *International Journal of Remote Sensing,* 7**,** 1475-1497.

Kaplowitz, M. 2000. Identifying ecosystem services using multiple methods: Lessons from the mangrove wetlands of Yucatan, Mexico. *Agriculture and Human Values,* 17**,** 169-179.

Karnieli, A., Agam, N., Pinker, R. T., Anderson, M., Imhoff, M. L., Gutman, G. G., Panov, N. & Goldberg, A. 2010. Use of NDVI and land surface

temperature for drought assessment: Merits and limitations. *Journal of Climate,* 23**,** 618-633.

Kattelus, M., Salmivaara, A., Mellin, I., Varis, O. & Kummu, M. 2015. An evaluation of the Standardized Precipitation Index for assessing inter-annual rice yield variability in the Ganges–Brahmaputra–Meghna region. *International Journal of Climatology*.

Kaymaz, I. 2005. Application of kriging method to structural reliability problems. *Structural Safety,* 27**,** 133-151.

Kogan, F. & Sullivan, J. 1993. Development of global drought-watch system using NOAA/AVHRR data. *Advances in Space Research,* 13**,** 219-222.

Kogan, F. 1995. Application of vegetation index and brightness temperature for drought detection. *Advances in Space Research,* 15**,** 91-100.

Kogan, F. N. 1997. Global Drought Watch from Space. *Bulletin of the American Meteorological Society,* 78**,** 621-636.

Kogan, F. N. 2000. Contribution of remote sensing to drought early warning. *Early warning systems for drought preparedness and drought management***,** 75-87.

Krishnaswamy, J., Bawa, K. S., Ganeshaiah, K. & Kiran, M. 2009. Quantifying and mapping biodiversity and ecosystem services: Utility of a multi-season NDVI based Mahalanobis distance surrogate. *Remote Sensing of Environment,* 113**,** 857-867.

Kuenzer, C., Dech, S. & Wagner, W. 2015. *Remote Sensing Time Series: Revealing Land Surface Dynamics*, Springer.

Lanfredi, M., Simoniello, T. & Macchiato, M. 2004. Temporal persistence in vegetation cover changes observed from satellite: Development of an estimation procedure in the test site of the Mediterranean Italy. *Remote Sensing of Environment,* 93**,** 565-576.

Li, F., Zhao, W. & Liu, H. 2015. Productivity responses of desert vegetation to precipitation patterns across a rainfall gradient. *Journal of plant research,* 128**,** 283-294.

Lin, M.-L., Cao, Y., Juan, C.-H., Chen, C.-W., Hsueh, I.-C., Wang, Q.-B. & Lee, Y.-T. Monitoring drought dynamics in the ejin oasis using drought indices from modis data. IGARSS 2008-2008 IEEE International Geoscience and Remote Sensing Symposium, 2008. IEEE, IV-834-IV-837.

Liverman, D. M. 1999. Vulnerability and adaptation to drought in Mexico. *Nat. Resources J.,* 39**,** 99.

Llorens, L., Penuelas, J., Beier, C., Emmett, B., Estiarte, M. & Tietema, A. 2004. Effects of an experimental increase of temperature and drought on the photosynthetic performance of two ericaceous shrub species along a north–south European gradient. *Ecosystems,* 7**,** 613-624.

Los, S. O., Weedon, G. P., North, P., Kaduk, J., Taylor, C. & Cox, P. 2006. An observation-based estimate of the strength of rainfall-vegetation interactions in the Sahel. *Geophysical Research Letters,* 33.

Lotsch, A., Friedl, M. A., Anderson, B. T. & Tucker, C. J. 2003. Coupled vegetation-precipitation variability observed from satellite and climate records. *Geophysical Research Letters,* 30.

Lugo Hubp, J., Aceves Quesado, J. F. & Espinosa Pereño, R. 1992. Rasgos geomorfológicos mayores de la península de Yucatán. *Revista mexicana de ciencias geológicas,* 10**,** 143-150.

MacGillivray, C., Grime, J. & Team, T. I. S. P. 1995. Testing predictions of the resistance and resilience of vegetation subjected to extreme events. *Functional Ecology***,** 640-649.

Magaña, V. 1999. Los Impactos de El Niño en México. Centro de Ciencias de la Atmósfera, Universidad Nacional Autónoma de México, México, con apoyo de la Dirección General de protección civil, Secretaría de Gobernación, México, 228 pp.

Magaña, V., Amador, J. A. & Medina, S. 1999. The midsummer drought over Mexico and Central America. *Journal of Climate,* 12**,** 1577-1588.

Magaña, V. O., Vázquez, J. L., Pérez, J. L. & Pérez, J. B. 2003. Impact of El Niño on precipitation in Mexico. *GEOFISICA INTERNACIONAL-MEXICO-,* 42**,** 313-330.

Manobava, M. 2003. *The responses of terrestrial vegetation to el Nino southern oscillation perturbation.* PhD, Kingston University London.

Márdero, S., Nickl, E., Schmook, B., Schneider, L., Rogan, J., Christman, Z. & Lawrence, D. 2012. Sequías en el sur de la península de Yucatán: análisis de la variabilidad anual y estacional de la precipitación. *Investigaciones Geográficas, Boletín del Instituto de Geografía***,** 19.

Marin, S., Pacheco, G. & Mendez, R. 2004. Hidrogeología de la Península de Yucatán. *El agua en México vista desde la academia***,** 159.

Marquínez, J., Lastra, J. & García, P. 2003. Estimation models for precipitation in mountainous regions: the use of GIS and multivariate analysis. *Journal of hydrology,* 270**,** 1-11.

McFeeters, S. 1996. The use of the Normalized Difference Water Index (NDWI) in the delineation of open water features. *International journal of remote sensing,* 17**,** 1425-1432.

McKee, T. B., Doesken, N. J. & Kleist, J. The relationship of drought frequency and duration to time scales. Proceedings of the 8th Conference on Applied Climatology, 1993. American Meteorological Society Boston, MA, 179-183.

McVicar, T. & Bierwirth, P. 2001. Rapidly assessing the 1997 drought in Papua New Guinea using composite AVHRR imagery. *International Journal of Remote Sensing,* 22**,** 2109-2128.

Méndez, M. & Magaña, V. 2010. Regional aspects of prolonged meteorological droughts over Mexico and Central America. *Journal of Climate,* 23**,** 1175-1188.

Mendez Perez, J. M. 2003. *Un estudio de eventos hidrometeorológicos extremos en la Republica Mexicana.* Masters, Universidad Nacional Autónoma de México.

Mendoza, B., Jáuregui, E., Diaz-Sandoval, R., García-Acosta, V., Velasco, V. & Cordero, G. 2005. Historical droughts in central Mexico and their relation with El Niño. *Journal of applied meteorology,* 44**,** 709-716.

Mendoza, B., Velasco, V. & Jáuregui, E. 2006. A study of historical droughts in southeastern Mexico. *Journal of Climate,* 19**,** 2916-2934.

Mendoza, B., Garcia-Acosta, V., Velasco, V., Jauregui, E. & Díaz-Sandoval, R. 2007. Frequency and duration of historical droughts from the 16th to the 19th centuries in the Mexican Maya lands, Yucatan Peninsula. *Climatic Change,* 83**,** 151-168.

Meng, L., Ford, T. & Guo, Y. 2016. Logistic regression analysis of drought persistence in East China. *International Journal of Climatology*.

Metcalfe, S. E., Barron, J. A. & Davies, S. J. 2015. The Holocene history of the North American Monsoon:'known knowns' and 'known unknowns' in understanding its spatial and temporal complexity. *Quaternary Science Reviews,* 120**,** 1-27.

Miles, L., Newton, A. C., DeFries, R. S., Ravilious, C., May, I., Blyth, S., Kapos, V. & Gordon, J. E. 2006. A global overview of the conservation status of tropical dry forests. *Journal of Biogeography,* 33**,** 491-505.

Miranda, F. & Hernández, X. E. 1963. *Los tipos de vegetación de México y su clasificación*, Colegio de Postgraduados, Secretaría de Agricultura y Recursos Hidráulicos.

Miranda, F. 1964. *Vegetación de la península yucateca: Rasgos fisiográficos, la vegetación*, Colegio de Postgraduados, Escuela Nacional de Agricultura.

Murphy, P. G. & Lugo, A. E. 1986. Ecology of tropical dry forest. *Annual review of ecology and systematics***,** 67-88.

Murtagh, F. & Legendre, P. 2011. Ward's hierarchical clustering method: clustering criterion and agglomerative algorithm. *arXiv preprint arXiv:1111.6285*.

Myneni, R. B., Hall, F. G., Sellers, P. J. & Marshak, A. L. 1995. The interpretation of spectral vegetation indexes. *Geoscience and Remote Sensing, IEEE Transactions on,* 33**,** 481-486.

NADM. 2016. *North American Drought Portal.*

Narasimhan, B. & Srinivasan, R. 2005. Development and evaluation of Soil Moisture Deficit Index (SMDI) and Evapotranspiration Deficit Index (ETDI) for agricultural drought monitoring. *Agricultural and Forest Meteorology,* 133**,** 69-88.

NDMC, N. D. M. C. 2015. *Program to Calculate Standardized Precipitation Index* [Online]. Available: http://drought.unl.edu/MonitoringTools/DownloadableSPIProgram.aspx [Accessed 2015].

Neeti, N., Rogan, J., Christman, Z., Eastman, J. R., Millones, M., Schneider, L., Nickl, E., Schmook, B., Turner, B. L. & Ghimire, B. 2012. Mapping seasonal trends in vegetation using AVHRR-NDVI time series in the Yucatán Peninsula, Mexico. *Remote Sensing Letters,* 3**,** 433-442.

Nicholson, S. E., Davenport, M. L. & Malo, A. R. 1990. A comparison of the vegetation response to rainfall in the Sahel and East Africa, using normalized difference vegetation index from NOAA AVHRR. *Climatic Change,* 17**,** 209-241.

Niemeyer, S. & Vogt, J. 2003. Integration of operationally available remote sensing and synoptic data for surface energy balance modelling and

environmental applications on the regional scale. *Remote Sensing and Climate Modeling: Synergies and Limitations.* Springer.

NOAA. 2016. *Historical Hurricane Tracks* [Online]. Available: https://coast.noaa.gov/hurricanes/ [Accessed].

Olson, C. F. 1995. Parallel algorithms for hierarchical clustering. *Parallel computing,* 21**,** 1313-1325.

Ordonez, E. 1936. Principal physiographic provinces of Mexico. *AAPG Bulletin,* 20**,** 1277-1307.

Orellana, R., Espadas, C., Conde, C. & Gay, C. 2009. *Atlas Escenarios de cambio climático en la península de Yucatán,* Centro de Investigación Científica de Yucatán Mérida.

Ortega-Gaucin, D. & Velasco, I. 2014. Aspectos socioeconómicos y ambientales de las sequías en México. *Aqua-LAC,* 5**,** 78-90.

Otto, M., Höpfner, C., Curio, J., Maussion, F. & Scherer, D. 2016. Assessing vegetation response to precipitation in northwest Morocco during the last decade: an application of MODIS NDVI and high resolution reanalysis data. *Theoretical and Applied Climatology,* 123**,** 23-41.

Palmer, W. C. 1965. *Meteorological drought*, US Department of Commerce, Weather Bureau Washington, DC.

Pearson, R. L. & Miller, L. D. Remote mapping of standing crop biomass for estimation of the productivity of the shortgrass prairie. Remote Sensing of Environment, VIII, 1972. 1355.

Peng, D., Zhang, B., Liu, L., Chen, D., Fang, H. & Hu, Y. 2012. Seasonal dynamic pattern analysis on global FPAR derived from AVHRR GIMMS NDVI. *International Journal of Digital Earth,* 5**,** 439-455.

Pennington, T. D. & Sarukhan, J. 1998. Árboles tropicales de México. *Manual para la identificacion de las principales especies. Universidad Nacional Autonoma de Mexico: Mexico,* 521.

Peralta-Hernández, A., Barba-Martínez, L., Magaña-Rueda, V., Matthias, A. & Luna-Ruíz, J. 2008. Temporal and spatial behavior of temperature and precipitation during the canícula (midsummer drought) under El Niño conditions in central México. *Atmosfera,* 21**,** 265-280.

Peters, A. J., Walter-Shea, E. A., Ji, L., Vina, A., Hayes, M. & Svoboda, M. D. 2002. Drought monitoring with NDVI-based standardized vegetation index. *Photogrammetric engineering and remote sensing,* 68**,** 71-75.

Piao, S., Fang, J., Ji, W., Guo, Q., Ke, J., Tao, S. & Woods, K. 2004. Variation in a satellite-based vegetation index in relation to climate in China. *Journal of vegetation science,* 15**,** 219-226.

Pinty, B. & Verstraete, M. 1992. GEMI: a non-linear index to monitor global vegetation from satellites. *Vegetatio,* 101**,** 15-20.

Pinzon, J. E. & Tucker, C. J. 2014. A non-stationary 1981–2012 AVHRR NDVI3g time series. *Remote Sensing,* 6**,** 6929-6960.

Poorter, L., Bongers, F., Aide, T. M., Zambrano, A. M. A., Balvanera, P., Becknell, J. M., Boukili, V., Brancalion, P. H., Broadbent, E. N. & Chazdon, R. L. 2016. Biomass resilience of Neotropical secondary forests. *Nature,* 530**,** 211-214.

Proud, S. R. & Rasmussen, L. V. 2011. The influence of seasonal rainfall upon Sahel vegetation. *Remote sensing letters,* 2**,** 241-249.

Rada, J. M. D., García, R. D., García-Contreras, G., Morín, J. A., Lugo, E. A., González, M. E. M. & Hernández, M. A. 2015. Conservation and Use. *Biodiversity and Conservation of the Yucatán Peninsula.* Springer.

Richardson, A. J. & Weigand, C. 1977. Distinguishing vegetation from soil background information. *Photogrammetric Engineering and Remote Sensing,* 43.

Rock, B. N., Williams, D. & Vogelmann, J. Field and airborne spectral characterization of suspected acid deposition damage in red spruce (Picea rubens) from Vermont. Machine Processing of Remotely Sensed Data Symposium, 1985. 71-81.

Rondeaux, G., Steven, M. & Baret, F. 1996. Optimization of soil-adjusted vegetation indices. *Remote Sensing of Environment,* 55**,** 95-107.

Rosén, E. 1995. Periodic droughts and long-term dynamics of alvar grassland vegetation on Öland, Sweden. *Folia Geobotanica,* 30**,** 131-140.

Rosenmeier, M. F., Hodell, D. A., Brenner, M., Curtis, J. H. & Guilderson, T. P. 2002. A 4000-year lacustrine record of environmental change in the southern Maya lowlands, Peten, Guatemala. *Quaternary Research,* 57**,** 183-190.

Rossi, S. & Niemeyer, S. 2012. Drought Monitoring Using Fraction of Absorbed Photosynthetically Active Radiation Estimates Derived from MERIS. *Remote Sensing of Drought.* CRC Press.

Rouse Jr, J., Haas, R., Deering, D., Schell, J. & Harlan, J. 1974. Monitoring the vernal advancement and retrogradation (green wave effect) of natural vegetation.

Rousseeuw, P. J. 1987. Silhouettes: a graphical aid to the interpretation and validation of cluster analysis. *Journal of computational and applied mathematics,* 20**,** 53-65.

Rueda, V. O. M. & García, C. G. 2002. Vulnerabilidad y adaptación regional ante el cambio climático y sus impactos ambientales, sociales y económicos. *Gaceta ecológica***,** 7-23.

Rzedowski, J. 1978. Vegetacion de Mexico. *Limusa, Mexico*.

Salas, M. A., Cerda, M. E. H., Cruz, J. V., Romero, E. A. & Barrié, C. T. L. 2014. The Influence of Strong El Nino Phases on the Rainfall Over the Yucatan Peninsula, Mexico. *Analele stiintifice ale Universitatii" Alexandru Ioan Cuza" din Iasi-seria Geografie,* 60**,** 15-28.

Saleska, S. R., Didan, K., Huete, A. R. & Da Rocha, H. R. 2007. Amazon forests green-up during 2005 drought. *Science,* 318**,** 612-612.

Sánchez-Sánchez, O., Islebe, G. A., Ramírez-Barajas, P. J. & Torrescano-Valle, N. 2015. Natural and Human Induced Disturbance in Vegetation. *Biodiversity and Conservation of the Yucatán Peninsula.* Springer.

Sánchez-Azofeifa, G. A., Quesada, M., Rodríguez, J. P., Nassar, J. M., Stoner, K. E., Castillo, A., Garvin, T., Zent, E. L., Calvo-Alvarado, J. C. & Kalacska, M. E. 2005. Research Priorities for Neotropical Dry Forests1. *Biotropica,* 37**,** 477-485.

Schmidt, M., Klein, D., Conrad, C., Dech, S. & Paeth, H. 2014. On the relationship between vegetation and climate in tropical and northern Africa. *Theoretical and applied climatology,* 115**,** 341-353.

Schultz, P. & Halpert, M. 1993. Global correlation of temperature, NDVI and precipitation. *Advances in Space Research,* 13**,** 277-280.

Simoniello, T., Lanfredi, M., Liberti, M., Coppola, R. & Macchiato, M. 2008. Estimation of vegetation cover resilience from satellite time series. *Hydrology and Earth System Sciences Discussions Discussions,* 5**,** 511-546.

Smart, P. L., Beddows, P. A., Coke, J., Doerr, S., Smith, S. & Whitaker, F. F. 2006. Cave development on the Caribbean coast of the Yucatan Peninsula, Quintana Roo, Mexico. *Special Papers-Geological Society Of America,* 404**,** 105.

Srivastava, S., Jayaraman, V., Nageswara Rao, P., Manikiam, B. & Chandrasekhar, M. 1997. Interlinkages of NOAA/AVHRR derived integrated NDVI to seasonal precipitation and transpiration in dryland tropics. *International Journal of Remote Sensing,* 18**,** 2931-2952.

Steven, M. D., Malthus, T. J. & Baret, F. 2016. Chapter 8: Towards Standardisation of Vegetation Indices. *Remote Sensing Handbook.*

Stringfield, V. & LeGrand, H. 1976. Karst hydrology of northern Yucatan Peninsula, Mexico.

Svoboda, M., Hayes, M. & Wood, D. 2012. Standardized precipitation index user guide. *World Meteorological Organization Geneva, Switzerland*.

Tadesse, T., Wardlow, B. D., Hayes, M. J., Svoboda, M. D. & Brown, J. F. 2010. The vegetation outlook (VegOut): A new method for predicting vegetation seasonal greenness. *GIScience & Remote Sensing,* 47**,** 25-52.

Tetetla-Rangel, E., Durán, R., Hernández-Stefanoni, J. L. & Dupuy, J. M. 2012. Distribución espacial de la riqueza de especies leñosas raras de la Península de Yucatán y su relación con las áreas naturales protegidas. *Tropical Conservation Science,* 5**,** 320-339.

Torrescano-Valle, N. & Folan, W. J. 2015. Physical Settings, Environmental History with an Outlook on Global Change. *Biodiversity and Conservation of the Yucatán Peninsula.* Springer.

Torrescano-Valle, N. & Islebe, G. A. 2015. Holocene paleoecology, climate history and human influence in the southwestern Yucatan Peninsula. *Review of Palaeobotany and Palynology,* 217**,** 1-8.

Townshend, J. R. & Justice, C. 1986. Analysis of the dynamics of African vegetation using the normalized difference vegetation index. *International Journal of Remote Sensing,* 7**,** 1435-1445.

Tucker, C., Vanpraet, C., Boerwinkel, E. & Gaston, e. A. 1983. Satellite remote sensing of total dry matter production in the Senegalese Sahel. *Remote Sensing of Environment,* 13**,** 461-474.

Tucker, C. & Sellers, P. 1986. Satellite remote sensing of primary production. *International Journal of Remote Sensing,* 7**,** 1395-1416.

Tucker, C. J., Vanpraet, C. L., Sharman, M. & Van Ittersum, G. 1985. Satellite remote sensing of total herbaceous biomass production in the Senegalese Sahel: 1980–1984. *Remote sensing of environment,* 17**,** 233-249.

Tucker, C. J., Newcomb, W. W., Los, S. O. & Prince, S. D. 1991. Mean and inter-year variation of growing-season normalized difference vegetation index for the Sahel 1981-1989. *International Journal of Remote Sensing,* 12**,** 1133-1135.

Turner, B., Villar, S. C., Foster, D., Geoghegan, J., Keys, E., Klepeis, P., Lawrence, D., Mendoza, P. M., Manson, S. & Ogneva-Himmelberger, Y. 2001. Deforestation in the southern Yucatán peninsular region: an integrative approach. *Forest Ecology and Management,* 154**,** 353-370.

Turner, B. 2010. Sustainability and forest transitions in the southern Yucatan: The land architecture approach. *Land Use Policy,* 27**,** 170-179.

Turner II, B., Geoghegan, J. & Foster, D. R. 2004. *Integrated land-change science and tropical deforestation in the southern Yucatán: Final frontiers*, Oxford University Press on Demand.

Tüshaus, J. 2013. Comparison of Medium Spatial Resolution ENVISAT-MERIS and Terra-MODIS Hyper-temporal Time Series for Vegetation Decline Analysis: A Case Study in Central Asia. *Remote Sensing,* 5**,** 1-17.

Udelhoven, T., Stellmes, M., del Barrio, G. & Hill, J. 2009. Assessment of rainfall and NDVI anomalies in Spain (1989–1999) using distributed lag models. *International Journal of Remote Sensing,* 30**,** 1961-1976.

Unal, Y., Kindap, T. & Karaca, M. 2003. Redefining the climate zones of Turkey using cluster analysis. *International Journal of Climatology,* 23**,** 1045-1055.

USDM. 2016. *U.S. Drought Monitor Classification Scheme* [Online]. Available: http://droughtmonitor.unl.edu/aboutus/classificationscheme.aspx [Accessed 2016].

Valdez-Hernández, M., Sánchez, O., Islebe, G. A., Snook, L. K. & Negreros-Castillo, P. 2014. Recovery and early succession after experimental disturbance in a seasonally dry tropical forest in Mexico. *Forest Ecology and Management,* 334**,** 331-343.

Valdez-Hernández, M., González-Salvatierra, C., Reyes-García, C., Jackson, P. C. & Andrade, J. L. 2015. Physiological Ecology of Vascular Plants. *Biodiversity and Conservation of the Yucatán Peninsula.* Springer.

Vázquez-Domínguez, E. & Arita, H. T. 2010. The Yucatan peninsula: biogeographical history 65 million years in the making. *Ecography,* 33**,** 212-219.

Vázquez, I. T. 1999. El clima de la selva baja caducifolia en México. *Investigaciones Geográficas (Mx)***,** 40-52.

Verbesselt, J., Zeileis, A. & Herold, M. 2012. Near real-time disturbance detection using satellite image time series. *Remote Sensing of Environment,* 123**,** 98-108.

Villers-Ruiz, L. & Trejo-Vázquez, I. 1997. Assessment of the vulnerability of forest ecosystems to climate change in Mexico. *Climate Research,* 9**,** 87-93.

Wang, J., Price, K. & Rich, P. 2001. Spatial patterns of NDVI in response to precipitation and temperature in the central Great Plains. *International Journal of Remote Sensing,* 22**,** 3827-3844.

Wardlow, B., Anderson, M. & Verdin, J. 2012a. Remote sensing of drought. *CRC, Boca Raton*.

Wardlow, B., Tadesse, T., Brown, J., Callahan, K., Swain, S. & Hunt, E. 2012b. Vegetation Drought Response Index. *Remote Sensing of Drought.* CRC Press.

Wei, H., Heilman, P., Qi, J., Nearing, M. A., Gu, Z. & Zhang, Y. 2012. Assessing phenological change in China from 1982 to 2006 using AVHRR imagery. *Frontiers of Earth Science,* 6**,** 227-236.

Werick, W., Willeke, G., Guttman, N., Hosking, J. & Wallis, J. 1994. National drought atlas developed. *Eos, Transactions American Geophysical Union,* 75**,** 89-90.

White, D. & Hood, C. 2004. Vegetation patterns and environmental gradients in tropical dry forests of the northern Yucatan Peninsula. *Journal of vegetation science,* 15**,** 151-160.

Whitmore, T. J., Brenner, M., Curtis, J. H., Dahlin, B. H. & Leyden, B. W. 1996. Holocene climatic and human influences on lakes of the Yucatan Peninsula, Mexico: an interdisciplinary, palaeolimnological approach. *The Holocene,* 6**,** 273-287.

Wilhite, D. A. 2000. Drought as a natural hazard: concepts and definitions.

Wilhite, D. A. & Vanyarkho, O. 2000. Drought: Pervasive impacts of a creeping phenomenon. *Drought: A global assessment,* 1**,** 245-255.

Wilhite, D. A. 2012. *Drought Assessment, Management, and Planning: Theory and Case Studies: Theory and Case Studies*, Springer Science & Business Media.

Wilson, E. M. 1980. Physical geography of the Yucatan Peninsula. *Yucatan: A World Apart. University of Alabama Press, Tuscaloosa, AL***,** 5-40.

WMO 1989. Calculation of monthly and annual 30-year standard normals.

Wooldridge, J. 2012. *Introductory econometrics: A modern approach*, Cengage Learning.

Wu, C., Niu, Z., Tang, Q. & Huang, W. 2008. Estimating chlorophyll content from hyperspectral vegetation indices: Modeling and validation. *Agricultural and Forest Meteorology,* 148**,** 1230-1241.

Wu, H., Hayes, M. J., Weiss, A. & Hu, Q. 2001. An evaluation of the Standardized Precipitation Index, the China-Z Index and the statistical Z-Score. *International journal of climatology,* 21**,** 745-758.

Yang, W., Yang, L. & Merchant, J. 1997. An assessment of AVHRR/NDVI-ecoclimatological relations in Nebraska, USA. *International Journal of Remote Sensing,* 18**,** 2161-2180.

Zhao, M. & Running, S. W. 2010. Drought-induced reduction in global terrestrial net primary production from 2000 through 2009. *science,* 329**,** 940-943.

APPENDIX 1

Table A- 1. List of 229 meteorological stations at the Yucatan Peninsula. Highlighted cells represent the 98 stations after data cleaning from section (see section 3.2.1.1).

Station	Latitude	Longitude	Altitude	State	Start	End	Duration (years)	% of data (1980-2011)
Abala	**20.65**	**-89.68**	**17**	**Yuc**	**May-67**	**Dec-14**	**47**	**90.47**
Acanceh	**20.81**	**-89.45**	**14**	**Yuc**	**May-78**	**Nov-08**	**30**	**71.42**
Adolfo Lopez Mateos	19.63	-88.69	54	Qroo	Mar-79	Dec-12	33	57.14
Agua Blanca	18.01	-88.82	62	Qroo	Jan-85	Dec-12	27	57.14
Akil	**20.24**	**-89.32**	**26**	**Yuc**	**Jan-77**	**Nov-08**	**31**	**69.04**
Altamira	18.58	-90.26	100	Camp	Jan-68	Dec-75	7	4.76
Alvarado	18.02	-89.27	170	Camp	Apr-97	Dec-11	14	33.33
Alvaro Obregon	**18.29**	**-88.64**	**37**	**Qroo**	**Aug-64**	**Dec-12**	**48**	**88.09**
Andres Quintana Roo	19.16	-88.10	16	Qroo	Jan-90	Dec-12	22	47.61
Bacalar	18.68	-88.38	2	Qroo	Jun-62	Jun-73	11	9.52
Becal	**20.43**	**-90.03**	**16**	**Camp**	**May-74**	**Dec-11**	**37**	**71.42**
Becanchen	19.87	-89.22	150	Yuc	Aug-52	Dec-14	62	59.52
Bolonchen	**20.00**	**-89.75**	**120**	**Camp**	**Jan-53**	**Jun-14**	**61**	**97.61**
Buctzotz	**21.21**	**-88.80**	**6**	**Yuc**	**Dec-53**	**Nov-08**	**55**	**83.33**
C.e.p. Tizimin	21.18	-87.98	26	Yuc	Jan-84	Nov-87	3	7.14
C.i.a.p.y.	**20.43**	**-89.76**	**50**	**Yuc**	**Mar-69**	**Dec-05**	**36**	**83.33**
Cacalchen	21.02	-89.23	12	Yuc	Jan-86	Dec-00	14	33.33
Calkini (dge)	**20.37**	**-90.05**	**15**	**Camp**	**Jan-82**	**Dec-11**	**29**	**71.42**
Calkini (smn)	20.36	-90.05	15	Camp	May-50	Dec-75	25	7.14
Calotmul	**21.02**	**-88.18**	**23**	**Yuc**	**May-82**	**Nov-08**	**26**	**64.28**
Camp (dge)	**19.84**	**-90.53**	**10**	**Camp**	**Jan-52**	**Dec-11**	**59**	**97.61**
Campo Experimental El Tormento	18.60	-90.72	50	Camp	Jun-77	Dec-00	23	52.38
Canasayab	19.29	-90.58	37	Camp	Jul-75	Dec-14	39	50.00
Cancun	21.16	-86.82	9	Qroo	Apr-88	Dec-14	26	52.38
Candelaria	19.74	-88.96	52	Qroo	Jan-98	Dec-14	16	38.09
Candelaria (dge)	**18.18**	**-91.05**	**50**	**Camp**	**Jan-61**	**Dec-85**	**24**	**61.90**
Candelaria (smn)	18.18	-91.05	40	Camp	Jun-44	Dec-11	67	26.19
Canki	19.99	-90.12	50	Camp	Jan-89	Dec-11	22	52.38
Cansancab	21.15	-89.10	7	Yuc	Sep-78	Jan-88	10	23.80
Cantamayec	20.47	-89.08	24	Yuc	Jan-98	Nov-14	16	4.76
Carolina	21.14	-89.46	5	Yuc	Jan-84	Feb-94	10	19.04
Castamay	19.84	-90.43	25	Camp	Apr-78	Apr-87	9	23.80

Catzin	20.76	-87.86	30	Yuc	Apr-82	May-12	30	52.38
Cayo Arcas	20.20	-91.96	6	Camp	Aug-29	May-87	58	30.95
Cayo Arenas	22.12	-91.40	3	Camp	Aug-29	Dec-85	56	28.57
Celestun (dge)	**20.86**	**-90.40**	**3**	**Yuc**	**Jan-61**	**Dec-05**	**44**	**80.95**
Celestun (smn)	20.85	-90.40	3	Yuc	May-43	Nov-83	40	28.57
Central Vallarta	20.86	-87.05	11	Qroo	Jan-00	Dec-12	12	23.80
Chac Cheito	19.05	-90.41	90	Camp	Jan-96	Dec-11	15	38.09
Chacchoben	**18.98**	**-88.21**	**15**	**Qroo**	**Aug-72**	**Dec-11**	**39**	**85.71**
Chacsinkin	20.17	-89.02	37	Yuc	Dec-69	Feb-72	3	7.14
Champoton (dge)	**19.36**	**-90.72**	**10**	**Camp**	**Jan-86**	**Dec-11**	**25**	**61.90**
Champoton (smn)	19.35	-90.72	10	Camp	Jan-21	Dec-85	64	38.10
Chan Cenote	**20.99**	**-87.78**	**30**	**Yuc**	**Jun-78**	**Dec-05**	**27**	**66.67**
Chanchichimila	**20.39**	**-88.48**	**26**	**Yuc**	**Aug-52**	**Dec-14**	**62**	**90.48**
Chemax	**20.65**	**-87.94**	**26**	**Yuc**	**Apr-78**	**Nov-07**	**29**	**71.43**
Chetumal (dge)	**18.50**	**-88.33**	**11**	**Qroo**	**Aug-52**	**Dec-12**	**60**	**90.48**
Chicbul	**18.78**	**-90.92**	**25**	**Camp**	**Jul-77**	**Dec-11**	**34**	**83.33**
Chicxulub Puerto	**21.29**	**-89.61**	**3**	**Yuc**	**Mar-63**	**Nov-07**	**44**	**90.48**
China	**19.67**	**-90.47**	**10**	**Camp**	**Apr-83**	**Dec-11**	**28**	**69.05**
Chochola	20.75	-89.83	14	Yuc	May-82	Dec-14	32	59.52
Chunchintok	19.36	-89.58	150	Camp	Jan-89	Dec-11	22	54.76
Chunchucmil	20.64	-90.22	13	Yuc	May-82	Nov-07	25	59.52
Coba	**20.49**	**-87.74**	**5**	**Qroo**	**Jul-71**	**Dec-12**	**41**	**61.90**
Cocoyol	18.17	-88.82	66	Qroo	Jul-54	Jan-72	18	7.14
Colonia Yuc	21.21	-87.73	17	Yuc	Aug-82	Dec-86	4	9.52
Conhuas	18.54	-89.92	170	Camp	Mar-79	Dec-11	32	57.14
Conkal	21.07	-89.52	9	Yuc	Oct-76	Dec-14	38	33.33
Cozumel (dge)	20.51	-86.95	6	Qroo	Jan-94	Dec-12	18	21.43
Cristobal Colon	18.22	-89.45	250	Camp	Jan-98	Dec-11	13	33.33
Cuzama	20.74	-89.32	10	Yuc	Jan-86	May-12	26	35.71
Dos Aguadas	18.13	-89.14	164	Qroo	Mar-99	Dec-12	13	28.57
Dzan	**20.36**	**-89.48**	**26**	**Yuc**	**Aug-66**	**Dec-07**	**41**	**90.48**
Dzibalchen	**19.46**	**-89.74**	**110**	**Camp**	**Jan-52**	**Dec-11**	**59**	**71.43**
Dzidzantum	21.26	-89.05	5	Yuc	Apr-86	Nov-07	21	50.00
Dzilam De Bravo	**21.39**	**-88.89**	**2**	**Yuc**	**Jan-61**	**Nov-07**	**46**	**88.10**
Dzitas	**20.84**	**-88.53**	**30**	**Yuc**	**Aug-52**	**Nov-07**	**55**	**83.33**
Dzitbalche	**20.32**	**-90.06**	**30**	**Camp**	**Jun-82**	**Dec-11**	**29**	**69.05**
Dziuche	**19.90**	**-88.81**	**37**	**Qroo**	**Apr-77**	**Dec-12**	**35**	**69.05**
Dzonot Ake	21.24	-87.94	16	Yuc	Mar-82	Nov-07	25	59.52
Dzonot Carretero	21.40	-87.88	9	Yuc	Oct-75	Jun-82	7	7.14
E.t.a. 006 Tenabo	20.05	-90.20	7	Camp	Feb-73	Mar-79	6	16.67

E.t.a. 086 Calkini	20.37	-90.05	15	Camp	Sep-73	Dec-82	9	19.05
E.t.a. 169 San Diego	20.20	-89.28	33	Yuc	Jan-61	Feb-83	22	21.43
E.t.a. 443 Espita	21.01	-88.30	27	Yuc	Dec-75	Sep-83	8	7.14
Edzna I	19.46	-90.10	125	Camp	Jul-72	Apr-83	11	19.05
Edzna Ii	**19.53**	**-90.19**	**30**	**Camp**	**Jan-81**	**Dec-11**	**30**	**73.81**
El Carmen (dge)	18.65	-91.75	3	Camp	Jan-55	Oct-77	22	9.52
El Carmen (smn)	**18.65**	**-91.76**	**5**	**Camp**	**Dec-26**	**Dec-11**	**85**	**64.29**
El Cuyo	**21.52**	**-87.68**	**7**	**Yuc**	**Dec-54**	**Dec-14**	**60**	**64.29**
El Zapote	18.22	-91.80	10	Camp	Jan-96	Jun-10	14	30.95
Entre Hermanos	18.46	-91.14	40	Camp	Jan-98	Dec-11	13	28.57
Escarcega (dge)	18.60	-90.73	85	Camp	Jan-61	May-88	27	42.86
Escarcega (smn)	18.60	-90.74	80	Camp	Nov-43	Dec-11	68	57.14
Espita	21.01	-88.28	25	Yuc	Apr-43	Dec-07	64	57.14
F.i.u.a.d.y. (periferico)	21.05	-89.65	9	Yuc	Sep-82	Aug-00	18	26.19
Felipe Carrillo Puerto (dge)	**19.58**	**-88.05**	**17**	**Qroo**	**Aug-52**	**Dec-11**	**59**	**95.24**
Felipe Carrillo Puerto (obs)	19.57	-88.05	10	Qroo	Jan-05	Dec-11	6	14.29
Halacho	20.49	-90.08	23	Yuc	Jan-98	Nov-07	9	23.81
Hecelchakan (dge)	20.18	-90.13	15	Camp	Apr-44	Dec-85	41	38.10
Hecelchakan (smn)	20.20	-90.12	50	Camp	Jan-86	Dec-11	25	59.52
Hocaba	20.82	-89.24	15	Yuc	Jun-78	Jun-97	19	30.95
Holca	**20.76**	**-88.93**	**22**	**Yuc**	**Apr-78**	**Nov-07**	**29**	**69.05**
Hool	**19.51**	**-90.41**	**25**	**Camp**	**Jun-62**	**Nov-11**	**49**	**100.00**
Hopelchen	**19.76**	**-89.84**	**100**	**Camp**	**Feb-44**	**Dec-14**	**70**	**83.33**
Hospital Morelos De Chetumal	18.50	-88.30	12	Qroo	Apr-03	Dec-12	9	21.43
Huhi	20.73	-89.16	14	Yuc	Jan-87	Jun-92	5	14.29
Hunucma	21.02	-89.88	6	Yuc	Dec-74	Sep-93	19	30.95
I.n.i.arroyo Caechet	**18.57**	**-88.46**	**26**	**Qroo**	**Jan-82**	**Dec-12**	**30**	**69.05**
Ideal	20.88	-87.55	22	Qroo	Jan-91	Dec-12	21	45.24
Ingenio Catmis	**19.96**	**-88.95**	**41**	**Yuc**	**May-54**	**Sep-08**	**54**	**80.95**
Inip	18.25	-88.63	2	Qroo	Jun-82	Dec-92	10	26.19
Isla Aguada	**18.78**	**-91.49**	**1**	**Camp**	**Mar-59**	**Dec-11**	**52**	**100.00**
Isla Arenas	**20.69**	**-90.45**	**1**	**Camp**	**Feb-70**	**Jan-12**	**42**	**100.00**
Isla Holbox	21.53	-87.38	10	Qroo	Jan-61	Dec-89	28	45.24
Isla Mujeres	21.24	-86.74	5	Qroo	Jan-61	Dec-72	11	4.76
Isla Perez	22.39	-89.67	3	Camp	Jan-30	Oct-83	53	21.43
Iturbide	**19.58**	**-89.60**	**80**	**Camp**	**May-67**	**Dec-11**	**44**	**97.62**
Izamal Escuela	**20.94**	**-89.03**	**13**	**Yuc**	**Jan-61**	**Nov-07**	**46**	**64.29**
Jose Maria Morelos	19.74	-88.71	26	Qroo	Apr-99	Dec-12	13	26.19

Juan Sarabia	18.50	-88.48	27	Qroo	Jan-05	Dec-12	7	16.67
Kantemo	21.15	-88.96	7	Yuc	Jan-85	Dec-00	15	11.90
Kantunilkin	**21.10**	**-87.49**	**15**	**Qroo**	**Aug-52**	**Dec-12**	**60**	**85.71**
Kinchil	**20.91**	**-89.96**	**8**	**Yuc**	**May-66**	**May-08**	**42**	**83.33**
Kuxeb	**20.86**	**-87.87**	**21**	**Yuc**	**Mar-82**	**Nov-07**	**25**	**61.90**
La Esperanza	18.17	-90.08	290	Camp	Jan-65	Aug-81	16	28.57
La Presumida	**19.80**	**-88.75**	**16**	**Qroo**	**Nov-65**	**Dec-12**	**47**	**97.62**
La Union Ii	18.39	-88.91	133	Qroo	Jan-05	Dec-12	7	14.29
Laguna Guerrero	18.70	-88.26	3	Qroo	Dec-02	Dec-12	10	21.43
Laguna Kana	19.50	-88.40	23	Qroo	Jan-98	Nov-12	14	28.57
Leona Vicario	**20.99**	**-87.20**	**8**	**Qroo**	**Jan-61**	**Dec-12**	**51**	**76.19**
Limones	**19.02**	**-88.11**	**9**	**Qroo**	**Jan-79**	**Dec-12**	**33**	**73.81**
Loche	**21.39**	**-88.15**	**15**	**Yuc**	**Jan-61**	**Nov-07**	**46**	**90.48**
Los Pozos	18.55	-88.48	33	Qroo	Oct-62	Jul-95	33	59.52
Mahahual	18.71	-87.71	4	Qroo	May-99	Dec-11	12	11.90
Mamantel	**18.52**	**-91.09**	**12**	**Camp**	**Jan-78**	**Dec-11**	**33**	**78.57**
Maxcanu	20.60	-90.00	12	Yuc	Aug-52	Oct-87	35	33.33
Merida (obs)	20.95	-89.65	11	Yuc	Apr-86	Nov-08	22	42.86
Merida Centro	**20.97**	**-89.62**	**9**	**Yuc**	**Jan-61**	**May-12**	**51**	**69.05**
Merida Santiago	20.98	-89.58	10	Yuc	Mar-82	Aug-88	6	16.67
Miguel Hidalgo	17.98	-90.83	67	Camp	Oct-64	Dec-89	25	42.86
Mococha	**21.11**	**-89.45**	**20**	**Yuc**	**Mar-77**	**Dec-14**	**37**	**73.81**
Molino Chumpan	**17.94**	**-91.74**	**10**	**Camp**	**May-78**	**Dec-11**	**33**	**71.43**
Monclova	**18.06**	**-90.82**	**100**	**Camp**	**Jan-61**	**Dec-11**	**50**	**95.24**
Morocoy	18.60	-88.81	68	Qroo	Jan-98	Dec-12	14	16.67
Motul	**21.08**	**-89.28**	**7**	**Yuc**	**Aug-52**	**Dec-14**	**62**	**97.62**
Muna	**20.49**	**-89.71**	**29**	**Yuc**	**Jul-58**	**Dec-14**	**56**	**92.86**
Nabula	21.03	-88.09	23	Yuc	May-82	Nov-88	6	16.67
Nanzal	18.26	-91.30	10	Camp	Jan-65	Aug-76	11	9.52
Nicolas Bravo Km. 71	**18.46**	**-88.93**	**109**	**Qroo**	**Jan-61**	**Dec-11**	**50**	**92.86**
Nilchi	**19.85**	**-90.27**	**10**	**Camp**	**Jun-64**	**Dec-11**	**47**	**97.62**
Noh Yaxche	**19.61**	**-90.22**	**30**	**Camp**	**Aug-78**	**Dec-11**	**33**	**80.95**
Nuevo Xcan	20.88	-87.58	26	Qroo	Jan-61	Dec-90	29	30.95
Nunkini	20.39	-90.14	25	Camp	Jun-82	Jan-98	16	38.10
Otilio Montaño	19.01	-88.83	103	Qroo	Jan-00	Dec-12	12	19.05
Oxcutzcab	**20.29**	**-89.39**	**26**	**Yuc**	**Jan-77**	**Nov-07**	**30**	**66.67**
Pablo T. Burgos	18.30	-90.70	50	Camp	Jan-98	Dec-11	13	33.33
Palizada	**18.25**	**-92.09**	**4**	**Camp**	**Nov-44**	**Dec-11**	**67**	**100.00**
Palmar De Vista Alegre	18.15	-92.02	3	Camp	Aug-67	Dec-71	4	4.76
Palmas	19.23	-88.12	14	Qroo	Jan-60	Dec-89	29	42.86

Panaba	21.30	-88.27	19	Yuc	Oct-75	Oct-01	26	38.10
Pedro Antonio De Los Santos	18.95	-88.16	10	Qroo	Jan-82	Nov-11	29	59.52
Peto (dge)	**20.12**	**-88.95**	**35**	**Yuc**	**Oct-59**	**Nov-07**	**48**	**90.48**
Peto (smn)	20.12	-88.97	34	Yuc	Jul-04	Dec-04	0	2.38
Piste	20.69	-88.58	25	Yuc	May-82	Nov-07	25	52.38
Pixoyal (dge)	18.93	-90.60	40	Camp	Jan-61	Dec-90	29	45.24
Pixoyal (smn)	18.93	-90.60	40	Camp	Jun-44	Dec-11	67	35.71
Placeres	18.16	-89.42	230	Camp	Feb-69	Jun-74	5	9.52
Playa Del Carmen	20.63	-87.08	9	Qroo	Jan-98	Dec-14	16	28.57
Pocboc	20.24	-90.10	10	Camp	Jan-02	Dec-11	9	23.81
Pocyaxun	**19.73**	**-90.35**	**20**	**Camp**	**Nov-82**	**Dec-11**	**29**	**66.67**
Pomuch	20.14	-90.17	10	Camp	Jan-96	Dec-11	15	38.10
Pucte	**18.23**	**-88.67**	**35**	**Qroo**	**Jul-71**	**Dec-12**	**41**	**88.10**
Puerto Morelos	20.85	-86.87	6	Qroo	Jan-61	Dec-98	37	59.52
Pustunich	**19.14**	**-90.48**	**30**	**Camp**	**Feb-52**	**Dec-11**	**59**	**97.62**
Reforma	18.81	-88.57	23	Qroo	Jan-98	Dec-12	14	30.95
Rio Indio	18.97	-87.62	2	Qroo	Mar-67	Dec-69	2	0.00
Rio Lagartos	**21.59**	**-88.15**	**4**	**Yuc**	**Apr-62**	**Nov-07**	**45**	**88.10**
Saban	20.03	-88.54	31	Qroo	Jan-86	Dec-12	26	57.14
Sabancuy	**18.97**	**-91.18**	**5**	**Camp**	**Nov-53**	**Dec-14**	**61**	**97.62**
Sacalum	20.50	-89.59	22	Yuc	Jan-77	Sep-89	12	30.95
San Diego Buenavista	19.86	-89.30	83	Yuc	Aug-82	Nov-07	25	52.38
San Felipe Bacalar	18.76	-88.34	19	Qroo	Feb-79	Jul-90	11	26.19
San Isidro	**18.63**	**-91.05**	**10**	**Camp**	**Apr-58**	**Dec-11**	**53**	**64.29**
San Juan Bautista	19.87	-89.93	90	Camp	Jan-97	Dec-11	14	35.71
San Roman	21.22	-88.50	9	Yuc	Jan-69	Jul-73	4	9.52
Santa Cristina	**19.82**	**-90.38**	**10**	**Camp**	**Nov-76**	**Dec-11**	**35**	**83.33**
Santa Cruz Chico	18.92	-88.28	20	Qroo	Jul-54	Dec-90	36	30.95
Santa Elena	**20.33**	**-89.64**	**43**	**Yuc**	**Mar-69**	**Nov-07**	**38**	**90.48**
Santa Rosa	19.95	-88.88	33	Yuc	Apr-66	Mar-72	6	4.76
Señor	**19.85**	**-88.14**	**21**	**Qroo**	**Jun-71**	**Dec-12**	**41**	**78.57**
Sergio Butron Casas	**18.51**	**-88.57**	**32**	**Qroo**	**Apr-77**	**Dec-12**	**35**	**73.81**
Siho Chac	**19.51**	**-90.58**	**15**	**Camp**	**Sep-82**	**Dec-11**	**29**	**71.43**
Silvituc	**18.64**	**-90.30**	**75**	**Camp**	**Apr-58**	**Dec-11**	**53**	**95.24**
Sisal	**21.17**	**-90.03**	**4**	**Yuc**	**Dec-57**	**Sep-07**	**50**	**83.33**
Solferino	**21.35**	**-87.43**	**14**	**Qroo**	**Jan-69**	**Dec-11**	**42**	**97.62**
Sotuta (dge)	**20.60**	**-89.01**	**21**	**Yuc**	**Jan-61**	**Nov-07**	**46**	**90.48**
Sotuta (smn)	20.60	-89.02	3	Yuc	Dec-42	Dec-90	48	45.24
Tabi	**20.23**	**-89.53**	**50**	**Yuc**	**Jan-77**	**Oct-08**	**31**	**69.05**

Tampak	19.57	-88.70	45	Qroo	Aug-52	Dec-87	35	42.86
Teabo	**20.41**	**-89.29**	**26**	**Yuc**	**Apr-78**	**Nov-07**	**29**	**69.05**
Tecnologico Chetumal	18.52	-88.30	9	Qroo	Jan-85	Dec-12	27	59.52
Tekax De Alvaro Obregon	**20.21**	**-89.29**	**31**	**Yuc**	**Aug-52**	**Dec-00**	**48**	**69.05**
Tekax Unidad	**20.17**	**-89.24**	**28**	**Yuc**	**Jan-77**	**Nov-07**	**30**	**73.81**
Telchac Puerto	**21.34**	**-89.27**	**2**	**Yuc**	**Aug-52**	**Nov-07**	**55**	**90.48**
Telchaquillo	**20.64**	**-89.46**	**10**	**Yuc**	**Aug-52**	**Nov-07**	**55**	**83.33**
Temax	21.16	-88.96	13	Yuc	Jul-84	Nov-07	23	35.71
Tenabo (dge)	20.04	-90.23	10	Camp	Jul-82	Aug-85	3	9.52
Tenabo (smn)	20.03	-90.23	7	Camp	May-50	Oct-74	24	11.90
Ticul	20.40	-89.56	30	Yuc	Jan-77	Dec-14	37	61.90
Tihosuco	**20.19**	**-88.37**	**33**	**Qroo**	**Aug-52**	**Dec-11**	**59**	**88.10**
Tinun	**19.96**	**-90.23**	**50**	**Camp**	**Jul-78**	**Dec-11**	**33**	**78.57**
Tixmehuac	**20.23**	**-89.11**	**33**	**Yuc**	**May-62**	**May-07**	**45**	**73.81**
Tixmucuy	19.60	-90.28	34	Camp	Jan-84	Dec-11	27	66.67
Tizimin	**21.16**	**-88.17**	**14**	**Yuc**	**May-69**	**Dec-14**	**45**	**76.19**
Triangulo Oeste	20.98	-92.30	1	Camp	Aug-29	Oct-87	58	21.43
Tulum	**20.23**	**-87.46**	**10**	**Qroo**	**Jul-64**	**Dec-12**	**48**	**78.57**
Tzucacab	**20.07**	**-89.04**	**36**	**Yuc**	**May-78**	**Jan-07**	**29**	**61.90**
Uman	20.88	-89.75	11	Yuc	Dec-74	Dec-91	17	19.05
Valladolid (dge)	20.70	-88.22	22	Yuc	Aug-52	Dec-77	25	19.05
Valladolid (obs)	20.69	-88.20	23	Yuc	Aug-90	Dec-05	15	30.95
Valle Hermoso	**19.19**	**-88.52**	**21**	**Qroo**	**Jun-71**	**Dec-12**	**41**	**73.81**
Victoria	**20.79**	**-87.28**	**15**	**Qroo**	**May-65**	**Dec-11**	**46**	**78.57**
Vista Alegre	18.04	-91.66	10	Camp	Jan-96	Dec-10	14	35.71
Xbonil	**18.64**	**-90.17**	**70**	**Camp**	**Aug-63**	**Oct-03**	**40**	**73.81**
Xcalak	18.27	-87.84	3	Qroo	Jan-72	Dec-11	39	30.95
Xcupil (dge)	**19.66**	**-89.86**	**60**	**Camp**	**Jan-44**	**Dec-71**	**27**	**95.24**
Xcupil (smn)	19.72	-89.85	80	Camp	Jan-82	Dec-00	18	4.76
X-Hualtez	21.12	-88.64	11	Yuc	Jan-77	Jun-10	33	45.24
Xmaben	19.23	-89.31	130	Camp	Feb-66	Jan-77	11	16.67
Xocnaceh	20.34	-89.48	31	Yuc	Aug-52	Oct-88	36	35.71
Xpichil	**19.69**	**-88.38**	**28**	**Qroo**	**Jan-61**	**Dec-11**	**50**	**97.62**
Xpugil	18.51	-89.40	250	Camp	Jul-71	Dec-11	40	11.90
Xul	**20.10**	**-89.46**	**92**	**Yuc**	**May-69**	**Dec-03**	**34**	**71.43**
Yalsihon	21.41	-88.51	8	Yuc	Mar-82	Nov-07	25	54.76
Yaxcaba	20.53	-88.83	29	Yuc	Sep-62	Dec-90	28	47.62
Yohaltun	19.02	-90.32	30	Camp	Jun-80	Jun-11	31	14.29
Yokdzonot Presentado	20.97	-87.91	20	Yuc	May-82	May-95	13	28.57
Zoh Laguna	**18.59**	**-89.42**	**265**	**Camp**	**Jun-49**	**Dec-11**	**62**	**80.95**

APPENDIX 2

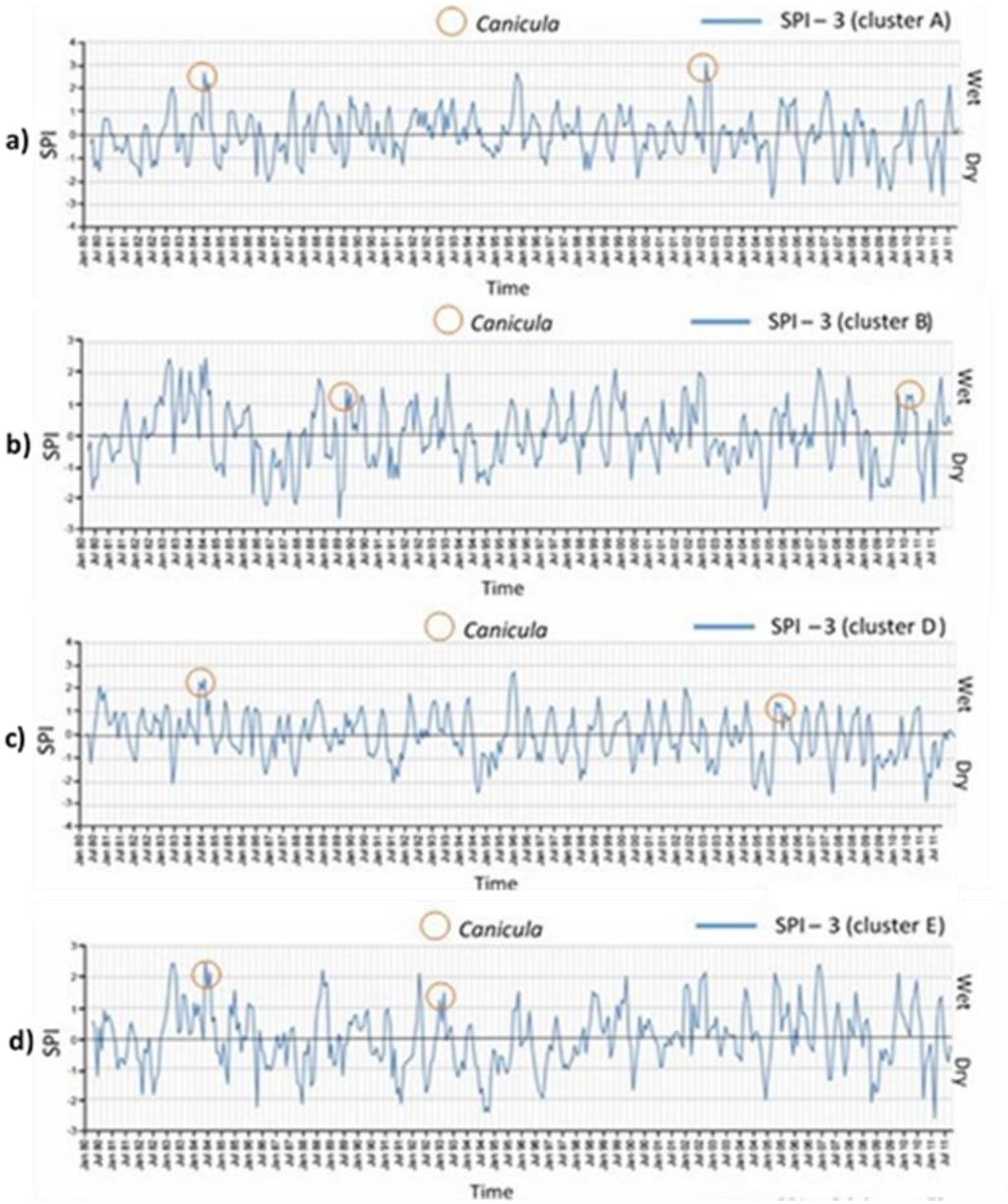


Figure B - 1. 3-month SPI values for cluster a) A, b) B, c) D, and d) E. These plots are the same as in section 3.4.1 but arranged by SPI rather than clusters

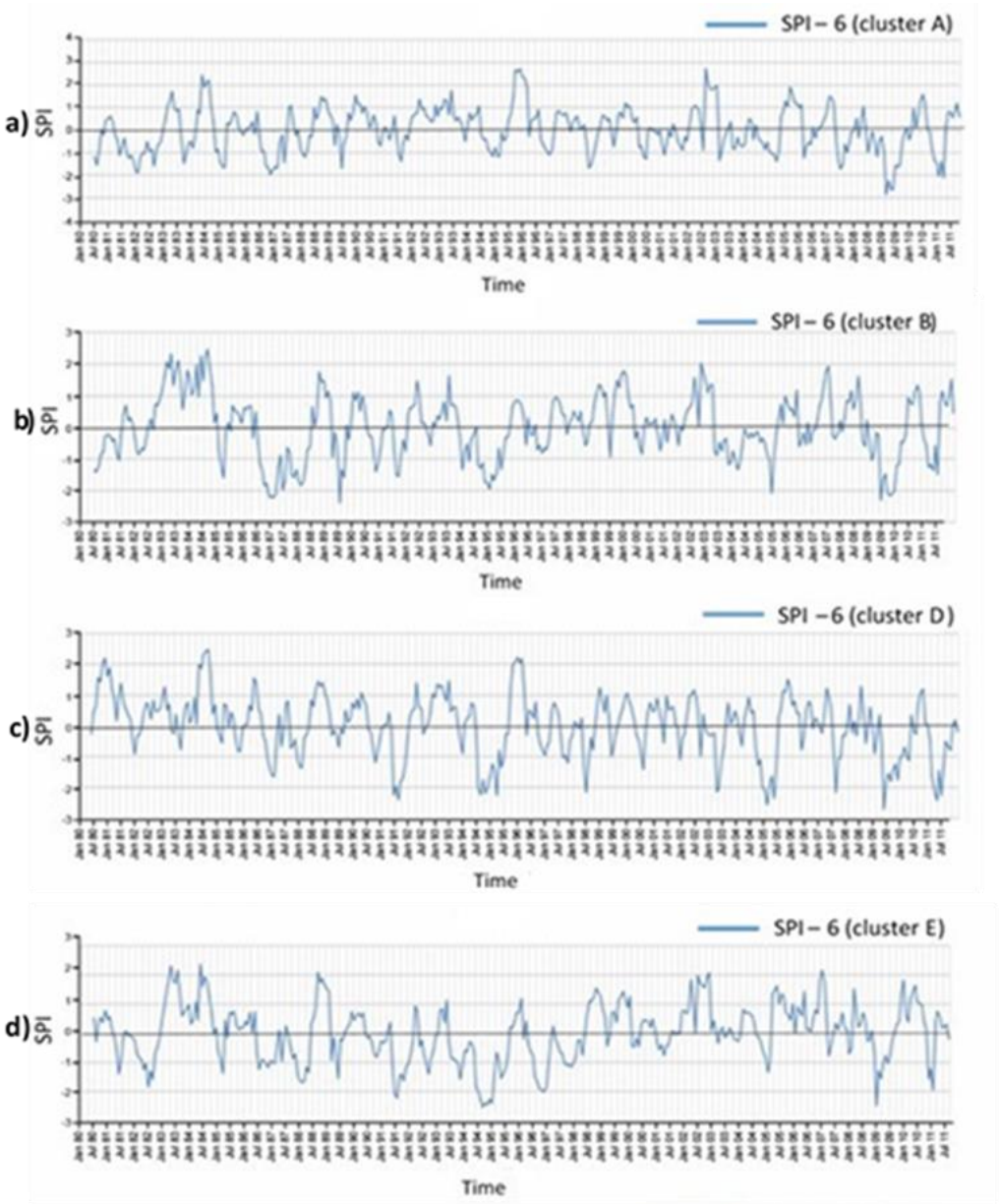


Figure B - 2. 6-month SPI values for cluster a) A, b) B, c) D, and d) E. These plots are the same as in section 3.4.1 but arranged by SPI rather than clusters

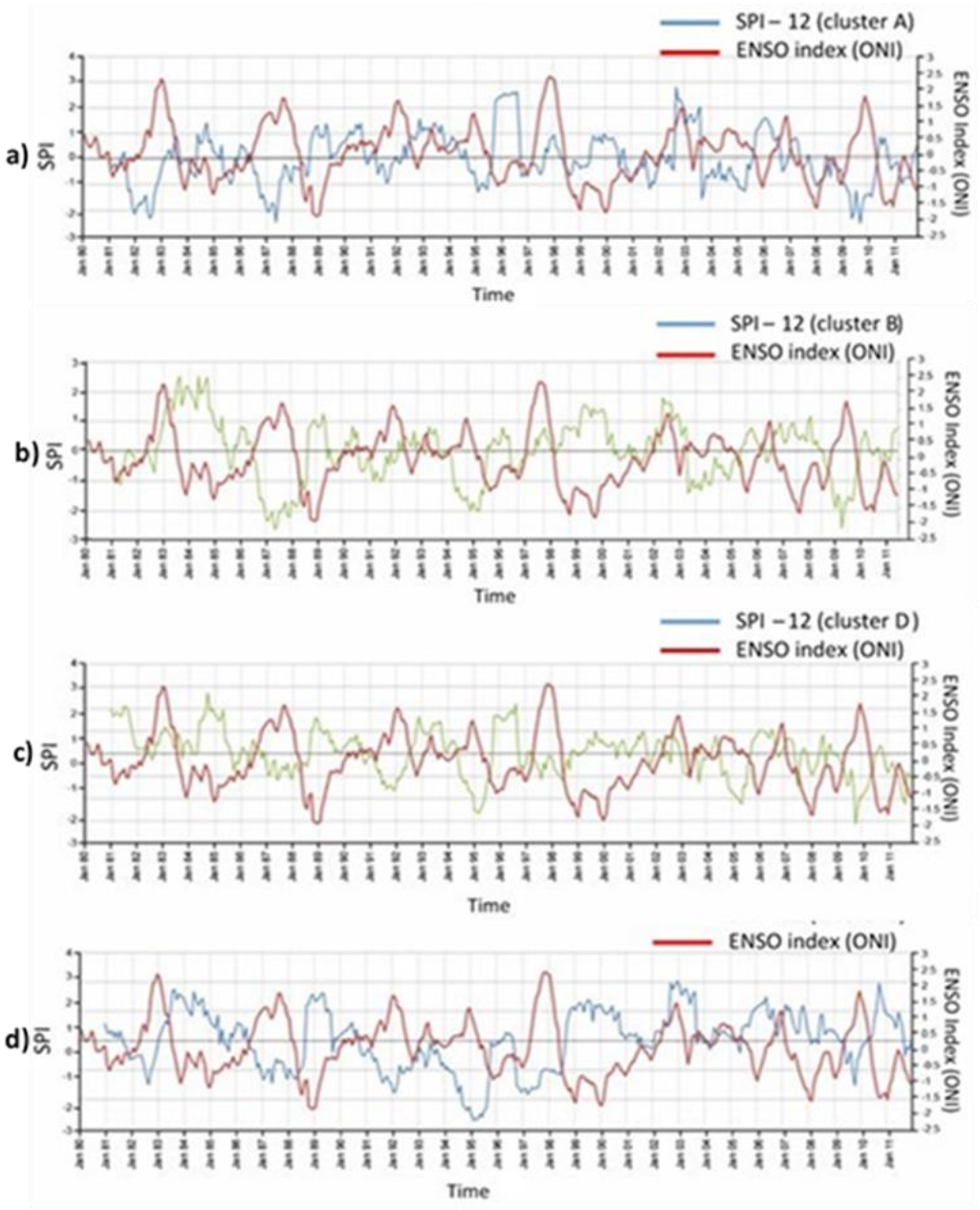


Figure B - 3. 12--month SPI values for cluster a) A, b) B, c) D, and d) E. These plots are the same as in section 3.4.1 but arranged by SPI rather than clusters. All plots include the Oceanic Niño Index in the secondary axis

APPENDIX 3

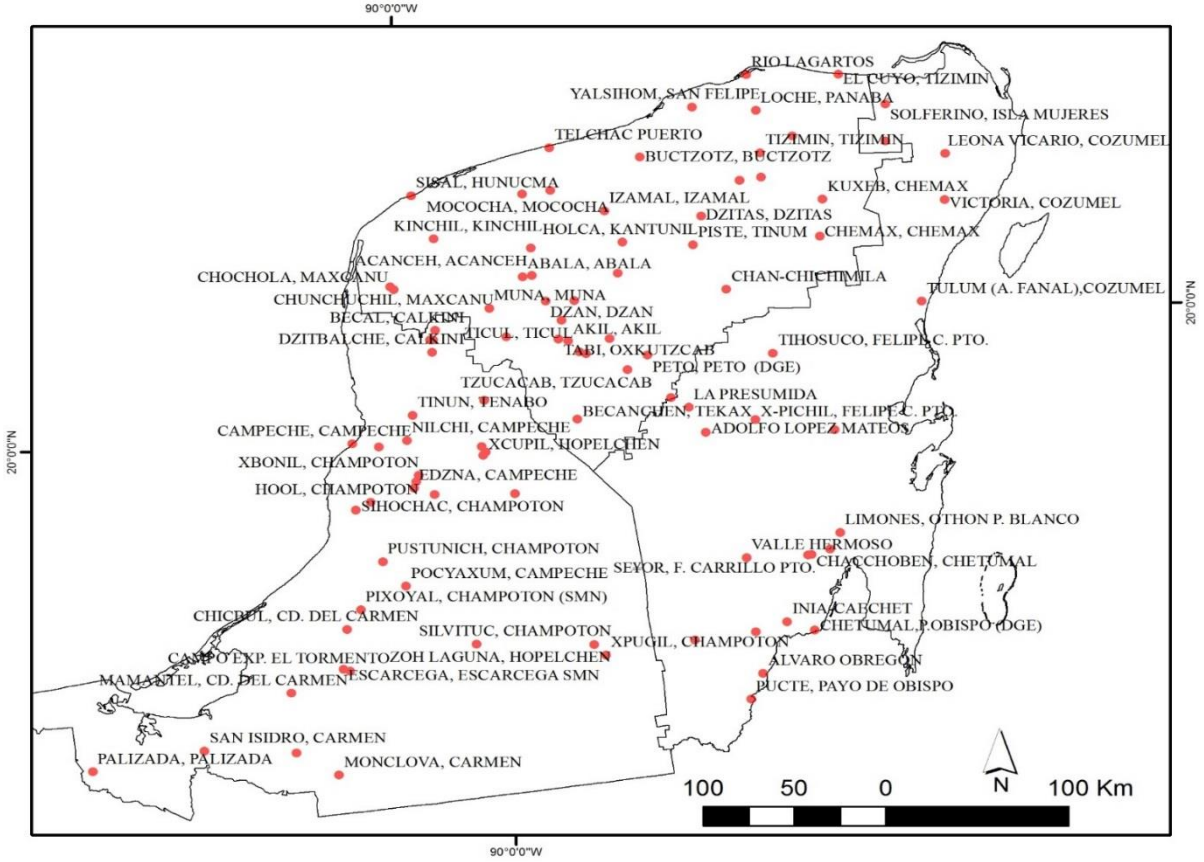


Figure A - 1. Location and names of meteorological stations at the Yucatan Peninsula

APPENDIX 4

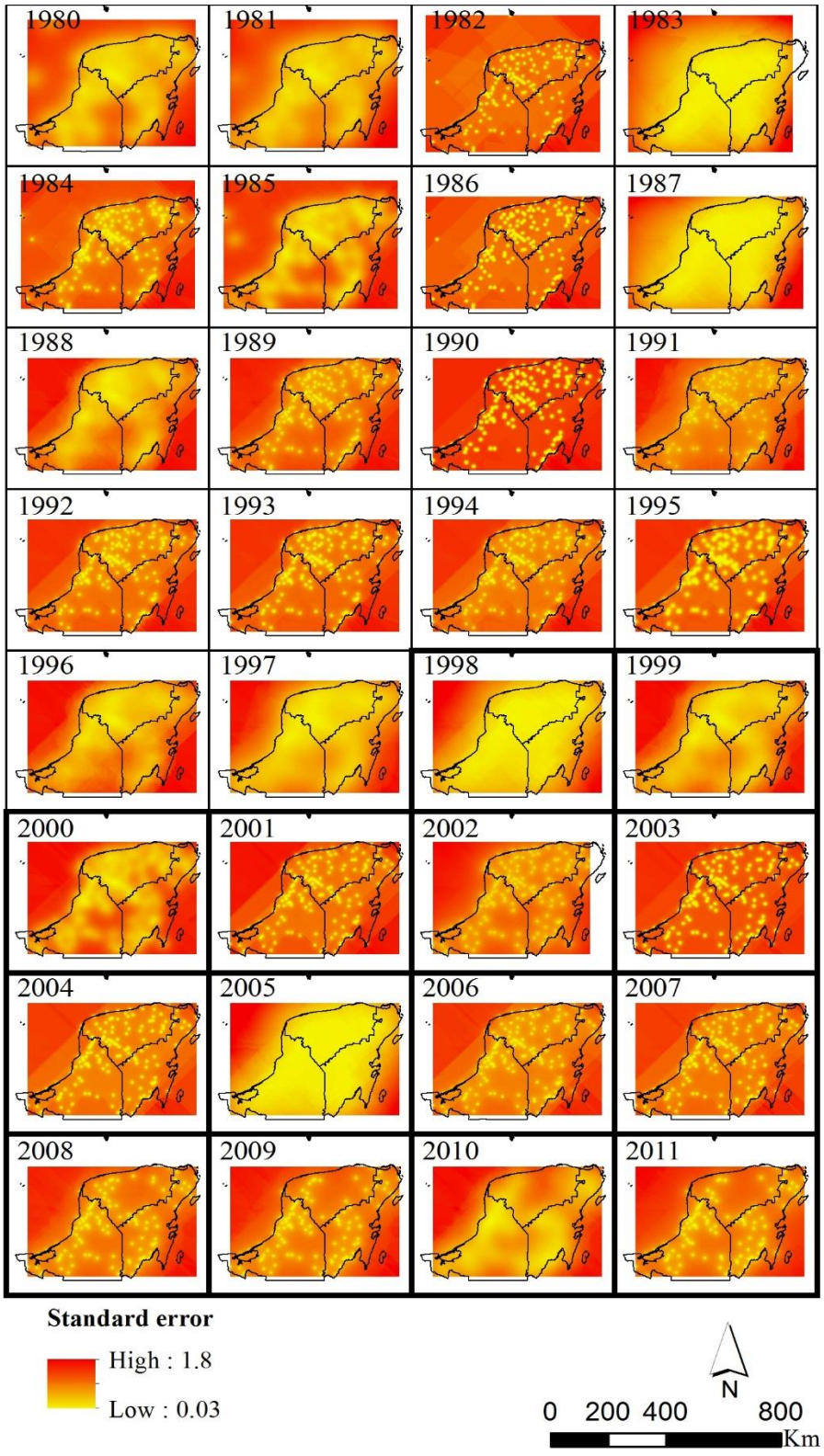


Figure C-1. Standard error estimated from kriging analysis presented in section 3.3.2.